UNIVERSITEIT VAN PRETORIA
UNIVERSITY OF PRETORIA
YUNIBESITHI YA PRETORIA

Identification of bioactive ingredients from *Cleome gynandra* and the physicochemical study of their microencapsulation in beta-cyclodextrin

By

Buntubonke Gom

Submitted in partial fulfilment of the requirements for the degree

***Philosophiae Doctor* Chemistry**

In the Faculty of Natural and Agricultural Sciences

University of Pretoria

Pretoria

South Africa

February 2022

Submission of declaration

I,**Buntubonke Gom** declare that the thesis, which I hereby submit for the degree *Philosophiae Doctor* at the University of Pretoria, is my own independent work and has not previously been submitted by me for a degree at this or any other tertiary institution.

Signature: **Date**:

Plagiarism declaration

Full names	Buntubonke Gom
Student number	16401655
Topic of work	Identification of bioactive ingredients from *Cleome gynandra* and the physicochemical study of their microencapsulation in beta-cyclodextrin

Declaration

1. I understand what plagiarism is and am aware of the University's policy in this regard.

2. I declare that this thesis is my own original work. Where other people's work has been used (either from a printed source, internet or any other source), this has been properly acknowledged and referenced in accordance with the requirements as stated in the University's plagiarism prevention policy.

3. I have not used another student's past written work to hand in as my own.

4. I have not allowed, and will not allow, anyone to copy my work with the intention of passing it off as his or her own work.

Signature: Date:

Acknowledgements

I would like to give sincere thanks to the following:

My supervisors Professor VJ Maharaj (University of Pretoria), Dr Nomusa Dlamini (CSIR) and Dr Philip Labuschagne (CSIR) for their invaluable guidance, encouragement,patience and scientific contributions throughout thisPhD research. Dr Lonji Kalombo for his expert advice and assistance on spray dryer.

The Council for Scientific and Industrial Research (CSIR) for creating the platform tomaking this collaboration possible and for their funding, Dr Malefa Tselenyana for assistance with enzyme-based assays and the team of colleagues at the CSIR. The Department of Science and Innovation (DSI) for their financial support and funding conference attendances.

The Chemistry Department at the University of Pretoria: Dr Mamoalosi Selepe for help with the use of NMR, HPLC and optical rotation equipment, and her expert advice.Madelien Wooding for running samples on the UPLC-QTOF-MS and her advice, and the past and present members of the Bioprospecting group under Prof VJ Maharaj for their valuable scientific discussions. I am grateful to Dr Frederick Malanfor assistance with single crystal X-ray diffraction data-collection and structure solution. Dr Winile Mavuso for assistance with melting point apparatus use.

Professor Lyndy J McGaw at the Faculty of Veterinary Science at Onderstepoortand her group of students for assistance with bacterial studies. Special thanks to Ibukun Michael Famuyide for assistance with bioautography and MIC studies.

Professor SubbaRao V. Madhunapantulafor guidance in cell culture and cancer cytotoxicity studies performed as part of training at the Cellular and Molecular Biology centre, Department of Biochemistry, JSS Medical College, JSS University, Mysuru, Karnataka, in India. Special thanks to B. G. Vidya, K. G. Mahadeva Swamy and Venugopal R. Bovilla for their expertise and assistance in cell culture and cancer cytotoxicity assay.

My wife Funeka for her understanding, great support and encouragement throughout my PhD research. And my mother Nomakholwa Mzondofor her great parenthood, support and encouragement throughout my studies.

Summary

The aim of this study was to unearth some of the ingredients that pose the bioactive nature of *Cleome gynandra*, isolating such ingredients and proving their biological efficacy, a discovery stage towards commercialisation. This was motivated by literature on indigenous use and scientific literature where the potential health benefits of *Cleome gynandra*, as one of the marginalised plants, have been demonstrated. A further aim was to use physicochemical and biological methods to investigate the feasibility of supercritical CO_2 fluid and spray dryer inclusion complexation of selected isolated biological ingredients with β-cyclodextrin. This was motivated by the notion that such inclusion might result in favourable alterations in the physical properties of these bioactive compounds (e.g. increased aqueous solubility and improved biological accessibility) and hence render them in more suitable form for eventual incorporation into pharmaceutical formulations.

In this thesis, single solvent system extraction, sequential extraction and supercritical fluid extraction were used to prepare several extracts which were initially selectively investigated for their inhibition of selected enzymes (α-glucosidase, α-amylase, renin, HMG-CoA reductase and xanthene oxidase), inhibition of selected bacteria strains (*Staphylococcus aureus* and *Escherichia coli*) and cancer cytotoxicity of lung cancer A549 cell line. The greatest enzyme based activity was seen against α-glucosidase where the ethyl acetate, acetone, *n*-hexane and supercritical fluid (CO_2-ethanol) extracts exhibited activities with 91.76 ± 1.16, 89.97 ± 1.77, 92.67 ± 0.17 and 96.55 ± 0.15 %inhibition, respectively, at 200 µg/mL. In bacterial assays, the ethanol extract exhibited the greatest inhibition activity against *Escherichia coli* with the MIC value 0.052 ± 0.016 mg/mL while in lung cancer cytotoxicity assays the *n*-hexane extract was the most active (>84% inhibition in the concentration range of 0.125 – 1.00 mg/mL, over 48-hour incubation and >75 % over 24-hour incubation).

The solvent-solvent partition product of the ethyl acetate extract, pEtOAc fraction, displayed IC50 value 8.75 µg/mL, better than the 25.40 µg/mL of the crude extract and 37.10 µg/mL of

the positive control. This fraction was further fractionated using column chromatography *via* a bioassay-guided fractionation approach resulting in seven semi-pure fractions displaying activities in the range 82.0 – 98.4 %inhibition at 25 µg/mL. Chemical profiling using UPLC-QTOF-MS led to several unidentified high molecular mass compounds and a novel compound cleogynone A.

Fractionation of the ethanol extract was followed by bioautographic antibacterial analysis of 22 fractions against both *Escherichia coli* and *Staphylococcus aureus* where the brightest spot of largest diameter indicative of the greatest activity was located against *Escherichia coli* and the most active fraction was further fractionated *via* semi-preparative HPLC yielding eight semi-pure sub-fractions with MIC values in the range 0.012 – 0.094 mg/mL comparable to gentamicin the positive control. Chemical profiling of the active fraction and sub-fractions using UPLC-QTOF-MS and MassLynx data processing led to the tentative identification of rutin, kaempferol-3-glucoside-3''-rhamnoside and isorhamnetin 3-O-robinoside as possible biomarkers, while processing using the Waters® UNIFI® Scientific Information System led to the identification of rutin (quercetin-3-O-rutinoside) and nictoflorin (kaempferol 3-O-rutinoside) as the major compounds and kaempferol, quercetin and nepitrin were represented by minor peaks. Purchased standards for nictoflorin and rutin displayed no inhibition of *Escherichia coli*.

Bioassay-guided fractionation of the *n*-hexane extract initially using column chromatography for lung cancer cytotoxicity led to several active fractions. Three semi-pure and most abundant, reasonably active fractions of mid-polarity were further fractionated using a combination of flash column chromatography and preparative thin-layer chromatography to yield two novel compounds, cleogynone A and cleogynone B whose molecular ions were identified using UPLC-QTOF-MS and chemical structures were elucidated using NMR with their crystal structures subsequently determined by single crystal X-ray diffraction. A known compound, named here, cleogynone C was confirmed by comparison of the NMR data to those in literature. Further characterisation of the pure compounds involve melting point analysis, IR, and optical rotation analysis. These three compounds were evaluated for their

invitro anticancer activity against lung cancer (A549), breast cancer (MDA-MB-468) and colorectal cancer (HCT116 and HCT15) in the concentration range 0.39 – 25.0 µg/mL. Against the colorectal cancer (HCT15), cleogynone A, B and C showed the highest activities 82.97±0.56, 81.74±0.34 and 83.67±3.16 % inhibition, respectively, at 25 µg/mL concentration over 48 hr treatment. Cleogynones B and C showed the greatest activity of 89.34±5.46 and 87.76±1.22 % inhibition activity, respectively, against HCT116 over 24 hr treatment at the highest test concentration (25 µg/mL). The compounds displayed moderate activity with the highest activity 66.58±1.30 %inhibition displayed by cleogynone C against breast cancer (MDA-MB-468) while all three compounds displayed poor activity against lung cancer (A549) ≤ 51.38±0.39 at the highest concentration (25 µg/mL).

Several β-CD *n*-hexane formulations were prepared *via* supercritical CO_2 technique at varying temperature, pressure and exposure time to study the effect of varying such operating parameters on the feasibility of the formulation, while one β-CD-*n*-hexane complex formulation was obtained *via* the spray-drying technique for comparison. The solubility assessments were achieved by area integrating the peaks of chromatographic profiles generated using UPLC-QTOF-MS. Formulation was successful in improving the aqueous solubility for most of the supercritical CO_2 formulations as well as the spray-dried formulation. High pressure formulation conditions enhance the formulation but negatively impacts the aqueous solubility. While formulations *via* the supercritical CO_2 technique did not show improvement of anticancer activity the spray drying technique resulted in the greatest anticancer activity improvement. The aqueous solubility of the novel compounds cleogynone A and cleogynone B was not improved in the presence of β-CD in water, no improvement of anticancer activity against the lung-, breast- and colorectal cancer cell lines.

This is the first comprehensive systematic study on the isolation, purification, identification and structure elucidation of known and novel bioactive ingredients from *Cleome gynandra* and physicochemical study of the interaction between ingredients of leaf extract of *Cleome gynandra* with β-cyclodextrin, and isolated ingredients and the results reported here should

be of significant interest in the further development and application of these bioactive components.

Table of Contents

List of Figures

Chapter 2

Chapter 3

Chapter 4

Chapter 5

List of Tables

Chapter 2

Chapter 3

Chapter 4

Chapter 5

List of abbreviations

5-FU	5-fluorouracil
Abl	Abelson proto-oncogene
ACE	Angiotensin-converting enzyme
AIDS	Acquired Immunodeficiency Syndromes
ARC	Agricultural Research Council
ARC-VOP	Agricultural Research Council – Vegetable and Ornamental Plants
AT1 receptors	Angiotensin II subtype 1 receptors
BCL2	B-cell lymphoma 2
BCR	Breakpoint cluster region gene
C. gynandra	*Cleome gynandra*
CD	Cyclodextrin
CDCl3	Deuterated Chloroform
CEF	Cchloroform : ethylacetate : formic acid
CFU	Colony forming units
COSY	^{1}H-^{1}H Correlation Spectroscopy
CSIR	Council for Scientific and Industrial Research
DADS	Diallyl disulphide
DCM	Dichloromethane
DEPT	Distortionless Enhancement by Polarization Transfer
DMEM	Dulbecco's Modified Eagle Medium
DMEM	Dulbecco's Modified Eagle Medium
DMMA	Dimethoxymethylamphetamine
DMSO	Dimethyl sulfoxide
DNS	3, 5-dinitrosalicylic acid
DPP-4	Dopamine agonist, dipeptidyl peptidase-4
E. coli	*Escherichia coli*
EGFR	Epidermal growth factor receptor
EGFR	Endothelial growth factor
EMR	Endoscopic mucosal resection
EMW	Ethyl acetate : methanol : water
EPMR	Endoscopic piecemeal mucosal resection
ERBB2	Human epidermal growth factor 2
ESI	Electrospray Ionization
EtOAc	Ethyl acetate
EtOH	Ethanol
FBS	Fetal bovine serum
FDA	Food and Drug Administration
FRET	Fluorescence resonance energy transfer
FTIR	Fourier Transform Infra-red
GC	Gas Chromatography
Gras	"generally regarded as safe"
HCV	Hepatitis C virus
HER2/neu	Human epidermal growth factor receptor 2
HIV	Human Immunodeficiency Virus

HMBC	Heteronuclear Multiple Bond Correlation
HMG-CoA	β-Hydroxy β-methylglutaryl-Coenzyme A
HPLC	High-Performance Liquid Chromatography
HPLC-UV-vis	High-performance liquid chromatography ultraviolet/visible
HRESIMS	High resolution electrospray ionization mass spectrometry
IC_{50}	Half-maximal inhibitory concentration
INT	*p*-iodonitrotetrazolium violet
IR	Infra-red
LC	Liquid Chromatography
LDL	Low density lipoprotein
LP-1	Glucagon-like peptide-1
m/z	Mass to charge ratio
MeOH	Methanol
MHA	Mueller Hinton ager
MIC	Minimum inhibitory concentration
MS	Mass Spectrometry
Mult.	Multiplicity
NADPH	Nicotinamide adenine dinucleotide phosphate
NMR	Nuclear Magnetic Resonance
NOESY	Nuclear Overhauser Effect Spectroscopy
NSCLC	Non-small cell lung cancer
PC	Positive control
PKCα	Protein kinase C alpha
p-NPG	*p*-nitro-phenyl-α-D-glucopyranoside
PPHG	Postprandial hyperglycaemia
ppm	Parts per million
QTOF	Quadrupole time-of-flight
RAS	Renin–angiotensin system
S. aureus	*Staphylococcus aureus*
SC-CO_2	Supercritical carbon dioxide
SCXRD	Single Crystal X-ray Diffraction
SGLT	Sodium-glucose transporter
SRB	Sulforhodamine B
TB	Tuberculosis
TCA	Trichloroacetic acid
TCA	Trichloroacetic acid
TFA	Trifluoroacetic acid
TLC	Thin-Layer Chromatography
Tot.	Total
Uniq.	Unique
UPLC-QTOF-MS	Ultra-performance liquid chromatography quadrupole time of flight mass spectrometer
UV	Ultra violet
VC	Vehicle control
WHO	World Health Organization

Chapter 1:

Introduction

1.1. Background

In search for biological species from which products such as pharmaceuticals and other commercially valuable ingredients can be obtained. Indigenous knowledge plays a vital role in narrowing the search pool, a bioprospecting approach. Given the great wealth of such knowledge with regards to plant use, scientific verification of the claims is necessary to bridge the gap towards product development. Plants have been used in traditional systems in varying manner to benefit communities in their food, medicines and holistic healing needs. There is a great wealth of herbs and edible plants claimed to possess medicinal properties that have not been absolutely screened and commercially exploited, *Cleome gynandra (C. gynandra)* is one such plant. It is used as a source of food and as a medicinal plant by some rural communities around the world [1]. *C. gynandra* has benefited traditional systems worldwide for the treatment of various diseases and is renowned for its nutritional and antioxidant properties [1,2]. The health promoting properties of *C. gynandra* highlight an opportunity for studies towards developing its health products - which are usually obtained in the form of extracts. Plant constituents are generally known to possess poor physicochemical properties, such as low aqueous solubility [3]. While in order to be readily delivered to the cellular membrane the bioactive components must have a certain minimum level of aqueous solubility, most plant constituents are lacking in this regard. In fact, many promising active pharmaceutical ingredients fall out in the development stages due to insufficient solubility [4,5]. Cyclodextrins (CDs) offer a solution, as they are able to incorporate a variety of molecules in their hydrophobic cavity resulting in a complex that is more water soluble than the uncomplexed molecule [6].

In search for bioactive ingredients for protection against- and treatment of diseases, the natural products approach has demonstrated solid capability throughout history.

1.2. The role of natural products in combating diseases

Historically, mankind has had varying ways of using natural products, such as marine organisms, microorganisms, animals and plants, in medicines to fight against sicknesses. Western medicine was introduced in countries such as China in the sixteenth century and underwent no development until the nineteenth century. In the nineteenth century it was a German pharmacist who isolated morphine, a pharmacologically active compound [7]. Countless bioactive compounds thereafter been isolated from natural products. The natural products approach of drug discovery has largely benefited some medicines such as antihypertensive, anticancer and antimigraine medication [7]. Natural products have been vital in the development of antibacterial drugs such as macrolides, β-lactams, lincosamides, lipopeptides, streptogramins, cephalosporines, glycopeptides, tetracyclines, chloramphenicol, rifamycins, and aminoglycosides. Only the sulfonamide, nitroimidazole, quinolone, trimethoprim and oxazolidinone are synthetically derived [8]. In view of the antifungal drugs, polyenes and griseofulvin are natural products and echinocandins are semi-synthetic derivatives from natural products. There are numerous natural products active against various diseases such as Fumagillin as antiparasitic, viramidine against HCV, betulinic acid against HIV replication, ω-Conotoxin for the treatment of neuropathic pain, huperzine for the treatment of Alzheimer's disease, and many more [8].

The development of synthetic techniques has resulted in a decrease in the role of natural products in drug discovery, the greatest decline seen over the last 3 decades, yet the importance of natural products has been widely demonstrated [7,9]. Cooper stated that, despite recent advances that result in rapid generation of new compounds, the pharmaceutical industry still heavily relies on undiscovered possibilities from nature [10].

While about 40% of prescription drugs are natural-based-products, 49% of new chemical products registered by the U.S. Food and Drug Administration (FDA) are natural products or derivatives thereof [11,12]. Furthermore, with advances in separation techniques for natural products and spectroscopic approaches for structure elucidation, the screening of natural product mixtures can now be achieved in time-frame comparable to high-throughput screening campaign [13,14].

Natural products have certain physical and chemical properties that render them amenable to actively engage biological targets. They generally have increased numbers of sp^3-hybridised carbons and chiral centre, they have larger macrocyclic aliphatic rings, fewer aromatic rings, increased oxygen content and lower nitrogen content. As thus, they are more complex three-dimensional structures and therefore effectively engage relative biologically relevant receptors or targets, in contrast with the more planer and less steriochemically complex synthetic compounds libraries [15]. Of the natural products that eventually get marketed, a huge majority originate from plants. Nearly 80% of the world's population still relies on herbal drugs for their health care [16].

1.3. Indigenous plants as source of biologically active ingredients

Plants are ubiquitous and relatively easily accessible, hence their predilection. The route of using nature's providence is usually guided by indigenous knowledge, and such knowledge had been passed down from generation to generation. Indigenous plants are those that are found in a particular locale that have existed for a long time. For centuries indigenous medicinal plants have been used worldwide for the treatment of various maladies including cancer, diabetes and tuberculosis and other mild complaints such as arthritis, stomach issues, common colds, menstrual problems and many more [2,17–21]. Communities have over centuries developed indigenous knowledge on the use of plants to benefit themselves in varying manner.

According to the World Health Organization (WHO) [22], about 20 000 medicinal plants are in existence in 91 countries, 12 mega biodiversity countries included. South Africa alone possesses about 9% of all known plant species on earth. Taking all of this into account it is evident that blindly searching for medicinal plants with a particular biological possession would be highly implausible. And thus taking on the footsteps on indigenous knowledge holders has been deemed as a provident narrowing strategy. There is great wealth of knowledge with regards to indigenous plant use in South Africa alone that poses to be commercially valuable. Combining such knowledge with science has the potential to bring forth some plants that have been marginalised due to the production and consumption of cash crops.

The collaboration of companies such as Smith-Kline Beecham with organic chemists from the CSIR and botanists from the National Botanical Institute (National Herbarium) in Pretoria implemented the bioprospecting approach. While a project on edible plants which constituted the first work on Hoodia was initiated at the time at the CSIR [23,24]. A bioprospecting project initiated in 1993 at the CSIR resulted in a number of scientific discoveries such as the isolation of monatin (a sweetener) from *Sclerocjiton illicifilius*, and the discovery of P57 (an appetite suppressant), from *H. gordonii*[24].

Examples of medicinal plants that have eventually landed on the market include honeybush (*Cyclopia intermedia, C. genistoides*) and rooibos (*Aspalathus linearis*) amongst others [19,24]. The research followed the traditional use by the Khoi-people, and its herbal benefits. Aloes *(Aloe), Hypoxis, Bowiea, Siphonochilus*, and *Scilla*, and essential oil plants buchu (*Agathosma betulina* and *Agathosma crenulata*) are other medicinal plants. Companies such as Phyto Nova Ltd were also responsible for producing new crops and new herbal health care products, such as those developed from *S. frutescens*, *S. Aesthiopicus* and *W. Salutaris*, *M. Tortuosum*[19,24,25].

It is estimated that greater than 70 % of the population in South Africa use traditional remedies while a large part of the day-to-day medicine is still derived from plants [19]. large volumes of plants or the extracts thereof are sold in the informal and commercial sectors of the economy. Traditional Healers play a huge role and the conversion of the indigenous knowledge is being taken into account. The Agricultural Research Council (ARC) does a collection of genebank maintenance and the determination of propagation methods of establishment [2,26].

C. gynandra has been deemed worthy of this study towards developing edible plant products with health benefits. Cited for immunomodulatory, antioxidant, anti-carcinogenic, analgesic, anti-inflammatory properties and lysosomal stability actions amongst others, *C. gynandra* grows abundantly in South African provinces such as Limpopo, North-West, Mpumalanga and Gauteng and is distributed across tropical and subtropical regions of the world such as Asia and the Middle East [27–31].

1.4. Developing potentially commercial products from *C. gynandra*

Developing health beneficiating food extracts is the notion of positive prevention and treatment of diseases *via* a safe approach. The medicinal properties of *C. gynandra* highlight an opportunity for studies towards its nutraceutical and/or pharmaceutical development. The ultimate products should be produced *via* green technologies and have proven biological efficacy and safety. Some potential health and nutritional benefits of *C. gynandra* have been documented, however, there is a need to also realise the economic potential of this plant by developing products that can be commercialised. Ingredients from leaf extracts of *C. gynandra* qualify for development as bio-accessible medicinal ingredients with proven health benefits. Natural health products have gained popularity to the point of becoming complementary alternative therapies [13,32,33]. Preparation of plant derived medicines involve the use of the whole plant or parts such as the roots, flowers, stems, fruits, leaves or

seeds [32] while the processing steps may involve cleaning and inspection, oven drying, grinding, and extraction and fractionation [34]. A modern approach to drug discovery from plants critically comprises identification and purification of the biologically active constituents, whereby the available constituents of the plant with inherent biological activity and even their concentrations are determined. The common sensitive techniques for the separation and isolation procedures are Liquid chromatography (LC), High-Performance Liquid Chromatography (HPLC) and Thin-Layer Chromatography (TLC), whilst Ultra-violet (UV), Infra-red (IR), Mass Spectrometry (MS) and Nuclear Magnetic Resonance (NMR) as well as X-ray diffraction are the spectroscopic techniques are used for structural elucidation. It is important to standardise medicinal plant preparations in order to be assured of the consistency of the chemical profile the biological potency [35]. Quality control for batch to batch reproducibility is vital and can be achieved by chemical fingerprinting using Ultra-Performance Liquid Chromatography Quadrupole time of flight Mass Spectrometry (UPLC-QTOF-MS). When used for commercial purposes natural medicinal products must meet the requirements that are no less than scientific evidence of safety and efficacy and must be obtained following good manufacturing procedures for safety and quality to be assured.[9,36]. *C. gynandra* has been traditionally used as a leafy vegetable and therefore safety concerns are negligible. Towards ascertaining bioavailability of the final product, techniques for improvement of physicochemical properties are in place, such as modification of ingredients *via* soft non-covalent methods of molecule modification that maintain the chemical integrity while improving its bio-accessibility improving the chances of the final product eventually developed as a commercial product with proven efficacy.

1.5. Problem statement

With increasing incidences of chronic diseases worldwide there is a growing need not only for new drugs but for preventative approaches. The role of natural products in drug discovery has been demonstrated, and thus taking this route is justified. To this day there are large numbers of marginalised plants with medicinal implications. Backing evidence exists in the literature where the potential health benefits of *C. gynandra,* one of the marginalised plants, have been demonstrated. It is necessary to unearth the ingredients that pose its bioactive nature. Isolating such ingredients and proving their biological efficacy will serve as the first step towards the development of the plant's nutraceutical, pharmaceutical and/or food products. In addition, CDs play an added advantage of improving the poor physicochemical properties of bioactive ingredients expected for the plant ingredients and therefore studies focused on microencapsulating the bioactive ingredients will better the chances of eventually developing medicinal products or food health products of *C. gynandra*. No such study has hitherto been undertaken.

1.6. Aims and objectives

The study aims at developing health products from *C. gynandra* using green technologies and to validate its potential health benefits and functionality. Further, to improve the chances of the expected bioactive ingredients being eventually developed as market ready products by improving their inherent physicochemical properties such as solubility towards eventually improving their bioavailability.

The specific objectives of the study were as follows:

- Prepare laboratory and bench scale plant extracts of natural bioactive molecules using food grade and green technologies. Followed by identification and quality control using chromatographic techniques such as UPLC-QTOF-MS.

- Identification of the best extraction methods for ingredients with a particular bioactivity from *C. gynandra* leaves.
- Bioactivity based fractionation of bioactive crude extracts and isolation of the bioactive compounds using separation techniques such as HPLC, column chromatography and thin layer chromatography.
- Identification of bioactive components and structure elucidation of any resulting novel compounds using NMR, Single Crystal X-ray diffraction, FTIR and other relevant techniques.
- Assessment of the solubility and stability of the bioactive components.
- Attempts at improving the physicochemical properties of isolated bioactive ingredients by preparing their inclusion complexes using selected beta-CD as hosts. Solid-state inclusion complexation of bioactive extracts with CDs using supercritical carbon dioxide (SC-CO_2) technology and studies on the impact of operating parameters on physicochemical properties such as solubility. Complexation techniques such as spray drying for comparative studies with the SC-CO_2 technique.
- Determination of bioactivity and physicochemical properties of the formulations, such as solubility.

Chapter 2 describes the overall crude extraction of *C. gynandra* leaves using organic solvents (*n*-hexane, ethyl acetate, ethanol, water, hydro-alcohol, acetone) as well as supercritical CO_2 extraction technology. Biological assessment of the crude extracts against various biological targets (α-amylase, α-glucosidase, xanthine oxidase, HMGCoA reductase, renin, lung cancer cell line, *staphylococcus aureus*, *Escherichia coli*) and chemical analysis of the extract using UPLC-QTOF-MS.

Chapter 3 describes the fractionation of selected extracts with α-glucosidase inhibition and extracts with bacterial inhibition activity, UPLC-QTOF-MS profiling of such bioactive fractions, and further identification of compounds using UNIFI®.

In Chapter 4 the anticancer components of *C. gynandra* are located *via* bioassay-guided fractionation and some major compounds as constituent ingredients of the active fractions are isolated. Structure solution of known compound(s) and structure elucidation of the novel compounds is described in Chapter 3 and purely isolated compounds are further assessed for their lung cancer, colorectal cancer and breast cancer cytotoxicity.

Chapter 5 describes formulation studies of the anticancer ingredients of the *n*-hexane extract *via* the supercritical CO_2 technology as well as the spray drying technique, and solubility assessment of the formulations.

Chapter 6 is the general conclusion chapter.

References

1. Narendhirakannan, R.T.; Subramanian, S.; Kandaswamy, M. Free radical scavenging activity of *Cleome gynandra L*. leaves on adjuvant induced arthritis in rats. **2005**, 71–80.

2. Jansen Van Rensburg, W.S.; Venter, S.L.; Netshiluvhi, T.R.; Van Den Heever, E.; Vorster, H.J.; De Ronde, J. a. Role of indigenous leafy vegetables in combating hunger and malnutrition. *South African J. Bot.***2004**, *70*, 52–59, doi:10.1016/S0254-6299(15)30268-4.

3. Coimbra, M.; Isacchi, B.; Van Bloois, L.; Torano, J.S.; Ket, A.; Wu, X.; Broere, F.; Metselaar, J.M.; Rijcken, C.J.F.; Storm, G.; et al. Improving solubility and chemical stability of natural compounds for medicinal use by incorporation into liposomes. *Int. J. Pharm.* 2011, *416*, 433–442.

4. Strickley, R.G. Solubilizing Excipients in Oral and Injectable Formulations. *Pharm. Res.***2004**, *21*, 201–230, doi:10.1023/B:PHAM.0000016235.32639.23.

5. Jing, W.; Liu, R.; Du, W.; Luo, Z.; Guo, P.; Zhang, T.; Zeng, A.; Chang, C.; Fu, Q. Pharmacokinetic and Metabolic Characteristics of Herb-Derived Khellactone Derivatives, A Class of Anti-HIV and Anti-Hypertensive: A Review. *Molecules***2016**, *21*, 314, doi:10.3390/molecules21030314.

6. Del Valle, E.M.M. Cyclodextrins and their uses: A review. *Process Biochem.***2004**, *39*, 1033–1046, doi:10.1016/S0032-9592(03)00258-9.

7. Yuan, H.; Ma, Q.; Ye, L.; Piao, G. The traditional medicine and modern medicine from natural products. *Molecules***2016**, *21*, doi:10.3390/molecules21050559.

8. Butler, M.S. Natural products to drugs: Natural product derived compounds in clinical trials. *Nat. Prod. Rep.***2005**, *22*, 162–195, doi:10.1039/b402985m.

9. Cordell, G.A.; Colvard, M.D. Natural products and traditional medicine: Turning on a paradigm. *J. Nat. Prod.***2012**, *75*, 514–525, doi:10.1021/np200803m.

10. Cooper, E.L. Drug Discovery, CAM and Natural Products. *Evidence-Based Complement. Altern. Med.***2004**, *1*, 215–217, doi:10.1093/ecam/neh032.

11. Strobel, G.; Daisy, B. Bioprospecting for Microbial Endophytes and Their Natural Products. *Microbiol. Mol. Biol. Rev.***2003**, *67*, 491–502, doi:10.1128/mmbr.67.4.491-502.2003.

12. Asiimwe, S.; Kamatenesi-Mugisha, M.; Namutebi, A.; Borg-Karlsson, A.K.; Musiimenta, P. Ethnobotanical study of nutri-medicinal plants used for the management of HIV/AIDS opportunistic ailments among the local communities of western Uganda. *J. Ethnopharmacol.***2013**, *150*, 639–648, doi:10.1016/j.jep.2013.09.017.

13. Harvey, A.L. Natural products in drug discovery. *Drug Discov. Today***2008**, *13*, 894–901, doi:10.1016/j.drudis.2008.07.004.

14. Sanchez, S.; Demain, A.L. Secondary metabolites. *Compr. Biotechnol.***2019**, 131–143, doi:10.1016/B978-0-444-64046-8.00012-4.

15. Wright, G.D. Unlocking the potential of natural products in drug discovery. *Microb. Biotechnol.***2019**, *12*, 55–57, doi:10.1111/1751-7915.13351.

16. Tiwari, S. Plants: A Rich Source of Herbal Medicine. *J. Nat. Prod.***2008**, *1*, 27–35.

17. Joshi, A.R.; Joshi, K. Indigenous knowledge and uses of medicinal plants by local communities of the Kali Gandaki Watershed Area, Nepal. *J. Ethnopharmacol.***2000**, *73*, 175–183, doi:10.1016/S0378-8741(00)00301-9.

18. Yirga, G. Assessment of indigenous knowledge of medicinal plants in Central Zone of Tigray, Northern Ethiopia. *African J. Plant Sci.***2010**, *4*, 006–011.

19. Coetzee, C.; Jefthas, E.; Reinten, E. Indigenous Plant Genetic Resources of South Africa. *ASHS Press.***1999**, 160–163.

20. Rankoana, S.A. Sustainable use and management of indigenous plant resources: A case of Mantheding community in Limpopo Province, South Africa. *Sustain.***2016**, *8*, doi:10.3390/su8030221.

21. Reinten, E.Y.; Coetzee, J.H. Commercialization of South African Indigenous Crops: Aspects of Research and Cultivation of Products. *Trends New Crop. New Uses***2002**, 76–80.

22. Egdahl, A. WHO: World Health Organization.

23. Maharaj, V.; Senabe, J.; Horak, R. Hoodia, a case study at CSIR. **2008**, 3–6.

24. Van Wyk, B.E. The potential of South African plants in the development of new medicinal products. *South African J. Bot.***2011**, *77*, 812–829, doi:10.1016/j.sajb.2011.08.011.

25. Lindsey, K.; Motsei, M.; Jäger, A. Screening of South African food plants for antioxidant activity. *J. Food Sci.***2002**, *67*, 2129–2131, doi:10.1111/j.1365-2621.2002.tb09514.x.

26. Kelly, J.P.; Kaufman, D.W.; Kelley, K.; Rosenberg, L.; Anderson, T.E.; Mitchell, A.A. Recent trends in use of herbal and other natural products. *Arch. Intern. Med.***2005**, *165*, 281–286, doi:10.1001/archinte.165.3.281.

27. Bala, A.; Kar, B.; Haldar, P.K.; Mazumder, U.K.; Bera, S. Evaluation of anticancer activity of Cleome gynandra on Ehrlich's Ascites Carcinoma treated mice. *J. Ethnopharmacol.***2010**, *129*, 131–134, doi:10.1016/j.jep.2010.03.010.

28. Mishra, S.S.; Moharana, S.K.; Dash, M.R. Review on cleome gynandra. *Int. J. Res. Pharm. Chem.***2011**, *1*, 681–689.

29. Narendhirakannan, R.T.; Subramanian, S.; Kandaswamy, M. Anti-inflammatory and lysosomal stability actions of *Cleome gynandra L.* studied in adjuvant induced arthritic rats. *Food Chem. Toxicol.***2007**, *45*, 1001–1012, doi:10.1016/j.fct.2006.12.009.

30. Prajapati, R.; Kalariya, M.; Umbarkar, R.; Parmar, S.; Sheth, N. *Colocasia esculenta*: A potent indigenous plant. *Int. J. Nutr. Pharmacol. Neurol. Dis.* 2011, *1*, 90.

31. Mnzava, N.A.; Chigumira Ngwerume, F. *Cleome gynandra L.* Available online: https://www.cabi.org/isc/datasheet/119802 (accessed on Aug 9, 2021).

32. Veeresham, C. Natural products derived from plants as a source of drugs. *J. Adv. Pharm. Technol. Res.***2012**, *3*, 200–201, doi:10.4103/2231-4040.104709.

33. Harvey, A.L. Screening Methods for Drug Discovery from Plants. In *Plant Bioactives and Drug Discovery: Principles, Practice, and Perspectives*; 2012; pp. 489–498 ISBN

9780470582268.

34. Cechinel-Filho, V. *Plant Bioactives and Drug Discovery*; John Wiley & Sons, Incorporated, 2012.

35. Ong, E.S. Extraction methods and chemical standardization of botanicals and herbal preparations. *J. Chromatogr. B Anal. Technol. Biomed. Life Sci.***2004**, *812*, 23–33, doi:10.1016/j.jchromb.2004.07.041.

36. Munhoz, A.C.M.; Frode, T.S. *Isolated Compounds from Natural Products with Potential Antidiabetic Activity - A Systematic Review*; 2018; Vol. 14; ISBN 6661705051.

Chapter 2:

Extraction of *Cleome gynandra* leaves, bioactivity assessment of extracts and chemical analysis using UPLC-QTOF-MS

2.1. Introduction

2.1.1. Background

Nature provides natural products with endless variety of structural composure. Such components have many functions and may possess biological properties that prove them beneficial to humans. Unearthing such molecules may help better human health and in improvement of medicines, proving pivotal in healthcare. Natural products may also be developed as functional foods with health benefits or nutraceutical agents as a preventative medicinal approach. Past research has shown that plants in particular have been invaluable reservoirs of potent biological products [1]. A relatively small percentage of the known plant species have been extensively studied in the pharmacological aspect. Despite the historical decline in natural products research in pharmaceutical industry, recent technological advances have resulted in renewed interest [1,2]. The WHO estimated that 65 percent of the world population relies on plant-derived traditional medicines for their primary health care. Research has shown that 61 percent of the 877 new small-molecule chemical compounds registered as drugs worldwide during the period 1981 – 2002 have a natural products origin [2,3]. The journey to discovering new biologically active agents, having selected the plant species, begins with extraction. The extract is chemically screened and subjected to various biological or pharmacological targets in order to distinguish between new components and known components in the crude extract, and further to providing quality control of the extract. Targeted isolation may then follow for constituents presenting novel spectroscopic

properties. There are numerous techniques related to metabolites identification methods which the principal operation is described.

This chapter focusses on extraction of the leaves of *C. gynandra*, biological assessment against various biological targets and chemical analysis of extract using UPLC-QTOF-MS.

2.1.2. Extraction

Extraction is one of the first steps towards obtaining medicines from plants and food ingredients. This process is characterised by physicochemical wetting, penetration and swelling by solvents contact with plant substrate, followed by separation of substances into soluble and insoluble constituents from surfaces of disrupted cells and dissolution of plan inherent componentsand theirdiffusive transfer to the external environment [4]. The efficiency of the extraction process is dependent on the chemical affinity of the substances for the extractor solvent. The extraction operation can be influenced by factors related to: physical properties of plant material and chemical composition, the process (such as agitation, temperature), and product specifications (nature of solvent) [4]. The choice of method, solvent and ratio of drug to solvent is not only based on efficiency of the process, but also the ease of operation, safety, cost effectiveness, time and energy efficiency. The plant material for extraction may be dry and ground or fresh in cases where the activity is affected by dryness. The choice of solvent(s) and method is crucial for achieving the particular desired outcome. Once the constituents responsible for activity are identified the goal is to obtain them in high yields through the extraction process. Quality control is vital at each stage to ascertain that the stability and structural integrity of the bioactive compounds is maintained, and that the extraction is reproducible.

2.1.2.1. Maceration extraction

This process will generally involve placing the prepared plant material in a vessel and adding a suitable solvent. The container is normally closed to limit solvent evaporation. Water, ethanol and hydro-alcoholic solvent systems are the “generally regarded as safe” (GRAS) solvents of choice in this study, with ethyl acetate and acetone as additional solvents in this respect. The plant material must be fully immersed in the solvent during this type of extraction. The extraction system may be allowed to stand for a specific period of time to allow the solvent to diffuse through the cell wall, sometimes with occasional shaking. When equilibrium is reached, the solution is filtered either using a cloth or filter paper. The insoluble plant material could be subjected to further extraction cycles with fresh solvent multiple times. The maceration in water is normally not prolonged for too long as this can present fungal contamination, which does not occur in alcohol or hydro-alcoholic solutions. The final step will generally involve evaporating the solvent and concentration of the extract. Different drying and concentration techniques may be used, such as vacuum distillation and the use of stream of air.

2.1.2.2. Supercritical fluid extraction technique

The technology of supercritical fluids is exploited due to its solvent strength and physical properties of the immanent compound at temperature and pressure about its critical point [5]. Each compound has its characteristic phase diagram and the location of the critical point will differ from compound to compound. At the critical point the gas and liquid phases merge to form a single homogeneous fluid phase. Beyond the critical point is the supercritical fluid region. The supercritical fluid is highly dense, and possesses low viscosity and diffusive intermediate between gas and liquid. These characteristics make supercritical fluids powerful solvents. The physicochemical affinity of the solute for the solvent and the apparent density

of the solvent determine the solubility of a compound in a supercritical solvent [5]. Supercritical CO_2 technique (SC-CO_2) has been receiving increased attention over the past recent years due to the adjustability of the supercritical fluid properties [6]. SC-CO_2 is the technique of choice due to its safety and the mild temperature and pressure required to achieve the supercritical state. Further, since CO_2 is gaseous at ambient conditions and thus eliminating residual solvent problem it is an ideal substitute for organic solvents. The solid-liquid extraction in supercritical fluid extraction technique involves non-steady transfer of solutes from a solid to a fluid. Researchers label the physicochemical properties of supercritical-CO_2 to facilitate mass transfer. According to Dìaz-Reinoso et al.[7] plant materials havevarious solutes extractable at different ratesdependant on their location (outer surface, pores, vacuoles, etc.) and partition coefficients, and that SC-CO_2 extraction involves: transport of CO_2 from the bulk solution to the external surface of the particle, CO_2 penetration and diffusion in the solid matrix, solubilisation of the components, transport of the solutes through the solid matrix, and transport of the solutes from the external surface of the solid to the bulk solution. Garlic is used as a food ingredient and as a nutraceutical and has many medicinal implications including treatment of cardiovascular disease and cancer to name a few. A study involved the used SC-CO_2 to obtain garlic extract in order to compare with the conventional extracts in terms of yield and quality [8]. Temperature and pressure conditions could be optimised to obtain the best possible yield. Comparison study of the extraction of essential oil from dried star anise fruits (*Illicium verum H*) on the yield and the time of extraction, revealed that extraction with SC-CO_2 yielded 9.8% more essential oil than the conventional steam distillation method [9]. The effects of pressure and temperature on the solubility of flaxseed oil using this technique of SC-CO_2 was investigated, a maximum solubility of 11.3 mg oil/g CO_2, was obtained at 70°C/55 MPa, however, the yield obtained after 3 h of extraction at this condition was only 66% of the total available oil of the flaxseed. Determination of the lipid composition and free fatty acids and tocol (tocopherol and tocotrienol) contents of the oils obtained by both SC-CO_2 and petroleum ether extraction revealed that the α-linolenic acid content of the SC-CO_2-extracted oil was higher than that

obtained by solvent extraction. Furthermore, using an entrainer with CO_2 in supercritical fluid extraction provides another dimension in the extraction and therefore may enhance solvation strength. Machmudah et al.[10] conducted a study to extract astaxanthin from *Haematococcus pluvialis* using the supercritical fluid extraction technique,higher CO_2 flow rate increased the amount of the total extract while the amount of astaxanthin content in the extract almost did not change. When ethanol was used as a co-solvent, higher amount of astaxanthin was extracted while working at moderate pressure and temperature at similar conditions.

The mild critical temperature and pressure conditions and the increased solvating power motivated the use of supercritical fluid CO_2 with ethanol as an entrainer, as one of the extraction processes in this study.

2.1.3. Biological assays

The initial screening approach in early stages in drug discovery move beyond observation of the effect in whole organism, but the application of robust conditions in assay development to provide methods that can be run in microplates where interaction between drug and target are detected by sensitive readouts that are generally light-based(absorbance, fluorescence, or chemilominescence) and such approach is the same for natural products as for synthetic compounds[11]. In order to demonstrate reliability, negative and positive controls are included, while optimisation of the reagents concentrations and the time course of the assay is essential to maximise signal to noise ratio. Any assay is susceptible to false positives and it may be necessary, therefore, to have a backup test method or readout equipment to confirm the results [11]. There are many sources of false positives - such as polyphenolic tannins which are generally assumed to precipitate proteins and therefore are a source of false positives during crude extract screening. High throughput screening approach, which

involves rapid screening of very large numbers of test samples, works well when there is a defined biological target such as a receptor or enzyme [11,12]. Fifty percent of currently used drugs are thought to act through G-protein-coupled receptors and there is a considerable number of these receptors whose functions remain uncovered [11,12].

Cell-based assays have become more popular for drug discovery and such are more advantageous than molecular based assays as the activity is detected against a functioning pathways as opposed to assuming a target specific role or mechanism of action. Some biologically active compounds may be unable to penetrate the cell membrane and these will be missed in cell-based assays, this is when chemical modification may be necessary to improve their bioavailability[12]. The simplest cell-based assays are those that measure cell viability or cell proliferation. Kits are commercially available that detect cell multiplication and cell death. Both molecular and cell-based assays were employed to assess the activity of the crude extracts herein. In this study, enzyme based assays involved were α-amylase-, α-glucosidase-, HMG-CoA-, renin-, and xanthine oxidase inhibition assay. Further assays involved were cell based anticancer assays for lung cancer cytotoxicity. Bacterial growth inhibition assays against *Escherichia coli* and *Staphylococcus aureus,* were also employed.

2.1.3.1. The role of α-amylase and its inhibition for management of diabetes

The enzyme α-amylase (α-1, 4-glucan-4-glucanohydrolases) is secreted in the pancreas and salivary glands and is vital in digestion of starch and glycogen. It is found in microorganisms, plants and higher organisms. This enzyme catalyses the initial step in the hydrolysis of starch to a mixture of smaller oligosaccharides consisting of maltose, maltotriose and branched oligosaccharides of α-(1-6) and α-(1-4) oligo-glucans [13,14]. Such oligosaccharides are further degraded to glucose by α-glucosidase and the glucose is then absorbed into the blood stream. Rapid degradation of dietary starch by α-amylase leads to

elevated postprandial hyperglycaemia (PPHG). Hyperglycaemia is a condition resulting in excessive glucose in the bloodstream. Since α-amylase hydrolyses starch to glucose its inhibition is a therapeutic strategy for disorders of carbohydrate uptake such as diabetes and obesity. Inhibition of α-amylase limits postprandial glucose levels by delaying the process of carbohydrate hydrolysis and absorption [15]. Inhibitors of α-amylase are expected to be better suppressors of PPHG, since these inhibitors do not result in an abnormal accumulation of maltose which result in side effects such as abdominal pain, flatulence and diarrhoea [16]. There are several drugs targeted for carbohydrate-hydrolysing enzymes clinically, however, it is necessary to develop a large inhibitor pool as a strategic move against resistance to existing drugs. Literature indicates that a variety of plants possess α-amylase inhibition, with about 800 species displaying antidiabetic properties[14]. Themain plant derived compounds with hyperglycaemic activity fall in the categories alkaloids, glycosides, steroids, terpenoids, hypoglycans, galactomannan gum, peptidoglycans, polysaccharides, glycopeptides, and guanidine[14].

2.1.3.2. The role α-glucosidase and its inhibition for management of diabetes

α-glucosidase is a membrane-bound intestinal enzyme responsible for hydrolysing oligosaccharides, trisaccharides and disaccharides to glucose and other monosaccharides [17].This enzyme, therefore, controls the rate of glucose absorption. Inhibition of α-glucosidase retards the process of breaking down carbohydrate consequently delaying glucose absorption and therefore lowering PPHG. Controlling hyperglycaemia is a vital part in the treatment of diabetes mellitus - a chronic disease that affects the body from sufficiently using the energy from food. This metabolic disorder is characterised by abnormal increase in blood glucose level [18]. There exist three types of diabetes mellitus. Type 1 and type 2 are insulin-dependent and non-insulin-dependent, respectively. The third type is gestational diabetes, and this type is prevalent in pregnant women [15]. The most common type,

accounting for over 90% of diabetes cases in adult population is type 2 diabetes [15]. While there are other proposed methods to counter type 2 diabetes, decreasing PPHG is a prominent therapeutic approach, achieved by impairing the action of carbohydrate hydrolases, such as α-amylases and α-glucosidase in the digestive system [15]. α-glucosidase inhibitors in therapeutic use are acarbose, miglitol and voglibose. Even though these inhibitors effectively control postprandial blood glucose levels, they have been associated with harmful side effects, by that means necessitating the search for new inhibitors [15,19]. Plants possess a variety of classes of compounds, exhibiting different medicinal properties. Researchers have identified and isolated compounds with α-glucosidase inhibition properties. Yin et al. (2014) summarised a collection of over 400 published α-glucosidase inhibitors isolated from different medicinal plants [19]. They alluded that the compounds showed high α-glucosidase inhibition and merited clinical development for treatment of diabetes mellitus.

2.1.3.3. HMG-CoA reductase and its inhibition for management of hypercholesterolemia

Hypercholesterolemia (high cholesterol levels) is associated with increased risk of atherosclerosis, which might result in angina, heart attack, stroke and peripheral vascular disease [20]. High cholesterol level is accountable for one-third of all cases of ischemic heart disease and increased risks of stroke [21]. While the major rate-limiting step invoves the conversion of 3-hydroxy-3-methylglutaryl coenzyme A (HMG-CoA) to malonate and coenzyme A in sterol biosynthesis [22], the enzyme that catalyses this reaction if HMG-CoA reductase, a transmembrane glycoprotein[23]. Inhibitors of the enzyme HMG-CoA reductase act by inducing the expression of low density lipoprotein (LDL) receptors in the liver, in so doing enhancing the catabolism of plasma LDL, lowering the plasma concentration of cholesterol [23,24]. This enzyme is thus the target of widely used drugs called statins which

are used for the therapeutic reduction of high plasma cholesterol levels [20,25]. Statins are associated with several side effects, in view of this the current study explores plant based ingredients as possible inhibitors of HMG-CoA reductase. Traditional medicines have demonstrated capable in the treatment and eradicating cardiovascular problems as well as associated metabolic disorders[26].

2.1.3.4. Renin and its inhibition for management of vascular diseases

Once released into the blood stream the enzyme renin,mainly secreted from the kidney, targets angiotensinogen. Cleavage of angiotensinogen by renin results in angiotensin I which is further converted to angiotensin II by angiotensin converting enzyme (ACE). Angiotensin II, binds to angiotensin II subtype 1 receptors (AT1 receptors). This cascade is called the renin–angiotensin system (RAS).The blood vessels consequently constrict and the blood pressure elevates; further imminent are changes in renal glomerular and tubular function, inflammation and fibrosis in the kidney, as well as hypertrophy, fibrosis and vasoconstriction in the heart [27,28]. Some clinical interventions in the RAS involve ACE inhibitors andrenin inhibitors.

2.1.3.5. Xanthine oxidase and its inhibition for management of hyperuricemia

An elevation of uric acid level in the blood is called hyperuricemia. Gouty arthritis is the result of such high uric acid blood levels and it treatment involves the use of uricosuric drugs to increase the renal excretion of uric acid, thereby lowering the serum urate concentration, a well-established therapeutic approach[29,30]. The evidence of some degree of uric acid overproduction in gouty arthritis patience is the rational approach to therapy involving decreasing uric acid production [29], therefore inhibition of the terminal steps of uric acid

formation is the method of inhibition involved herein. Uric acid in the human arises from the oxidation of both hypoxanthine and xanthine and is catalysed by the enzyme xanthine oxidase (found in the liver, intestinal mucosa, serum and lungs) [29–31].

2.1.3.6. Plant extracts for bacterial inhibition

The bacterial pathogens chosen in this study were *Escherichia coli* (*E. coli*) and *Staphylococcus aureus* (*S. aureus*). Pathogenic *E. coli*is associated with diseases such as thrombocytopenic purpura, haemolytic uremic syndrome and diarrhoea [32]. *S. aureus* is amongst the leading microbes responsible for skin infection such as boils, abscesses, carbuncles and sepsis of wounds, it further produces toxins causing diarrhoea and vomiting [33].*S. aureus* is susceptible to antibiotics [37]

.*Escherichia coli and Staphylococcus aureus and their relevance to this study*

E. coli, a rod-like, Gram-negative bacillus, which may have whip-like flagella to help it navigate the environment, or hair-like pili for attachment to surfaces or other cells [34]. *E. coli* can grow in both oxygen abundant and oxygen deprived conditions, however, its growth is halted in extreme temperature or pH conditions. *E. coli* is found in the gut microbiomes of mammals, and less commonly constituted in the gut microbiomes of birds, reptiles and fish, also in soil, water, plants and food [34,35]. It is an all-rounder, most of its strains exhibiting commensalism, and other of its strains possessing varying pathogenic abilities [35]. *E. coli* may cause intestinal or extra-intestinal diseases in humans and other animal hosts. Some of the diseases that may be caused by *E. coli* include diarrhoea, ulcerative colitis, haemolytic uremic syndrome and thrombocytopenic purpura [32,36].

Current antibiotics are losing efficacy due to inclining resistant strains causing diseases [38]. And as the worldwide trend is towards minimising the use of antibiotics in food animals. It is not surprising that scientists are looking for alternative ways to combat infectious microbes. A number of plants have been claimed to have medicinal benefits against infectious

diseases which affect both humans and animals. As a result, efforts have been made to carry out research into traditional medicines, presenting ideal alternatives to the currently used antimicrobial agents.

2.1.3.7. Lung cancer

Cancer takes second place in the leading causes of death worldwide[39,40]. Cancer cases are mainly reported in developing countries, and South Africa has shown an increase in lung cancer cases linked to diseases such as tuberculosis (TB) and acquired immunodeficiency syndromes (AIDS) [41]. Tobacco smoking is one of the major causes of lung cancers, 80%–90% of cases arise in cigarette smokers, and a 20- to 30 fold increased risk of developing lung cancer is reported for a lifetime smoker compared to a lifetime non-smoker[42]. There are several systems of therapy directed at certain targets that have recently been introduced in clinical trial for the treatment of lung cancer as well as other types of cancers [42,43]. Such therapeutic strategies include inhibitors of Ras activation and function (such as farnesyltransferase inhibitors),epidermal growth factor receptor (EGFR) inhibitors, HER2/neu receptor inhibitors and other tyrosine kinase inhibitors, matrix metalloproteinase inhibitors, vaccines against tumour mutated or specifically expressed peptides, and gene replacement therapy to name a few. Available chemotherapy has limited beneficial effects, whilethe rationally targeted approach has been stimulated by clinical success of BCR/Abl and c-kit inhibitors in chronic myelogenous leukaemia and gastrointestinal stromal tumours [42]. Lung cancer cytotoxicity assay has been chosen herein for preliminary screening.

2.1.4. UPLC-QTOF-MS for chemical analysis of crude extracts

Ultra-performance liquid chromatography/ quadrupole time-of-flight mass spectroscopy (UPLC-QTOF-MS) has, in recent years, seen great recognition as a highly efficient technique for profiling in metabolism studies. The chromatographic profile of an extract presents some common chemical constituents with biological activity that will ultimately represent a chromatographic fingerprint of a herbal medicine[44]. Chromatographic fingerprints, aid in the accurate identification and authentication of herbal medicines even if the concentration of characteristic marker constituents may slightly differ for different samples [44]. It isvital, therefore,to acquire reliable chromatographic fingerprints as representative chemically characteristic component of the complex mixture. Marker compounds that verify the identity and potency of the extract can be identified through chemical fingerprinting of active extracts. Further, the markers are important in confirming the correct botanical identity of the starting material.

2.1.4.1. High performance- and ultra-performance liquid chromatography

Because of many factors including: high accuracy and precision, its versatility, ease of use, compound specificity, ease of sample preparation, rapid analysis time and high sensitivity, high-performance liquid chromatography (HPLC) is considered as the separation technique of choice in various applications [45]. In this technique solvent is forced through a tightly packed column by pumps in high pressure, the column itself connects to a variety of sensitive detectors[46]. Instead of the polar phases as it is the case with thin-layer chromatography and column chromatography (which is discussed in chapter 3), highly nonpolar phases, called ‘reverse-phase’ packing are used. Such phase is achieved by bonding multiple hydrocarbons to the silica gel particles surfaces in order to attain a nonpolar surface. The elution order will be an opposite of the behaviour on alumina or silica

column. The polar compounds elute first on this type of column as the more nonpolar components adhere longer to the stationary phase.

Smaller particles are used to shorten the diffusion path of the analyte in packed column LC, this approach improves separation efficiencies. The simplified van Deemter equation signifies this. It describes the relation between efficiency (*H*), the linear velocity (*v*) and the particle size,

$$H = 2\lambda dp + \frac{2\gamma Dm}{v} + f(k)\frac{d_p^2}{Dm}v = A + {}^{B}/_{v} + C \quad (1)$$

where *λ* is a packing constant, *γ* an obstruction factor for diffusion in a packed bed, *D*m is the diffusion coefficient in the mobile phase and *f*(*k*)the function of the retention factor (*k*) [45–47]. A van Deemter curve aids in the investigation of chromatographic performance [45,46]. A, B and C are constants,the term A is independent of velocity and smallest when the packed column particles are small and uniform. B represents axial diffusion or the natural diffusion tendency of molecules and diminished at high flow rates and so this term is divided by v. The term C is due to kinetic resistance to equilibrium in the separation process. The kinetic resistance is the time lag involved in moving from the gas phase to the packing stationary phase and back again. The greater the flow of gas, the more a molecule on the packing tends to lag behind molecules in the mobile phase. Thus this term is proportional to v.

The principles of ultra-performance liquid chromatography (UPLC) are similar to those of HPLC, the basic distinction is in the design of the column material particle size, less than 2 µm,this, greatly enhancing the performance resulting in maximised advantages in the column use, crafting a powerful, robustand reliable solution [45,47]. The recent introduction of UPLC instrumentation of columns packed with 1.7 µm particles able to withstand liquid flow at pressures up to 1034 barof its capabilitiesextends the limits of what has been thus far achievable on commercial HPLC instrumentation [47].

2.1.4.2. Mass Spectrometry and the quadrupole time of flight capability

The technique of mass spectrometry (MS) utilises the degree of deflections of charged particles by a magnetic field to find the relative masses of molecular ions and fragments. This method provides a great deal of information that assist in determining molecular mass, assist in structure elucidation, and in verifying the identity of known substances in extracts [47].

The sample is normally vaporised and bombarded by a beam of electrons of high-energy (usually at 70 eV) in order to produce gas phase ions of the compound [48]. The molecular ion is weaker than the original molecule and will undergo further fragmentation to result in either a radical and an ion, or a molecule and a new radical cation. Each ion can, in turn, undergo fragmentation, and so on. The ions are then separated according to their mass-to-charge ratio (*m/z*) and are detected in proportion to their abundance. A mass spectrum of the molecule is ultimately produced and is a plot of ion abundance versus mass-to-charge ratio [48].

Different mass analysers are in existence; including triple quadrupoles and ion traps. Ion trap provides well-established metabolite experiments such as neutral loss and product ion scanning,triple quadrupole on the other hand allows MSn for metabolite structural elucidation. These analysers both provide nominal mass accuracy and may not be well poised in untargeted metabolite profiling experiments such as herbal metabolomics [49]. Orthogonal acceleration time-of-flight mass spectrometry (TOFMS), in turn, allows the generation of mass information with greater accuracy and precision [49]. Candidate empirical formulae at the 3–5 ppm error range, can be deduced from such accurate mass thus significantly reducing the number of possible structures of putative metabolites with molecular masses of a few hundred Dalton (Da).

2.2. *Cleome gynandra*

2.2.1. Plant description, distribution and habitat

Cleome gynandra (*bangala*, *lerotho*, spider flower, spider plant, African cabbage, cat's whiskers, *oorpeultjie*, *snotterbelletjie*) belongs to the *Capparaceae* family and is reported to have originated in tropical Africa or South-east Asia [50,51]. It was distributed to other tropical and subtropical countries in the Northern and Southern hemisphere [50]. *C. gynandra* is frost tender, erect, annual herb which can grow up to 0.6 m - 0.9 m high; it is a leaf at one stage and a flower at another [50,52]. *C. gynandra* has taproot with secondary roots and root hairs. The stem is granular, mostly with hair and longitudinal parallel lines [52,53]. Pigmentation varies from green to pink and violet to purple. The plant has branches which may become woody at a later stage of the plant's life. The plant has compound and lobed leaves with 3 – 5 leaflets. Its flowers are white or purple in a long terminal cluster with the separate flowers attached by short, equal stalks at equal distances along a central stem up to 30 cm [52,53]. seeds are brown, circular in outline measuring 1.5 mm in a diameter, with obscurely netted surface [53,54].

Figure 2.1: *Image of Cleome gynandra* [53].

2.2.2. Traditional uses

C. gynandra is used predominantly as a leafy vegetable. Its tender leaves or young shoots and often the flowers are boiled in a stew or as a side dish [54] while dried leaves are ground and incorporated in weaning foods. In some countries, only this leafy vegetable is available during the relish-gap period, thereby playing a significant role in household food security during drought [50,51]. In traditional systems worldwide it is used to treat many diseases and is also used in various traditional culinary systems for its nutritional and antioxidant properties [52,55]. In India it is used by traditional healers for the treatment of various diseases including epilepsy, irritable bowel syndrome and in protozoal and worm infections [52]. In western Uganda extracts of the plant is also used to induce labour during childbirth [56]. The plant is high in protein and amino acids, and its minerals content deems it highly economically important as it can be grown and cultivated easily [52,57].

2.2.3. Scientific studies on nutritional constituents and the biological properties of *C. gynandra* extracts

C. gynandra has been cited to have immunomodulatory, antioxidant, anti-carcinogenic, analgesic, anti-inflammatory properties and lysosomal stability actions [52]. Work is reported proving the anticancer activity of the methanol extract of *C. gynandra* in Swiss albino mice against ehrlich ascites carcinoma [58], demonstration of the anti-inflammatory activity of the ethanolic extract of *C. gynandra* leaves and the capacity to stabilise lysosomal enzyme activities in the plasma and liver of control and experimental rats [59]. *C. gynandra* has been used traditionally to treat microbial diseases [60]. Different researchers have conducted studies to assess the capabilities of *C. gynandra* extracts as antimicrobial agents. The methanol extracts of *C. gynandra* against different fungi and bacterial strains including *E. coli and S. aureus*,using disc diffusion assay proved to possess high antibacterial and antifungal activity [61]. Ethanol and ethyl acetate extracts from leaves of *C. gynandra* amongst other plant species from the same family, against several bacterial pathogens including *E. coli* and *S. aureus* showed positive reactions on all tested organisms [62]. Ranjitha et al. conducted a phytochemical investigation of *n*-hexane extract of *C. gynandra* leaves [63] In the study 4 compounds were identified (α-amyrin acetate, α-amyrin, sitosterol, stigmasetrol) using GC-MS technique. The compounds were isolated and tested in different antimicrobial assays exhibiting moderate activity against *S. aureus* and *C. albicans*, but low activity against *E. coli* and *C. glabrata*. Studies involving methanol, chloroform, aqueous, petroleum ether and *n*-hexane extract of *C. gynandra* against some bacteria and fungi isolated from patients with infectious diarrhoea had been conducted [64]. The *in vitro* screening was carried out using Enterotoxigenic *E. coli*, *Salmonella typhimurium, Salmonella entertidis, Shigella dysentriae, Shigella flexineri, Candida albicans, Candida tropicalis and Candida krusei*. The methanol extract showed good activity compared to aqueous and chloroform extract while petroleum ether and *n*-hexane extract showed no activity. In addition, the methanol extracts

phytochemical analysis showed the presence of carbohydrates, alkaloids, flavonoids, amino acids, steroids, sterols and saponins.

Literature indicates that there is a significant interest on the antimicrobial activity of *C. gynandra*. And it is quite evident, studying different research outputs, that *C. gynandra* proves to possess *E. coli* and *S. aureus* inhibitory properties. Furthermore, the polar extracts of *C. gynandra* leaves prove more potent, in this regard. While the classes of compounds *via* preliminary phytochemical identifications by different research groups are revealed. It still remains unclear which compounds are responsible for the antimicrobial activity, particularly *E. coli and S. aureus* inhibitory activity, microbes chosen in this study. Furthermore, while Ranjitha et al. isolated 4 compounds from *n*-haxane extract of *C. gynandra* leaves these showed poor *E. coli* inhibitory activity [63]. Reports by other researchers indicate that the polar compounds may be responsible for the potency against *E. coli* [61,62,64]. There is a need to identify the compounds responsible for the microbial inhibitory properties of *C. gynandra*. Identifying natural compounds responsible for *E. coli* growth inhibition will add great value since it has a broad spectrum of lifestyles and phenotypes, and thus is a well-suited model organism to study bacterial evolution and adaptation to different growth conditions and niches [35]. And also to note, as alluded earlier, *E. coli* is responsible for a number of infectious diseases such as diarrhoea and thrombosis notwithstanding the world trends towards lessening the antibiotic use on animal food products, natural alternatives are necessary. This study realises the opportunity to identify and isolate the ingredients responsible for the inhibition of microbes such as *E. coli* and *S. aureus*.*C. gynandra* has numerous biologically active phytochemicals such as triterpenes, tannins, anthroquinones, flavonoids, saponins, steroids, resins, lectins, glycosides, sugars, phenolic compounds, and alkaloids in its methanolic extract, the compounds are thought to be responsible for the anti-arthritic properties [59]. Furthermore, a study showed the total extractable phenolic content to be 3.94 ± 0.09 mg garlic acid equivalent per gram of dry weight while the total flavonoid concentration as 2.19 ± 0.11 mg catechin equivalents per gram of dry weight. Total iridoid

content was 9.14 ± 0.20 mg harpagoside equivalents per gram of dry weight [65]. Studies on its nutritional content reveal that *C. gynandra* is high in beta-carotene and vitamin B_2 as well as in selected minerals such as iron, zinc, magnesium, calcium and phosphorus [66]. And further the nutrient content per edible portion of leaves of *C. gynandra* which includes protein, riboflavin, vitamin A and C, dietary fibre was studied [67]. The antioxidant enzymes of *C. gynandra* are able to cope with the formation of reactive oxygen species under drought stress [68] and flavonoids mediate antioxidant activity of *C. gynandra* in some chronic inflammatory cells *via* its free radical scavenging activity, it is proposed that the high content of phenolic compounds is responsible for the antioxidant property [69]. Such reported findings reveal that indigenous vegetables such as *C. gynandra* have higher levels of phytochemicals and also exhibit more potent antioxidant activity compared to the commercial varieties. A further study showed that planting of *C. gynandra* in beds of cut-flower roses significantly reduces red spider mite (Tetranych usurticae Koch) infestation without any negative effect on productivity or flower quality [55].

These findings not only reveal the high medicinal properties of *C. gynandra* but also prove that it is amongst the most nutritious leafy vegetables.

Regardless of the elaborate evidence that *C. gynandra* possesses medicinal components, very little has been reported towards isolation and identification of the ingredients responsible for the inherent biological activities. Dammerane triterpenoids from *C. gynandra* were previously isolated without any biological studies [70]. To the best of our knowledge there are no reported studies involving the isolation and naming of compounds from *C. gynandra* leavesresponsible for bioactivity, leaving the gap for this study. In this chapter we report bioactivity of several extracts from the leaves of *C. gynandra* that may lead to the identification and isolation of bioactive compounds and its further development of potentially commercial products.

2.3. Materials and methods

2.3.1. Plant harvesting and preparation

C. gynandra was harvested from the Agricultural Research Council – Vegetable and Ornamental Plants (ARC-VOP) (Roodeplaat, Pretoria, South Africa) in November 2016, and identified by Dr Willem Jansen Van Rensburg. A voucher specimen (TOT8420) was deposited at the ARC-VOP laboratory. The leaf material was carefully examined and the healthy leaf material was dried using an oven heat at 50 °C followed by dry storage. The dried leaves were ground to fine particles size using a Lasec polymix PX-MFC 90 D grinder, Kinematica AG (Switzerland), before extraction, not only to maximise surface area and obtain homogeneity but also to rupture the plant organ, tissue and cell structures exposing the solutes to the extraction solvent.

2.3.2. Extractions materials

Analytical grade extraction solvents (*n*-hexane, ethanol, acetone, ethyl acetate, methanol and dichloromethane) were purchased from Radchem pty (Ltd) (South Africa), or MERCK (Sigma Aldrich) (South Africa). Milli-Q® water was used in preparative experimentations involving the use of water. All chemicals were used without further purification.

2.3.3. General extraction methods

The general extraction techniques employed were divided into three categories: 1) extraction *via* single solvent system, 2) supercritical fluid extraction and 3) sequential organic solvent extraction.

2.3.3.1. Batch extraction of dry leaf material usingasingle solvent system

The dried ground leaf material (amounts varying as per solvent extraction) was immersed separately in a selected solvent or solvent mixture, at 1:10 *m/v* ratio. The contents were constantly stirred using a stirrer plate and stirrer bar at room temperature with repeated extraction of plant residue (1hr, 18hr and 1hr), with filtering after each interval using a Buchner funnel. The filtrates were combined. The combined filtrates were evaporated using a *Buchi* rotary evaporator and/or a *genevoc SP Scientific* genevac EZ-2 centrifugal evaporator or left to dry in a fume hood. The plant material was extracted separately with water, ethanol, ethanol/water (50:50), ethyl acetate, *n*-hexane and acetone to give 6 extracts.

Liquid-Liquid partitioning of the EtOAc extract

The EtOAc extract (18 g) was dissolved in *n*-hexane (200 ml) and sonicated for 2 min to which 90% ethanol (200 ml) was added. A separating funnel was used for the liquid-liquid partitioning and the content was shaken several times. The *n*-hexane layer was evaporated to dryness and the resulting fraction named p-hexane. The 90% EtOH layer was evaporated and the dry mass was re-suspended in ethyl acetate (200 ml) to which water (200 ml) was added and the combination shaken in separating funnel. The contents were allowed to settle and the resulting two layers were collected separately. The resulting fractions from the EtOAc phase and that from the water phase were named p-EtOAc and p-water, respectively. The partitioning of the EtOAc extract is illustrated in Figure 2.2.

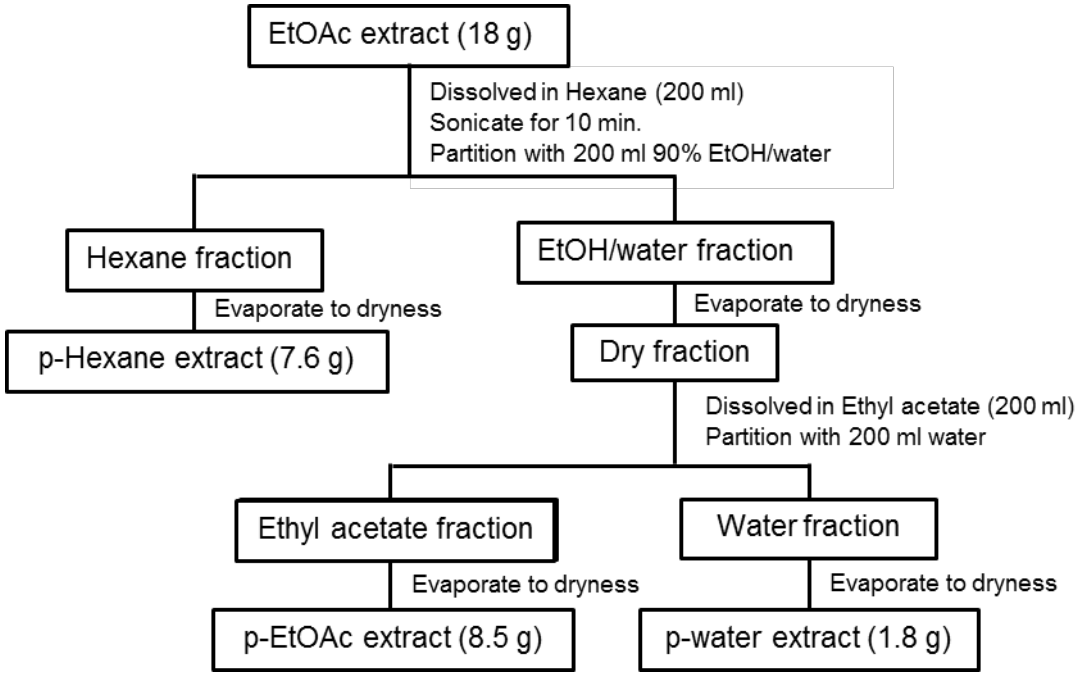

Figure 2.2: *Liquid-liquid partitioning of EtOAc extract.*

2.3.3.2. Supercritical fluid extraction of dried leaf material

A Waters MV-10 ASFE supercritical fluid extraction system (Figure 2.3) using the software ChromScope for the supercritical fluid extraction of the plant material with analytical grade ethanol and carbon dioxide.

Figure 2.3: *Image of a Waters MV-10 ASFE Supercritical Fluid Extraction system* [71].

Dried *C. gynandra* leaf material (100 g) was subjected to supercritical fluid extraction in an extraction chamber. The ethanol flow rate was varied from 0 – 1.5 mL/min while that of CO_2 was maintained at 5 ml/min. The pressure conditions varied from 100 – 350 bar while the temperature conditions initiated at 35 °C and with a maximum of 80 °C. The gradient extraction conditions are shown in Table 2.1. After extraction the filtrate was allowed to evaporate in a fume hood to yield approximately 3.5 mg of the sc(CO_2-EtOH) extract.

Table 2.1: *Extraction conditions via the supercritical fluid extraction method.*

Ethanol Flow rate (mL/min)	CO_2 Flow (mL/min)	Temp. (°C)	Pressure (bar)	Dynamic duration 1 (min)	Static duration (min)	Dynamic duration 2 (min)	Cycles	Make-up Flow (mL/min)
0,0	5	35	100	5	20	10	4	0,5
0,0	5	35	100	1	1	3	1	1,0
0,0	5	40	250	5	20	10	2	0,5
0,0	5	40	350	5	20	10	3	0,5
0,0	5	40	200	1	1	3	1	1,0
0,2	5	50	100	5	20	7	3	0,5
0,4	5	60	200	5	20	7	3	0,5
0,6	5	70	300	5	20	7	3	0,5
0,8	5	70	310	5	20	7	3	0,5
1,0	5	80	320	5	20	7	3	0,5
1,2	5	80	330	5	20	7	3	0,5
1,5	5	80	340	5	20	7	3	0,5
1,5	5	80	350	5	20	7	3	0,5
0,0	5	80	150	5	1	5	1	0,5
1,0	5	80	100	5	0	10	2	0,5
0,0	5	80	100	5	0	10	1	1,0

2.3.3.3. Sequential extraction of plant dried leaf material

This extraction method involved soaking leaf material in different solvents sequentially in the order from least polar to most polar, in the order –*n*-hexane, dichloromethane, ethyl acetate and methanol. The sequential extraction followed the order illustrated in Figure 2.4 for the extraction of dried leaves (500 g) of *C. gynandra* ground to fine particles (~ 40 µm) at room temperature. Plant material was soaked in *n*-hexane (5 L × 1h, 5L × 18h and 5L × 1h) with

constant stirring then filtered between each extraction. The *n*-hexane extracts were evaporated to dryness at 40 °C under vacuum by a rotary evaporator and combined yielding 13 g of the extract. The residual plant material was further soaked in dichloromethane (5L × 1h, 5L × 18h and 5L × 1h) at room temperature with stirring then filtered between each extraction. The dichloromethane extracts were evaporated to dryness at 40 °C under vacuum by a rotary evaporator to obtain 18 g of the extract. The resulting residual plant material was further soaked in ethyl acetate (5 L × 1h, 5L × 18h and 5L ×1h) at room temperature with constant stirring then filtered between each extraction. The combined ethyl acetate extracts were evaporated to dryness at 50 °C under vacuum by a rotary evaporator to obtain 19 g of the extract. Finally, the residual plant material was further soaked in methanol (5L × 1h, 5L × 18h and 5L × 1h) at room temperature with stirring then filtered between each extraction. The methanol extracts were combined and evaporated to dryness at 60 °C under vacuum by a rotary evaporator to obtain 16 g of the extract. The extracts obtained are named: *n*-hexane-, seq-DCM-, seq-EtOAc- and seq-MeOH extract, according to the extraction sequence.

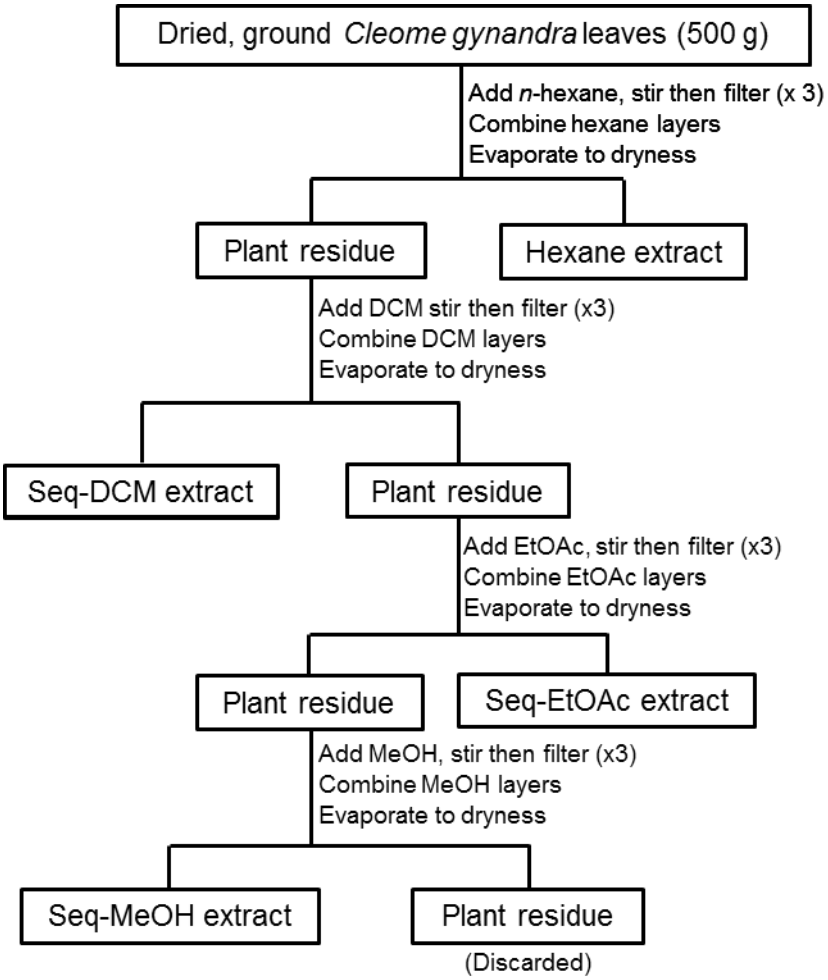

Figure 2.4: *An illustration of the sequential extraction procedure followed using n-hexane, dichloromethane, ethyl acetate and methanol to obtain the extracts labelled as n-hexane, seq-DCM, seq-EtOAc and seq-MeOH.*

2.3.4. Enzyme-based biological assays

The crude extracts prepared using single solvent system and supercritical fluid extraction were subjected to enzyme-based bio-assays. The enzyme assays were selected to assess the potential of the extracts ingredients as anti-diabetic-, anti-hypertension-, anti-cholesterol-, cardio-protective and anti-uricemic agents. The selected enzyme-based assays were α-amylase-, α-glucosidase-, xanthene oxidase-, HMG-CoA reductase-, and renin inhibition.

2.3.4.1. Materials for enzyme-based assays

All chemicals, reagents, standards and enzymes for the enzyme assays were purchased from Sigma Aldrich unless specified otherwise. For the α-amylase and α-glucosidase assays: 1% soluble starch as the substrate (Sigma, S2004), human salivary α-amylase (Sigma, E8140), α-glucosidase (from *Saccharomyces cerevisiae*), phosphate buffer (pH 6.9) (Sigma, S0751), standard inhibitors, acarbose (Sigma A8980) and α-amylase inhibitor from wheat seed (Sigma A1520), 3, 5-dinitrosalicylic acid (DNS) reagent (Sigma, D0550) and potassium sodium tartrate (S6170). For the HMG-CoA assay: HMG-CoA Reductase Assay Kit (Sigma, CS1090), the kit contained the substrate solution (HMG-CoA), enzyme (HMG-CoA reductase), NADPH (nicotinamide adenine dinucleotide phosphate), assay buffer and a standard inhibitor, pravastatin. For the renin inhibition assay: Renin assay kit (Sigma, MAK157-1KT). The kit contained the substrate, renin and assay buffer. The inhibitor, aliskiren was purchased separately (Sigma, CDS023114). Xanthine oxidase inhibition assay: Dimethoxymethylamphetamine (DMMA), xanthine oxidase assay kit (Sigma, MAK078-1KT). The contents of the kit included xanthine oxidase, fluorescent peroxidase substrate and assay buffer. A Tecan Infinite® F500 microplate reader was used for colorimetric readings where enzyme-based assays were involved.

The percentage inhibition for the enzyme assays was calculated using the formula:

$$\%Inhibition = \frac{Abs_{control} - Abs_{extract}}{Abs_{control}} \quad (2)$$

The mean values were obtained from triplicate experiments.

2.3.4.2. α-Amylase inhibition assay

α-Amylase inhibition assay uses calorimetry and measures the extent of the hydrolysis of starch to glucose by using a 3, 5-dinitrosalicylic acid (DNS) reagent. The hydrolysis yields a brown-coloured product which can be detected at 540 nm.

In a 96-well plate, 30 µL phosphate buffer (20 mM, pH 6.9) and 10 µL α-amylase (100 µg/mL) were added to the control wells. The blank wells contained 40 µL phosphate buffer. The positive control well contained, 20 µL acarbose (1 mg/mL in water), 10 µL phosphate buffer and 10 µL α-amylase. The extract was prepared as 1 mg/mL solution in ethanol, 20 µL was added in the extract test well, with 10 µL phosphate buffer and 10 µL α-amylase. Further, extract control wells contained 80 µL phosphate buffer and 20 µL extract. Experiments were performed in triplicate for three different sets and mean ± standard error of the mean were calculated. The plates were incubated at 37°C for 30 min. After the pre-incubation, 60 µL substrate of 1% starch solution was added to each well and incubated at 37 °C for 15 min. Using 1.0 mL DNS reagent the reaction was terminated and the plate was placed in boiling water bath for 5 min. After this cooled to room temperature. The final test concentration was 200 µg/mL for crude extracts, and the absorbance was read at 540 nm using the Tecan Infinite® F500 microplate reader.

2.3.4.3. α-Glucosidase inhibition assay

α-Glucosidase inhibition assay measures the hydrolysis of *p*-nitrophenyl-α-D-glucopyranoside to glucose and *p*-nitrophenyl. The resulting yellow-coloured product can be detected at 405 nm. In a 96-well plate, 30 µL phosphate buffer (20 mM, pH 6.9) and 10 µL α-glucosidase (100 µg/mL) were added to the control wells. The blank wells contained 40 µL phosphate buffer. The positive control well contained, 20 µL dimethoxymethylamphetamine (DMMA) (1 mg/mL), 10 µL phosphate buffer and 10 µl α-glucosidase. The extract was

prepared as 1 mg/mL solution in ethanol, 20 µL was added in the extract test well, with 10 µL phosphate buffer and 10 µL α-glucosidase. Further, extract controls contained 80 µL phosphate buffer and 20 µL test extract. The plates were incubated at 37°C for 30 min. After the pre-incubation, 60 µL substrate was added to each well and incubated at 37 °C for 15 min. The final test concentration was 200 µg/mLand varying in the case were IC_{50} value determination was involved, and the absorbance was read at 405 nm using theTecan Infinite® F500 microplate reader. Experiments were performed in triplicate and mean ± standard error of the mean was calculated.

2.3.4.4. HMG-CoA reductase inhibition assay

A stock solution of 1 mg/mL in 10% ethanol (EtOH) and 90% phosphate buffer (pH 6.9) was prepared for all test samples (extracts). The extracts were screened at a final concentration of 200 µg/mL. The assay buffer was added to the blank wells (92 µL), inhibitor wells (90 µL), control wells (91 µL) solvent control and sample wells (71 µL). The inhibitor wells contained 1 µL pravastatin, the solvent control contained 20 µL solvent and sample wells contained 20 µL of prepared stock solution. To all the wells 2 µL NADPH and 1 µL HMG-CoA reductase (HMGR) were added. The sample controls contained no enzyme nor substrate but 78 µL assay buffer, 2 µL NADPH and 20 µL of the samples.

The plates were incubated for 30 minutes, then 6 µL of substrate solution was added to all the wells and the absorbance was read immediately at 340 nm the Tecan Infinite® F500 microplate reader. A kinetics program was used to measure the decrease in absorbance at 2 min intervals for 30 min. The plates were agitated for 10 seconds before the first measurement. The enzyme activity was measured by the decrease in absorbance due to the decrease in NADPH. Enzyme inhibition was characterised by no change or very slow rate of decrease in absorbance compared to the control.

2.3.4.5. Renin inhibition assay

The renin activity assay is determined by using a fluorescence resonance energy transfer (FRET) peptide containing a fluorescence quencher. Cleavage of the peptide by renin results in a fluorescent product which can be detected at λex = 535 nm/λem = 612 nm. Stock solutions of test samples were prepared at 2 mg/mL either in aqueous phosphate buffer solution (pH 6.9) or 10% ethanol and 90% phosphate buffer (pH 6.9). All extracts were screened at a final concentration of 200 µg/mL.

The assay buffer was added to the blank wells (50 µL), control wells (30 µL), inhibitor, solvent control and sample wells (10 µL). The inhibitor wells contained 10 µL aliskiren (100 µg/mL), the solvent control and test sample wells each contained 20 µL of the prepared stock. To all, except the blank well, 20 µL renin (100 ng/mL) was added. For each test sample, a sample blank was prepared with 30 µL assay buffer and 20 µL test sample. The plates were incubated for 30 min, then 50 µL of substrate solution was added to all the wells and the plates were incubated for further 60 min. Renin activity was measured by the increase in fluorescence measured using the Tecan Infinite® F500 microplate reader and thus inhibition of renin was characterized by a decrease in fluorescence compared to the control.

2.3.4.6. Xanthine oxidase inhibition assay

For each extract a stock solution was prepared at 1 mg/mL in 10% ethanol (EtOH) and 90% phosphate buffer (pH 6.9). All samples were screened at a final concentration of 200 µg/mL. The assay buffer was added to the wells for blank (46 µL), control (44 µL) and inhibitor well, solvent control and sample wells (34 µL). The extract was prepared as 1 mg/mL solution in ethanol and 10 µL was added in the extract test well, 10 µL of 10% ethanol in phosphate buffer in the solvent well. 1 mg/mL positive control was prepared in phosphate buffer and 10

µL was added in the positive control well. Except the blank well, all the other wells contained 2 µL xanthine oxidase. Sample blanks contained 38 µl assay buffer and 10 µL test sample. The plates were incubated for 30 minutes (min) at room temperature, after which 2 µL of xanthine oxidase was added to all the wells followed by 2 µL of fluorescent peroxidase substrate. The plates were further incubated for 2 min and kinetic measurements were taken for 1 hour with 5 min intervals. Xanthine oxidase activity was indicated by the increase in fluorescence and inhibition of xanthine oxidase was characterised by the decrease in fluorescence measured using the Tecan Infinite® F500 microplate reader. The kinetics graphs were plotted using GraphPad Prism 5 (GraphPad Software, Inc., California).

2.3.4.7. Determination of IC_{50} values

The fractions obtained *via* the liquid-liquid partitioning of EtOAc were further assessed for α-glucosidase inhibition activity, along with the original EtOAc crude, at different concentrations (200, 100, 50, 25, 12.5, 6.25, 3.13, 1.56, 0.78, 0.39 µg/mL) to achieve their inhibition curves, and their IC_{50} values were calculated using GraphPrism.

2.3.5. Antibacterial activity assay

The EtOH-, EtOAc-, acetone- and *n*-hexane extract were screened for antibacterial activity against *E. coli* and *S. aureus*.

2.3.5.1. Bacterial strains and their culturing

S. aureus ATCC 29213 and *E. coli* ATCC 27853 were the strains used for antibacterial assays. The strains were maintained in Mueller Hinton ager (MHA) (Fluka, Spain). The

organisms were sub-cultured every 2 weeks. Before testing, the bacterial inoculums were prepared and cultivated in Mueller Hinton broth for 12 hr at incubation temperature 37 °C. The bacterial cultures were serially diluted (10-fold increments) in sterile broth to obtain cell suspension of 1.0 x 10^5 CFU/ml (colony forming units per ml).

2.3.5.2. Determination of minimum inhibitory concentration

The minimum inhibitory concentration (MIC) for the selected crude extracts against bacteria were evaluated using the serial microdilution assays [72,73]. The test solution (1 – 0.008 mg/mL) was serially diluted 50% with water and the sample with the highest test concentration was dissolved in 10% ethanol in water. The dilutions were prepared in 96-well microtitre plates. Bacterial culture (100 µL) was then added to each well before incubation for 24 hr at 37 °C. The bacterial inhibition was visualised by adding 40 µl of aqueous *p*-iodonitrotetrazolium violet (INT) (Sigma Aldrich) to each well. The plates were incubated for a further 1 hr and the MIC was determined as the lowest sample concentration that inhibited microbial growth, as indicated by the visible reduction in the red colour, visually inspected.

2.3.6. Anticancer assays

Crude extracts prepared from the sequential extraction method discussed in section 2.1.1.1 were initially evaluated for their lung cancer cytotoxicity in the A549 cell line.

2.3.6.1 Cell culture

All cell lines were cultured at 37°C, 5% CO_2, in Dulbecco's Modified Eagle Medium (DMEM) containing high glucose (containing 4.5 g/L glucose, sodium bicarbonate and phenol red),

supplemented with 10 % fetal bovine serum (FBS), Glutamax (2 mM) and PenStrep (0.5 mg/ml).

2.3.6.2 General method for anticancer bioactivity assay

Cells were trypsinized at 10,000 cells per well in a 100 µL volume plated in 96 well plate. The cells were incubated in CO_2 to reach 60 - 70% confluence, at which point, they were treated with increasing concentration (0.125, 0.25, 0.50 and 1 mg/mL) of test sample (initially reconstituted in 10%DMSO and diluted with H_2O at 1mg/mL) along with positive control (Cisplatin-100 µM and/or diallyl disulphide (DADS) 1mM), incubated over 24 hours and 48 hours and cell viability determined using sulforhodamine B (SRB) assay. After 24- and 48-hour incubation cells were fixed using 50 µL of 50% trichloroacetic acid (TCA) was added to each well, and the plates were kept at 40 °C for 60 min. After fixation of cells, the wells were carefully washed with slow running tap water, and subsequently the plates were allowed to dry. One hundred microliters of SRB was added to each well and the plates incubated for 30 min. Excess unbound SRB was removed and the plates washed with 1% acetic acid. The washed wells were allowed to dry at room temperature. The protein bound SRB was dissolved in 100 µL of 10 mM tris base solution and the absorbance read at 510 nm on a multimode plate reader (ParkinElmer, Massachusetts, USA).

2.3.7. Ultra-performance Liquid Chromatography Quadrupole time-of-flight Mass Spectrometry

UPLC-QTOF-MS was used to generate chromatograms for the chemical fingerprints of the extracts. UPLC was performed using a Waters Acquity UPLC system (Waters Corp., MA USA), equipped with a binary solvent delivery system and an autosampler.

The extracts were reconstituted in methanol to a concentration of 1 mg/mL then centrifuged at 10000 rpm for 2 min. Separation was performed on a Waters BEH C18, (2.1 mm × 100 mm, 1.7 µm column). The mobile phase consisted of solvent A: 0.1% formic acid in purified water and solvent B: acetonitrile with 0.1% formic acid. The gradient elution was optimized as follows: 3% B (0-0.1 min), 3-30% B (0.1-6.0 min), 30% B (6.0-9.0 min), 30-100% B (9.0-20.0 min), 100% B (20.0-23.5 min), 100-3% B (23.5-24.0), 3% B (24.0-25.0). The flow rate was kept at 0.400 mL/min and the injection volume was 5 µL. The column temperature was 40 °C.

For MS conditions a Waters Synapt G2 high definition QTOF mass spectrometer equipped with an ESI source was used to acquire negative and positive ion data. The system was driven by MassLynx V 4.1 software (Waters Inc., Milford, Massachusetts, USA) for data acquisition. MS calibration was performed by direct infusion of 5 mM sodium formate solution at a flow rate of 10 µL/min and using Intellistart functionality over the mass range of 50 - 1200 Da. The MS source parameters were set as follows for both the positive and negative mode: Source temperature 110 °C, sampling cone 25 V, extraction cone 4.0 V, desolvation temperature 300 °C, cone gas flow 10 l/h, desolvation gas flow (500 l/h). The capillary was 2.8 kV in the positive and 2.6 kV in the negative modes.

Acquisition

A 2 ng/µL solution of leucine encephalin was used as the lockspray solution that was constantly infused at a rate of 2 µL/min through a separate orthogonal ESI probe to compensate for experimental drift in mass accuracy. Trap collision energies were 30 V (high) and (10 V) for the low energy.

Chemical profiling

Compounds were tentatively identified by generating molecular formulas using MassLynx V 4.1 based on their iFit value, and by comparison of MS/MS fragmentation pattern with that of

matching compounds. Identification of known compounds was effected using online databases such as *Chemspider, PubChem, the Dictionary of Natural Products, MassBank, Metlin and MefFusion.*

2.4. Results and discussion

2.4.1. Single solvent system and the SCF extraction

The solvent systems used to obtain the different extracts *via* the single solvent system method were water, ethanol, ethanol/water (50:50), ethyl acetate, *n*-hexane and acetone. The solvents were selected based on their acceptance as food grade and also for comparative purposes as in the case of *n*-hexane. The results for extraction are summarised in Table 2.2.

Table 2.2: *Batch extraction yields summary*

Solvent system	Plant material (g)	Extract (g)	%Yield
Ethanol	450	35	7.8
Ethyl acetate	500	19	3.8
N-hexane	500	13	2.6
Acetone	103	5	4.9
Ethanol:water (50:50)	100	8	8.0
Water	126	2	1.6
sc(CO_2& ethanol)	100	1	1.0

The best extraction yield was obtained for the ethanol extract and the lowest yield was obtained with water. This can be expected as ethanol is able to extract both polar and non-polar compounds. Water is suitable for extracting polar compounds and the leaves of *C. gynandra* seem to possess a relatively few of these as the water extraction yield was the lowest in batch extraction. *N*-hexane on the other hand gives high yields in the extraction of non-polar and neutral analytes particularly oils and produced relatively low yield compared to the rest of the solvents employed herein. It is evident that the majority of analytes in *C.*

gynandra leaves are medium polar. The supercritical fluid extraction which involved supercritical CO_2 and ethanol gave the lowest extraction yield i.e. 100 g of plant material resulted in 1 g of extract, a 1 % yield. The supercritical method of extraction used an equipment designed for analytical purposes. While CO_2 is expected to return low yields, as it boasts in the extraction of oils, as discussed earlier, the presence of ethanol was expected to increase the yield as its presence was expected to expand the pool of extractable components, however, this was not the case. This could be due to the equipment only allowing a small amount of plant material to be extracted at a time and perhaps the temperature, pressure and flow rate conditions were not the optimum conditions for such extraction.

2.4.2. Sequential extraction

Sequential extraction of the dried, ground leaves (500 g) of *C. gynandra* as discussed in section 2.3.3.3 gave a yield of 13 g *n*-hexane extract, 18 g seq-DCM extract, 19 g seq-EtOAc extract, and 16 g seq-MeOH extract. This indicates a 66 g total extractable content, a 13.2 % overall extraction yield. The *n*-hexane extract contributed the lowest yield at 2.6 % while the highest yield was seen for seq-EtOAc, 38 %, see Table 2.3. These extracts were evaluated for their anticancer activity towards identifying the bioactive compounds.

Table 2.3: *Sequential extraction yields*

Extract	**Extract (g)**	**%Yield**
N-hexane	13	2.6
Seq-DCM	18	3.6
Seq-EtOAc	19	3.8
Seq-MeOH	16	3.2
Total extractable	66	13.2

2.4.3. Biological activity assays of extracts against α-amylase and α-glucosidase

All the extracts that were tested for their inhibition of α-amylase (EtOH, water, EtOH-water, sc(CO_2-EtOH), EtOAc, acetone and *n*-hexane) were inactive against this enzyme (Table 2.4). This result was unexpected as Sangameswaran et al.[74] in their study reported α-amylase inhibitory effect of the ethanol extract from *C. gynandra* leaves to be ranging between 13.21 % and 65.34 % when studied at concentrations 10 –100 µg/mL. Furthermore, in the same study, at the same concentration range the inhibitory effect of the aqueous extract was found to be ranging from 10.76% to 48.59%. The reported IC_{50} of ethanol extract was found to be 77.53 ± 0.15 µg/mL, and that of the water extract was 123.5 ± 0.40 µg/mL. The possible explanation for the lack of activity for all the extracts against α-amylase may be due to the over-saturation of the enzyme as the concentration of 200 µg/mL may have been too high.

In contrast, when assayed for α-glucosidase inhibition the extract sc(EtOH-CO_2) exhibited the highest inhibition compared to other extracts tested, a 96.55 ± 0.15 %inhibition when tested at 200 µg/mL and compared favourably to the positive control, acarbose (97.56 ± 0.10 %), while the EtOH extract gave a 61.09 ± 2.16 % inhibition at the same test concentration (Table 2.4). The EtOAc, acetone and *n*-hexane extracts also exhibited good inhibition activity against α-glucosidase with 91.76 ± 1.16, 89.97 ± 1.77 and 92.67 ± 0.17 %inhibition, respectively. This result revealed that the active compounds against α-glucosidase are in all likelihood medium to non-polar compounds, and this argument is further solidified by the water extract showing no activity.

Table 2.4: *Inhibition activity (%) of crude extracts against alpha amylase and alpha glucosidase.*

Extract	α-Amylase assay % Inhibition ± SD	α-Glucosidase assay % Inhibition ± SD
EtOH extract	-19.81 (0)	61.09 ± 2.16
EtOH/H_2O extract	-17.81 (0)	-12.55 (0)
Water extract	-9.51 (0)	-17.86 (0)
sc(EtOH-CO_2) extract	-17.80 (0)	96.55 ± 0.15
N-hexane extract	-32.87 (0)	92.67 ± 0.17
EtOAc extract	-12.46	91.76 ± 1.16
Acetone extract	-10.35	89.97 ± 1.77
	Controls	
Acabose	81.82 (0.81)	
DMMA		97.56 (0.10)
10% Ethanol	-18.89 (0)	-2.50 (0)

Ethanol falls under ‘generally regard as safe’ chemicals and its use is found vastly across fields.Alcohol is the principle ingredient in alcoholic beverages like beer, wine or brandy. It is also an ingredient in a range of products, such as personal care and beauty products, paints and varnishes and fuel. Developing an ethanol extract for commercial purposes as food, herbal or nutraceutical products would be less restricting and would be preferred. On the other hand, the supercritical fluid extraction technology ensures safety as well as green measures of extraction. The extract sc(CO_2-EtOH) showed the highest inhibition activity and thus merited further steps towards identifying the active components, however, the major obstacle was that very little quantity of plant could be extracted, limited by the instrument capability as it is an analytical design.

Ethyl acetate is listed as a FDA approved solvent, and the extract EtOAc exhibited 91.76 ± 1.16 % inhibition of α-glucosidase while the extraction yield was relatively appreciable at about 3.8 % per leaf mass. EtOAc extract was therefore subjected to solvent-solvent partitioning to attempt concentrating the bioactive constituents to possibly improve activity.

2.4.4. Evaluation of α-glucosidase inhibition for the liquid-liquid partitioned fractions

The fractions produced through liquid-liquid partitioning i.e. p-hexane and p-water showed limited inhibition of α-glucosidase with IC_{50} values greater than 130 ug/mL (Figure 2.5).

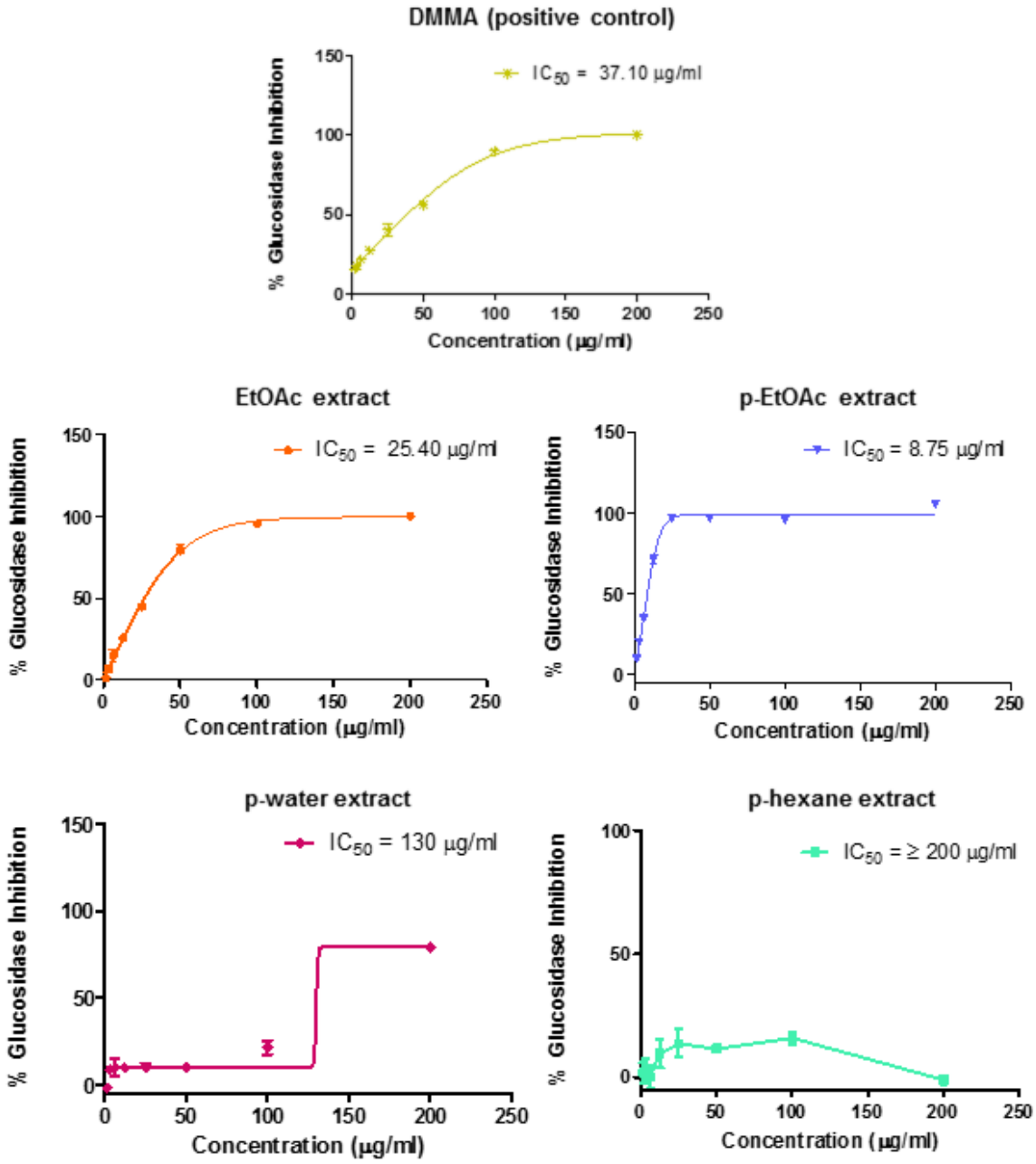

Figure 2.5: *Inhibition curves and IC_{50} values of extracts tested for the inhibition of α-glucosidase.*

The ethyl acetate liquid-liquid fraction showed excellent activity with an IC_{50} value of 8.75 µg/mL which was an improvement compared to that of the parent extract, 24.40 µg/mL. This

also compared favourably with the positive control DMMA with an IC_{50} of 37.10 µg/mL. The results showed that the active compounds were retained in the ethyl acetate fraction indicating that these were in all likelihood medium polar compounds since the *n*-hexane with non-polar compounds and the water with the polar compounds did not exhibit any appreciable activity. This warranted the further chemical characterisation of the ethyl acetate extract and the partition p-EtOAc, the results of which are discussed in section 2.4.10.

2.4.5. Effect of extracts on HMG-CoA reductase

The enzyme activity was measured by the decrease in absorbance due to the decrease in NADPH, therefore, inhibition of the enzyme by pravastatin was recognized by the unchanged or very slow rate of decrease in absorbance of NADPH compared to the control. Figure 2.6 demonstrates the activity of pravastatin as the rate of decrease in NADPH absorbance is slower in the presence of pravastatin compared to the control. As the test samples were dissolved in 10 % ethanol it was vital to have ethanol as a control and very small activity was observed which was subtracted for test samples.

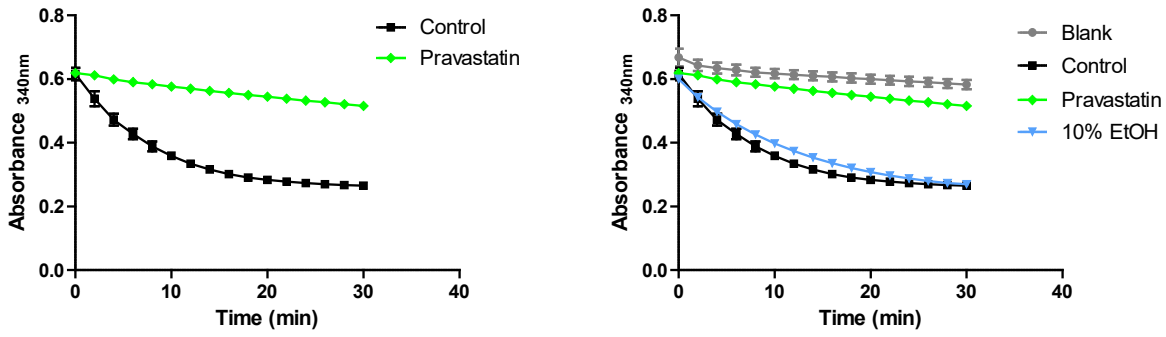

Figure 2.6: *The activity of the inhibitor, pravastatin (green), against HMG-CoA reductase (black) action and the controls.*

The EtOH-, *n*-hexane-, acetone and EtOAc extracts were tested in the assay at 200 µg/mL. The kinetics for the assay are shown in Figure 2.7. The competition for site of the

components in the *n*-hexane and those in the EtOAc extracts versus the substrate is evident as the NADPH absorbance increases with time thus revealing the activity of these extracts towards retarding catalytic action of HMG-CoA reductase and thus reducing the oxidation of NADPH by the catalytic subunit of HMG-CoA reductase in the presence of the substrate. The EtOAc- and *n*-hexane extracts were effective in inhibiting the action of HMG-CoA reductase. The EtOH and acetone extracts exhibited poor activity.

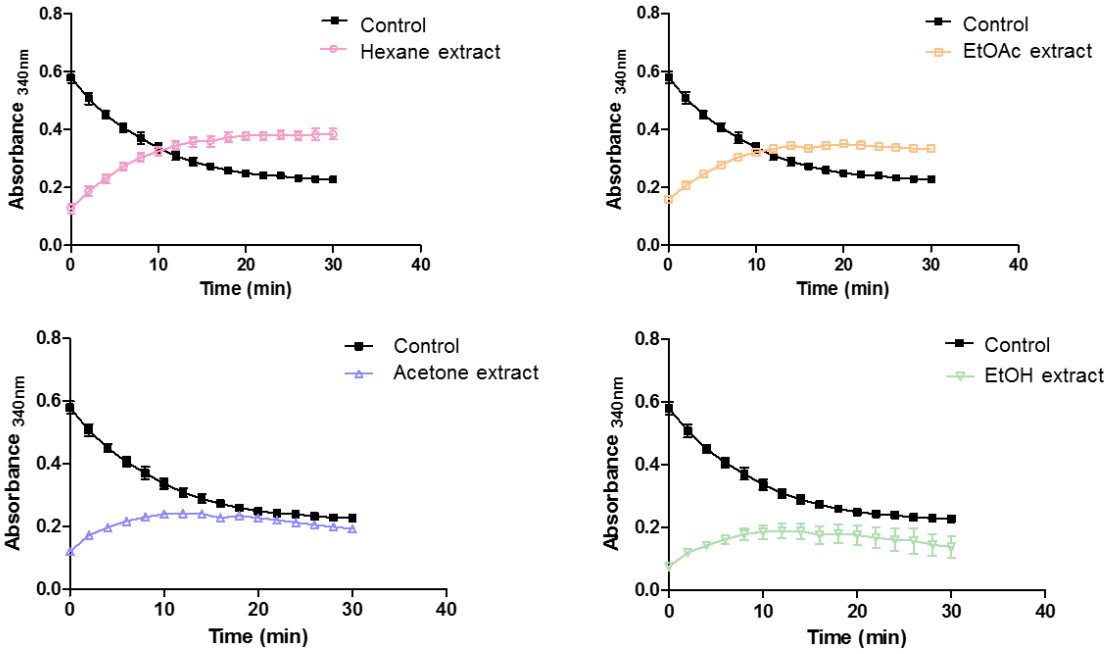

Figure 2.7: *HMG-CoA reductase inhibition of extracts at 200 µg/mL.*

The results show that the effect of concentration of NADPH on the action of HMG-CoA reductase at 200 µg/mL for the EtOAc and *n*-hexane extract is time dependant. The bioactive components are likely medium polar to none polar constituents as the EtOAc and *n*-hexane extracts exhibited activity while the acetone and EtOH extracts were inactive.

2.4.6. Evaluation of extracts for the inhibition of renin

The renin activity is measured by the increase in fluorescence, therefore, inhibition of renin by aliskiren was recognized by the decrease in fluorescence compared to the control. Thus, the samples that have an inhibitory effect on renin will show a fluorescence that is lower than that of the control and the percentage inhibition can be calculated. The solvent control, 10% EtOH showed very low effect on renin action (0.86 ± 0.74%). This effect was subtracted from that of the extracts dissolved in 10% ethanol to correct for the inhibition due to the solvent. The EtOH extract and the EtOH-water extract at 200 µg/ml displayed moderate activity, 68.06 ± 1.78 % and 52.72 ± 1.37 % inhibition, respectively, while aliskiren used as a positive control exhibited 100.72 ± 0.25 % inhibition at 100 µg/mL (Table 2.5). The sc(CO_2-EtOH) extract exhibited poor activity, 29.34 ± 1.26 % inhibition while the water extract revealed no activity. Aliskerin is one of the inhibitors widely used in the treatment of hypertension, and is also used for treating heart failure and diabetic nephropathy [28]. The EtOH extract exhibited good activity and merits further studies towards identification of compounds responsible for the activity. The activity displayed by the EtOH extract is due to the medium polar compounds since the water extract exhibited no activity, while the EtOH-water extract displayed poor activity, indicating that the polar compounds may not possess renin inhibition properties.

Table 2.5: *Renin inhibition of crude extracts at 200 µg/mL and the positive control, aliskiren at 100 µg/mL.*

Extract	**Renin % Inhibition ± SD**
EtOH extract	68.06 ± 1.78
EtOH-water extract	52.72 ± 1.37
Water extract	-107 (0)
sc(CO_2-EtOH)	29.34 ± 1.26
Controls	
10% EtOH	0.86 ± 0.74
Aliskiren	100.72 ± 0.25

2.4.7. Xanthine oxidase inhibition activity of the extracts

Xanthine oxidase activity assay is determined by a coupled enzyme assay, which results in a colorimetric or fluorometric product, proportional to the hydrogen peroxide generated. One of the commercial inhibitors of xanthine oxidase is allopurinol. The kinetics curve demonstrating the inhibition of xanthine oxidase action is seen in Figure 2.8 for allopurinol at 100 µg/ml, wherein the rate of production of hydrogen peroxide is seen to decrease compared to the control, indicative of the retardation of the enzyme activity in the presence of allopurinol.

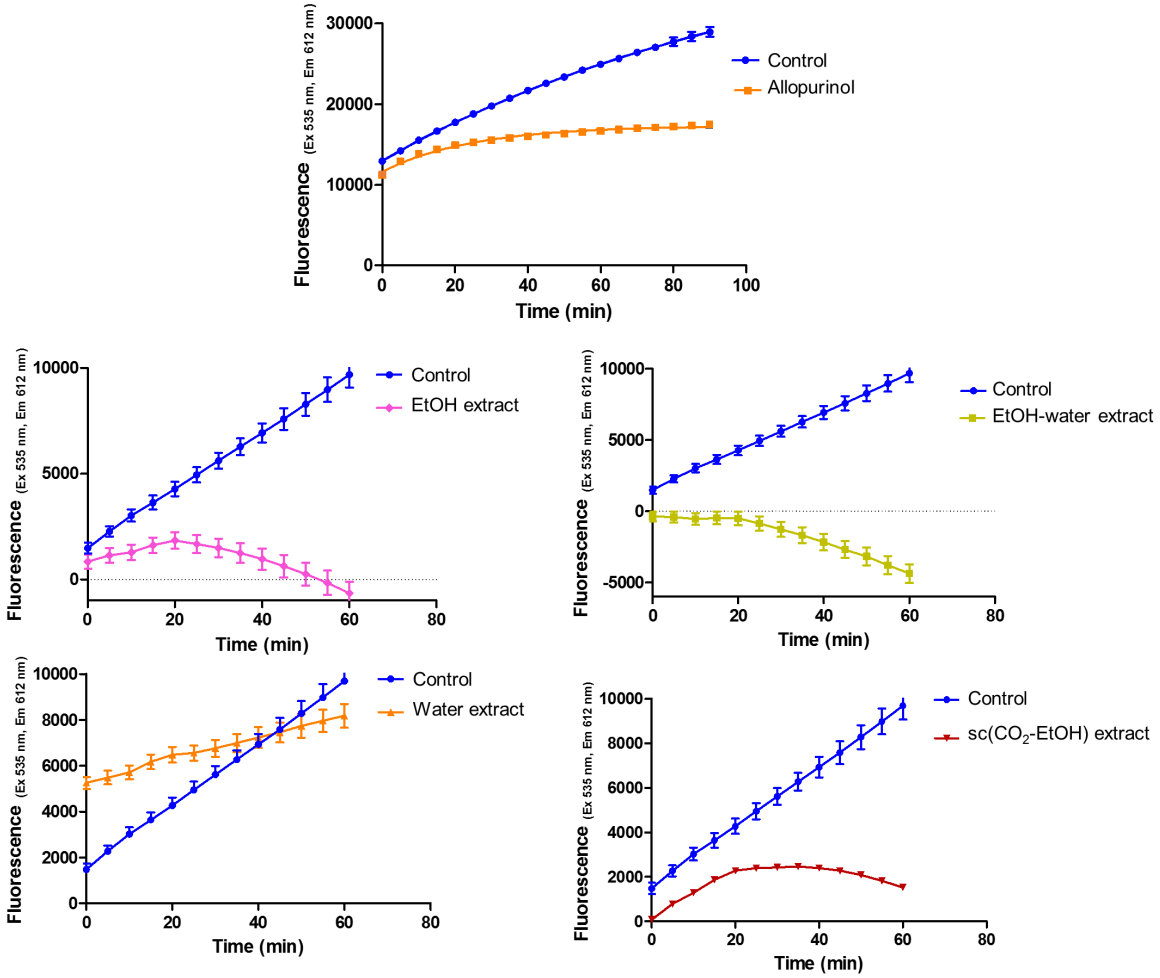

Figure 2.5: *Xanthine oxidase inhibition kinetics curves of allopurinol (100 µg/mL) (positive control) water-, EtOH-water-, EtOH- and sc(CO_2-EtOH) extract at 200 µg/mL.*

Retardation of the enzyme activity was seen for the EtOH-, EtOH-water- and sc(CO_2-EtOH), which displayed high activity as the rate of decrease was much greater at 200 µg/ml as

illustrated by the respective kinetics curves. The water extract displayed no activity. The effective extraction of biologically active ingredient against xanthine oxidase from *C. gynandra* leaf extract was evident with the ethanol, 50% ethanol in water and supercritical ethanol-CO_2 extraction media. These extracts merit development as herbal medicines for the management of diseases such as gout. It can also be said that the active compounds are medium polar, and that polar compounds are less active as the water extract showed poor activity.

2.4.8. Extract inhibition of *Escherichia coli* and *Staphylococcus aureus*

The EtOH-, EtOAc-, acetone- and *n*-hexane extracts were tested to determine their inhibition of *S. aureus* and *E. coli* growth. Of the four extracts, the EtOH extract exhibited the greatest inhibition activity against *E. coli*. The MIC for the ethanol extract against *E. coli* was 0.052 ± 0.016 mg/mL, comparable to 0.037 ± 0.013 mg/mL of gentamicin, the positive control. The acetone extract exhibited the highest activity against *S. aureus* at 0.25 ± 0.00 mg/mL (Table 2.5). This result warranted studies towards identification of the bioactive compounds. Chemical characterisation of the extract is discussed in section 2.4.10.

Table 2.6: *Minimum inhibition concentration of EtOH-, EtOAc-, acetone- and n-hexane extract against S. aureus and against E. coli.*

Extract	Mean MIC (mg/mL) and standard deviations	
	S. aureus	***E. coli***
EtOH	0.458 ± 0.102	0.052 ± 0.016
EtOAc	0.333 ± 0.129	0.146 ± 0.051
Acetone	0.25 ± 0.00	0.167 ± 0.065
N-hexane	>1	1.00 ± 0.00
Gentamicin (+ve control)	0.047 ± 0.017	0.037 ± 0.013

2.4.9. Evaluation of the anticancer activity of the extracts obtained *via* the sequential extraction method

The extracts obtained *via* the sequential extraction technique *vizn*-hexane, seq-DCM, seq-EtOAc and seq-MeOH extract, were assessed for their lung cancer cytotoxicity against A549 cell line. Table 2.7 displays the anticancer screening results for the extracts, wherein the *n*-hexane extract was the most active (>84% inhibition in the concentration range of 0.125 – 1.00 mg/mL, over 48-hour incubation and >75 % over 24-hour incubation). This result warranted the isolation and identification of the compounds responsible for activity and such study is discussed in detail in Chapter 4.

Table 2.7: *Comparative assessment of cytotoxic potential of sequential solvent extracts of Cleome gynandra against A549 lung cancer cell line.*

Extract	Concentration (mg/mL)	Growth inhibition (%) at 24 h (Mean±SE)	Growth inhibition (%) at 48 h (Mean±SE)
Vehicle control #		9.4±1.96	-2.46±2.15
***N*-hexane extract**	0.125	75.05±0.20	84.87±0.05
	0.25	78.61±0.73	87.18±0.13
	0.50	78.10±0.23	87.27±0.18
	1.00	77.53±0.77	87.08±0.18
Dichloromethane extract	0.125	-5.55±7.22	16.01±5.78
	0.25	12.39±2.82	46.07±2.80
	0.50	22.45±0.49	64.64±1.68
	1.00	25.70±2.52	66.44±1.91
Ethyl acetate extract	0.125	16.3 8±2.71	38.29±0.86
	0.25	34.71±1.86	63.46±0.64
	0.50	42.04±1.39	75.24±1.27
	1.00	56.42±1.25	74.35±0.79
Methanol extract	0.125	16.69±3.84	5.55±0.60
		10.95±3.73	-1.03±1.75
	0.50	9.92±1.20	2.36±1.26
	1.00	12.98±0.78	14.86±1.21

The final concentration of respective vehicle control in the treatment media is 1%

2.4.10. UPLC-QTOF-MS chemical analysis of extracts

UPLC-QTOF-MS was used to obtain a chemical fingerprint that can be used in the future to show batch to batch reproducibly, for extracts that proved reasonably potent in biological assays, and thus, worth pursuing further studies for. Compounds were tentatively identified by first generating the molecular formula using MassLynx V 4.1 based on their isotopic fit value (iFit value), and thereby obtaining accurate mass and by comparison of MS/MS fragmentation pattern with that of matching compounds from selected databases (*viz. Chemspider, The Dictionary of Natural Products, PubChem, MassBank, Metlin and Metfusion)*. The selected extracts were the EtOAc extract and the fraction pEtOAc for α-glucosidase inhibition, the EtOH extract for antimicrobial activity, and the *n*-hexane extract for anticancer activity.

2.4.10.1. Chemical profiling of the ethyl acetate extract and the fraction pEtOAc

A chemical analysis of pEtOAc, the fraction prepared *via* liquid-liquid partitioning of EtOAc extract, and the parent EtOAc extract was undertaken to identify the compounds represented by common peaks which could be responsible for the observed α-glucosidase inhibition activity. The chemical fingerprint of the extract generated using UPLC-QTOF-MS operating in the ESI positive mode, for both EtOAc and pEtOAc, is shown in Figure 2.9. A total of six peaks were selected for identification of the chemical structures based on their mass data and their purity (no interfering peaks). Of these, two compounds were tentatively identified and one identified as a novel compound (Table 2.8).

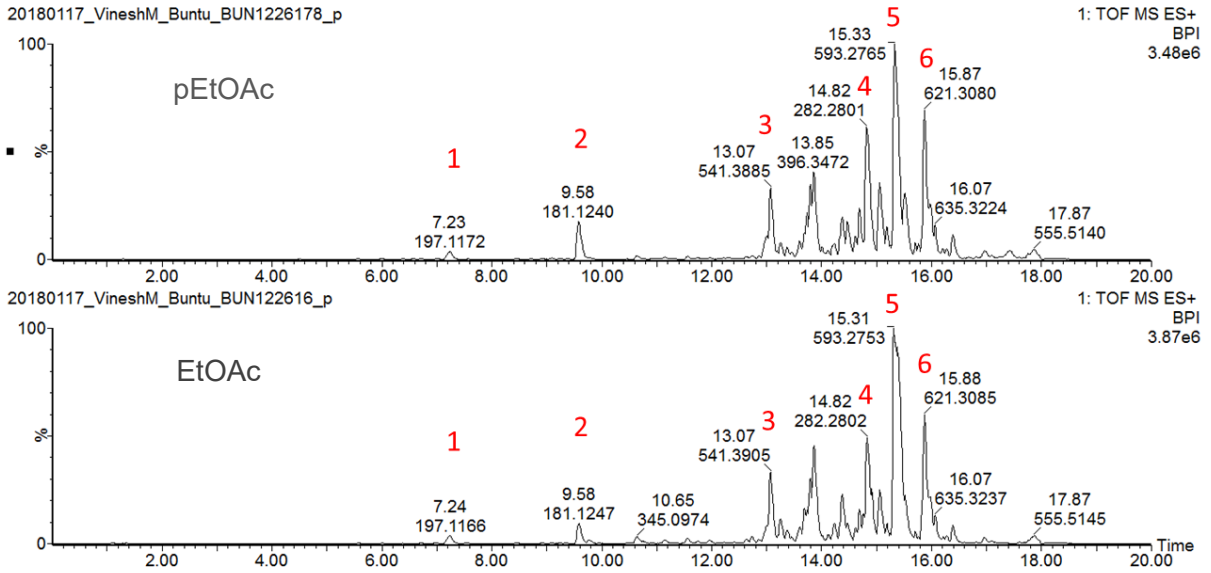

Figure 2.9: *ESI positive mode BPI chromatogram of the extract EtOAc and the fraction pEtOAc. A total of six compounds were selected for tentative identification. Three compounds were tentatively identified as Aspergone E (peak 1), dihydroactinidiolide (peak 2), cleogynone A, and the rest were unidentified (peak 4, 5 & 6).*

EtOAc and pEtOAc showed similar profiles and showed minor peaks in the 7 to 10-minute (polar-medium polar) region and major peaks in the region 13 to 16 minutes (medium polarity region). This distribution of peaks reveals that the extract is composed mainly of medium to non-polar constituents. Using the ESI positive mode two compounds were tentatively identified and one was identified as a novel compound, which is isolated in this work, cleogynone A (**1**) (isolation and structure elucidation discussed in chapter 4) (Table 2.8). The two medium polar peaks, at *m/z* 197.1172 retention time 7.23 minutes, and at *m/z* 181.1240 retention time9.58 minutes were tentatively identified as aspergone E (**2**) and dihydroactinidiolide (**3**), respectively, while medium-nonpolar peak at *m/z* 599.3914 retention time 13.07 minutes was identified as cleogynone A (**1**) (Figure 2.10).

Literature reveals that aspergone E (**2**) was isolated from an ethyl acetate extract of a marine sponge-derived *Aspergillus* sp. strain OUCMDZ-1583, and proved to possess α-glucosidase inhibitory activity [75]. In the reported study aspergone E displayed IC_{50} value of 1.30 mM, comparable to acarbose (IC_{50} = 0.95 mM). The molecular formula of aspergone E,

as in this study, was established as $C_{11}H_{16}O_3$ from an HRESIMS peak at *m/z* 219.0989 $[M + Na]^+$. It can thus be one of the compounds contributing toward the α-glucosidase activity exhibited by both the EtOAc extract and the fraction pEtOAc.

Dihydroactinidiolide (**3**), was first isolated from *Actinidia polygama (A. polygama)* and is also found in tobacco, tea, coffee and other fruits [76–78]. It is an important aroma constitute of cigar, tobacco and tea and is largely racemic (from tobacco (R)-isomer of 30% ee, from *A. polygama* (S)-isomer of 6% ee) [78]. No reported α-glucosidase activity was found for dihydroactinidiolide.

Table 2.8: *Chemical profile of ethyl acetate extract of C. gynandra leaves.*

Peak #	**Retention time (min)**	**Acquired $[M + Na]^+$ /$[M + H]^+$**	**Formula of possible structure**	**Theoretical $[M + H]^+$ / $[M + Na]^+$ *m/z***	**Calculated accurate mass (Da)**	**Possible structures**	**Mass error (ppm)**	**Observed ions**	
1	7.23	219.0990 $[M + Na]^+$	$C_{11}H_{16}O_3$	219.0997	196.1099	Aspergone E	-3.0	219.0990	$[M + Na]^+$
								197.1172	$[M + H]^+$
								179.1064	$[M + H]^+ - H_2O$
2	9.58	203.1055 $[M + Na]^+$	$C_{11}H_{16}O_2$	203.1048	180.1150	Dihydroactinidiolide	3.4	203.1055	$[M + Na]^+$
								181.1240	$[M + H]^+$
3	13.07	599.3914 $[M + Na]^+$	$C_{34}H_{56}O_7$	599.3924	576.4026	Cleogynone A	-1.7	599.3907	$[M + Na]^+$
								542.3971	$[M - H_2O - OH]^+$
								541.3893	$[M - 2H_2O]^+$
								499.3787	$[M - CH_3CO_2H - H_2O]$
								481.3682	$[M - CH_3CO_2H - 2H_2O]$
								439.3576	$[M - 2CH_3CO_2H - H_2O]$
								421.3470	$[M - 2CH_3CO_2H - 2H_2O]$
								413.3056	$[M - C_7H_{14}O_3 - H_2O]$
								277.2168	$[M - C_{16}H_{28}O_5]$
4	14.82	304.2620 $[M + Na]^+$	$C_{18}H_{35}NO$	304.2616	281.2719	Unidentified	1.3	304.2620	
								282.2801	
								283.2841	
5	15.31	593.2765 $[M + H]^+$	$C_{34}H_{40}O_9$	593.2751	592.2672	Unidentified	1.9	593.2753	
								533.2540	
								505.2237	
								461.2320	
								447.2166	
6	15.88	621.3076 $[M + H]^+$	$C_{36}H_{44}O_9$	621.3064	620.2985	Unidentified	2.4	621.3079	
								593.2768	
								561.2867	
								535.2715	
								507.2766	

								461.2342	
								447.2185	
								435.2546	
								419.2233	
								405.2083	
								132.1035	
								86.0982	

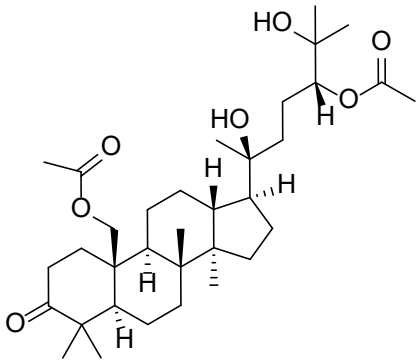

Peak 3: Cleogynone A (**1**)

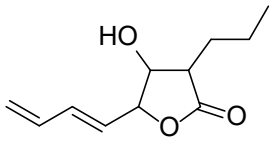

Peak 1: Aspergone E (**2**)

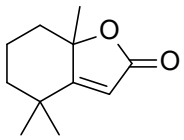

Peak 2: Dihydroactinidiolide (**3**)

Figure 2.6: *Chemical structures of compounds identified from the extracts EtOAc and pEtOAc.*

2.4.10.2. Chemical profiling ethanol extract

The EtOH extract showed peaks mainly within the 9 to 18-minute range of the 25-minute chromatogram with a few peaks in the 0 to 9-minute. This distribution of peaks reveals that the extract is composed mainly medium-polar to non-polar constituents. The chemical fingerprint of the extract generated using UPLC-QTOF-MS operating in both the ESI negative and positive mode is shown in Figure 2.11. A total of fifteen peaks were selected for identification of the chemical structures based on their mass data and their purity (no interfering peaks), using both the ESI positive and negative modes. Of these, five compounds were tentatively identified (Table 2.9 and Table 2.10).and their chemical structures are shown in Figure 2.12, the remaining could not be identified. Using the ESI negative mode three compounds within the range 0 – 4 min, *m/z* 341.1067 retention time

0.61 min, *m/z* 609.1453 retention time 3.42 min and at *m/z* 593.1506 retention time 3.80 min, were tentatively identified as sucrose, rutin (**4**) and nicotiflorin (**5**). The compounds represented by the peaks 4, 5, 6, 7 and 8 all have exact masses greater than 700 (see Table 2.9) and using their exact masses and molecular formulas obtained using MassLynx as well as the Dictionary of Natural Products and LIPID MAPS® Lipidomics Gateway (online libraries), these compounds fall in the category, glycerolipids. To the best of our knowledge, however, the compounds represented by the peaks described could not be matched with any known compounds, based on their MS fragmentation. Examples of such glycerolipids are shown in Figure 2.13. Naturally occurring triacylglycerols are biosynthesised from a pool of five or more fatty acids, and derivatives with two or three different acyl groups are usually formed; symmetrical triacylglycerols are less often produced [79]. The number of possible triacylglycerols increases rapidly with the number of different acids present in the fatty acid pool. With two acids, eight triacylglycerols (including enantiomers) are formed. The number of possible triacylglycerols that can be formed from 20 fatty acids, with all isomers distinguished (including optical isomers) is 8000 [79].

Using the ESI positive mode one compound, *m/z* 181.1223 retention time 6.91 min was tentatively identified as dihydroactinidiolide, and another compound, *m/z* 599.3922 retention time 10.63 min was identified as cleogynone A. These were also tentatively identified from the EtOAc extract and discussed in section 2.4.10.1 earlier, and are shown in Figure 2.10, above.

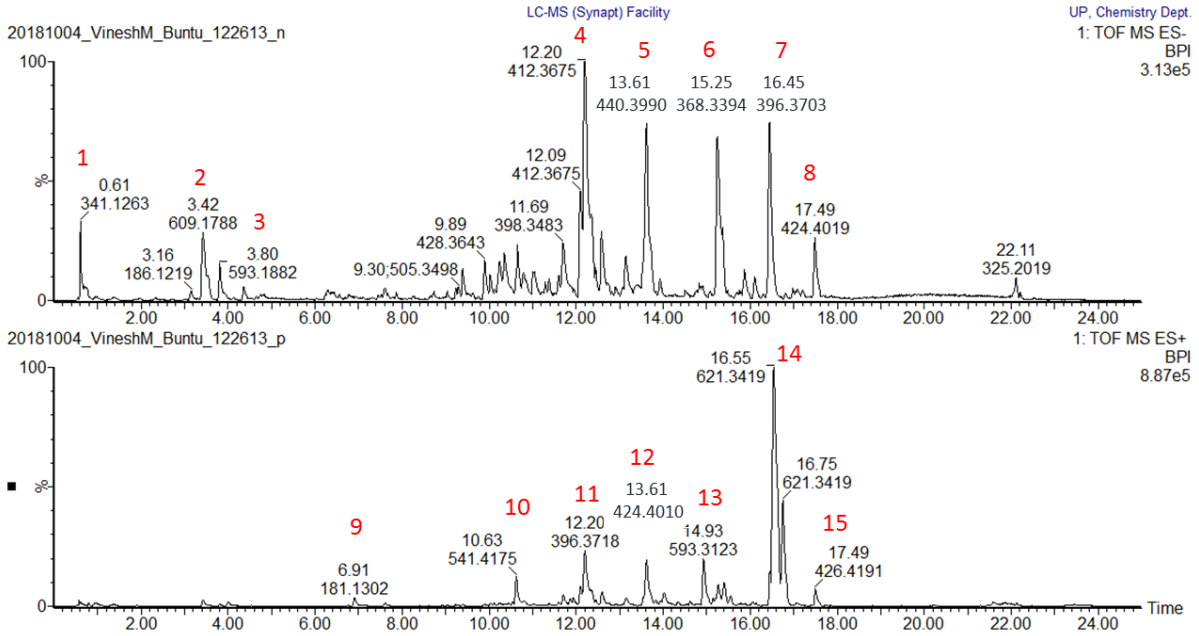

Figure 2.7:*ESI positive and negative mode BPI chromatogram of the EtOH extract. A total of five compounds were identified. From the ESI positive mode a novel compound cleogynone A (peak 10) was identified and dihydroactinidiolide (peak 9) was tentatively identified, while in the ESI negative mode three compounds were tentatively identified as sucrose (peak 1), rutin (peak 2) and nicotiflorin (peak 3). The remaining peaks could not be identified.*

Rutin is a constituent of many plants, presence in over 30 families, mostly dicotyledons [80–83]. It is also produced by *Aspergillus flavus L7*[84]. Its first isolation was from *Ruta graveolens*. Some of its biological importance involve anti-oedemic, anti-inflammatory, anti-thrombotic, anti-hypotensive, spasmolytic, anti-haemorrhagic properties, neuroprotective, antioxidant and anti-HIV activity [81–84].

Kaempferol-3-O-rutinoside or nicotiflorin has been isolated from numerous plant species, examples are *Sophora japonica, Chromolaena moritziana, Mitracarpus scaber* [85]. It was reported to possess antimicrobial activity against *E. coli, P. aeruginosa, P. mirabilis, K. pneumonia, A. baumannii, S. aureus, E. faecalis, B. subtilis, C. albicans, C.* krusei [86], it is thus one of the components responsible for growth inhibition activity against *E. coli* and *S. aureus* in this study.

Table 2.9:*Chemical profile of the ethanol extract using the ESI negative mode.*

Peak #	Retention time (min)	Acquired $[M - H]^-$/ $[M + Na - 2H]^-$	Formula of possible structure	Theoretical $[M - H]^-$ / $[M + Na - 2H]^-$ *m/z*	Calculated accurate mass (Da)	Possible structures	Mass error (ppm)	Observed ions	
1	0.61	341.1067 $[M - H]^-$	$C_{12}H_{22}O_{11}$	341.1084	342.1162	Sucrose	-5.0	341.1064	$[M - H]^-$
								179.0520	$[M - C_6H_{11}O_6]^-$
2	3.42	609.1453 $[M - H]^-$	$C_{27}H_{30}O_{16}$	609.1456	610.1534	Rutin	-0.5	609.1453	$[M - H]^-$
								302.0366	$[M - C_{15}H_{10}O_7]^-$
								301.0313	$[M - C_{15}H_9O_7]^-$
								300.0252	$[M - C_{15}H_8O_7]^-$
								271.0221	$[M - C_{14}H_7O_6]^-$
3	3.80	593.1506 $[M - H]^-$	$C_{27}H_{30}O_{15}$	593.1506	594.1585	Nicotiflorin	0.0	593.1506	$[M - H]^-$
								286.0406	$[M - C_{15}H_{10}O_6]^-$
								285.0374	$[M - C_{15}H_9O_6]^-$
								284.0303	$[M - C_{15}H_8O_6]^-$
								255.0270	$[M - C_{14}H_7O_5]^-$
								227.0323	$[M - C_{13}H_7O_4]^-$
4	12.20	847.6786 $[M + Na - 2H]^-$	$C_{53}H_{94}O_6$	847.6792	826.7050	Unidentified, possibly glycerolipid	-0.7	847.0771	
								512.2087	
								412.3418	
								368.3524	
								366.3347	
								310.3097	
								183.0104	
								130.0851	
5	13.61	903.7391 $[M + Na - 2H]^-$	$C_{57}H_{102}O_6$	903.7418	882.7676	Unidentified, possibly glycerolipid	-3.0	903.7391	
								881.7589	
								555.2868	
								540.2997	
								440.3727	
								396.3819	
								394.3679	
								183.0093	
								130.0845	
6	15.25	737.6425 $[M + Na - 2H]^-$	$C_{47}H_{88}O_4$	737.6424	716.6683	Unidentified, possibly glycerolipid	0.1	737.6425	
								468.2411	
								369.3182	
								368.3152	
								324.3261	
								183.0097	
								130.0849	
								100.9314	
7	16.45	793.7080 $[M + H]^-$	$C_{53}H_{94}O_4$	793.7074	794.7152	Unidentified, possibly glycerolipid	0.8	793.7080	
								497.2759	
								496.2740	
								397.3506	
								396.3472	
								352.3580	
								183.0084	
								130.0849	
								100.9300	
8	17.49	849.7698 $[M + H]^-$	$C_{57}H_{102}O_4$	849.7700	850.7778	Unidentified	-0.2	849.7698	
								525.3071	
								524.3051	
								425.3819	
								424.3778	
								380.3889	
								339.2003	
								183.0089	
								130.0847	
								100.9314	

Table 2.10:*Chemical profile of the ethanol extract using the ESI positive mode.*

Peak #	Retention time (min)	Acquired $[M + Na]^+$ /$[M + H]^+$	Formula of possible structure	Theoretical $[M + H]^+$ / $[M + Na]^+$ *m/z*	Calculated accurate mass (Da)	Possible structures	Mass error (ppm)	Observed ions	
9	6.91	181.1223 $[M - H]^+$	$C_{11}H_{16}O_2$	181.1229	180.1150	Dihydroactinidiolide	-3.3	203.1044	$[M + Na]^+$
								181.1229	$[M + H]^+$
10	10.63	599.3922 $[M + Na]^+$	$C_{34}H_{56}O_7$	599.3924	576.4026	Cleogynone A	-0.7	599.3922	$[M + Na]^+$
								542.3928	$[M - H_2O - OH]^+$
								541.3894	$[M - 2H_2O]^+$
								499.3787	$[M - CH_3CO_2H - H_2O]^+$
								481.3677	$[M - CH_3CO_2H - 2H_2O]^+$
								439.3567	$[M - 2CH_3CO_2H - H_2O]^+$
								421.3470	$[M - 2CH_3CO_2H - 2H_2O]^+$
11	12.20	396.3717				unidentified			
12	13.61	424.3792				unidentified			
13	14.93	975.5656 $[M - H]^+$	$C_{53}H_{82}O_{16}$	975.5681	974.5603	unidentified	-2.6	593.2753	
								533.2540	
								505.2237	
								461.2320	
								447.2166	
14	16.55	621.3080 $[M - H]^+$	$C_{36}H_{44}O_9$	621.3064	620.2985	unidentified	2.6	621.3079	
								593.2768	
								561.2867	
								535.2715	
								507.2766	
								461.2342	
								447.2185	
								435.2546	
								419.2233	
								405.2083	
								132.1035	
								86.0982	
15	17.54	797.5174 $[M + Na]^+$	$C_{45}H_{74}O_{10}$	797.5180	774.5282	Unidentified, possibly glycerol	-0.8	915.5291	
								797.5174	
								686.5311	
								621.3111	
								558.4856	
								448.3759	
								426.3937	
								408.3828	
								86.0962	

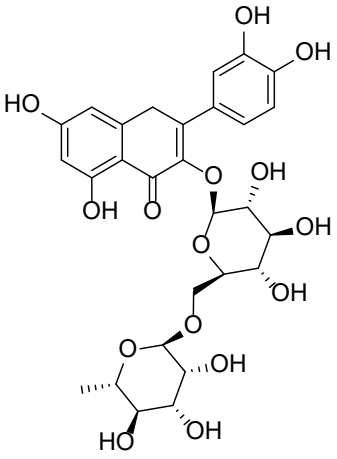

Peak 2: Rutin (**4**)

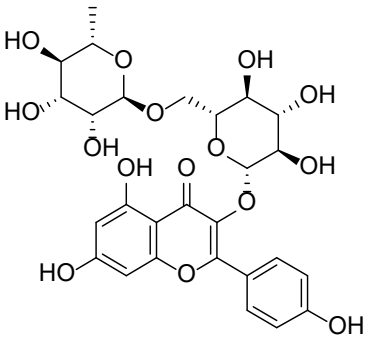

Peak 3: Nicotiflorin (**5**)

Figure 2.82:*Chemical structures of nicotiflorin and rutin, two of the compounds identified from the EtOH extract.*

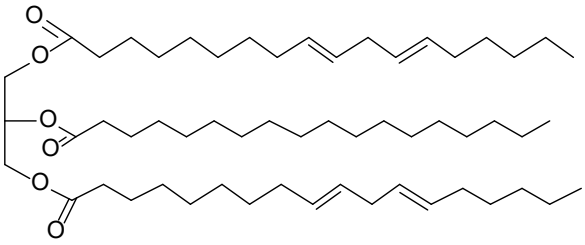

a,ß-Dilinoleomyristin (**6**)

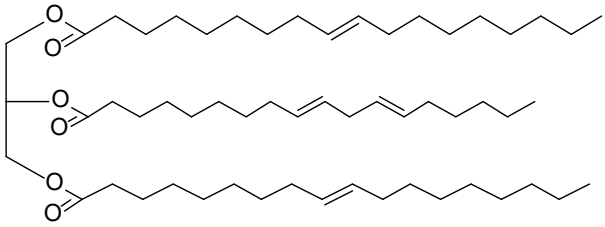

Glycerol 2-(9Z,12Z-octadecadienoate) 1,3-di-(9Z-octadecenoate) (**7**)

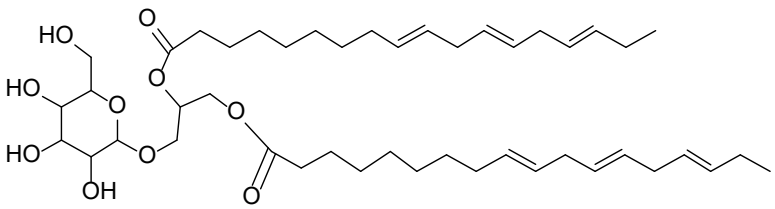

Glycerol 1,2-dialkanoates; Glycerol 1,2-di-(9Z,12Z,15Z-octadecatrienoate), 3-O-ß-D-Galactopyranoside (**8**)

Figure 2.93:*Chemical structures of some examples of compounds belonging to the category glycerolipids.*

2.4.10.3. Chemical profiling *n*-hexane extract

The *n*-hexane extract showed peaks only within the 6 to 25-minute range of the 25-minute chromatogram. This distribution of peaks reveals that the extract is composed mainly non-polar constituents. Chemical profiling of the *n*-hexane extract was necessary for quality control purposes. The chemical fingerprint of the extract generated using UPLC-QTOF-MS operating in both the ESI positive mode is shown in Figure 2.14. Using the ESI positive modes, eight major peaks were analysed resulting in tentative identification of one compound, namely, dihydroactinidiolide (peak 1), and the identification of cleogynone A (peak 2), both which had already been identified as present in EtOH and EtOAc extracts, the rest could not be identified. The compounds represented by the peaks 4, 5, 6, 7 and 8 all have exact masses greater than 700 and were found to fall in the category glycerolipids, similar components as in the case of EtOH extract and could not be matched with any known compounds, comparing their MS fragmentation, to the best of our knowledge.

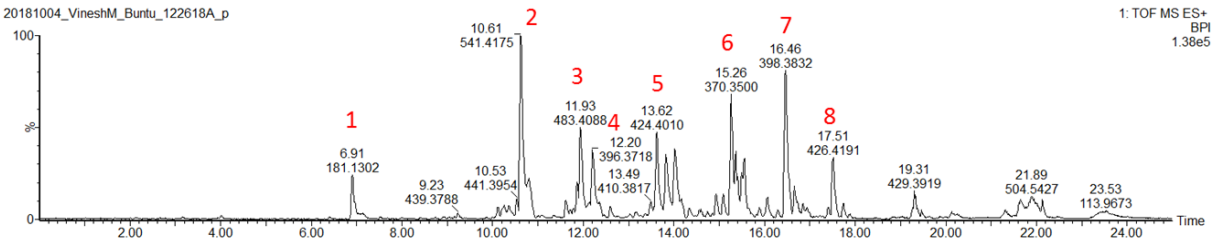

Figure 2.10: *ESI positive mode BPI chromatogram of the n-hexane extract. Eight peaks were selected for identification. Cleogynone A (peak 2) was identified and dihydroactinidiolide (peak 1) was tentatively identified, peak 3 could not be identified, while peak 4, 5, 6, 7 and 8 were found to belong to the category of glycerol lipids but could not be identified.*

This extract was further fractionated towards isolating, purifying and identifying the active ingredients. And several compounds were isolated and their structures elucidated in chapter 4.

2.5. Conclusion

This preliminary assessment opens stage for further studies veered at identifying the compounds responsible for activity. In particular, this may present drug leads for future discoveries to add to the medicines bank as the world is in search for new drugs in combatting the increasing incidences of chronic diseases. In chapter 3 work towards identification of some ingredients that may be responsible for the α-glucosidase inhibition of EtOAc extract which exhibited greater than 90% inhibition activity and an IC_{50} value 25.40 µg/ml, a better activity than the positive control, will be discussed. The partitioning of the EtOAc was effective in concentrating bioactive components in the pEtOAc extract exhibiting an IC_{50} value 8.75 ug/ml, almost 3 times better than that of the crude extract and thus meriting further studies towards identification of the ingredients responsible for activity, discussed in the next chapter. Furthermore, the *n*-hexane extract displayed high activity against lung cancer cell line A549 compared to other extracts prepared *via* the sequential extraction method and therefore merits further analysis and possible identification of the bioactive compounds, and in chapter 4 the isolation of cancer active compounds from this extract and further cancer assessment will be discussed. It can further be concluded, in this chapter, that the EtOH extract can be developed as an antibacterial, particularly for management of sicknesses such as diarrhoea which may be caused by bacteria such as *E. coli.* Furthermore, the *C. gynandra* leaf extracts are seen to generally possess four or five major common peaks at medium-polar to non-polar end on UPLC MS analysis. Some of the compounds represented by these common peaks were tentatively identified, while one compound isolated in this study was found present in the extracts EtOAc, EtOH and *n*-hexane. Most of the components represented by these peaks could not be identified and future work should involve their isolation and identification. Further extracts showed varying biological activities against enzymatic assays xanthine oxidase inhibition, renin inhibition and HMGCoA reductase inhibition and certainly studies involving identifying the compounds

represented by the common peaks may help to unearthing either novel compounds or revealing known compounds responsible for such biological properties.

The results in this chapter reveal that the leaves of *C. gynandra* possess medicinal ingredients which can be developed into agents, either as nutraceutical, functional foods, herbal medicines or pharmaceutical, potentially, for management of and protection against various diseases. The inherent ingredients have the potential for treatment of cancer, hyperglycaemia, cholesterol, management of heart diseases, management and prevention of gout, management of hypertension as well as treatment and prevention of diarrhoea, to name a few.

2.6. References

1. Cechinel-Filho, V. *Plant Bioactives and Drug Discovery*; John Wiley & Sons, Incorporated, 2012;
2. Veeresham, C. Natural products derived from plants as a source of drugs. *J. Adv. Pharm. Technol. Res.***2012**, *3*, 200–201, doi:10.4103/2231-4040.104709.
3. Cragg, G.M.; Grothaus, P.G.; Newman, D.J. Natural Products in drug discovery : Recent advances. In *Plant Bioactives and Drug Discovery: Principles, Practice, and Perspectives.*; 2012; pp. 1–27.
4. Queiroz, E.F.; Hostettmann, K.; Wolfender, J.L. Modern Approaches in the Search for New Active Compounds from Crude Extracts of Natural Sources. In *Plant Bioactives and Drug Discovery: Principles, Practice, and Perspectives*; 2012; pp. 43–80 ISBN 9780470582268.
5. Palmer, M.V.; Ting, S.S.T. Applications for supercritical fluid technology in food processing. *Food Chem.***1995**, *52*, 345–352, doi:10.1016/0308-8146(95)93280-5.
6. Banchero, M.; Manna, L. Investigation of the piroxicam/hydroxypropyl-β-cyclodextrin inclusion complexation by means of a supercritical solvent in the presence of auxiliary agents. *J. Supercrit. Fluids***2011**, *57*, 259–266, doi:10.1016/j.supflu.2011.04.006.
7. Díaz-Reinoso, B.; Moure, A.; Domínguez, H.; Parajó, J.C. Supercritical CO_2 extraction and purification of compounds with antioxidant activity. *J. Agric. Food Chem.***2006**, *54*, 2441–2469, doi:10.1021/jf052858j.
8. Del Valle, J.M.; Mena, C.; Budinich, M. Extraction of garlic with supercritical CO_2 and conventional organic solvents. *Brazilian J. Chem. Eng.* 2008, *25*, 535–542.
9. Tuan, D.Q.; Ilangantileket, S.G. Liquid CO_2 extraction of essential oil from Star anise fruits (Illicium verum H.). *J. Food Eng.***1997**, *31*, 47–57, doi:10.1016/S0260-8774(96)00030-1.
10. Machmudah, S.; Shotipruk, A.; Goto, M.; Sasaki, M.; Hirose, T. Extraction of Astaxanthin from Haematococcus p luvialis Using Supercritical CO_2 and Ethanol as Entrainer. *Ind. Eng. Chem. Res.***2006**, *45*, 3652–3657, doi:10.1021/ie051357k.
11. Harvey, A.L. Natural products in drug discovery. *Drug Discov. Today***2008**, *13*, 894–901, doi:10.1016/j.drudis.2008.07.004.
12. Harvey, A.L. Screening Methods for Drug Discovery from Plants. In *Plant Bioactives and Drug Discovery: Principles, Practice, and Perspectives*; 2012; pp. 489–498 ISBN 9780470582268.
13. Kamtekar, S.; Keer, V.; Patil, V. Estimation of phenolic content, flavonoid content, antioxidant and alpha amylase inhibitory activity of marketed polyherbal formulation. *J. Appl. Pharm. Sci.***2014**, *4*, 61–65, doi:10.7324/JAPS.2014.40911.
14. de Sales, P.M.; de Souza, P.M.; Simeoni, L.A.; Magalhães, P. de O.; Silveira, D. α-amylase inhibitors: A review of raw material and isolated compounds from plant source. *J. Pharm. Pharm. Sci.***2012**, *15*, 141–183, doi:10.18433/j35s3k.
15. Su, C.H.; Hsu, C.H.; Ng, L.T. Inhibitory potential of fatty acids on key enzymes related to type 2 diabetes. *BioFactors***2013**, *39*, 415–421, doi:10.1002/biof.1082.
16. Kim, J.S.; Kwon, C.S.; Son, K.H. Inhibition of alpha-glucosidase and amylase by luteolin, a flavonoid. *Biosci. Biotechnol. Biochem.***2000**, *64*, 2458–2461,

doi:10.1271/bbb.64.2458.

17. Rosa, M.M.; Dias, T. Commonly used endocrine drugs. *Handb. Clin. Neurol.***2014**, doi:10.1016/B978-0-7020-4087-0.00054-1.

18. Hanefeld, M.; Mertes, G. Treatment: Alpha Glucosidase Inhibitors. *Ref. Modul. Biomed. Sci.***2018**, doi:10.1016/B978-0-12-801238-3.65370-9.

19. Yin, Z.; Zhang, W.; Feng, F.; Zhang, Y.; Kang, W. α-Glucosidase inhibitors isolated from medicinal plants. *Food Sci. Hum. Wellness***2014**, *3*, 136–174, doi:10.1016/j.fshw.2014.11.003.

20. Tobert, J.A. Lovastatin and beyond: The history of the HMG-CoA reductase inhibitors. *Nat. Rev. Drug Discov.***2003**, *2*, 517–526, doi:10.1038/nrd1112.

21. Marahatha, R.; Basnet, S.; Bhattarai, B.R.; Budhathoki, P.; Aryal, B.; Adhikari, B.; Lamichhane, G.; Poudel, D.K.; Parajuli, N. Potential natural inhibitors of xanthine oxidase and HMG-CoA reductase in cholesterol regulation: in silico analysis. *BMC Complement. Med. Ther.***2021**, *21*, 1–11, doi:10.1186/s12906-020-03162-5.

22. Holdgate, G.A.; Ward, W.H.J.; McTaggart, F. Molecular mechanism for inhibition of 3-hydroxy-3-methylglutaryl CoA (HMG-CoA) reductase by rosuvastatin. *Biochem. Soc. Trans.***2003**, *31*, 528–531, doi:10.1042/BST0310528.

23. Koning, A.J.; Roberts, C.J.; Wright, R.L. Different subcellular localization of Saccharomyces cerevisiae HMG-CoA reductase isozymes at elevated levels corresponds to distinct endoplasmic reticulum membrane proliferations. *Mol. Biol. Cell***1996**, *7*, 769–789, doi:10.1091/mbc.7.5.769.

24. Jones, P.H. Comparing HMG-CoA reductase inhibitors. *Clin. Cardiol.***2003**, *26*, 15–20, doi:10.1002/clc.4960261306.

25. Istvan, E.S.; Deisenhofer, J. The structure of the catalytic portion of human HMG. *Biochim. Biophys. Acta***2000**, *1529*, 9–18.

26. Charan, J.; Riyad, P.; Ram, H.; Purohit, A.; Ambwani, S.; Kashyap, P.; Kumar, S.; Singh, G.; Alqarawi, A.A.; Hashem, A.; et al. *Ameliorations in the Biomarker Indices of Dyslipidemia and Atherosclerotic Plaque by the Inhibition of HMG – CoA Reductase and Antioxidant Potential of Phytoconstituents of an Aqueous Seed Extract of Acacia Senegal (L .) Willd in Rabbits*; 2021;

27. Stanton, A. Potential of renin inhibition in cardiovascular disease. *JRAAS - J. Renin-Angiotensin-Aldosterone Syst.***2003**, *4*, 6–10, doi:10.3317/jraas.2003.008.

28. Jensen, C.; Herold, P.; Brunner, H.R. Aliskiren: The first renin inhibitor for clinical treatment. *Nat. Rev. Drug Discov.***2008**, *7*, 399–410, doi:10.1038/nrd2550.

29. Klinenberg, J.R.; Goldfinger, S.E.; Seegmiller, J.E. The Effectiveness of the Xanthine Oxidase Inhibitor Allopurinol in the Treatment of Gout. *Am. Coll. Physicians***1965**, *62*, 639–647.

30. Carcassi, A.; Marcolongo, R.; Marinello, E.; Riario-Sforza, G.; Boggiano, C. Liver xanthine oxidase in gouty patients. *Arthritis Rheum.***1969**, *12*, 17–20, doi:10.1002/art.1780120104.

31. Guerciolini, R.; Szumlanski, C.; Weinshilboum, R.M. Human liver xanthine oxidase: Nature and extent of individual variation. *Clin. Pharmacol. Ther.***1991**, *50*, 663–672, doi:10.1038/clpt.1991.205.

32. Voravuthikunchai, S.P.; Limsuwan, S. Medicinal Plant Extracts as Anti–*Escherichia coli* O157:H7 Agents and Their Effects on Bacterial Cell Aggregation. *J. Food*

*Prot.***2006**, *69*, 2336–2341, doi:10.4315/0362-028X-69.10.2336.

33. Maregesi, S.M.; Pieters, L.; Ngassapa, O.D.; Apers, S.; Vingerhoets, R.; Cos, P.; Berghe, D.A.V.; Vlietinck, A.J. Screening of some Tanzanian medicinal plants from Bunda district for antibacterial, antifungal and antiviral activities. *J. Ethnopharmacol.***2008**, *119*, 58–66, doi:10.1016/j.jep.2008.05.033.

34. Blount, Z.D. The unexhausted potential of *E. coli*. *Elife***2015**, *4*, 1–12, doi:10.7554/eLife.05826.

35. Leimbach, A.; Hacker, J.; Dobrindt, U. *E. coli* as an All-Rounder: The Thin Line Between Commensalism and Pathogenicity. *Curr. Top. Microb. Immunol.***2013**, *358*, 3–32.

36. Jahani, S.; Saeidi, S.; Javadian, F.; Akbarizadeh, Z.; Sobhanizade, A. Investigating the Antibacterial Effects of Plant Extracts on Pseudomonas aeruginosa and Escherichia coli. *Int. J. Infect.***2016**, *3*, doi:10.17795/iji-34081.

37. Chambers, H.F.; DeLeo, F.R. Waves of Resistance: Staphylococcus aureus in the Antibiotic Era. *Nat Rev Microbiol.***2009**, *7*, 629–641, doi:10.1038/nrmicro2200.Waves.

38. Chukwuka, K.S.; Ikheloa, J.O.; Okonko, I.O.; Moody, J.O.; Mankinde, T.A. The antimicrobial activities of some medicinal plants on *Escherichia coli* as an agent of diarrhea in livestock. *Adv. Appl. Sci. Res.***2011**, *2*, 37–48.

39. S. C. Gupta, J. H. Kim, S. Prasad, B.B.A. Regulation of survival, proliferation, invasion, angiogenesis, and Cancer metastasis of tumor cells through modulation of inflammatory pathways by nutraceuticals. *Cancer Metastasis Rev***2010**, *29*, 405–434, doi:10.1007/s10555-010-9235-2.Regulation.

40. Agency, I. Cancer WHO. *Cancer* 2017.

41. Molatlhegi, R.P.; Phulukdaree, A.; Anand, K.; Gengan, R.M.; Tiloke, C.; Chuturgoon, A.A. Cytotoxic effect of a novel synthesized carbazole compound on A549 lung cancer cell line. *PLoS One***2015**, *10*, 1–14, doi:10.1371/journal.pone.0129874.

42. Minna, J.D.; Roth, J.A.; Gazdar, A.F. Focus on lung cancer. *Cancer Cell***2002**, *1*, 49–52, doi:10.1016/S1535-6108(02)00027-2.

43. Gibbs, J.B. Mechanism-based target identification and drug discovery in cancer research. *Science (80-.).***2000**, *287*, 1969–1973, doi:10.1126/science.287.5460.1969.

44. Chothani, D.L.; Patel, M.B.; Mishra, S.H. HPTLC Fingerprint Profile and Isolation of Marker Compound of Ruellia tuberosa . *Chromatogr. Res. Int.***2012**, *2012*, 1–6, doi:10.1155/2012/180103.

45. Taleuzzaman, M.; Ali, S.; Sj, G.; Ss, I. Ultra Performance Liquid Chromatography (UPLC) - A Review. **2015**, *2*.

46. Chawla, G.; Ranjan, C. Principle, Instrumentation, and Applications of UPLC: A Novel Technique of Liquid Chromatography. *Open Chem. J.***2016**, *3*, 1–16, doi:10.2174/1874842201603010001.

47. de Villiers, A.; Lestremau, F.; Szucs, R.; Gélébart, S.; David, F.; Sandra, P. Evaluation of ultra performance liquid chromatography. Part I. Possibilities and limitations. *J. Chromatogr. A***2006**, *1127*, 60–69, doi:10.1016/j.chroma.2006.05.071.

48. de Hoffmann, E.; Stroobant, V. *Mass spectrometry*; Third Edit.; John Wiley & Sons, Ltd: Chinchester, England, 2007; ISBN 9780470033104.

49. Chan, E.C.Y.; Yap, S.L.; Lau, A.J.; Leow, P.C.; Toh, D.F.; Koh, H.L. Ultra-

performance liquid chromatography/time-of-flight mass spectrometry based metabolomics of raw and steamed Panax notoginseng. *Rapid Commun. Mass Spectrom.***2007**, *21*, 519–528, doi:10.1002/rcm.2864.

50. Chweya, J.A.; Mnzava, N.A. *Cat ' s whiskers. Cleome gynandra L. Promoting the conservation and use of underutilized and neglected crops*; 11th ed.; The International Plant Genetic Resources Institute: Rome, Italy, 1997; ISBN 9290433035.

51. Ekpong, B. Effects of seed maturity, seed storage and pre-germination treatments on seed germination of *cleome* (*Cleome gynandra L.*). *Sci. Hortic. (Amsterdam).***2009**, *119*, 236–240, doi:10.1016/j.scienta.2008.08.003.

52. Mishra, S.S.; Moharana, S.K.; Dash, M.R. Review on *Cleome gynandra.Int. J. Res. Pharm. Chem.***2011**, *1*, 681–689.

53. Mnzava, N.A.; Chigumira Ngwerume, F. *Cleome gynandra L*. Available online: https://www.cabi.org/isc/datasheet/119802 (accessed on Aug 9, 2021).

54. Jansen Van Rensburg, W.S.; Venter, S.L.; Netshiluvhi, T.R.; Van Den Heever, E.; Vorster, H.J.; De Ronde, J. a. Role of indigenous leafy vegetables in combating hunger and malnutrition. *South African J. Bot.***2004**, *70*, 52–59, doi:10.1016/S0254-6299(15)30268-4.

55. Nyalala, S.; Grout, B. African spider flower (*Cleome gynandra L./Gynandropsis gynandra* (L.) Briq.) as a red spider mite (Tetranychus urticae Koch) repellent in cut-flower rose (*Rosa hybrida L.*) cultivation. *Sci. Hortic. (Amsterdam).***2007**, *114*, 194–198, doi:10.1016/j.scienta.2007.06.010.

56. Kamatenesi-Mugisha, M.; Oryem-Origa, H. Medicinal plants used to induce labour during childbirth in western Uganda. *J. Ethnopharmacol.***2007**, *109*, 1–9, doi:10.1016/j.jep.2006.06.011.

57. Gao, Z.J.; Liu, J.B.; Xiao, X.G. Purification and characterisation of polyphenol oxidase from leaves of *Cleome gynandra L*. *Food Chem.***2011**, *129*, 1012–1018, doi:10.1016/j.foodchem.2011.05.062.

58. Bala, A.; Kar, B.; Haldar, P.K.; Mazumder, U.K.; Bera, S. Evaluation of anticancer activity of *Cleome gynandra* on Ehrlich's Ascites Carcinoma treated mice. *J. Ethnopharmacol.***2010**, *129*, 131–134, doi:10.1016/j.jep.2010.03.010.

59. Narendhirakannan, R.T.; Subramanian, S.; Kandaswamy, M. Free radical scavenging activity of *Cleome gynandra L* . leaves on adjuvant induced arthritis in rats. **2005**, 71–80.

60. Bala, A.; Haldar, P.K.; Kar, B.; Naskar, S.; Saha, P.; Kundusen, S.; Gupta, M.; Mazumder, U.K. Antioxidant activity of the fractions of *Cleome gynandra* promotes antitumor activity in ehrlich ascites carcinoma. *Asian J. Chem.***2011**, *23*, 5055–5060.

61. Sridhar, N.; Surya Kiran, B.V.V.S.; Tharaka Sasidhar, D.; Kanthal, L.K. In vitro antimicrobial screening of methanolic extracts of *Cleome chelidonii* and *Cleome gynandra*. *Bangladesh J. Pharmacol.***2014**, *9*, 161–166, doi:10.3329/bjp.v9i2.17759.

62. Kapoor, B.B.S.; Mishra, R. Antimicrobial Screening of Some capparidaceous Medicinal Plants of North-West Rajasthan. **2013**, *1*, 20–22.

63. J. Ranjitha; Bakiyalakshmi, K.; Anand, M.; Sudha, P.N. Phytochemical Investigation of *n*-Hexane Extract of Leaves of *Cleome gynandra*. *Asian J. Chem.***2009**, *21*, 3455–3458.

64. Uma, B.; Prabhakar, K.; Rajendran, S.; Sarayu, Y.L. A study on phytochemical

screening and antimicrobial activity of *Cleome gynandra L.* against infectious infantile diarrhoea. *Pharmacologyonline***2009**, *2*, 12–16.

65. Moyo, M.; Amoo, S.O.; Ncube, B.; Ndhlala, A.R.; Finnie, J.F.; Van Staden, J. Phytochemical and antioxidant properties of unconventional leafy vegetables consumed in southern Africafile:///C:/Users/u16401655/Downloads/Eloff 1998.pdf file:///C:/Users/u16401655/Downloads/Masoko 2005.pdf. *South African J. Bot.***2013**, *84*, 65–71, doi:10.1016/j.sajb.2012.09.010.

66. Schönfeldt, H.C.; Pretorius, B. The nutrient content of five traditional South African dark green leafy vegetables-A preliminary study. *J. Food Compos. Anal.***2011**, *24*, 1141–1146, doi:10.1016/j.jfca.2011.04.004.

67. Van Jaarsveld, P.; Faber, M.; van Heerden, I.; Wenhold, F.; Jansen van Rensburg, W.; van Averbeke, W. Nutrient content of eight African leafy vegetables and their potential contribution to dietary reference intakes. *J. Food Compos. Anal.***2014**, *33*, 77–84, doi:10.1016/j.jfca.2013.11.003.

68. Uzilday, B.; Turkan, I.; Sekmen, A.H.; Ozgur, R.; Karakaya, H.C. Comparison of ROS formation and antioxidant enzymes in *Cleome gynandra* (C 4) and *Cleome spinosa* (C 3) under drought stress. *Plant Sci.***2012**, *182*, 59–70, doi:10.1016/j.plantsci.2011.03.015.

69. Bala, A.; Kar, B.; Karmakar, I.; Kumar, R.B.S.; Haldar, P.K. Antioxidant activity of Cat's whiskers flavonoid on some reactive oxygen and nitrogen species generating inflammatory cells is mediated by scavenging of free radicals. *Chin. J. Nat. Med.***2012**, *10*, 321–327, doi:10.1016/S1875-5364(12)60065-X.

70. Das, P.C.; Patra, A.; Mandal, S.; Mallick, B.; Das, A.; Chatterjee, A. Cleogynol, a novel dammarane triterpenoid from *Cleome gynandra*. *J. Nat. Prod.***1999**, *62*, 616–618, doi:10.1021/np9803528.

71. Waters Corporation MV-10 ASFE System: System guide for ChromScope v1.20 Available online: https://www.waters.com/webassets/cms/support/docs/715003818reva.pdf (accessed on Apr 18, 2021).

72. Eloff, J.N. A sensitive and quick microplate method to determine the minimal inhibitory concentration of plant extracts for bacteria. *Planta Med.***1998**, *64*, 711–713, doi:10.1055/s-2006-957563.

73. Masoko, P.; Eloff, J.N. The diversity of antifungal compounds of six South African Terminalia species (Combretaceae) determined by bioautography. *African J. Biotechnol.***2005**, *4*, 1425–1431, doi:10.5897/AJB2005.000-3183.

74. Sangameswaran, B.; Venkataraman, S.; ShriShastikaa, S.; Sudhakaran, S.; Suganya, E.; Sureshkumarand, S.; Vasavi, P. Study of Preliminary Phytochemical Anti-Diabetic Property of *Cleome Gynandra.World J. Pharm. Res. World J. Pharm. Res. SJIF Impact Factor***2017**, *6*, 598–614, doi:10.20959/wjpr201712-9549.

75. Kong, F.; Zhao, C.; Hao, J.; Wang, C.; Wang, W.; Huang, X.; Zhu, W. New α-glucosidase inhibitors from a marine sponge-derived fungus, Aspergillus sp. OUCMDZ-1583. *RSC Adv.***2015**, *5*, 68852–68863, doi:10.1039/c5ra11185d.

76. Sakan, T.; Isoe, S.; Hyeon, S.B. The structure of actinidiolide, dihydroactinidiolide and actinidol. *Tetrahedron Lett.***1967**, *8*, 1623–1627, doi:10.1016/S0040-4039(00)70326-1.

77. Albone, E.S. Dihydroactinidiolide in the supracaudal scent gland secretion of the red fox. *Nature***1975**, *256*, 575, doi:10.1038/256575a0.

78. Dabdoub, M.J.; Silveira, C.C.; Lenardão, E.J.; Guerrero, P.G.; Viana, L.H.; Kawasoko, C.Y.; Baroni, A.C.M. Total synthesis of (±)-dihydroactinidiolide using selenium-stabilized carbenium ion. *Tetrahedron Lett.***2009**, *50*, 5569–5571, doi:10.1016/j.tetlet.2009.07.067.

79. Gronowitz, S.; Herslof, B.; Ohlson, R.; Toregard, B. ences in acyl group length as in 1 , 2-distearoyl-3-acetyl-sn-glycerol . Measurements were only carried out at the D-line . In 1965 Schlenk [7], measuring the ORD down to 300 nm , was able to demonstrate optical activity in several triglycerides , most. *Chem. Phys. Lipids***1975**, *14*, 174–188.

80. Hörhammer, L.; Wagner, H.; Arndt, H.G.; Kraemer, H.; Farkas, L. Syhthese natürlich vorkommender polyhydroxy-flavonol- glykoside. *Tetrahedron Lett.***1966**, *7*, 567–571, doi:10.1038/1831433c0.

81. Gullón, B.; Lú-Chau, T.A.; Moreira, M.T.; Lema, J.M.; Eibes, G. Rutin: A review on extraction, identification and purification methods, biological activities and approaches to enhance its bioavailability. *Trends Food Sci. Technol.***2017**, *67*, 220–235, doi:10.1016/j.tifs.2017.07.008.

82. Kim, H.; Kong, H.; Choi, B.; Yang, Y.; Kim, Y.; Mi, J.L.; Neckers, L.; Jung, Y. Metabolic and pharmacological properties of rutin, a dietary quercetin glycoside, for treatment of inflammatory bowel disease. *Pharm. Res.***2005**, *22*, 1499–1509, doi:10.1007/s11095-005-6250-z.

83. Kazuma, K.; Noda, N.; Suzuki, M. Malonylated flavonol glycosides from the petals of Clitoria ternatea. *Phytochemistry***2003**, *62*, 229–237, doi:10.1016/S0031-9422(02)00486-7.

84. Patil, M.P.; Patil, R.H.; Maheshwari, V.L. Biological Activities and Identification of Bioactive Metabolite from Endophytic Aspergillus flavus L7 Isolated from Aegle marmelos. *Curr. Microbiol.***2015**, *71*, 39–48, doi:10.1007/s00284-015-0805-y.

85. Nahrstedt, A.; Hungeling, M.; Petereit, F. Flavonoids from Acalypha indica. *Fitoterapia***2006**, *77*, 484–486, doi:10.1016/j.fitote.2006.04.007.

86. Orhan, D.D.; Özçelik, B.; Özgen, S.; Ergun, F. Antibacterial, antifungal, and antiviral activities of some flavonoids. *Microbiol. Res.***2010**, *165*, 496–504, doi:10.1016/j.micres.2009.09.002.

Chapter 3:

Fractionation of extracts, UPLC-QTOF-MS profiling of fractions with α-glucosidase inhibition and bacterial inhibition, and further identification of compounds using UNIFI®

3.1. Background

The biological activities of crude extracts from the leaves of *C. gynandra* were discussed in Chapter 2, *viz* the liquid-liquid partition of the ethyl acetate extract (pEtOAc) was most active for α-glucosidase inhibition while the ethanol extract was most active for the growth inhibition of *Escherichiacoli (E. coli)*.In this chapter, fractionation of the fraction pEtOAc and the ethanol extract with their α-glucosides inhibition and antibacterial properties against *E. coli* are discussed.

Bioassay-guided fractionation for α-glucosidase inhibition

Further fractionation of the fraction pEtOAc which was more active than the crude EtOAc extract against α-glucosidase in Chapter 2 is discussed here. Fractions of pEtOAc are obtained *via* column chromatography and evaluated for their α-glucosidase inhibitory activity. Selected active and abundant fractions are further assayed at different concentrations to study their behaviours at varying concentrations. Selected active fractions are further chemically profiled using UPLC-QTOF-MS towards identifying possibly known compounds.

Bioassay-guided fractionation for bacterial inhibition

The further fractionation of the EtOH extract *via* column chromatography and evaluation of the fractions for their growth inhibition of *E. colivia* thin-layer chromatographic bioautography, towards identifying the components responsible for the antimicrobial activity is discussed.

Staphylococcus aureus (*S. aureus*) inhibition was also included, only for comparative measures as the EtOH extract only showed moderate activity against *S. aureus*. Furthermore, the most active fraction(s) are chemically profiled *via* UPLC-QTOF-MS towards identifying possibly known components. Components of such potent fraction(s) are further isolated in attempts at purification using semi-preparative HPLC. The program UNIFI® was employed for the analysis of data generated by UPLC-QTOF-MS for the identification of known compounds that are constituents in the sub-fractions obtained *via* semi-preparative HPLC. The results discussed in this chapter form the basis of a discovery stage towards developing ingredients with potential as antimicrobial agents for the inhibition of *E. coli* and possibly *S. aureus*.

3.2. Type 2 diabetes and α-glucosidase inhibition

Inhibition of α-glucosidase, an enzyme involved in the digestion of carbohydrates, can significantly decrease the postprandial increase of blood glucose after a mixed carbohydrate diet and therefore can be an important strategy in the management of postprandial blood glucose level in type 2 diabetic patients and borderline patients [1]. Currently, there is renewed interest in functional foods and plant-based medicines modulating physiological effects in the prevention and cure of diabetes and obesity. Plant extracts have long been used for the ethnomedical treatment of diabetes in various systems of medicine and are currently accepted as an alternative for diabetic therapy.To mediate adverse effects of current agents and for provision of more candidates of drug choices, the search for new α-glucosidase inhibitors is necessary, and natural resources such as plants possess the potential therapeutic agents.

3.2.1 Type 2 diabetes

3.2.1.1. Brief background

High levels of sugar in the blood is termed hyperglycaemia, and this condition is a leading indicator of diabetes [2]. Uncontrolled diabetes over time leads to damage to body systems such as the nerves and blood vessels. Diabetes is the major cause of blindness, kidney failure, heart attacks, stroke and lower limb amputation [3]. In 2016, an estimated 1.6 million deaths were directly caused by diabetes while another 2.2 million deaths were attributable to high blood glucose in 2012 [4]. The World Health Organisation (WHO) further stated that almost half of all deaths attributable to high blood glucose occur before the age of 70 years. The WHO estimated that diabetes was the seventh leading cause of death in 2016 [4]. Type 2 diabetes results from the body's ineffective use of insulin. The majority of people with diabetes have type 2 diabetes and this number is estimated to be more than doubled from that of 2005 by 2030 [5].

3.2.1.2. Causes and risk factors

Type 2 diabetes is largely the result of excess body weight, physical inactivity and unhealthy diets [3–5]. It occurs more frequently in individuals with hypertension, dyslipidemia (abnormal cholesterol profile), and central obesity, and is a component of metabolic syndrome [4]. The condition is often genetic and may be caused by mutations in more than one gene, as well as by environmental factors [4,5].

3.2.1.3. Effective treatment

The increasing trend of type 2 diabetes has prompted alternative combatting strategies for new therapeutic agents. Over the last decade there has been evident improvement in drug

treatment for type 2 diabetes, however, drug resistance is still a concern [4]. α-Glucosidases inhibitors act against the enzyme in the small intestines by slowing down its process of breaking down oligosaccharides to glucose units, and thereby reduce the postprandial glucose levels and insulin responses [5]. Known inhibitors include acarbose, miglitol and voglibose (Figure 3.1), and are currently used clinically in combination with diet or other anti-diabetic agents to control blood glucose levels of patients [5,6].

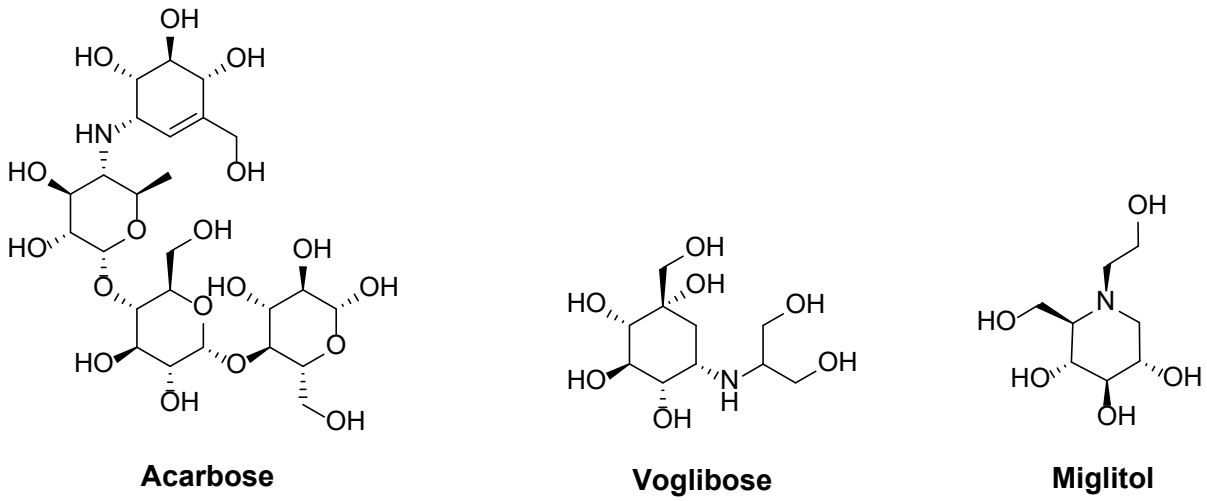

Figure 3.1: *Structures of some well-known alpha glucosidase inhibitors.*

Other antidiabetic agents include: biguanides, dopamine agonist, dipeptidyl peptidase-4 (DPP-4) inhibitors, glucagon-like peptide-1 receptor agonists (LP-1 receptor agonists), meglitinides, sodium-glucose transporter (SGLT) 2 inhibitors, sulfonylureas and thiazolidinediones [7].

3.2.1.4. Components from medicinal plants with antidiabetic properties

Some compounds reported from medicinal plants to possess anti-diabetic properties, include: saponins, flavonoids, alkaloids, anthraquinones, terpenes, coumarins, phenolics and polysaccharides [7,8]. Crude extracts of medicinal plants commonly used in the traditional

Chinese medical system and having demonstrated experimental or/and clinical anti-diabetic efficacy, include: Leguminosae, Cucurbitaceae, Araliaceae, Liliaceae, Chenopodiaceae, Solanaceae, Compositae, Campanulaceae, Cornaceae, Rhamnaceae, Scrophulariaceae, Euphorbiaceae, Ginkgoceae, Gramineae, Myrtaceae, Sterculiaceae, Annonaceae, Labiatae and Crassulaceae [7,8]. Munhoz et al. (2018) reviewed that, reported compounds from natural products, identified to have important anti-diabetic activity with defined mechanisms, include: quercetin, oleanolic acid, kaempferol, ursolic acid, rutin, β-sitosterol, and mangiferin [9] (Figure 3.2).

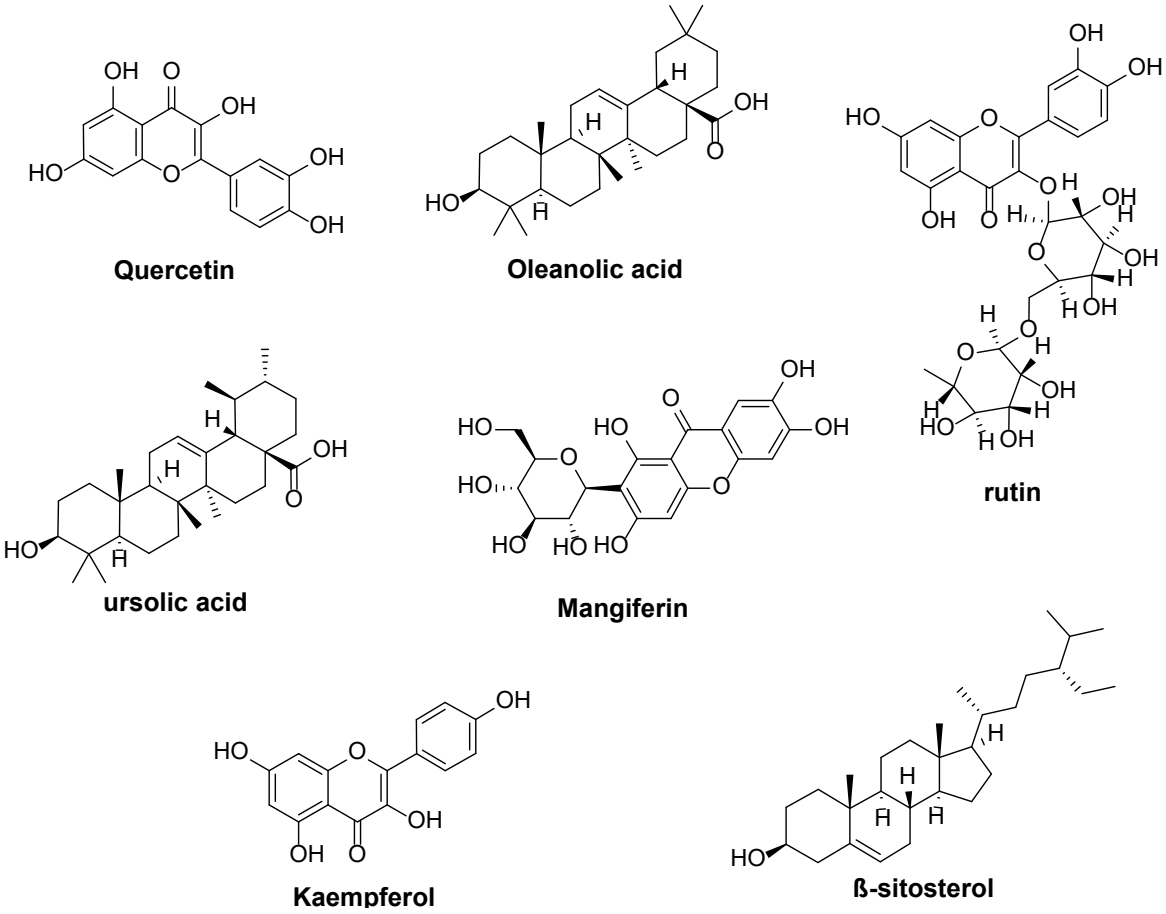

Figure 3.2: *Structures of some reported natural product-based compounds to have important anti-diabetic activity with defined mechanisms.*

3.3. *Escherichia coli, Staphylococcus aureus* and their growth inhibition

The increasing incidence of antibiotic resistance are undeniable, resulting in an absolute necessity to finding other alternative candidate agents for treatment than commonly utilised drugs [10]. Towards bacterial combatting strategies, the pharmaceutical and food industries have invested substantial resources in the search for new inhibitory compounds from natural resources [11]. Some known antibacterial compounds include: cephalosporin, macrolide, fluoroketolide, vancomycin, methicillin, penicillin, minocycline, fluoroquinoone, mononactam to name a few [12]. Some antibiotics discovered by classical screening include: novalactamycin, lysostaphin, pleuromutilins, fusidic acid, VIC 200107 and fidaxomicin [12]. Figure 3.3 displays chemical structures of some antibacterial agents. Some known animal growth promoting antibiotics include: bambermycin, bacitracin, monensin, salinomycin, virginiamycin, tylosin, spiramycin, ardacin and olaquindox, to name a few [13].

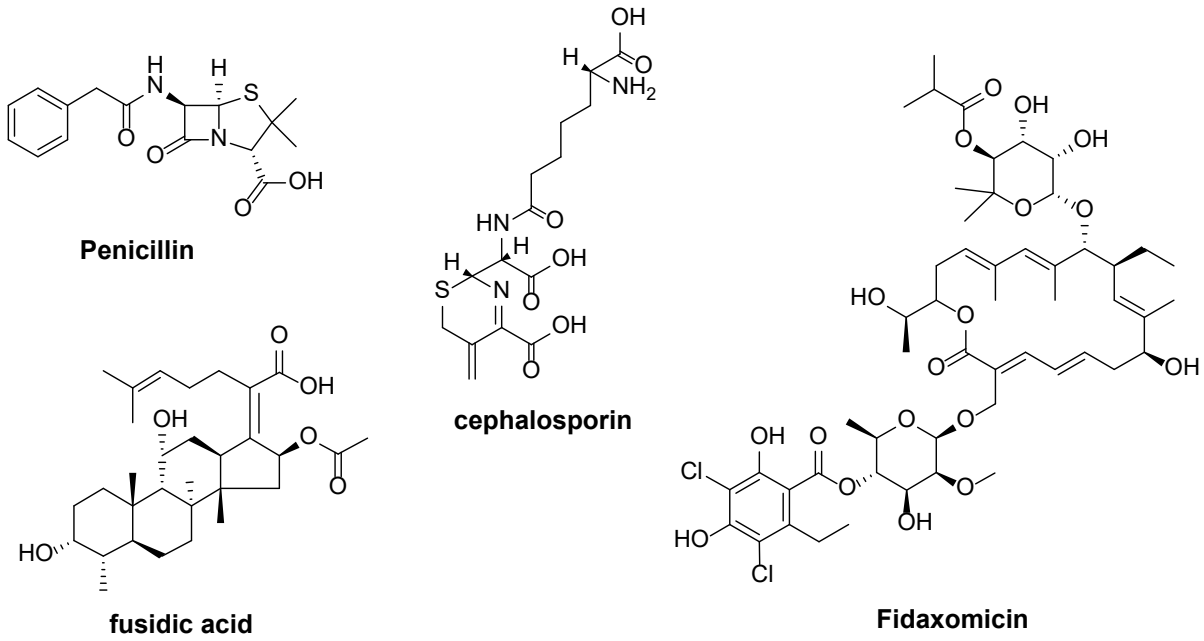

Figure 3.3: *Chemical structures of some of the known antibiotics.*

E. coli and *S. aureus* are becoming more and more resistant to conventional antibiotics [10]. The diarrhoeagenic strain of *E. coli* and *S. aureus* are known to cause gastrointestinal illness in humans and other animals [14]. It was reported that 79 % of *E. coli* strains were resistant to ampicillin and 30 % of strains were resistant to ciprofloxacin while 37 % of *S. aureus* strains were resistant to ciprofloxacin [14]. Certainly, there is a need to search for natural bioactive alternatives that can inhibit the growth of such pathogenic bacteria. The literature reports on potential ingredients from natural resources and antibacterial activity of *C. gynandra* are discussed in Chapter 2.

In Chapter 2, the EtOH extract exhibited the greatest inhibitory activity against *E. coli* compared to other extracts tested. The MIC value for the ethanol extract against *E. coli* was 0.052 ± 0.016 mg/mL, comparable to 0.037 ± 0.013 mg/mL of gentamicin, the positive control. This result warranted studies towards identifying the ingredients responsible for the good activity. While growth inhibition exhibited by the EtOH extract against *S. aureus* was moderate compared to other extracts, MIC value 0.458 ± 0.102 mg/mL, it was deemed necessary to also include *S. aureus* for comparative measures in the bioassay-guided fractionation study involved in this chapter.

3.3.1 Bioautography

Medicinal plants, vegetables and fruits are sources of a large number of bioactive scaffolds with therapeutic and nutraceutical importance. Dewanjee et al. (2015) stated that paper chromatography and TLC were tools in the screening of antimicrobial agents through bioautography. Three bioautographic methods, namely, (i) agar diffusion or contact bioautography, (ii) direct TLC bioautographic detection and (iii) immersion or agar overlay bioautography, are used to detect antimicrobial agents in a mixture of compounds [15].

Contact bioautography involves developing TLC plate or paper for compounds separation, and the antimicrobial agents diffuse from TLC plates or paper to an inoculated agar plate.

The chromatogram is placed face down onto the inoculated agar layer for a given period to allow diffusion. The chromatogram is, thereafter, removed and the agar layer is incubated. Zones of inhibition on the agar surface, corresponding to the spots in chromatographic plates, are indicative of the antimicrobial compound.

Direct TLC bioautography involves spraying or dipping the developed plates into a fungal or bacterial suspension. A suspension of test bacteria or fungi is used for the spraying or dipping purpose. Using a suspension of 106 CFU/mL could be employed for both bacteria and fungi. The bioautogram is then incubated for given period under humid condition. Visualisation of microbial growth is achieved by the use of tetrazolium salts. These salts are converted by the dehydrogenases of living microorganisms to intensely coloured formazan bioautogram and are re-incubated at 25 °C for 24 hr or at 37 °C for 3–4 hr. White zones against a purple background on the TLC plate indicate microbial inhibition activity.

Agar overlay is a combination of contact and direct bioautography. In this method, the chromatogram is covered with a molten, seeded agar medium. After solidification, incubation and staining (usually with tetrazolium dye), the inhibition or growth bands are visualised. For Gram-negative bacteria, an agar solution containing the red-coloured bacterium *Serracia marcescens* can be employed. The red-coloured gel is incubated overnight at room temperature and inhibition zones appear as white or pale yellow areas on a red background. With other, colourless, microorganisms, zones of inhibition are visualised with the aid of the dehydrogenase activity-detecting reagent, tetrazolium salt. Metabolically active microorganisms convert the tetrazolium salt into the corresponding intensely coloured formazan [15].

3.4. Materials and methods

Solvents and reagents (*n*-hexane, dichloromethane, chloroform, methanol, acetone, ethyl acetate, benzene, ethanol, ammonium hydroxide, sulphuric acid, vanillin and formic acid)

used for column chromatography, aluminium-backed thin-layer chromatography (TLC) and bioautography experiments were analytical grade purchased from MERCK (Sigma Aldrich, South Africa) or Radchem (Pty) Ltd (South Africa). Solvents and reagents (methanol, acetonitrile, formic acid and trifluoroacetic acid (TFA)) used for semi preparative HPLC were HPLC/Ultra-PLC grade, purchased from MERCK (Sigma Aldrich, South Africa). Milli-Q® water was used in all experimentations involving the use of water. All chemicals were used without further purification.

Silica gel 60 (0.063-0.2 mm; Macherey-Nagel GmbH & Co. KG, Düren, Germany) and Silica gel-60 (0.040-0.063 mm; Merck KGaA, Darmstadt, Germany) were used for open column chromatography. Aluminium-backed silica gel GF254 plates (Merck KGeA, Darmstadt, Germany) were used for TLC detection, while preparative TLC was achieved using TLC Silica gel 60 glass plates (Merck KGaA, Darmstadt, Germany).

3.4.1. Silica gel column chromatography and thin-layer chromatography for further fractionation of the fraction pEtOAc

The dried pEtOAc extract (8 g) was dissolved in ethyl acetate (30 ml) for fractionation by column chromatography with *n*-hexane as the starting solvent, followed by *n*-hexane/dichloromethane and dichloromethane/methanol mixtures at the end of the chromatography. The increasing polarity of the solvent system was as follows: 100% *n*-hexane, *n*-hexane/dichloromethane 9:1, 4:1, 7:3, 3:2, 1:1, 2:3, 3:7, 1:4 1:9, 100% dichloromethane, dichloromethane/methanol 9.5:0.5, 9:1, 8.5:1.5, 8:2 and 7:3. The eluents were collected in test tubes while the separation was monitored using TLC. Developed TLC plates were visualised under UV light at 254nm as well as by spraying with vanillin stain (MeOH, 30 ml; vanillin, 0.1 g; H_2SO_4, 1 ml dropwise). After visualisation, similar fractions were combined. The combined fractions were dried using a Büchi® Rotavapor® R-210 evaporator.

3.4.2. Silica gel column chromatography and thin-layer chromatography for fractionation of the ethanol extract

Silica gel 60 (0.063-0.2 mm; Macherey-Nagel GmbH & Co. KG,Düren, Germany) was used for open column chromatography. A glass silica column of 105 cm length and 21 cm circumference was used. The column was packed with a slurry suspension formed by mixing approximately 1200 g of dried silica gel with *n*-hexane. The dried EtOH extract (7 g) was dissolved in chloroform at saturation concentration and mixed with silica gel 60, and the extract infused silica was dried at room temperature. The dry extract infused silica was poured slowly onto the bed of the silica gel layer in glass column and allowed to settle. Initially *n*-hexane was used as the eluent. The polarity was increased gradually by mixing the *n*-hexane with dichloromethane, until 100% dichloromethane was reached, the polarity was further increased by mixing dichloromethane and methanol, until 30% methanol was reached, while the elution progress was monitored using TLC. Initially, a total of 135 fractions collected in test tubes were dried using a Büchi® Rotavapor® R-210 evaporator and reconstituted in small amount of solvent (either chloroform, acetone or methanol, depending on solubility) analysed by TLC using silica gel plates, and visualised under UV light at 254nm and/or by spraying with vanillin stain (MeOH, 30 ml; vanillin, 0.1 g; H_2SO_4, 1 ml dropwise). After visualisation, similar fractions were combined and allowed to dry under fume-hood.

3.4.3. Secondary fractionation of the most active antimicrobial fraction using semi-preparative HPLC

Development of a method for semi-preparative HPLC fractionation of the most bioactive EtOH primary fraction was performed using a Waters™ HPLC 660 Controller, Millipore, equipped with a Waters™ 996 Photodiode Array detector. Measurement processing was done using the Waters™ Millennium32 software. A Phenomenex, Luna, C_{18} 5 µm, 4.6 x 250 mm column was used. A gradient method was used for the selected most active fraction with

solvent A water with 0.05 % TFA, solvent B was 100% methanol. The gradient method used was 0%-3% B in 3 minutes, 3%-20% B in 8 minutes, 20%-60% B in 10 minutes, 60-60% 5 minutes, 60-75% B in 8, 75%-85% D in 5 minutes, 85%-97%D in 5 minutes, 97%-100% B in 5 minutes, 100%-50% B in 3 minutes, 50%-10% B in 3 minutes, 10%-3% B in 2 minutes.

Semi-preparative HPLC was carried out using the same instrument and column and the sample concentration was increased from 1 to 10 mg/mL and the injection volume from 5 – 20 µL up to 40 µL. The sample was filtered using a 0.45 PTFE filter before injection on semi-preparative HPLC. Several injections were necessary for accumulating sufficient quantities of isolates for further studies, while the flow rate was kept the same.

For each injection the fractions were collected at eight intervals chosen based on observed absorption in the UV-Vis range 200 – 800 nm, leading to 8 fractions. Each of the similar fractions were combined and the 8 fractions were dried using the Genevoc SP Scientific Genevac *EZ-2* centrifugal evaporator.

3.4.4. α-glucosidase inhibition assay

The enzyme α-glucosidase (*Saccharomyces cerevisiae*), 3, 5, di-nitro salicylic acid (DNS), *p*-nitro-phenyl-α-*D*-glucopyranoside (*p*-NPG), sodium dihydrogen phosphate and di-sodium hydrogen phosphate were purchased from Sigma-Aldrich. For the 25 µg/mL and 2.5 µg/mL test concentrations of the fractions in the α-glucosidase inhibition assay, the method was as follows:

In a 96-well plate, reaction mixture containing 30 µL phosphate buffer (20 mM, pH = 6. 9), 10 µL α-glucosidase (100 µg/mL) were added to the control wells. The blank wells contained 40 µL phosphate buffer. Fraction controls contain 60 µL phosphate buffer and 20 µL of test fraction. The positive control well contained, 20 µL dimethoxymethylamphetamine (DMMA) (1 mg/mL), 10 µL phosphate buffer and 10 µL α-glucosidase. To the test fraction wells 20 µL of fraction (0.1 mg/mL or 0.01 mg/mL) in DMSO was added with 10 µL phosphate buffer and

10 µL α-glucosidase. The plates were pre-incubated at 37°C for 15 min. Then, 40 µL *p*-NPG (5 mM) was added as a substrate and incubated further at 37°C for 20 minutes.

For dose dependant α-glucosidase inhibition of selected fractions at test concentrations 5, 20, 80, 320 µg/mL, the same method was followed as above. The only difference was that to the test fraction wells, 20 µL of varying concentrations of the fractions (0.02 mg/mL, 0.08 mg/mL, 0.32 mg/mL and 1.28 mg/mL) in DMSO was added with 10 µL phosphate buffer and 10 µL α-glucosidase and pre-incubated for 15 minutes. Then, 40 µL *p*-NPG (5 mM) was added as a substrate and incubated further at 37°C for 20 min.

The absorbance of the released *p*-nitrophenol was measured at 405 nm using the Tecan Infinite® F500 microplate reader. The results were expressed as percentage inhibition, which was calculated using the formula,

$$Inhibition\ activity\ (\%) = \left(1 - \frac{As}{Ac}\right) \times 100 \quad (1)$$

where, As is the absorbance in the presence of test substance and Ac is the absorbance of control.

3.4.5. Bacterial culture: *S. aureus* and *E. coli*

S. aureus (ATCC 29213) and *E. coli* (ATCC 25922) were the strains used for antibacterial assays. The strains were maintained in Mueller Hinton ager (MHA) (Fluka, Spain). The organisms were sub-cultured every 2 weeks. Before testing, the bacterial inoculums were prepared and cultivated in Mueller Hinton broth for 12 hr at incubation temperature 37 °C. The bacterial cultures were serially diluted (10 fold increments) in sterile broth to obtain cell suspension of 1.0 x 10^5 CFU/ml (colony forming units per ml).

3.4.6. Analysis of the EtOH fractions by TLC for antimicrobial analysis

TLC profiles of the EtOH fractions obtained using column chromatography for antimicrobial analysis were done on aluminium-backed silica gel plates. Either a combination of *n*-hexane and acetone or the solvent systems, chloroform: ethyl acetate: formic acid (5:4:1, intermediate polarity, acidic) and ethyl acetate: methanol: water (40:5.4:5, polar, neutral) were used to analyse 100 µg (10 µL of 10 mg/mL) of the fractions loaded in a band of 1 cm width on the TLC plates. Visible bands were marked under white light and ultraviolet light (254 nm and 360 nm wavelengths, Camac universal UV light lamp TL-600) before being sprayed with freshly prepared vanillin (0.1 g vanillin, 28 mL methanol, 1 mL,sulphuric acid) spray reagent. The plates were then heated to 110 °C for the colour development.

3.4.7. Qualitative antibacterial assay of EtOH fractions by TLC bioautography

Thin-layer chromatograms of the fractions were prepared as described earlier except that the plates were not sprayed with vanillin. The developed plates were allowed to dry overnight in a stream of cold air to completely remove the solvent. Each of the plates were wetted by spraying with an actively growing suspension of *E. coli* or *S. aureus* cultured for 18–24 hr at 37 °C. The plates were then incubated at 37 °C in a closed plastic humidified sterile container for 24 hr to promote bacterial growth on the plates. After incubation, the plates were sprayed with 2 mg/mL of freshly prepared *p*-iodonitrotetrazolium violet (INT) (Sigma Aldrich, South Africa) in sterile hot distilled water and incubated for a further 1–2 hr for the development of clear zones against a purple-red background which suggests inhibition of bacterial growth by the compounds separated on the chromatograms.

3.4.8. Quantitative antibacterial assay of the EtOH fractions by determination of minimum inhibitory activity

The minimum inhibitory concentration (MIC) for the fractions against bacteria were evaluated using the serial microdilution assays [16,17]. The sub-fractions obtained *via* preparative-HPLC were made up to a concentration of 10 mg/mL with DMSO, and 100 µL was added to the first well of a sterile 96-well microtitre plate and a 1:1 serial dilution was performed, initially, sterile distilled water was added. One-hundred microlitres of the prepared bacterial cultures were added to each well. The bacteria were exposed to final fraction concentrations of 0.02 to 2.5 mg/mL after the bacterial cultures were added to the diluents. Gentamicin (Sigma Aldrich, South Africa) and DMSO served as positive and negative controls, respectively, while broth alone served as sterility control. The microplates were then incubated overnight at 37 °C under aerobic conditions. After 16 –18 hr incubation, the presence of bacterial growth was detected by adding, to each well, 40 µL of 0.2 mg/mL INT and the plates were then further incubated at 37 °C for 2 hr. Bacterial growth in the wells appeared as red colour which is indicative of the reduction of INT to a red-coloured formazan. The MIC was determined visually as the lowest concentration that led to growth inhibition indicated by a reduction in the red colour [16–18].

3.4.9. UPLC-QTOF-MS conditions and method

The fractions and sub-fractions were reconstituted in methanol to a concentration of 1 mg/mL then centrifuged at 10000 rpm for 2 min. As in Chapter 2, UPLC was performed using a Waters Acquity UPLC system (Waters Corp., MA USA), equipped with a binary solvent delivery system and an autosampler. For the MS conditions, a Waters Synapt G2 high definition QTOF mass spectrometer equipped with an ESI source was used to acquire

negative and positive ion data. Similar method as described in Chapter 2 was used to maintain consistency and for any required comparisons.

Acquisition

A 2 ng/µL solution of leucine encephalin was used as the lockspray solution that was constantly infused at a rate of 2 µL/min through a separate orthogonal ESI probe to compensate for experimental drift in mass accuracy. Trap collision energies were 30 V (high) and (10 V) for the low energy. Data were not centroided during data acquisition in order to be used on UNIFI software. To ensure accurate MS analysis on MassLynx the data was mass corrected during analysis *via* a lockspray interface, with reference ion of $[M + H]^+$ (m/z 556.2771) in positive ion mode and $[M-H]^-$ (m/z 554.2615) in negative ion mode.

Chemical profiling

Compounds were tentatively identified by generating molecular formulas using MassLynx V 4.1 based on their iFit value, and by comparison of MS/MS fragmentation pattern with that of matching compounds. Identification of known compounds was effected using online databases such as *Chemspider, PubChem, the Dictionary of Natural Products, MassBank, Metlin and MefFusion.*

3.4.10. Analysis of the most active EtOH fraction using UNIFI®platform

Waters® UNIFI® Scientific Information System (version 1.9.2) was used for some library searching and report generation of the data acquired using MassLynx for the most active antimicrobial fraction and its sub-factions. An analytical workflow for ESI negative mode was created within UNIFI® and used to analyse the chromatographic and mass spectral components of the most active antimicrobial fraction utilising the various in-built tools such as the green tea library, and the Chinese traditional medicines library, and structure elucidation tool to effectively confirm the ingredients in the fraction [19,20].

The UNIFI® software also has a unique database function that allows users to quickly add new compounds and create a customized library of compounds, such in-house libraries were also used in the search. UNIFI® provides an elemental composition calculator that can determine a number of possible formulas for an accurate mass peak, based on isotope pattern matching and considering fragment ion peaks. A margin of error up to 5 ppm for identified compounds was allowed and the matching compounds would be generated based on predicted fragments from structure.

3.5. Results and discussion

3.5.1. Fractionation of the fraction pEtOAc

Column chromatography fractionation of pEtOAc initially led to more than 100 fractions collected, which were analysed by TLC, and according to the similarity of patterns, a total of 63 fractions were obtained after combining and were labelled F1 - F63. After drying, using a Büchi® Rotavapor® evaporator, the fractions were reconstituted in a small amount of appropriate solvent and the concentrated reconstitutes (F1 - F63) were analysed with TLC (*n*-hexane/acetone 7:3 and dichloromethane/methanol 8:2, depending on polarity), and similar fractions were further combined as illustrated in Figure 3.4. This led to 28 fractions numbered F1 - F5, F8, F9, F13, F14, F16 - F26, F40, F41, F43, F44, F47, F49, F50, F58. The weights of the final combined fractions ranged between 3 - 630 mg. The fractions were thereafter evaluated for their α-glucosidase inhibition towards identifying the bioactive ingredients.

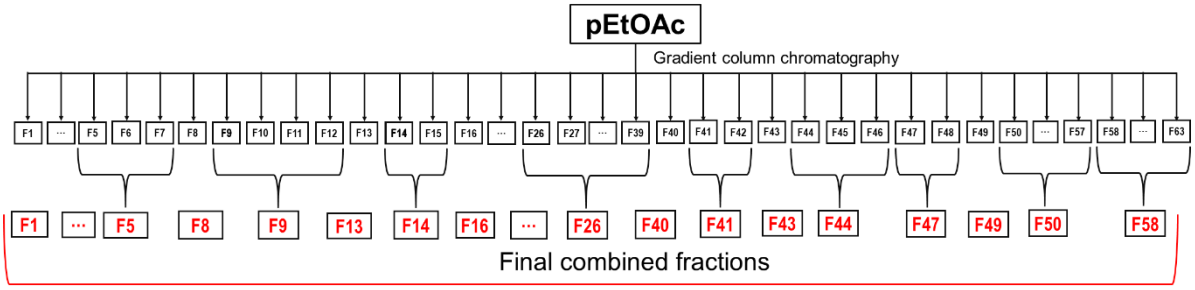

Figure 3.4: *An illustration of the combination of column chromatography eluted fractions and their numbering.*

3.5.2. The α-glucosidase inhibitory effect of the pEtOAc fractions

The percentage inhibition of twenty-eight fractions against α-glucosidase are shown Table 3.1. The factions which showed inhibition greater than 80 % at 25 µg/mL were further tested at 2.5 µg/mL. However, none of these fractions exhibited any appreciable inhibition at 2.5 µg/mL concentration. The standard reference compound, DMMA, showed α-glucosidase inhibitory activity of 96.83 % at 25 µg/mL and 99.81 % inhibition at 2.5 µg/mL. Fractions F41 and F47 displayed 98.36 and 98.41 %inhibition, greater than that exhibited by DMMA at 25 µg/mL.

Table 3.1: *α-glucosidase inhibition of fractions of pEtOAc at 25 µg/mL and 2.5 µg/mL, arranged from least to most polar as eluted from the column. The most active fractions are highlighted.*

Fractions	% Inhibition ± SD (25 µg/mL)	% Inhibition ± SD (2.5 µg/mL)
F1	5.03	
F2	0	
F3	52.30	
F4	62.26	9.92
F5	83.43	10.69
F8	50.81	
F9	0	
F13	43.72	
F14	34.51	
F16	76.26	10.03
F17	29.86	
F18	49.05	
F19	34.32	
F20	40.91	
F21	67.87	9.83
F22	87.09	16.09
F23	59.08	14.36
F24	26.16	

F25	89.85	16.39
F26	17.47	
F40	93.15	10.61
F41	98.36	14.24
F43	85.49	28.06
F44	82.00	13.66
F47	98.41	-41.21
F49	78.33	-39.21
F50	56.98	
F58	0.04	
DMMA (positive control)	96.83 ± 0.27	99.81 ± 0.04

The selected active fractions, F22, F25, F40, F41, F43, F44 and F47 eluted in the medium to polar regions during chromatography. A challenge on the components from *C. gynandra* was that a great majority of the compounds do not absorb UV-visible light, which presented difficulties in attempting to isolate the compounds that were responsible for the activity, as a result HPLC UV could not be used for further chromatographic separation.

For dose dependant α-glucosidase inhibition evaluation assay of selected fractions, priority was given to the most abundant fractions (30 – 630 mg) and the selected fractions were F5, F22, F40, F44, F49 and F50, assayed at test concentrations 5, 20, 80 and 320 µg/mL. The inhibition curves showing percentage inhibition *vs* concentration of the fractions are shown in in Figure 3.5. The fractions exhibited dose-dependent inhibition of α-glucosidase. These fractions were further subjected to chemical fingerprinting using UPLC-QTOF-MS, towards identifying known compounds that may be responsible for activity.

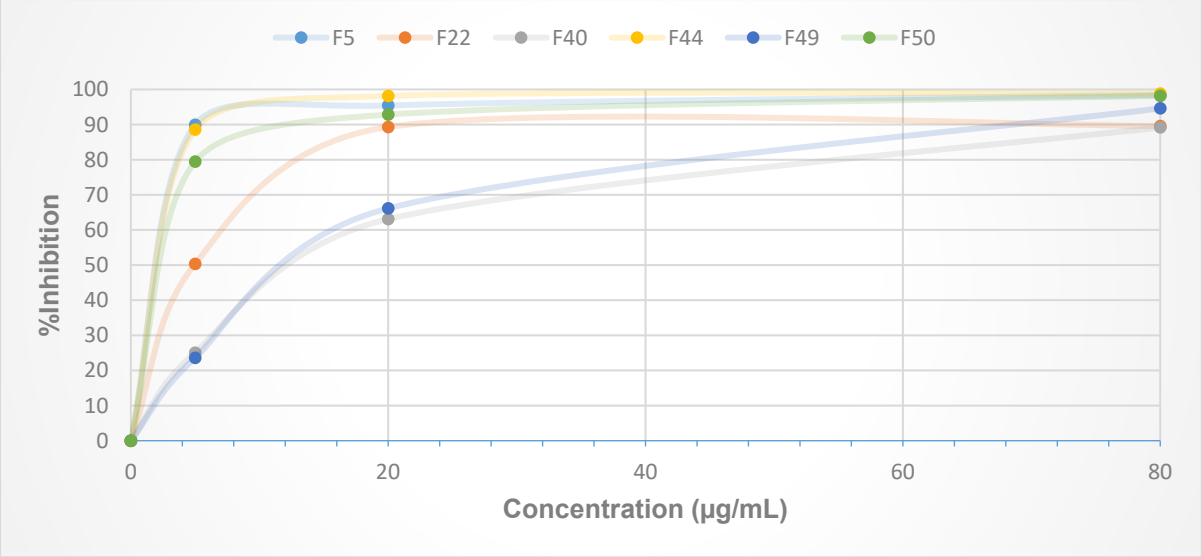

Figure 3.5: *Concentration dependency alpha glucosidase inhibition curves of the active fractions, F5, F22, F40, F44, F49 and F50, the 320 µg/mL point was excluded for clarity.*

3.5.3. Chemical profiling of the selected pEtOAc fractions using UPLC-QTOF-MS

Analysis of the UPLC-QTOF-MS data was used to tentatively identify the structures of the most prominent peaks which could be used as possible bioactivity markers in the selected fractions. The chromatographic profiles for the fractions F5, F22, F40, F44, F49 and F50 indicated that these possess different types compounds (Figure 3.6). Each fraction possessed different profiles with some peaks which overlapped especially between fraction F49 and F50. The tentatively identified major compounds are shown in Table 3.2. F22 displayed a prominent peak (peak 3) at 10.66 min with *m/z* 541.3951, analysis of the MS spectra revealed the parent ion with regards to this peak as 599.3922, $[M + Na]^+$ (calculated for 576.4026) and the compoundwas assigned the molecular formula $C_{34}H_{56}O_7$. The compound was identified as that newly isolated in this study, cleogynone A, for which the structure elucidation is detailed in Chapter 4. No known compounds could be identified owing to the lack of systematic research on *C. gynandra*. The parent ions of the major compounds that could not be attributed to any known compounds indicated that these compounds contain a large number of carbons and may indicate that these are novel

triterpenoids (Table 3.2). Attempts were made to purify the compounds using column chromatography and prep TLC and were unfortunately unsuccessful. For the polar components which make up the majority of the active region, HPLC UV could not be used due to lack of UV-invisibility of the compounds, as stated earlier. Further studies could involve using mass directed fractionation, which is not the scope of this work.

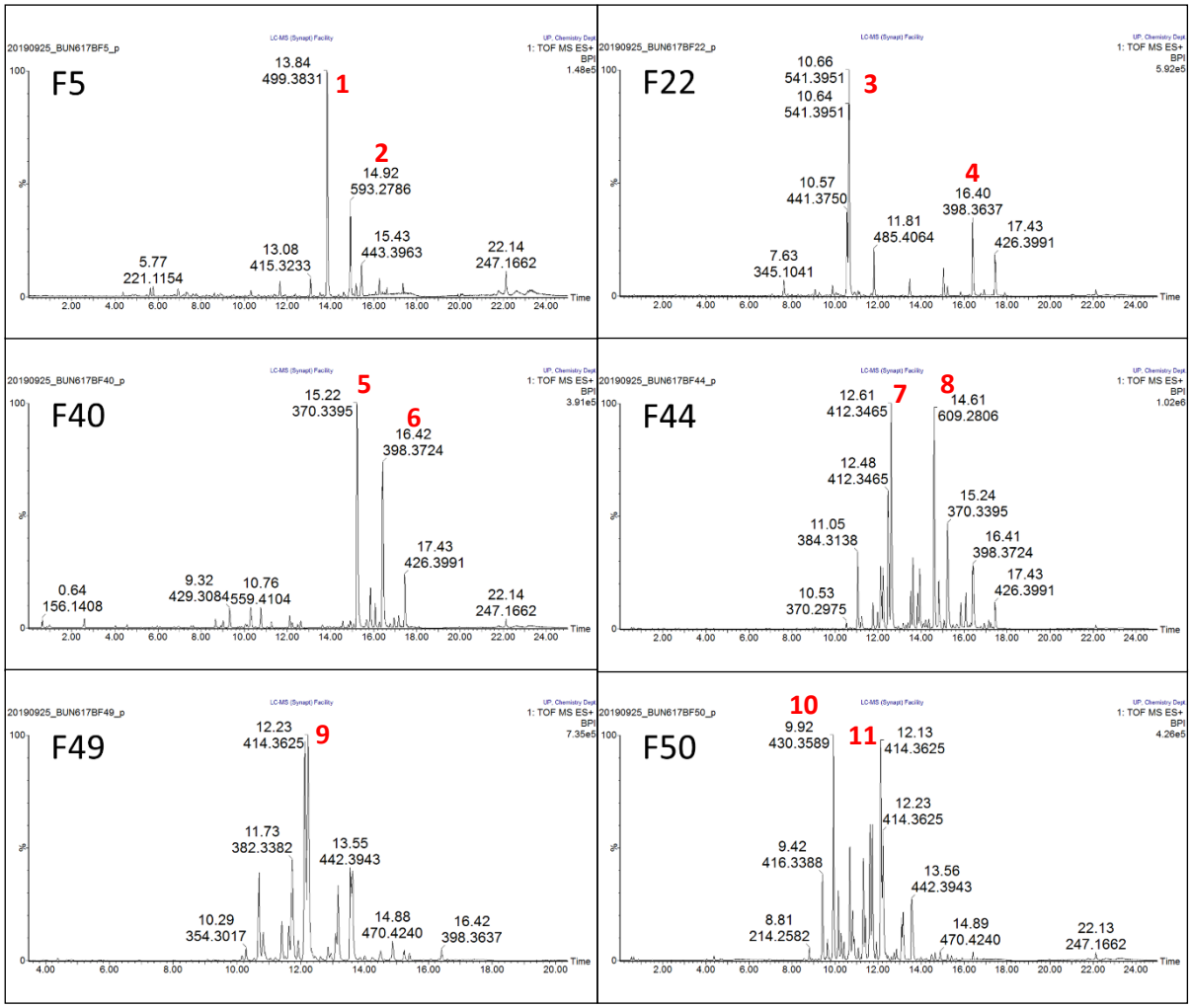

Figure 3.6: *ESI positive mode BPI chromatogram of the fractions F5, F22, F40, F44, F49 and F50 obtained from the pEtOAc active extract which α-glucosidase inhibition.*

Table 3.2: *Chemical profile of fractions of the partition pEtOAc.*

Peak #	Retention time (min)	Acquired[M + Na]$^+$ /[M + H]$^+$/[M + K]$^+$ *m/z*	Formula of possible structure	Theoretical [M + H]$^+$ / [M + Na]$^+$ / [M + K]$^+$ *m/z*	Calculated accurate mass (Da)	Possible compound	Mass error (ppm)	Observed ions/ (fragments)	
1	13.87	539.3716 [M + H]$^+$	$C_{34}H_{50}O_5$	539.3736	538.3658	Unidentified	-3.7	499.3794	
								479.3497	
								439.3594	
								421.3481	
2	14.94	593.2764 [M + H]$^+$	$C_{34}H_{40}O_9$	593.2751	592.2672	Unidentified	2.2	533.2540	
								505.2237	
								461.2320	
								447.2166	
3	10.66	599.3934 [M + Na]$^+$	$C_{34}H_{56}O_7$	599.3924	576.4026	Cleogynone A	1.7	599.3934	[M + Na]$^+$
								542.3945	[M - H_2O - OH]$^+$
								541.3909	[M - $2H_2O$]$^+$
								499.3800	[M - CH_3CO_2H - H_2O]$^+$
								421.3468	[M - $2CH_3CO_2H$ - $2H_2O$]$^+$
4	16.40	817.7045 [M + K]$^+$	$C_{50}H_{98}O_5$	817.7051	778.7414	Unidentified	-0.7	398.3636	
								399.3665	
5	15.22	739.6564 [M + K]$^+$	$C_{44}H_{92}O_5$	739.6582	700.6945	Unidentified	-2.4	761.6400	
								393.3231	
								392.3188	
								371.3405	
								370.3395	
								132.1024	
								86.0990	
6	16.42	795.7189 [M + K]$^+$	$C_{48}H_{100}O_5$	795.7208	756.7571	Unidentified	-2.4	421.3539	
								420.3503	
								399.3757	
								398.3724	
								132.1024	
								86.0990	
7	12.61	861.6243 [M + Na]$^+$	$C_{45}H_{90}O_{13}$	861.6279	838.6381	Unidentified	-4.2	450.2938	
								434.3280	
								412.3465	
								321.2364	
								132.1024	
								86.0990	
8	14.61	609.2711 [M + H]$^+$	$C_{34}H_{40}O_{10}$	609.2700	608.2622	Unidentified	1.8	591.2613	
								559.2346	
								531.2402	
								515.2449	
								485.2342	
9	12.23	827.7086 [M + K]$^+$	$C_{48}H_{100}O_7$	827.7106	788.7469	Unidentified	-2.4	436.3377	
								414.3568	
								396.3461	
								132.1020	
								86.0969	
10	9.92	897.6476 [M + H]$^+$	$C_{54}H_{88}O_{10}$	897.6456	896.6378	Unidentified	2.2	469.3029	
								468.2999	
								452.3292	
								431.3557	
								430.3526	
								412.3419	
								405.2962	
								86.0970	
11	12.09	865.6556 [M + Na]$^+$	$C_{52}H_{90}O_8$	865.6533	842.6636	Unidentified	2.7	458.3248	
								436.3408	
								414.3587	

								396.3478	
								320.2279	
								132.1018	
								86.0972	

3.5.4. EtOH extract fractions for antimicrobial activity against *E. coli* and *S. aureus*

The 135 fractions collected were concentrated and analysed using TLC (*n*-hexane/acetone 7:3 or dichloromethane/methanol 8:2, based on their polarity). The fractions showing similar profiles were combined resulting in a total of 22 fractions which were numbered F1 - F22 in the order of elution from the column. The fractions were dried using the Büchi® Rotavapor® evaporator, and their masses ranged between 5 – 220 mg. The fractions were evaluated for their antimicrobial activity against *E. coli* and *S. aureusvia* the TLC bioautography method.

3.5.5. Qualitative antibacterial activity of the EtOH extract fractions by TLC bioautography

The fractions F1 – F22 obtained using column chromatography were separated on aluminium-backed TLC (*n*-hexane: acetone (60:40)) for bioautographic antibacterial analysis against both *E. coli* and *S. aureus*. Figure 3.7 displays the TLC bioautograms, labelled a, b, c and d. The areas of the TLC bioautograms showing white clear zones in the pink background revealed the positions of the active compounds, and their retention factors (R_f) values were calculated.The greatest activity is depicted by F17 against *E. coli*, where the brightest spot was evident with R_f value = 0.08.

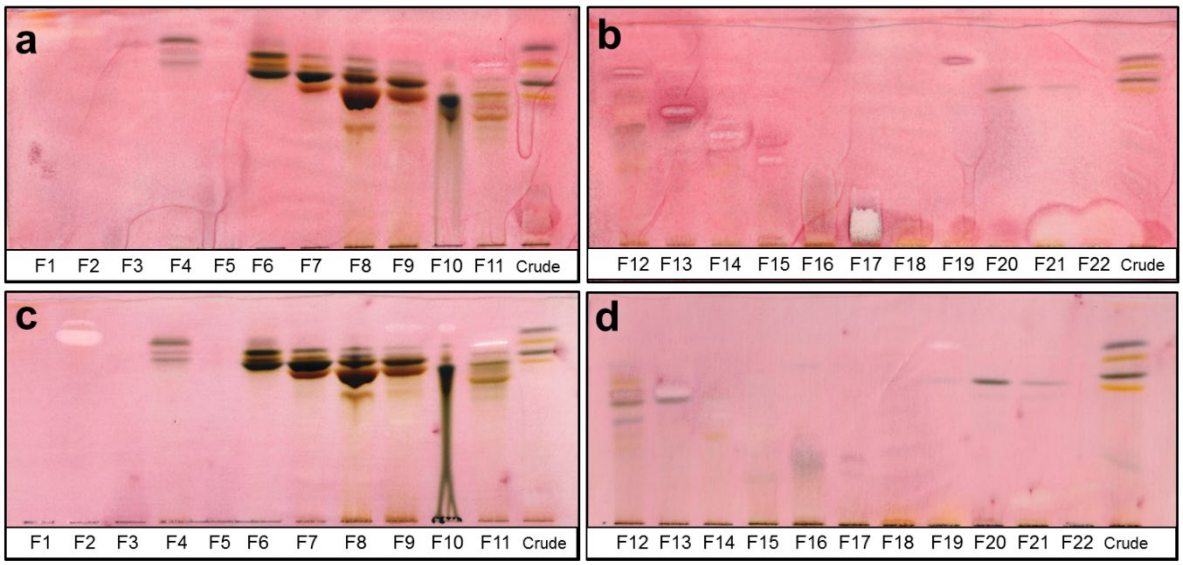

Figure 3.7: *Bioautograms of (a & b) Escherichia coli inhibition and (c and d) Staphylococcus aureus inhibition of the fractions (F1 – F22). The plates were developed with 60:40 n-hexane: acetone solvent system; white bands indicate compounds that inhibit the growth of the bacteria.*

The large diameter of the spot suggests that more than one compound is responsible for the activity. A bright spot was also evident for fraction F2 (R_f = 0.85) against *S. aureus*. F11 against *S. aureus* also revealed reasonable activity as a bright narrow spot is depicted (R_f = 0.79). The bioautograms demonstrated that the most active compounds against *E. coli* are polar compounds, whereas against *S. aureus* the most active compounds are non-polar. These results led to further fractionation of F17 using preparative HPLC towards purifying the possibly bioactive compound(s).

3.5.6. Semi-preparative HPLC fractionation of F17 and antibacterial minimum inhibitory activities of the sub-fractions

Eight fractions labelled F17A – F17H (2 – 20 mg) were collected at intervals chosen based on visible chromatographic peaks in the UV-Vis range. The fractions were further subjected to minimum inhibitory activity assays against both *E. coli* and *S. aureus*. The fractions all displayed activity comparable to gentamicin with MIC values in the range 0.012 – 0.094 mg/mL (Table 3.3). The diameter of the white spot, for F17, observed for bioautography was in support of this result, suggesting that there are several compounds responsible for the growth inhibition. Furthermore, prep-HPLC fractionation effectively removed any non-polar residue or remnants in the fraction that might reduce the activity.

Table 3.3: *Minimum inhibitory concentration (MIC) of eight sub-fractions from F17 (F17A-F17H), all fractions displayed inhibitory activity comparable to gentamicin.*

Fraction	**Mean MIC (mg/mL) and standard deviations**	
	Escherichia coli ATCC 25922	*Staphylococcus aureus* ATCC 29213
F17-A	0.0160±0.00	0.0630±0.00
F17-B	0.0310±0.00	0.0235±0.011
F17-C	0.0160±0.00	0.0235±0.011
F17-D	0.0235±0.010	0.0160±0.00
F17-E	0.0120±0.006	0.0940±0.044
F17-F	0.0160±0.00	0.0235±0.011
F17-G	0.0120±0.006	0.0630±0.00
F17-H	0.0120±0.006	0.0160±0.00
Gentamicin	0.0235±0.011	0.0310±0.00

3.5.7. Chemical profiling of the most active fraction, F17 using UPLC-QTOF-MS and MassLynx data processing towards identifying the bioactive compounds

Fraction F17 was selected as the most active fraction against *E. coli* and its chemical profile was generated using UPLC-QTOF-MS operating in the ESI negative mode (Figure 3.8). The full chromatographic profile of F17 displays major peaks in the region 12 - 16 minutes which are attributed to non-polar compounds. As discussed earlier (section 3.5.5) the zone of inhibition in the bioautography method was located at R_f = 0.08. The chromatographic

chemical analysis is focused in the region of 0 – 11 minutes. A total of six peaks were selected for identification based on their mass data and their purity (no interfering peaks). Using the ESI negative mode three compounds, at *m/z* 609.1546 retention time 6.34 minutes, at *m/z* 593.1492 retention time 7.01 minutes, and at *m/z* 623.1573 retention time 7.16 minutes were tentatively identified as rutin (peak 2), kaempferol-3-glucoside-3''-rhamnoside (peak 3) and isorhamnetin 3-O-robinoside (peak 4), respectively (Table 3.4). The chemical structures of the compounds identified are displayed in Figure 3.9. Rutin was already identified in the crude extract EtOH as described in Chapter 2.

Contradictions are found in the literature in terms of antimicrobial activity of rutin against *S. aureus* and *E. coli*. Gutierrez-Venegas et al. (2019) conducted a study that showed that rutin exhibited antimicrobial activity against microorganism present in tooth plaque which included *S. aureus* and *E. coli* (ATCC 25923)[21]. Nizer et al. (2020) conducted a study that showed lack of antimicrobial activity of rutin isolated from *Tontelea micrantha,* exhibiting greater than 500 µg/mL against both *S. aureus* (ATCC 29213) and *E. coli* (ATCC 25922) and also against several other microbes [22]. In their study Singh et al. (2008) showed that rutin exhibited an MIC of 0.07 mg/mL against *E. coli* (MTCC, 443) and *S. aureus* (MTCC, 96) [23]. The variation of the results may be attributed to different bacterial strains used.

No antibacterial studies were previously reported for kaempferol-3-glucoside-3''-rhamnoside and isorhamnetin 3-O-robinoside.

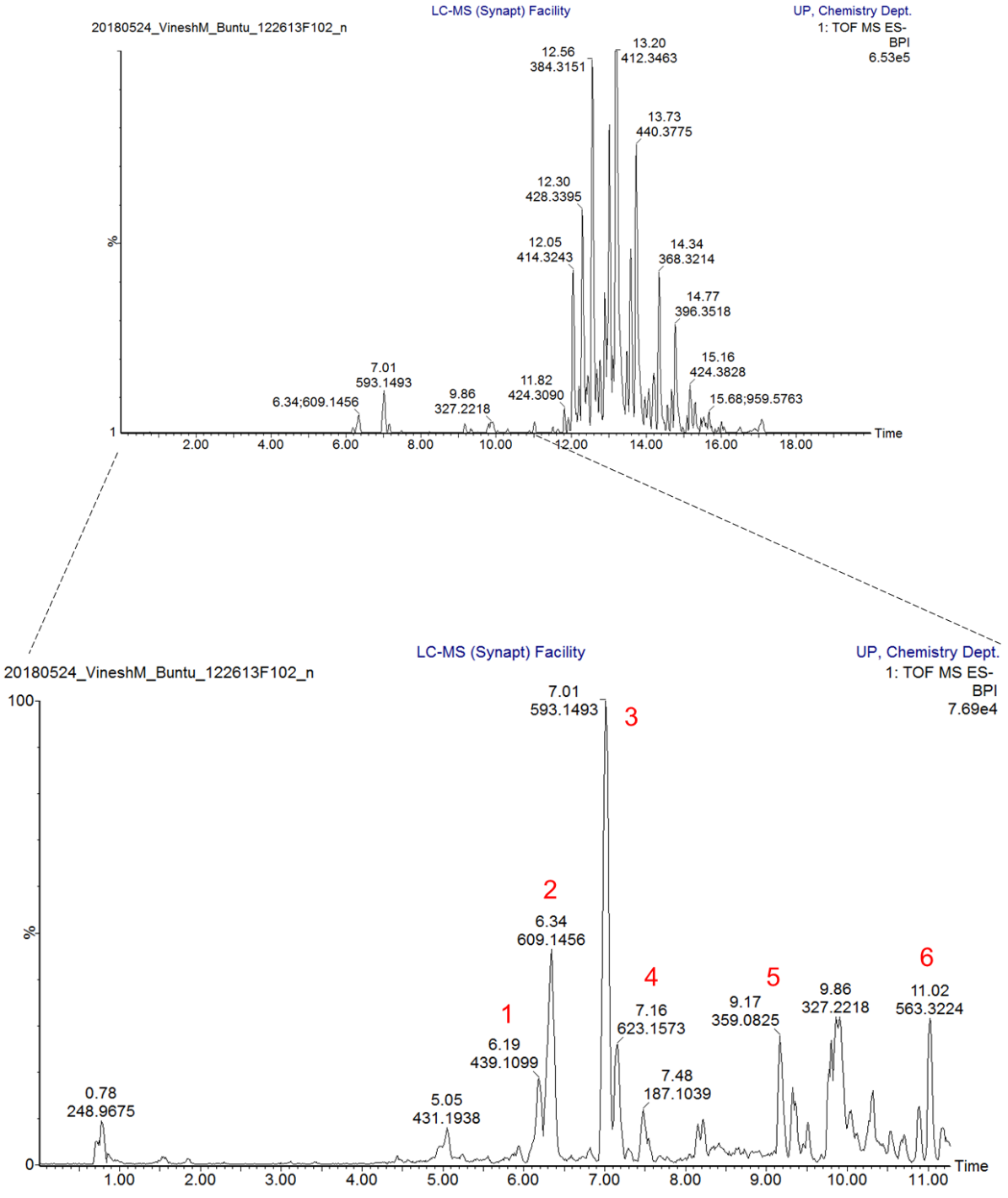

Figure 3.8: *ESI negative mode BPI chromatogram of the column chromatography obtained fraction F17 most active for E.coli inhibition in bioautography. Six peaks were selected for identification. Peaks 2, 3 and 4 were tentatively identified as rutin, kaempferol-3-glucoside-3"-rhamnoside and isorhamnetin 3-O-robinoside, respectively. The remaining of the peaks could not be identified.*

Table 3.4: *Chemical profile of fraction F17 from the EtOH extract.*

Peak #	Retention time (min)	Acquired [M - H]$^-$ *m/z*	Formula of possible structure	Theoretical [M - H]$^-$ *m/z*	Calculated accurate mass (Da)	Possible structures	Mass error (ppm)	Observed ions/ (fragments)	
1	6.20	439.1103	$C_{16}H_{24}O_{14}$	439.1088	440.1166	Unidentified	3.4	439.1103	
								440.1115	
								441.1087	
								329.1395	
2	6.34	609.1456	$C_{27}H_{30}O_{16}$	609.1456	610.1534	Rutin	0.0	609.1456	[M – H]$^-$
								302.0427	[M – H]$^-$ - $C_{12}H_{19}O_9$
								301.0407	[M – H]$^-$ - $C_{12}H_{20}O_9$
								300.0340	[M – H]$^-$ - $C_{12}H_{21}O_9$
								271.0311	[M - H]$^-$ - $C_{13}H_{22}O_{10}$
3	7.01	593.1492	$C_{27}H_{30}O_{15}$	593.1506	594.1585	Kaempferol-3-Glucoside-3"-Rhamnoside	-2.4	593.1492	[M - H]$^-$ - C12H
								286.0484	[M - H]$^-$ - $C_{12}H_{19}O_9$
								285.0457	[M - H]$^-$ - $C_{12}H_{20}O_9$
								284.0380	[M - H]$^-$ - $C_{12}H_{21}O_9$
								255.0360	[M - H]$^-$ - $C_{12}H_{22}O_{10}$
								227.0412	[M - H]$^-$ - $C_{14}H_{22}O_{11}$
4	7.16	623.1573	$C_{28}H_{32}O_{16}$	623.1612	624.1690	Isorhamnetin 3-O-robinoside	-6.3	623.1573	[M - H]$^-$
								316.0591	[M - H]$^-$ - $C_{12}H_{19}O_9$
								315.0545	[M - H]$^-$ - $C_{12}H_{20}O_9$
								314.0471	[M - H]$^-$ - $C_{12}H_{21}O_9$
								300.0293	[M - H]$^-$ - $C_{13}H_{23}O_9$
								299.0231	[M - H]$^-$ - $C_{13}H_{24}O_9$
5	9.16	359.0827	$C_{11}H_{20}O_{13}$	359.0826	360.0904	Unidentified	0.3	359.0827	
								344.0608	
								330.0428	
								329.0363	
								314.0142	
								301.0422	
								287.0205	
								286.0167	
								258.0242	
6	11.02	563.3224	$C_{31}H_{47}O_9$	563.3220		unidentified	0.7	563.3224	
								503.3042	
								322.1449	
								321.1433	
								130.0937	
								116.9340	
								96.9667	
								59.0199	

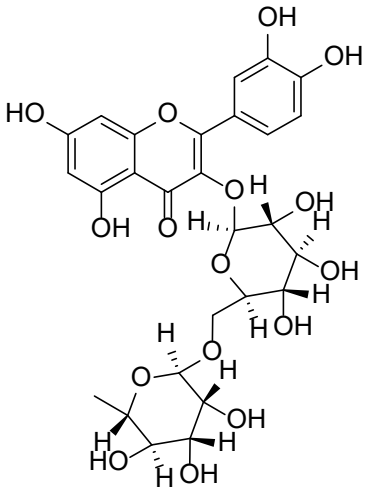

Peak 2: Rutin (**4**)

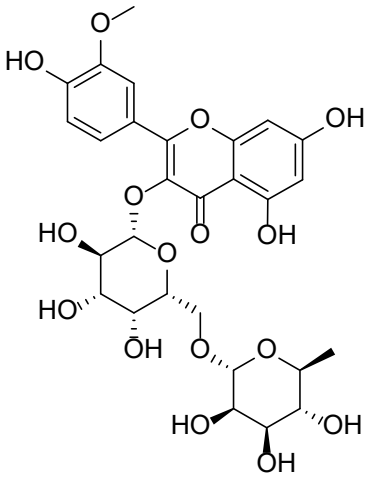

Peak 4: Isorhamnetin 3-*O*-robinoside (**10**)

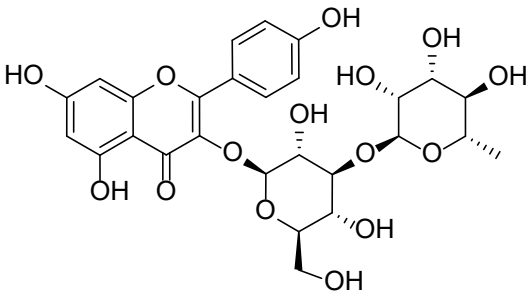

Peak 3: Kaempferol-3-glucoside-3''-rhamnoside (**9**)

Figure 3.9: *Chemical structures of rutin (peak 2),kaempferol-3-glucoside-3''-rhamnoside (peak 4) and isorhamnetin 3-O-robinoside (peak 4), the three compounds identified from fraction F17 of the EtOH extract.*

3.5.8. UNIFI® identification of compounds from the sub-fractions of F17

The major sub-fractions collected using the HPLC UV-vis technique were F17-E and F17-F, and using UNIFI® the major compounds from these fractions were identified as rutin (quercetin-3-*O*-rutinoside) and nictoflorin (kaempferol 3-*O*-rutinoside), at retention times 3.45 and 3.83 minutes, respectively, see Figure 3.10. Pure standards of these major compounds, rutin and nictoflorin, were purchased (Sigma Aldrich, South Africa) and further subjected to qualitative TLC bioautography (section 3.5.9). Furthermore, the compounds, kaempferol,

quercetin and nepitrin were identified as represented by minor peaks from the LCMS profiles of F17-E and F17-F using UNIFI® (Figure 3.10).

Nitiema et al. (2012), in their study showed that quercetin lacked inhibitory activity against *Enterobacter aerogenes* CIP 104 725, *E. coli* 81nr.149 SKN541, *Salmonella typhimurium* SKN533 and *Salmonella infantis* SKN 557, where the antibacterial test was performed by following agar disc diffusion method [24]. Kaempferol showed antimicrobial activity against *Bacillus cereus, B. subtills, S. aureus, Fusarium oxysporum, Macrophomina phaseoli, Diplodia oryzae, Rhizoctania solani, Helminthosporium turcicum, Aspergillus carneus,* except *B. mycoides, Sarcina lutea, E. coli and Candida albicans* by paper disc method [25]. Furthermore, Yamada et al. (1999), revealed that the MIC value of the kaempferol they isolated from the leaves of *Diospyros kaki* was 25.0, 100.0 and 50 µg/mL against *Staphilococcus mutans* K1, HS-6 and IFO 13955, respectively, and 25.0 µg/mL against *E. coli* B (IFO 13168), *E. coli* K-12 (IFO 3301), *Bacillus subtilis* (IFO 12210), and *S. aureus* (IFO 3060) [26]. This indicates that one of the minor compound identified, kaempferol is contributing to the antibacterial activity in this study. There are no antimicrobial studies reported for nepitrin.

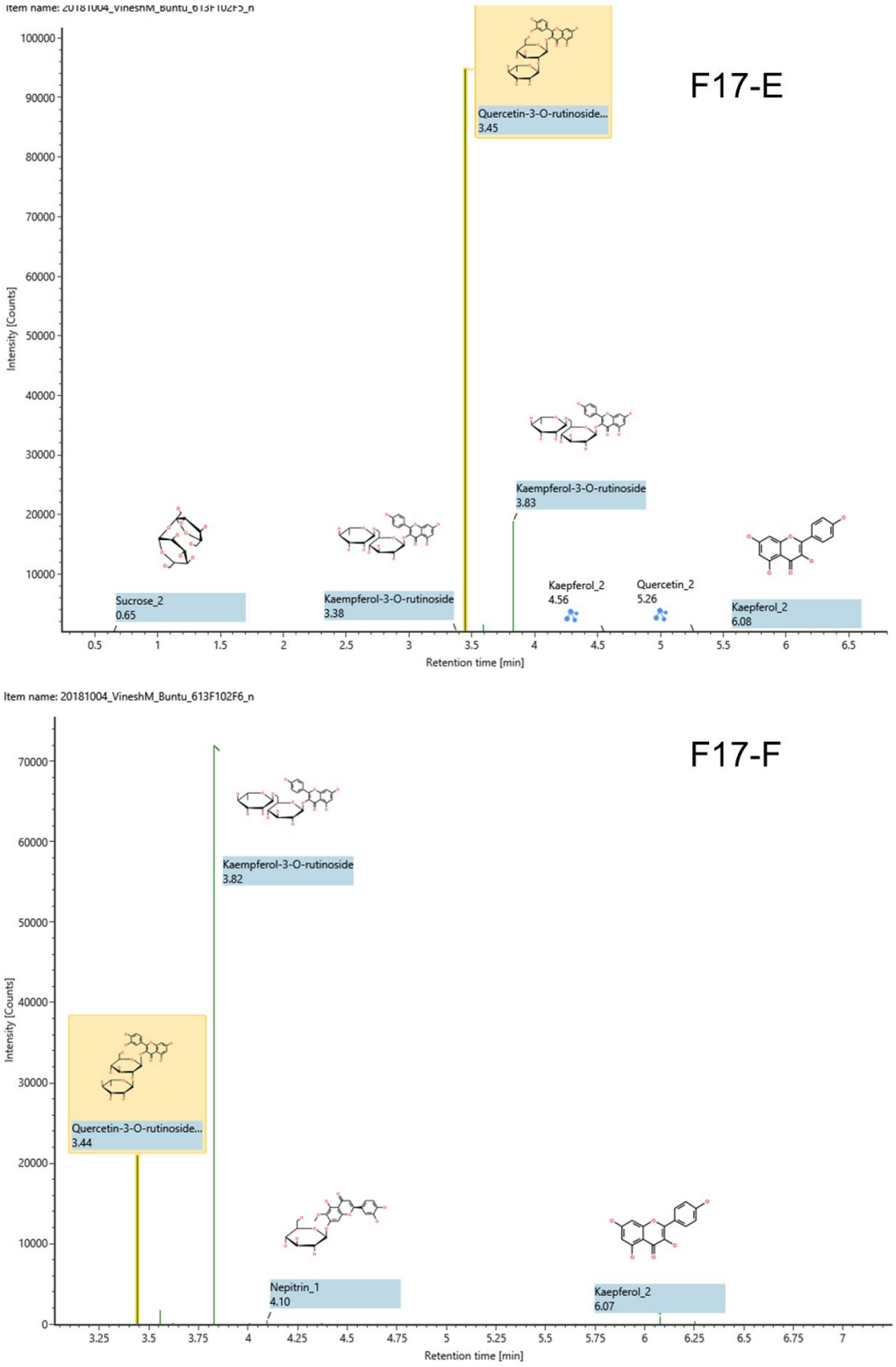

Figure 3.10: *UNIFI® identification of compounds from F17-E and F17-F. The compounds Quercetin-3-O-rutinoside and Kaempferol-3-O-rutinoside were identified as represented by the main peaks in these two fractions.*

3.5.9. Bioautography of purchased standards in comparison with the original fraction and extract

Qualitative bioautography assay was performed to evaluate the pure standards (rutin and nictoflorin) for their antimicrobial activity together with F17 and the crude extract all analysed on the same plates (Figure 3.11), Both the intermediate-acidic solvent system CEF (chloroform:ethylacetate:formic acid (5:4:1)) as well as the polar-neutral EMW (ethyl acetate:methanol:water (40:5.4:5)) were used for development of the plates. Figure 3.11 shows that both the pure standards are inactive as there are no bright spot to indicate activity on the plates even though they are the main ingredients.

Determination of the minimum inhibitory activity of nictoflorin and rutin against *E. coli* and *S. aureus* further revealed that these compounds exhibited no inhibition activity. This result is in line with Nizer et al. (2020) [21] who showed that rutin exhibits no inhibition activity against *E. coli* (ATCC 25922)and *S. aureus* (ATCC 29213). This is, however, contradicting Orhan et al. (2010) who reported nictoflorin and rutin as active against *E. coli* (ATCC 25922) [23]. Nictoflorin and rutin are therefore not responsible for the activity seen in this work regardless that some research proved them as active against the bacteria studied here, and this work agrees with the reports that indicate their lack of activity.

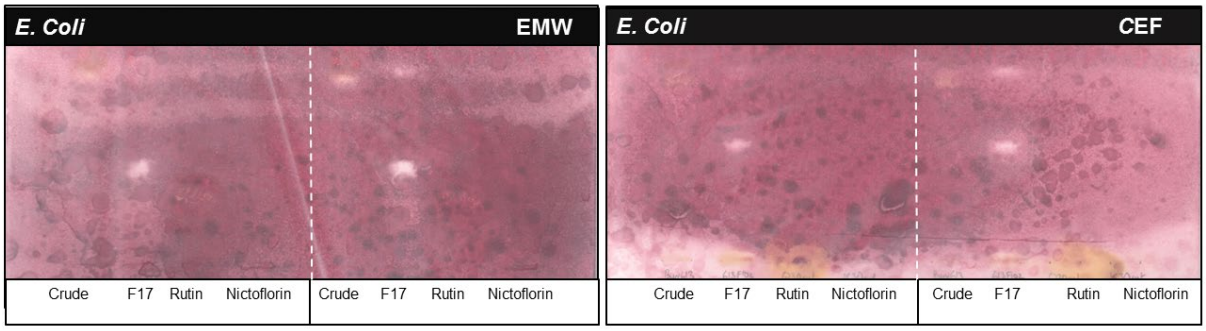

Figure 3.11: *Duplicated bioautograms of Escherichia coli inhibition of the pure standards. The plates were developed with solvent systems EMW and CEF. No activity evident proving that nicotiflorin and rutin are not responsible for the bioactivity.*

3.6. Conclusion

In this chapter the studies involving the fractionation of highly bioactive extracts were undertaken. The fractionation of two extracts is discussed. The EtOAc and EtOH extracts were fractionated towards identifying compounds responsible for α-glucosidase inhibition and antimicrobial (*E. coli* and *S. aureus*) inhibition, respectively.

Fractionation of the EtOH extract led to 22 fractions assessed for their inhibition of *E. coli* and *S. aureus via* the qualitative method of TLC bioautography. The most active fraction was F17 of the EtOH extract and this result led to its chemical analysis towards identifying the bioactive compounds. UPLC-QTOF-MS data analysis using molecular formulas generated using MassLynx, and by comparison of MS/MS fragmentation pattern using selected online libraries revealed three major compounds which were identified as rutin, kaempferol-3-glucoside-3''-rhamnoside and isorhamnetin 3-O-robinoside. Preparative HPLC-UV-vis fractionation of F17 led to semi-pure major compounds, that could not be separated, in two consecutive sub-fractions and all the 8 fractions obtained tested active in MIC. All the fractions were impure and, therefore, no compound structures could be elucidated. Analysis of the UPLC-QTOF-MS data, using the program UNIFI®, of the two major sub-fractions obtained *via* HPLC-UV-vis revealed the two major compounds as rutin, and nictoflorin.

Reference standards for rutin and nictoflorin were purchased, however, bioautography assessment of these compounds revealed that they were not responsible for the antimicrobial active. Furthermore, MIC evaluation of the pure standards against *E. coli* (ATCC 25922) and *S. aureus* (ATCC 29213), revealed no inhibitory activity. Moreover, three minor compounds from the two major sub-fractions obtained *via* HPLC-UV-vis were identified as quercetin, kaempferol and nepitrin. While there are no literature reports about antimicrobial activity studies on nepitrin, reports about quercetin indicated lack of activity, while kaempferol was indicated active against several strains of *E. coli* and *S. aureus* amongst other microbes. Kaempferol is, therefore, one of the compounds responsible of the biological activity. The major compounds identified exhibit no activity. Standards for two of the compounds identified using UPLC-QTOF-MS online libraries (*viz*. kaempferol-3-glucoside-3''-rhamnoside and isorhamnetin 3-O-robinoside) could not be obtained and no reports on the antimicrobial activity (*S. aureus* and *E. coli*) were found, indicating that these compounds are less researched, they could also be responsible for the antimicrobial activity. Based on the results in this chapter and the previous chapter, the potential for the components of the ethanol extract of *C. gynandra* leaves to be developed as antimicrobial agents against *E coli* and *S. aureus* is unquestionable.

Fractionation of the EtOAc extract led to 28 fractions assessed for their inhibition of α-glucosidase, revealing six most active fractions at 25 µg/mL. Some active fractions were selected based on their abundance and were assessed for their dose-dependent activity, and the fractions F5, F22, F40, F44, F49 and F50 showed concentration dependant activity. UPLC-QTOF-MS analysis revealed that most of the components responsible for α-glucosidase inhibition in *C. gynandra* leaves EtOAc extract are in the polar region. Isolation of the bioactive components *via* preparative HPLC-UV-vis could not be effected as the compounds do not absorb UV-vis light. A large majority of the compounds from the EtOAc extract of *C. gynandra* are unknown as searching the online libraries using MassLynx generated molecular masses and calculated exact masses, chemical formula as well as

fragmentation pattern comparison led to no positive identification of any known compounds. The only compound that could be identified was also a novel compound cleogynone A, whose structure is elucidated in Chapter 4.

While lack of reported research on isolation of compounds from *C. gynandra* makes this the first of its kind, it has posed a challenge in tackling this study. Future work, therefore, should attempt different methods towards identifying the most appropriate techniques and procedures to isolating the compounds from this plant, such as mass direct HPLC technique which were not the scope of this work. Based on the results in this chapter and the previous chapter, the potential for the components of ethyl acetate extract of *C. gynandra* leaves to be developed for the management of hyperglycaemia is undeniable. The major challenge which should be the bases of future work is fine tuning and identifying methodologies for isolating the polar components that are found to possess α-glucosidase inhibition activity that do not absorb UV-vis light, these have novel spectroscopic properties and are likely to be novel compounds.

3.7. References

1. Subramanian, R.; Asmawi, M.Z.; Sadikun, A. In vitro α-glucosidase and α-amylase enzyme inhibitory effects of Andrographis paniculata extract and andrographolide. *Acta Biochim. Pol.***2008**, *55*, 391–398, doi:10.18388/abp.2008_3087.

2. Assefa, S.T.; Yang, E.Y.; Chae, S.Y.; Song, M.; Lee, J.; Cho, M.C.; Jang, S. Alpha glucosidase inhibitory activities of plants with focus on common vegetables. *Plants***2020**, *9*, doi:10.3390/plants9010002.

3. Bourne, R.R.A.; Stevens, G.A.; White, R.A.; Smith, J.L.; Flaxman, S.R.; Price, H.; Jonas, J.B.; Keeffe, J.; Leasher, J.; Naidoo, K.; et al. Causes of vision loss worldwide, 1990-2010: A systematic analysis. *Lancet Glob. Heal.***2013**, *1*, 339–349, doi:10.1016/S2214-109X(13)70113-X.

4. Egdahl, A. WHO: World Health Organization.

5. Lam, S.H.; Chen, J.M.; Kang, C.J.; Chen, C.H.; Lee, S.S. α-Glucosidase inhibitors from the seeds of Syagrus romanzoffiana. *Phytochemistry***2008**, *69*, 1173–1178, doi:10.1016/j.phytochem.2007.12.004.

6. Butler, M.S. Natural products to drugs: Natural product derived compounds in clinical trials. *Nat. Prod. Rep.***2005**, *22*, 162–195, doi:10.1039/b402985m.

7. Hung, H.Y.; Qian, K.; Morris-Natschke, S.L.; Hsu, C.S.; Lee, K.H. Recent discovery of plant-derived anti-diabetic natural products. *Nat. Prod. Rep.***2012**, *29*, 580–606, doi:10.1039/c2np00074a.

8. Qi, L.-W.; Liu, E.-H.; Chu, C.; Peng, Y.-B.; Cai, H.-X.; Li, P. Anti-Diabetic Agents from Natural Products — An Update from 2004 to 2009. *Curr. Top. Med. Chem.***2010**, *10*, 434–457, doi:10.2174/156802610790980620.

9. Munhoz, A.C.M.; Frode, T.S. *Isolated Compounds from Natural Products with Potential Antidiabetic Activity - A Systematic Review*; 2018; Vol. 14; ISBN 6661705051.

10. Guisbiers, G.; Wang, Q.; Khachatryan, E.; Mimun, L.C.; Mendoza-Cruz, R.; Larese-Casanova, P.; Webster, T.J.; Nash, K.L. Inhibition of *E. Coli* and *S. aureus* with selenium nanoparticles synthesized by pulsed laser ablation in deionized water. *Int. J. Nanomedicine***2016**, *11*, 3731–3736, doi:10.2147/IJN.S106289.

11. Brehm-Stecher, B.F.; Johnson, E.A. Sensitization of Staphylococcus aureus and *Escherichia coli* to antibiotics by the sesquiterpenoids nerolidol, farnesol, bisabolol, and apritone. *Antimicrob. Agents Chemother.***2003**, *47*, 3357–3360, doi:10.1128/AAC.47.10.3357-3360.2003.

12. Jr, R.C.M. Discovering new antimicrobial agents. *Int. J. Antimicrob. Agents***2021**, *37*, 2–9, doi:10.1016/j.ijantimicag.2010.08.018.

13. Butaye, P.; Devriese, L.A.; Haesebrouck, F. Antimicrobial Growth Promoters Used in Animal Feed : Effects of Less Well Known Antibiotics on Gram-Positive Bacteria. *Clin. Microbiol. Rev.***2003**, *16*, 175–188, doi:10.1128/CMR.16.2.175.

14. Wulandari, A.P.; Primastia, N.; Sajuti, J.N. Sensitivity *Escherichia coli* and *Staphylococcus aureus* cause diarrhea to the fungi isolated from soft coral Sensitivity *Escherichia coli* and *Staphylococcus aureus* Cause Diarrhea to the Fungi Isolated from Soft Coral. *AIP Conf. Proc. 1744***2019**, *020005*, 1–5, doi:10.1063/1.4953479.

15. Dewanjee, S.; Gangopadhyay, M.; Bhattacharya, N.; Khanra, R.; Dua, T.K.

Bioautography and its scope in the field of natural product chemistry. *J. Pharm. Anal.***2015**, *5*, 75–84, doi:10.1016/j.jpha.2014.06.002.

16. Eloff, J.N. A sensitive and quick microplate method to determine the minimal inhibitory concentration of plant extracts for bacteria. *Planta Med.***1998**, *64*, 711–713, doi:10.1055/s-2006-957563.

17. Eloff, J.N. Avoiding pitfalls in determining antimicrobial activity of plant extracts and publishing the results. *BMC Complement. Altern. Med.***2019**, *19*, 1–8, doi:10.1186/s12906-019-2519-3.

18. Famuyide, I.M.; Aro, A.O.; Fasina, F.O.; Eloff, J.N.; Mcgaw, L.J. Antibacterial activity and mode of action of acetone leaf extracts of under-investigated Syzygium and Eugeia species on multi drug resisstant porcine diarrhoeagenic *E. coli*.pdf. **2019**, *9*, 1–14.

19. Yuk, J.; Narendrabhai Patel, D.; Qiao, L.; Isaac, G.; Yu, K. Detecting The “Un-Natural” In Natural Products Using Unifi Natural Product Application Solution. *Planta Med***2016**, *82*, OA44.

20. Deng, L.; Shi, A.M.; Liu, H.Z.; Meruva, N.; Liu, L.; Hu, H.; Yang, Y.; Huang, C.; Li, P.; Wang, Q. Identification of chemical ingredients of peanut stems and leaves extracts using UPLC-QTOF-MS coupled with novel informatics UNIFI platform. *J. Mass Spectrom.***2016**, *51*, 1157–1167, doi:10.1002/jms.3887.

21. Gutiérrez-Venegas, G.; Gómez-Mora, J.A.; Meraz-Rodríguez, M.A.; Flores-Sánchez, M.A.; Ortiz-Miranda, L.F. Effect of flavonoids on antimicrobial activity of microorganisms present in dental plaque. *Heliyon***2019**, *5*, doi:10.1016/j.heliyon.2019.e03013.

22. Nizer, W.S.D.C.; Ferraz, A.C.; Moraes, T.D.F.S.; Ferreira, F.L.; Magalhães, C.L.D.B.; Vieira-Filho, Sidney Augusto, Duarte, L.P.; Magalhães, J.C. De Lack of Activity of Rutin Isolated from Tontelea micrantha Leaves against Vero and BHK, Fungi, Bacteria and Mayaro virus and its in silico Activity. *J. Pharm. Negat. Results***2020**, *11*, 9–14, doi:10.4103/jpnr.JPNR.

23. Singh, M.; Govindarajan, R.; Rawat, A.K.S.; Khare, P.B. Antimicrobial Flavonoid Rutin from Pteris vittata L. against Pathogenic Gastrointestinal Microflora. *Am. Fern J.***2008**, *98*, 98–103.

24. Nitiema, L.W.; Savadogo, A.; Simpore, J.; Dianou, D.; Traore, A.S. In vitro antimicrobial activity of some phenolic compounds (coumarin and quercetin) against gastroenteritis bacterial strains. *Int. J. Microbiol. Res.***2012**, *3*, 183–187, doi:10.5829/idosi.ijmr.2012.3.3.6414.

25. El-Gammal, A.A.; Mansour, R.M.A. Antimicrobial Activities of Some Flavonoid Compounds. *Zentralbl. Mikrobiol.***1986**, *141*, 561–565, doi:https://doi.org/10.1016/S0232-4393(86)80010-5.

26. Yamada, Y.; Yamamoto, A.; Yoneda, N.; Nakatani, N. Identification of kaempferol from the leaves of Diospyros kaki and its antimicrobial activity against Streptococcus mutans. *Biocontrol Sci.***1999**, *4*, 97–100, doi:10.4265/bio.4.97.

Chapter 4:

Isolation, purification and structure elucidation of anticancer compounds from *Cleome gynandra* leaf extract

4.1. Background

Surgery, chemotherapy and radiotherapy are the conventional cancer treatments often supplemented by other complementary and alternative therapies [1]. Chemotherapy might be one of the most extensively studied methods in anticancer therapy, however, it is associated with toxicity and severe side effects [1]. Furthermore, multi-drug resistance is a greater challenge and thus further necessitating the search for new cancer drugs. With analysis of a number of chemotherapeutic agents and their sources indicating that over 60% of approved drugs are derived from natural compounds warranted the search for new ingredients as anticancer agents. Published research has indicated that *C. gynandra* extracts are active against cancer and some phytochemical studies have been conducted, however no studies have been reported on the systematic chemical analysis towards isolating and identifying the compounds responsible for the cancer activity. In this study lung cancer cytotoxicity of the crude extracts from *C. gynandra* leaves obtained *via* sequential extraction were screened and the *n*-hexane extract displayed the best activity (chapter 2). The technique UPLC-QTOF-MS was used to obtain the chemical fingerprint of the extract and the MS data for the resulting peaks were further studied towards identifying the components of the extract which was discussed in chapter 2. A large majority of the components of the *n*-hexane extract could not be identified using online libraries which warranted fractionation and isolation studies towards purifying and structure elucidation of the compounds responsible for the anticancer activity. In this chapter the *n*-hexane extract is subjected to bioassay-guided fractionation towards isolating and purifying the anticancer compounds.

4.2. Cancer

Cancer is a disease in which some of the cells grow uncontrollably, invading and destroying adjacent cells, where they may also spread to other parts of the body, and can start almost anywhere in the trillions of cells that make up a human body [2]. Migration of cancer to other parts of the body is called metastasis. Cancer has become a second leading life-threatening disease accounting for high mortality rates worldwide [3]. According to Gibbs (2000) cancer has become or shortly will become the leading disease-related cause of death in some areas of the world [4]. It is becoming a larger health problem and the medicines used as treatments have clear limitations [4]. Cancer accounted for 9.6 million deaths in 2018 [5]. Lung-, breast-, and colorectal cancers were the most prevalent, accounting for 2.09, 2.09 and 1.80 million cases, respectively, and hence these type of cancers selected for this study [5].

4.2.1. Lung cancer

Lung cancer, as the name suggests, begins in the lungs. The four major histologic types of lung cancer include squamous cell carcinoma, adenocarcinoma, large cell carcinoma, and small cell undifferentiated carcinoma, the combination accounting for greater than 90% of lung cancer cases [6,7]. Routine mortality statistics have confirmed that lung cancer became more frequent during the first half of the 20th century [7]. Increased death rates due to lung cancer have necessitated the search for potential novel anticancer compounds.

4.2.1.1. Potential causes and risk factors

Tobacco smoking is the major cause of lung cancers, 80%–90% of cases were shown to arise in cigarette smokers [6,7]. Tobacco smoke is known to contain over 20 known lung

cancer specific carcinogens and some reports indicate that, from such exposure, women may be at a higher risk of lung cancer [6]. Furthermore, studies indicate a 2.5-fold risk of lung cancer from family history, the familial association is most readily detected in lung cancer occurring in non-smokers [6]. While tobacco had been used for centuries worldwide the introduction of manufactured cigarettes with addictive properties, introducing inhalation of carcinogens, is what resulted in the surge in lung cancer cases [7]. In addition to smoking, an increase in lung cancer cases in South Africa is also attributed to factors such as environmental pollutants, occupational exposure and changing lifestyles [3]. The occupational and environmental factors include exposure to radon, arsenic, chromium, nickel, vinyl chloride, and ionizing radiation [8]. The risk of the disease is a joint consequences of the interrelationship between exposure to agents playing the aerologic (or protective) role and the individual susceptibility to such agents [7].

4.2.1.2. Effective treatment

Treatment differs according to the histologic type of cancer, the stage at presentation, and the functional evaluation of the patient [8]. Surgery is the treatment of choice for patients with stage I through IIIA non–small cell carcinoma.For patients undergoing complete resection and no preoperative chemotherapy, adjuvant chemotherapy is standard.Treatment for unresectable non–small cell carcinoma may involve radiotherapy and chemotherapy.The role of targeted therapies, specifically the antivascular endothelial growth factor agent bevacizumab (Avastin), has been examined in patients with advanced stage (IIIB and IV) non-squamous carcinoma. The combination of the vascular endothelial growth factor inhibitor bevacizumab and chemotherapy increases survival compared with chemotherapy alone [8,9]. Chemotherapy (combined with radiotherapy in limited stage disease) is the mainstay of treatment for small cell carcinoma [8]. Palliative and hospice care are important end-of-life treatment modalities. The primary care physician can help patients determine

what options may be most appropriate. Platinum-based chemotherapy remains the standard-of-care for most patients affected by advanced non-small cell lung cancer (NSCLC) and the platinum compounds currently used in NSCLC are cisplatin and carboplatin [10] while non-platinum-based combination therapies are reasonable alternatives in certain populations [9]. The structures of cisplatin, carboplatin andbevacizumab are shown in Figure 4.1. The National Cancer Institute of the United States of America listed cancer drugs approved by the Food and Drug Administration (FDA) for lung cancer, in August 2021 [11]. They stated that the individual drugs in the combinations were FDA-approved while the drug combinations themselves usually are not approved, although they are widely used. These are listed in Table 4.1.

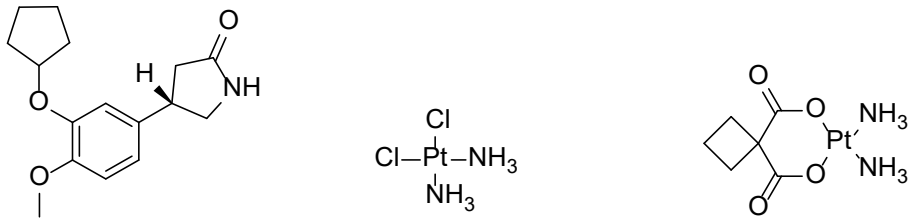

Bevacizumab **Cisplatin** **Carboplatin**

Figure 4.1: *Some examples of drugs used for lung cancer treatment.*

4.2.2. Breast cancer

Breast cancer incidence has increased dramatically elevating concern among physicians and women in general [12]. Breast cancer is a major affliction of women in affluent countries. Breast cancer is the commonest cause of cancer death in women worldwide [13]. The impact of breast cancer is magnified because women are at risk from their middle to later years. The incidence rates increase rapidly during the fourth decade and become substantial before the age of 50 thus creating a long-lasting source of concern for women and a need for vigilance [12]. Long-term increases in the incidence of breast cancer are being observed

worldwide in both industrialized and developing countries. Breast cancer is categorized into 3 major subtypes based on the presence or absence of molecular markers for oestrogen or progesterone receptors and human epidermal growth factor 2 (ERBB2; formerly HER2): hormone receptor positive/ERBB2 negative (70% of patients), ERBB2 positive (15%-20%), and triple-negative (tumours lacking all 3 standard molecular markers; 15%) [14].

Table 4.1: *Cancer drugs approved by the Food and Drug Administration (FDA) for lung cancer treatment therapy, published byThe National Cancer Institute of the United States government* [11].

Drugs Approved for Non-Small Cell Lung Cancer		Drugs Approved for Small Cell Lung Cancer	Drug Combinations Used to Treat Non-Small Cell Lung Cancer
• Abraxane • Afatinib Dimaleate • Afinitor (Everolimus) • Afinitor Disperz (Everolimus) • Alecensa (Alectinib) • Alectinib • Alimta • Amivantamab-vmjw • Atezolizumab • Avastin (Bevacizumab) • Bevacizumab • Brigatinib • Capmatinib Hydrochloride • Cemiplimab-rwlc • Ceritinib • Crizotinib • Cyramza (Ramucirumab) • Dabrafenib Mesylate • Dacomitinib • Docetaxel • Doxorubicin Hydrochloride • Durvalumab • Entrectinib • Erlotinib Hydrochloride • Gemcitabine Hydrochloride • Gemzar (Gemcitabine Hydrochloride) • Imfinzi (Durvalumab) • Everolimus Gavreto (Pralsetinib) • Gefitinib • Gilotrif (Afatinib Dimaleate) • Infugem (Gemcitabine Hydrochloride) • Ipilimumab • Iressa (Gefitinib) • Keytruda (Pembrolizumab) • Libtayo (Cemiplimab-rwlc) Lorbrena (Lorlatinib) • Lorlatinib • Lumakras (Sotorasib)	• Mekinist (Trametinib Dimethyl Sulfoxide) • Methotrexate Sodium • Mvasi (Bevacizumab) • Necitumumab • Nivolumab • Opdivo (Nivolumab) • Osimertinib Mesylate • Paclitaxel • Paclitaxel Albumin-stabilized Nanoparticle Formulation • Pembrolizumab • Pemetrexed Disodium • Portrazza (Necitumumab) • Pralsetinib • Ramucirumab • Retevmo (Selpercatinib) • Rozlytrek (Entrectinib) • Rybrevant (Amivantamab-vmjw) • Selpercatinib • Sotorasib • Tabrecta (Capmatinib Hydrochloride) • Tafinlar (Dabrafenib Mesylate) • Tagrisso (Osimertinib Mesylate) • Tarceva (Erlotinib Hydrochloride) • Taxotere (Docetaxel) • Tecentriq (Atezolizumab) • Tepmetko (Tepotinib Hydrochloride) • Tepotinib Hydrochloride • Trametinib Dimethyl Sulfoxide • Trexall (Methotrexate Sodium) • Vizimpro (Dacomitinib) • Vinorelbine Tartrate • Xalkori (Crizotinib) • Yervoy (Ipilimumab) • Zirabev (Bevacizumab) • Zykadia (Ceritinib)	• Afinitor (Everolimus) • Atezolizumab • Doxorubicin Hydrochloride • Durvalumab • Etopophos (Etoposide Phosphate) • Etoposide • Etoposide Phosphate • Everolimus • Hycamtin (Topotecan Hydrochloride) • Imfinzi (Durvalumab) • Lurbinectedin • Methotrexate Sodium • Nivolumab • Opdivo (Nivolumab) • Tecentriq (Atezolizumab) • Topotecan Hydrochloride • Trexall (Methotrexate Sodium) • Zepzelca (Lurbinectedin)	Carboplatin-Taxol Gemcitabine-Cisplatin

4.2.2.1. Potential causes and risk factors

Many of the established risk factors are linked to oestrogens [12,13]. Early menarche, late menopause, and obesity in postmenopausal women impose a risk [12,13]. The incidence is doubled among women with natural menopause after the age of 55 as compared with those

in whom it occurs before the age of 45 [12]. Breastfeeding probably has a protective effect as childbearing reduces risk while research further shows that early first birth and a larger number of births has greater protective effect [12,13]. Both oral contraceptives and hormonal therapy for menopause cause a small increase in breast-cancer risk which appears to diminish once use stops [12,13]. Physical activity is probably protective. Alcohol consumption has also increased the risk. Mutations in certain genes greatly increase breast-cancer risk but these account for a minority of cases [13].

A family history of breast cancer particularly when the diagnosis was made in the mother or a sister at a young age can be an important risk factor for breast cancer [12]. Exposure to ionizing radiation particularly between puberty and the age of 30 can substantially increase the risk of breast cancer [13]. Additional risk factors include tallness the use of oral contraceptives and user of oestrogen supplements [13].

4.2.2.2. Treatment

Local therapy for non-metastatic breast cancer consists of surgical resection and sampling or removal of axillary lymphnodes with consideration of postoperative radiation [14]. Currently, metastatic breast cancer remains incurable in virtually all affected patients. Surgery and radiation are typically used for palliation only in metastatic disease [14]. Medical therapy of breast cancer with anti-estrogens such as raloxifene or tamoxifen might avoid breast cancer in individuals who are at increased possibility of developing it [15]. Structures of some drugs used for treatment of breast cancer are shown in Figure 4.2.

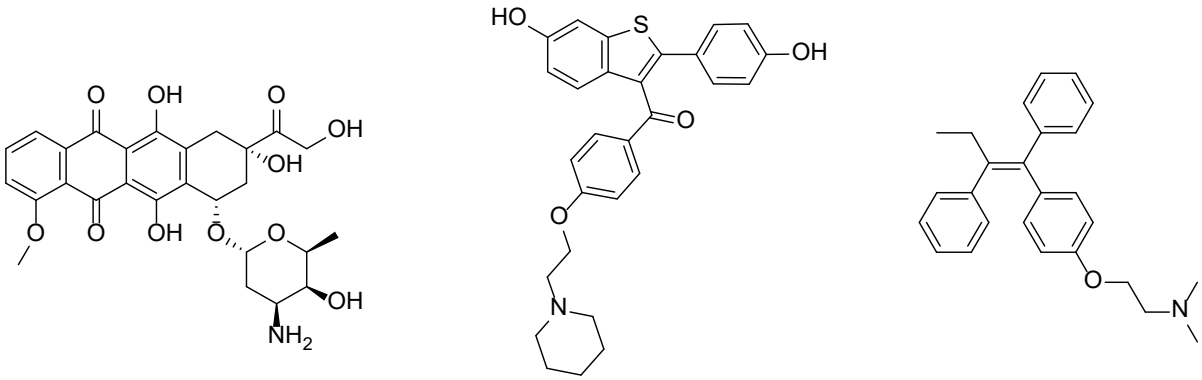

Doxorubicin **Raloxifen** **Tamoxifen**

Figure 4.2: *Some examples of structures of drugs used in breast cancer medical therapy.*

The cancer drugs approved by the FDA for breast cancer were published by the National Cancer Institute of the United States government [16]. Some drug combinations themselves usually are not approved, although they are widely used. These are listed in Table 4.2.

***Table 4.2**: Cancer drugs approved by the Food and Drug Administration (FDA) for breast cancer treatment therapy, published by The National Cancer Institute of the United States government* [16].

Drugs Approved to Treat Breast Cancer		Drugs Approved to Prevent Breast Cancer	Drug Combinations Used in Breast Cancer
• Abemaciclib • Abraxane (Paclitaxel Albumin-stabilized Nanoparticle Formulation) • Ado-Trastuzumab Emtansine • Afinitor (Everolimus) • Afinitor Disperz (Everolimus) • Alpelisib • Anastrozole • Aredia (Pamidronate Disodium) • Arimidex (Anastrozole) • Aromasin (Exemestane) • Capecitabine • Cyclophosphamide • Docetaxel • Doxorubicin Hydrochloride • Ellence (Epirubicin Hydrochloride) • Enhertu (Fam-Trastuzumab Deruxtecan-nxki) • Epirubicin Hydrochloride • Eribulin Mesylate • Everolimus • Exemestane • 5-FU (Fluorouracil Injection) • Fam-Trastuzumab Deruxtecan-nxki • Fareston (Toremifene) • Faslodex (Fulvestrant) • Femara (Letrozole) • Fluorouracil Injection • Fulvestrant • Gemcitabine Hydrochloride • Gemzar (Gemcitabine Hydrochloride) • Goserelin Acetate • Halaven (Eribulin Mesylate) • Herceptin Hylecta (Trastuzumab and Hyaluronidase-oysk) • Herceptin (Trastuzumab) • Ibrance (Palbociclib) • Infugem (Gemcitabine Hydrochloride) • Ixabepilone • Ixempra (Ixabepilone) • Kadcyla (Ado-Trastuzumab Emtansine)	• Keytruda (Pembrolizumab) • Kisqali (Ribociclib) • Lapatinib Ditosylate • Letrozole • Lynparza (Olaparib) • Margenza (Margetuximab-cmkb) • Margetuximab-cmkb • Megestrol Acetate • Methotrexate Sodium • Neratinib Maleate • Nerlynx (Neratinib Maleate) • Olaparib • Paclitaxel • Paclitaxel Albumin-stabilized Nanoparticle Formulation • Palbociclib • Pamidronate Disodium • Pembrolizumab • Perjeta (Pertuzumab) • Pertuzumab • Pertuzumab, Trastuzumab, and Hyaluronidase-zzxf • Phesgo (Pertuzumab, Trastuzumab, and Hyaluronidase-zzxf) • Piqray (Alpelisib) • Ribociclib • Sacituzumab Govitecan-hziy • Soltamox (Tamoxifen Citrate) • Talazoparib Tosylate • Talzenna (Talazoparib Tosylate) • Tamoxifen Citrate • Taxotere (Docetaxel) • Tecentriq (Atezolizumab) • Tepadina (Thiotepa) • Thiotepa • Toremifene • Trastuzumab • Trastuzumab and Hyaluronidase-oysk • Trexall (Methotrexate Sodium) • Trodelvy (Sacituzumab Govitecan-hziy) • Tucatinib • Tukysa (Tucatinib) • Tykerb (Lapatinib Ditosylate) • Verzenio (Abemaciclib) • Vinblastine Sulfate • Xeloda (Capecitabine) • Zoladex (Goserelin Acetate)	• Evista (Raloxifene Hydrochloride) • Raloxifene Hydrochloride • Soltamox (Tamoxifen Citrate) • Tamoxifen Citrate	**AC** • Doxorubicin (Adriamycin) • Cyclophosphamide **AC-T** • Doxorubicin (Adriamycin) • Cyclophosphamide • Paclitaxel (Taxol) **CAF** • Cyclophosphamide • Doxorubicin • Fluorouracil **CMF** • Cyclophosphamide • Methotrexate • Fluorouracil **FEC** • Fluorouracil • Epirubicin Hydrochloride • Cyclophosphamide **TAC** • Docetaxel (Taxotere) • Adriamycin • Cyclophosphamide

4.2.3. Colorectal cancer

Colorectal cancer is the fourth most common cancer in men and the third most common cancer in women worldwide [17]. The clinical behaviour results from interactions at many levels and it is challenging to understand the molecular basis of individual susceptibility to colorectal cancer [18]. About fifty percent of patients are cured by surgery alone while the other half however will eventually die due to metastatic disease, which includes approximately 25% of patients who have evidence of metastases at the time of diagnosis [19].

4.2.3.1. Potential causes and risk factors

With incidence rates varying approximately 20-fold worldwide, the highest rates are seen in the developing world [20]. The 20-fold international differences may be explained by dietary and other environmental differences. Colon and rectal cancers share many environmental risk factors and are both found in individuals with specific genetic syndromes. Colorectal cancer is known to occur more frequently in certain families and there are several rare genetic syndromes that are markers of high risk [20]. Colon cancer occurs with approximately equal frequency in men and women while rectal cancer is up to twice as common in men as in women [20]. Consumption of vegetables, fruits, fibre, and micronutrients is associated with lower risk while evidence is consistent with a stronger risk with saturated/animal fat than with total fat. A majority of studies indicate an increased risk or null with higher intake of meat [20]. Egg consumption, sugar intake, and frequency of eating are to some degree associated with increased risk, while complex carbohydrate, vitamin D, and vitamin E consumption are associated with possibly decreased risk of colorectal neoplasia [20]. The relationship between physical activity and reduced risk is the most consistent finding while obese individuals are at an increased risk of contracting colorectal

cancer. While alcohol consumption shows inconsistent relation to elevated risk, smoking shows no association. Nonsteroidal anti-inflammatory drugs, including aspirin have been consistently associated with a reduced risk of colorectal cancer [20].

4.2.3.2. Treatment

Depressed lesion confined to the mucosa or that only slightly invade the submucosa can be completely removed with an endoscopic mucosal resection (EMR) technique [21]. If the histologic analysis of the resected specimen shows that the cancer has massively invaded the submucosa or permeates the vessels, additional surgical resection is required to avoid risk of reoccurrence. Laterally spreading tumors are good indications for EMR or endoscopic piecemeal mucosal resection (EPMR). Lesions up to 25 mm in diameter can be removed by the EMR technique. Those larger than 25 mm would be treated with EPMR. Small flat adenomas up to 5 mm can be easily treated with the hot biopsy technique [21]. That 5 to 10 mm in diameter can be treated with the EMR technique. It may not be necessary, however, to treat all flat lesions because they are almost always non-invasive.

Treatment of colorectal cancer primarily uses fluorouracil, a fluorinated pyrimidine, which is thought to act primarily by inhibiting thymidylate synthase, the rate-limiting enzyme in pyrimidine nucleotide synthesis [22]. Advances in the systemic therapy of colorectal cancer are reported with significant progress in the treatment of colorectal cancer having been achieved with the approval of several new therapeutic agents that have greatly improved the outlook for patients diagnosed with resectable and metastatic disease [22]. Fluoropyrimidines such capecitabine and tegafur uracil are some of the effective treatment methods. Irinotecan is a semisynthetic derivative of the natural alkaloid camptothecin that is converted by carboxylesterases to SN-38. SN-38 causes DNA fragmentation and programmed cell death [22]. Oxaliplatin is a diaminocyclohexane platinum compound that

forms DNA adducts, leading to impaired DNA replication and cellular apoptosis. In patients with metastatic colon cancer, single-agent oxaliplatin has limited efficacy, but clinical benefit has been observed when it is administered with fluorouracil and leucovorin. Angiogenesis inhibitors are a recently recognized strategy to control malignant proliferation and spread [22]. Currently the most successful anti-angiogenic strategy has focused on inhibiting the vascular endothelial growth factor, a soluble protein that stimulates blood vessel proliferation. Bevacizumab is a humanised monoclonal antibody directed against vascular endothelial growth factor that has been examined in combination with chemotherapy in patients with advanced colorectal cancer [22]. Several ongoing studies are assessing the efficacy of combined treatment with monoclonal antibodies to vascular endothelial growth factor and EGFR in patients with metastatic colorectal cancer [22].

The use of a fluoropyrimidine, irinotecan, oxaliplatin, bevacizumab, and either cetuximab or panitumumab, in the treatment of patients with metastatic colorectal cancer is supported. The goal of ongoing adjuvant trials evaluating bevacizumab and cetuximab is to increase even further the improved rates of survival provided by fluorouracil, leucovorin and oxaliplatin [[22]].

Some drugs commonly used for colorectal cancer include: 5-fluorouracil (5-FU), capecitabine (xeloda), irinotecan (camptosar), oxaliplatin (eloxatin), trifluridine and tipiracil (lonsurf) [23]. Figure 4.3 illustrates some chemical structures of some common colorectal cancer therapeutic drugs.Drugs approved and used in the treatment of colorectal cancer are listed in Table 4.3.

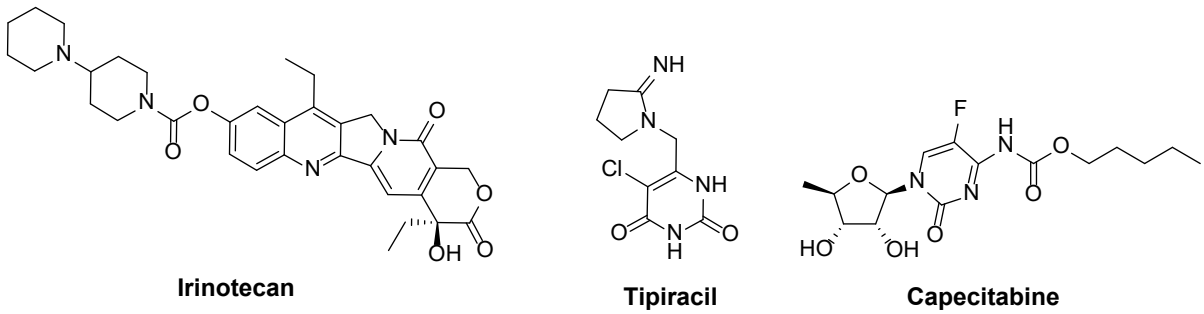

Figure 4.3: *Chemical structures of some drugs used for colorectal cancer treatment.*

Table 4.3: *Cancer drugs approved by the FDA for colorectal cancer treatment therapy, published by The National Cancer Institute of the United States government* [23].

Drugs Approved for Colon and Rectal Cancer	Drug combinations used	Drugs Approved for Gastroenteropancreatic Neuroendocrine Tumours
• Avastin (Bevacizumab) • Bevacizumab • Camptosar (Irinotecan Hydrochloride) • Capecitabine • Cetuximab • Cyramza (Ramucirumab) • Eloxatin (Oxaliplatin) • Erbitux (Cetuximab) • 5-FU (Fluorouracil Injection) • Fluorouracil Injection • Ipilimumab • Irinotecan Hydrochloride • Keytruda (Pembrolizumab) • Leucovorin Calcium • Lonsurf (Trifluridine and Tipiracil Hydrochloride) • Mvasi (Bevacizumab) • Nivolumab • Opdivo (Nivolumab) • Oxaliplatin • Panitumumab • Pembrolizumab • Ramucirumab • Regorafenib • Stivarga (Regorafenib) • Trifluridine and Tipiracil Hydrochloride • Vectibix (Panitumumab) • Xeloda (Capecitabine) • Yervoy (Ipilimumab) • Zaltrap (Ziv-Aflibercept) • Zirabev (Bevacizumab) • Ziv-Aflibercept	**CAPOX** • Capecitabine • Oxaliplatin **FOLFIRI** • Leucovorin Calcium (Folinic Acid) • Fluorouracil • Irinotecan Hydrochloride **FOLFIRI-BEVACIZUMAB** • Leucovorin Calcium (Folinic Acid) • Fluorouracil • Irinotecan Hydrochloride • + Bevacizumab **FOLFIRI-CETUXIMAB** • Leucovorin Calcium (Folinic Acid) • Fluorouracil • Irinotecan Hydrochloride • + Cetuximab **FOLFOX** • Leucovorin Calcium (Folinic Acid) • Fluorouracil • Oxaliplatin **FU-LV** • Fluorouracil • Leucovorin Calcium **XELIRI** • Capecitabine (Xeloda) • Irinotecan Hydrochloride **XELOX** • Capecitabine (Xeloda) • Oxaliplatin	• Afinitor (Everolimus) • Everolimus • Lanreotide Acetate • Somatuline Depot (Lanreotide Acetate)

4.2.4. Anticancer compounds from natural resources

Phytochemical compounds have in several cases been directly employed or chemically modified to develop chemicals used in modern medicine including anticancer drugs [24]. According with the FDA, more than the 60% of the drugs employed in cancer treatment are obtained from natural resources [24]. Garcia-Oliveira et al. (2021) summarized available information regarding the clinical status of the main plant compounds proposed for cancer treatment [24]. Vinka alkaloids, taxanes, camptothecin derivatives, podophyllotoxin and

derivatives and roscovitine were the most used in clinical studies. Major plant-based compounds widely used in treating cancers include vincristine, vinblastine, camptothecin, paclitaxel, irinotecan, topotecan, and etoposide [25]. Figure 4.4 displays some of these major plant-based compounds.

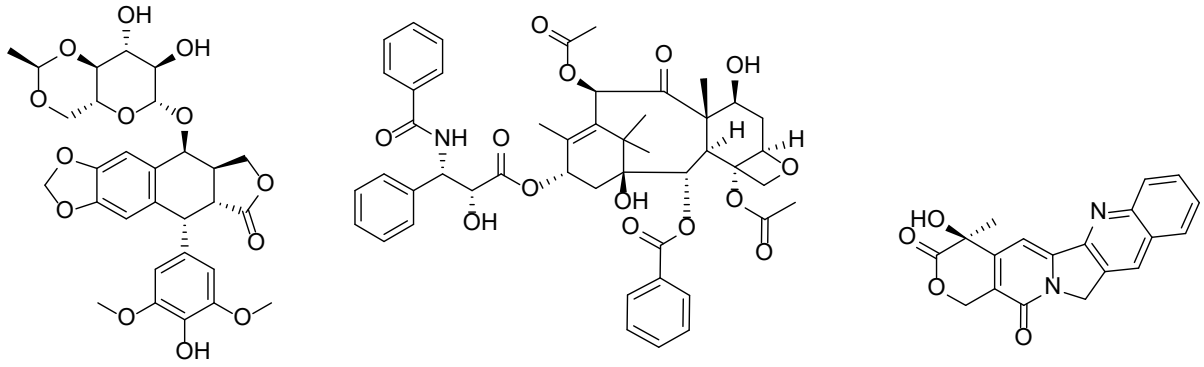

Figure 4.4: *Some examples of major plant-based compounds widely used in cancer therapy. Etoposide a semisynthetic derivative of podophyllotoxin from rhizomes (Podophyllum peltatum). Paclitaxel derived from the bark of the Pacific yew tree (Taxus brevifolia). Camptothecin is a naturally occurring alkaloid derived from the plant Camptotheca acuminate.*

A summary of current available information regarding the clinical status of the main plant based compounds proposed for cancer treatment is compiled [24]. An overview of the collected data supporting the development of plant compounds as anticancer agents including clinical trials and clinical uses are listed in Table 4.4 [24,25].

Table 4.4: *Plant-based anticancer compounds employed in clinical treatment of cancer* [24].

Compounds	Source-Extraction	Clinical Development	Commercial Name
Vinca alkaloids	*Catharanthus roseu* (Leaves) Isolated by semi-synthetic routes	In clinical use; combination trials	Vinorelbine, Vincristine, Vinblastine, Vindesine, Vinflunine, Vincamine, Vintafolide
Paclitaxel, docetaxel	*Taxus* spp. (Bark) Synthesis, semi-synthesis, and plant cell culture	In clinical use; Phase I-III clinical trials; early treatment settings; non-small lung cancer, breast cancer, ovarian cancer, Kaposi sarcoma. Research and development in alternative drug administration using nanoparticles, naocochealtes and nanoliposomes.	Taxol®, Taxotere®, Abraxane®, Jevtana®, Taxoprexin®, Xytotax®
Camptotecin, irinotecan	*Camptotheca acuminate* (leaves) Water extraction	Ovarian, lung, colorectal and pediatric cancer	Topotecan, irinotecan, belotecan
Podophyllotoxin and analogues	*Podophyllum* spp. (rhizome, roots) Alcohol extraction	Lymphomas and testicular cancer trials	No rentable
Roscovitine	*Raphanus sativus* (Radish) Chloroform extraction	Phase II clinical trials inEurope	Roscovitine, seliciclib

Many other potential plant secondary metabolites have been proven experimentally with anticancer properties and are under clinical or preclinical trial phase studies [24,25]. These positive results led to their evaluation in further clinical trials to estimate the suitability (preliminary efficacy, toxicity, pharmacokinetics, safety data, etc.) of the compounds as possible agents in new strategies for cancer therapy. Garcia-Oliveira et al. (2021) [24] have compiled a list of some examples of these compounds (Table 4.5).Some terpenoids isolated from African plants have shown good activities against various cancer cells. This includes oleanane-type triterpenoid saponins, gummiferaosides A, B and C (Albizia gummifera); caseanigrescen A, B, C and D (Casearia nigrescens); cardenolide glycosides, elaeodendroside V and W (Elaeodendron alluaudianum); crotobarin (human oral epidermoid carcinoma), HT29 (human colon adenocarcinoma), A549 (human lung adenocarcinoma) and HL60 (human promyelocytic leukemia) cell lines and crotogoudin (Croton barorum and Croton goudotii) [26].

Table 4.5: *Examples of clinical trials carried out with the selected phytochemical compounds* [24].

Compound	Type of Cancer	Main Results
Sulforaphane	Prostate	Reduction of prostate-specific antigen after prostatectomy/Lengthening of the on-treatment prostate-specific antigen doubling time
	Breast	Improved efficacy of doxorubicin, without any cytotoxic effect.
Resveratrol	Colorectal	Induction of apoptosis in malignant cells in hepatic metastasis.
	Breast	Reduction of DNA methylation of RASSF-1 and prostaglandin E2 expression.
	Prostate	Reduction of cancer recurrence.
Curcumin	Pancreas	Improved efficacy of gemcitabine, without any cytotoxic effect.
	Breast	Improved efficacy of paclitaxel, without any cytotoxic effect.
Quercetin	Gastric	High dietary intake is inversely related to the risk of cancer development.
Gingerol	Colorectal	Reduction of the risk of cancer development.
	Solid tumour	Enhanced antioxidant status of patients receiving chemotherapy/Improvement of general quality of cancer patients receiving chemotherapy.
Kaempferol	Ovarian Pancreatic	Reduction of the risk of cancer development.

Different classes of phenolic compounds have been reported with high anti-proliferative effects against cancer cell lines. Flavonoids from the genus *Dorstenia*, gancaonin Q, 6-prenylapigenin, 6,8-diprenyleriodictyol, and 4-hydroxylonchocarpin, inhibited the proliferation of a panel of 14 cancer cell lines including human CCRFCEM leukaemia cells and their multidrug-resistant subline, CEM/ADR5000, PF-382 leukaemia T-cells, and HL-60 promyelocytic leukaemia (moderately differentiated), MiaPaCa-2 and Capan-1pancreatic adenocarcinoma, MCF-7 breast adenocarcinoma, SW-680 colon carcinoma cells, 786-0 renal carcinoma cells, U87MG glioblastoma-astrocytoma cells, A549 lung adenocarcinoma, Caski and HeLa cervical carcinoma cells, Colo-38 skin melanoma cells [26].

Data available from the screening of some alkaloids are rather moderate. Acridone alkaloids isolated from the fruits of *Zanthoxylum leprieurii* helebelicine A, 3-hydroxy-1-methoxy-10-methyl-9-acridone, 1-hydroxy-3-methoxy-10-methyl-9-acridone and 1-hydroxy-2,3-dimethoxy-10-methyl-9-acridone showed moderate activity against human lung carcinoma cells A549 (IC_{50} values of 31 to 52μM) and colorectal adenocarcinoma cells DLD-1 (IC_{50} of 27 to 74μM). Cytotoxic compounds such as vinblastine and vincristine are present in the

Madagascar periwinkle (*Catharanthus roseus*) are highly active alkaloids. Some further well known anticancer alkaloids are veprisine and jatrorrhizine [26].

According to the National Cancer Institute plant screening program, a pure compound is generally considered to have *in vitro* cytotoxic activity if the IC_{50} value following incubation between 48 and 72 hr is less than 4 µg/mL. Furthermore, the cut-off point for good cytotoxic compound has also been established to be 10 µM [26].

4.3. Materials and methods

Solvents and reagents (*n*-hexane and acetone) used for column chromatography and aluminium backed thin-layer chromatography (TLC) were analytical grade purchased from MERCK (Sigma Aldrich, South Africa) or Radchem (Pty) Ltd (South Africa). Solvents and reagents (*n*-hexane, acetone, methanol and chloroform) used for preparative TLC were HPLC/Ultra-PLC grade, purchased from MERCK (Sigma Aldrich, South Africa). Milli-Q® water was used in preparative experimentations involving the use of water. All chemicals were used without further purification.

Silica gel 60 (0.063-0.2 mm; Macherey-Nagel GmbH & Co. KG, Düren, Germany) and Silica gel-60 (0.040-0.063 mm; Merck KGaA, Darmstadt, Germany) were used for open column chromatography. Silica gel GF_{254} plates (Merck KGeA, Darmstadt, Germany) were used for TLC detection while preparative TLC was achieved using TLC Silica gel 60 glass plates (Merck KGaA, Darmstadt, Germany).

4.3.1. Primary fractionation using column chromatography

Primary fractionation was achieved using column chromatography. A glass column of 105 cm length and 7 cm internal diameter with a reservoir of 2 L capacity was used. The column

was packed with a slurry suspension by mixing approximately 1380 g of dried silica gel with *n*-hexane. Dried *n*-hexane extract (2 g) was dissolved in *n*-hexane (15 ml) and the dissolved extract was poured slowly onto the bed of the silica gel layer in glass column and allowed to settle. Initially, 100 % *n*-hexane was used as the eluent after which the polarity was increased by mixing the hexane with acetone, while the elution progress was monitored using thin layer chromatography (TLC). The mobile phase was increased from 100 % *n*-hexane up to *n*-hexane:acetone (40:60). Sixty-three fractions were collected which were further analysed by TLC using silica gel plates and visualised under UV light at 254 nm as well as by staining with a vanillin stain (MeOH, 30 ml; vanillin, 0.1 g; H_2SO_4, 1 ml dropwise). TLC profiles of the fractions for anticancer analysis were obtained on aluminum-backed silica gel plates. A combination of *n*-hexane and acetone (*n*-hexane:acetone 80:20; 70:30; 60:40; 50:50 and 40:60) were used for TLC development for analysis of a solution of a 10 mg/mL of each of the fractions loaded on the TLC plates. Visible bands were marked under white light and ultraviolet light (254 nm and 360 nm wavelengths, Camac universal UV light lamp TL-600) before staining. The plates were then heated to 110 °C for colour development.

After visualisation, similar fractions were combined and dried using a *Buchi* rotary evaporator and/or a *Genevac SP Scientific* EZ-2 centrifugal evaporator.

4.3.2. Secondary fractionation *via* column chromatography and preparative TLC

The isolation and purification of the major and active compounds from active fractions obtained from the primary fractionation was achieved by column chromatography and preparative TLC. A glass silica column of 92 cm length and 9 cm circumference. 55 g dry silica was made into a slurry with *n*-hexane and selected active fraction(s) obtained fromprimary fractionation (200 mg) were dissolved in *n*-hexane (20 ml) and the dissolved fraction was poured slowly onto the bed of the silica gel layer in glass column and allowed to

settle, initially, 100 % *n*-hexane was used as the eluent. The polarity was increased gradually by mixing *n*-hexane with acetone, while the elution progress was monitored using TLC, fifteen fractions were collected. Semi-pure most abundant subfractions were purified *via* preparative TLC. Fourty and eighty milligrams of selected two subfractions was dissolved in chloroform and loaded as a band on the glass preparative TLC and developed with solvent system *n*-hexane-acetone (80:20). The Rf value of the band relating to the compound of interest to be purified was located on the preparative TLC glass by separating a 1.5 cm width strip at the edge of the glass silica plate by scrapping off a vertical line using a pencil tip. About 1 mg of the fraction was spotted on this separate strip on the glass silica plate to start on the same line as the purification sample in a parallel run. After development of the TLC, the edge of the strip was then stained with a vanillin stain (MeOH, 30 ml; vanillin, 0.1 g; H_2SO_4, 1 ml) and heated using a hair-dryer for colour development and different colour spots were visible. The respective band parallel of the visualised spot(s) of interest was scrapped off separately and extracted from silica using a mixture chloroform :methanol (7:3) while the silica was filter using a sintered glass funnel. The pure compounds were dried using a *Genevac SP Scientific* EZ-2 centrifugal evaporator.

4.3.3. Cancer cell culture

All cell lines were cultured at 37°C, 5% CO_2, in Dulbecco's Modified Eagle Medium (DMEM) containing high glucose (containing 4.5 g/L glucose, sodium bicarbonate and phenol red), supplemented with 10 % fetal bovine serum (FBS), Glutamax (2 mM) and PenStrep (0.5 mg/mL). Cell culture and cancer cytotoxicity studies were performed as part of training of myself at the cancer research laboratory (B. G. Vidya, K. G. Mahadeva Swamy and Venugopal R. Bovilla) led by professor SubbaRao V. Madhunapantula. The research laboratory is located at the Cellular and Molecular Biology centre, Department of Biochemistry, JSS Medical College, JSS University, Mysuru, Karnataka, in India.

4.3.4. Anticancer assays

Lung cancer (A549), breast cancer (MDA-MB-468) and colorectal cancer (HCT-15 and HCT-116) cells were trypsinized at 10,000 cells per well in a 100 µL volume plated in 96 well plate. The cells were incubated in CO_2 to reach 60 - 70% confluence, at which point were treated with increasing concentration of test sample along with positive control (Cisplatin-30.11 µg/mL and/or diallyl disulfide (DADS) 146.2 µg/mL), incubated over 24 hours and 48 hours and cell viability determined using sulforhodamine B (SRB) assay. After 24- and 48-hour incubation cells were fixed using 50 µl of 50% trichloroacetic acid (TCA) was added to each well, and the plates were kept at 4°C for 60 minutes. After fixation of cells, the wells were carefully washed with slow running tap water, and subsequently the plates were allowed to dry. One hundred microliters of SRB was added to each well and the plates incubated for 30 min. Excess unbound SRB was removed and the plates washed with 1% acetic acid. The washed wells were allowed to dry at room temperature. The protein bound SRB was dissolved in 100 µL of 10 mM tris base solution and the absorbance read at 510 nm on a multimode plate reader (PerkinElmer, Massachusetts, USA).

4.3.5. Structure elucidation and characterisation

NMR spectra were recorded on a Bruker Avance III-400 instrument (Bruker, Karlsruhe, Germany). ESI-MS data were obtained *via* ultra-performance liquid chromatography with an Acquity UPLC system coupled to a Waters Synapt G2 quadrupole time-of-flight (QTOF) mass spectrometer using an electrospray ionization technique operating in positive mode (Milford, Massachusetts, USA). IR spectra were recorded on a Perkin Elmer spectrum 100 FT-IR spectrophotometer (Waltham, Massachusetts, USA). Optical rotations were recorded on a Perkin Elmer Model 341 polarimeter. Single crystal X-ray data were collected using a Bruker D8 Venture diffractometer using monochromated CµKα (k = 1.54178 Å), a Photon 100 detector (Billerica, Massachusetts, USA) and APEX III control software (Bruker AXS

Inc.). Data reduction was performed using SAINT+ (Bruker AXS Inc.), and the intensities were corrected for absorption using SADABS (Bruker AXS Inc.). All structures were solved by direct methods using a SHELXS algorithm (Sheldrick, 2015a) and refined using the SHELXL program (Sheldrick, 2015b). All H atoms were placed in geometrically idealised positions and constrained to ride on their parent atoms.

4.4. Results and discussion

4.4.1. Primary fractionation using column chromatography

The fractions were initially collected in more than hundred test tubes which were analysed by TLC and according to the similarity of the patterns, a total of thirty-six final combined fractions were obtained. The solvent systems used for TLC analysis were *n*-hexane : acetone (7:3) and dichloromethane : methanol (8:2). The combined fractions were dried and labelled F1 – F36 and their weights were as follows: F1 (340 mg); F2 (432 mg); F3 (163 mg); F4 (594 mg) ; F5 (232 mg); F6 (75 mg); F7 (210 mg); F8 (9 mg); F9 (5 mg); F10 (48 mg); F11 (3 mg); F12 (42 mg); F13 (36 mg); F14 (49 mg); F15 (44 mg); F16 (59 mg); F17 (21 mg); F18 (16 mg); F19 (6 mg); F20 (8 mg); F21 (25 mg); F22 (22 mg); F23 (22 mg); F24 (23 mg); F25 (9 mg); F26 (2 mg); F27 (12 mg); F28 (2 mg); F29 (6 mg); F30 (4 mg); F31 (15 mg); F32 (19 mg); F33 (4 mg); F34 (12 mg); F35 (19 mg) and F36 (21 mg). Sixteen fractions (F1 – F7, F11, F13, F16, F19, F20, F22, F24, F32 and F35) were selected based on their purity on TLC (no overlapping spots) for *invitro* evaluation for their lung cancer cytotoxicity against lung cancer A549 cell line.

4.4.2. Lung cancer cytotoxicity of the primary fractions

The A549 lung cancer cell line was treated for 24 hr with each of the selected fractions (F1 – F7, F11, F13, F16, F19, F20, F22, F24, F32 and F35) at different concentrations (0.0625,

0.125, 0.25, 0.5 and 1 mg/mL). The concentration-based bioactivities of the tested fractions are displayed in Figure 4.5. F24, F32 and F35 were the the most active fractions displaying activities of 72.76, 78.83 and 86.46 % inhibition at 0.5 mg/mL. At the lowest test concentration (0.0625 mg/mL), the fractions F24, F32 and F35 displayed 53.08, 49.14 and 46.47 % inhibition, respectively. At the highest test concentration (1 mg/mL) the fractions F24, F32 and F35 displayed 32.71, 53.83 and 79.58 % inhibition, respectively. This was lower than the percentage inhibition at 0.5 mg/mL displayed by each of these fractions indicating that saturation was reached at this concentration. The fractions F6, F7 and F11 were identified as reasonably active, exhibiting 69.13, 66.57 and 62.68 % inhibition at 0.5 mg/mL, respectively. The percentage inhibition displayed at the highest concentration for each of these fractions was lower than that at 0.5 mg/mL once again indicating that the samples were saturated at this test concentration. Fraction F1 displayed the only concentration dependant activity over the entire range (0.0625 – 1 mg/mL) but the weakest activity overall of 4.94 % inhibition at the lowest concentration and 55.32 % inhibition at the highest concentration (1 mg/mL). Fractions F3, F4 and F5 also displayed good activity at 0.5 mg/mL, the highest activity of 71.26, 73.18 and 68.01 % inhibition, respectively. Fractions F6, F7 and F11 contained fewer compounds based on the TLC analysis relative to other fractions and were therefore given first preference towards further purification. Even though F24, F32 and F35 were the most active overall, these are polar fraction and would have required HPLC separation and since the major compounds from *C. gynandra* leaves were not UV active, these could not be purified by HPLC. Fractions F6, F7 and F11, however are mid-polar and therefore column chromatography and preparative TLC was used towards purifying their inherent compounds. These fractions were therefore selected for further work towards isolation of the possible bioactive compounds.

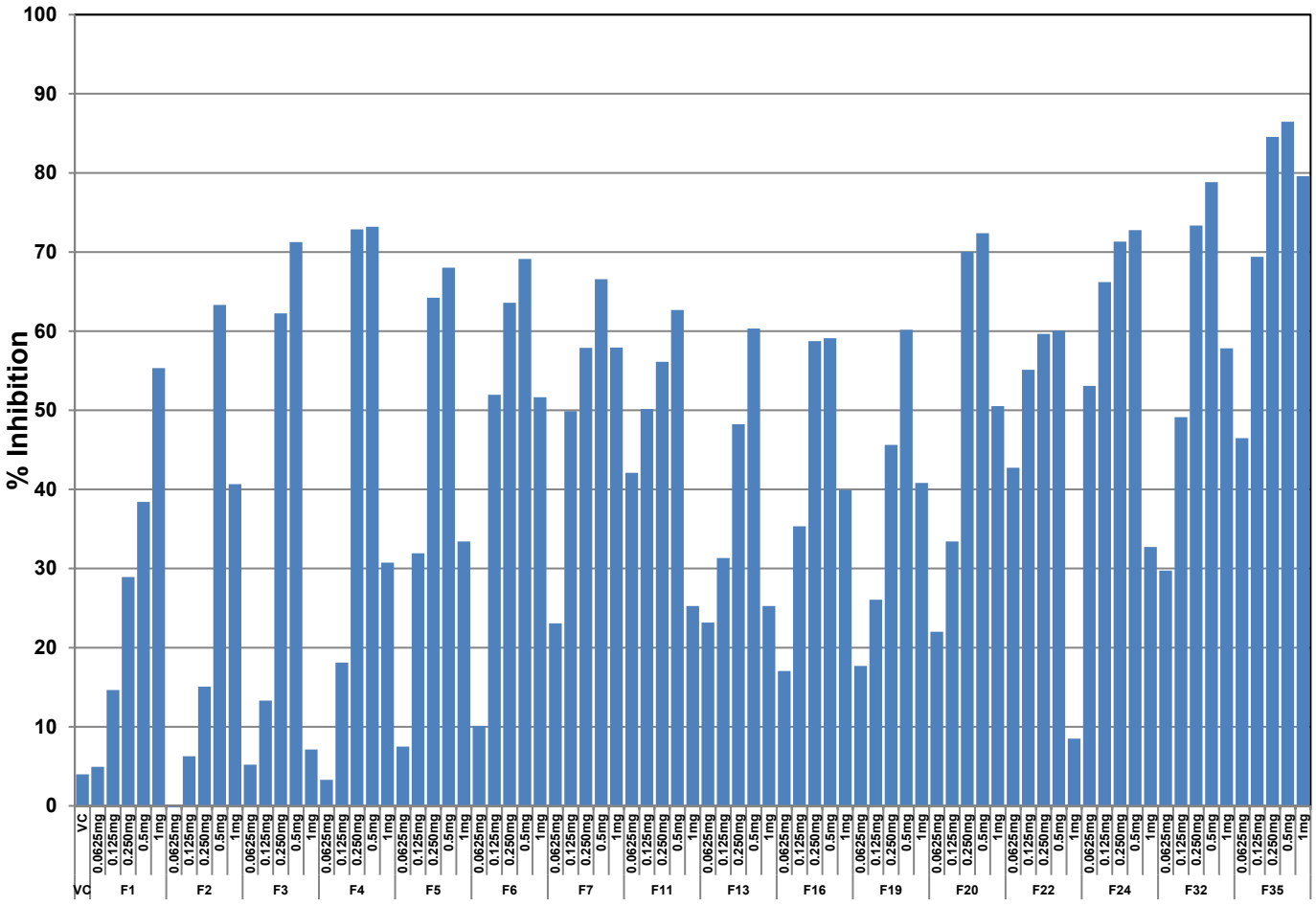

Figure 4.5: *Lung cancer (A549) cytotoxicity of fractions F1 – F7, F11, F13, F16, F19, F22, F24, F32 and F35. The cancer cell lines were treated with fractions for 24 hr.*

4.4.3. Secondary fraction of selected fractions using column chromatography and TLC towards purifying potential bioactive compounds

The fraction F7 was the most abundant of the three selected fractions, F6 (75 mg); F7 (210 mg) and F11 (3 mg). This necessitated its selection towards isolating and purifying its most abundant components, based on TLC analysis. Fraction F7 (200 mg) was therefore subjected to silica gel flash column chromatography (*n*-hexane : acetone 1:0 to 7:3, v/v) to yield fifteen subfractions (F7A–F7O) which were dried using the *Genevac SP Scientific* EZ-2 centrifugal evaporator. Subfraction F7G (80 mg) was subjected to preparative TLC (*n*-hexane-acetone 8:2, v/v) to yield compound **1** (29 mg) and compound **2** (24 mg). Subfraction

F7J (40 mg) was purified on preparative TLC (*n*-hexane-acetone 7:3, v/v) to yield compound **3** (11 mg).Compounds **1-3** were initially confirmed pure by UPLC-QTOF-MS and proton NMR.

4.4.4. Structure elucidation

4.4.4.1. Cleogynone A (1)

White crystalline, mp 180 – 181 °C; [α]20 D +184.5 (c 0.14, MeOH); UV (MeOH) λ_{max} (log ε): 202 (2.72), 219 (2.50), 282 (1.81) nm; IR v_{max}: 3466, 2960, 2929, 2860, 1723, 1462, 1376, 1267, 1250, 1122, 1072, 1039, 947, 742 cm^{-1}; HRESIMS *m/z*: 559.3999 $[M + H - OH]^+$ (calculated for C_{34} H_{56} O_7).

Compound **1** (Figure 4.6)**,** crystallised on drying in a centrifugal evaporator to yield colourless single crystalline material. The IR spectrum of compound **1** named cleogynone A revealed absorption at 3450, 1710, and 1270 cm^{-1}, which were attributed to hydroxyl, ketone and ester groups, respectively.

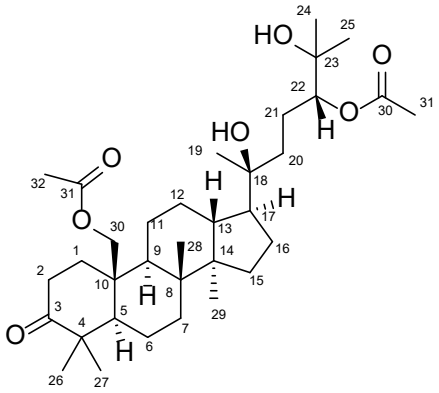

Figure 4.6: *Structure of compound **1** (cleogynone A) a novel dammerane-type triterpenoid with anticancer activity.*

Cleogynone A (**1**) was assigned the molecular formula C_{34} H_{56} O_7 from its HRESIMS (*m/z* 559.3999,[M + H - OH]$^+$), ^{1}H and ^{13}C NMR (including DEPT) and single crystal X-ray crystallographic data (SCXRD) with seven degrees of unsaturation. The ^{1}H NMR of cleogynone A (**1**) (Table 4.6) revealed nine singlet methyl groups at δ_H 2.05 (3H, s), 1.90 (3H, s), 1.14 (6H, s), 1.06 (3H, s), 1.02 (3H, s), 0.90 (3H, s), 0.88 (3H, s) and 0.84 (3H, s), the presence of one oxygenated methine at δ_H 4.74 (1H, dd, *J* = 10.3, 2.4 Hz) and one oxygenated methylene with protons at δ_H 4.18 (1H, d, *J* = 11.7 Hz) and 4.00 (1H, d, *J* = 11.7 Hz). In addition, two proton resonances at δ_H 2.50 (1H, m) and 2.28 (1H, m) from one methylene were seen. Several protons for methylenes and methines overlap in the range between δ_H 1.18 and 1.78, one of the methylenes had one proton at δ_H 2.08 (1H, m) and the other embedded within the overlapping range. Two protons, at δ_H 2.01 (2H, s) further revealed the presence of two hydroxyl groups.

Inspection of the ^{13}C NMR spectrum together with the DEPT spectrum suggested that cleogynone A (**1**) was a triterpenoid derivative with 34 carbons (Table 4.6), consisting of nine methyl carbons, eleven sp^3 methylenes (including one oxy-methylene at δ_C 64.5), five sp^3 methines (including one oxy-methine at δ_C 80.5), six sp^3 quaternary carbons (including two oxygen carrying at δ_C 75.1 and 72.5), and three sp^2 quaternary carbons (carbonyls at δ_C 171.2, 171.3 and 216.9). Apart from three carbonyl groups,the remaining elements of unsaturation were attributed to four rings, indicating that cleogynone A (**1**)is a tetracyclic triterpenoid.

The ^{1}H-^{1}H COSY correlation (Figure 4.7) between δ_H 1.56, 2.08 (H-1)/δ_H 2.28, 2.50 (H-2) and the HMBC correlations (Figure 4.7) from H-1 (δ_H 2.08, 1.56), H-2 (δ_H 2.50, 2.28), H-26 (δ_H 1.02) and H-27 (δ_H 0.90) to C-3 (δ_C 216.9) of cleogynone A (**1**) confirmed the existence of a ketone at C-3 and that C-4 is substituted by two methyls. Furthermore, the correlations from H-30 (δ_H 4.00, 4.18) to C-1 (δ_C 34.5), C-5 (δ_C 52.6), C-9 (δ_C 51.6) and C-31 (δ_C 171.3), and from H-32 (δ_H 1.90) to C-31 (δ_C 171.3) demonstrated the substitution of C-10 with a

methylene further linked to an acetyl group. A second acetyl group is located at C-22 as demonstrated by the HMBC correlations between H-22 (δ_H 4.74) and C-33 (δ_C 171.2), H-34 (δ_H 2.05) and C-33 (δ_C171.2). The aforementioned information helped establish the vicinity of the three carbonyl groups contained in the structure.

Table 4.6:*^{1}H (400 MHz) and ^{13}C NMR spectroscopic data for cleogynone A (**1**) in $CDCl_3$.*

Position	δ_H (ppm), (mult., *J* in Hz)	δ_C (ppm)
1	2.08 (m)	34.5
	1.56 (m)	
2	2.50 (m)	34.4
	2.28 (m)	
3	-	216.9
4	-	45.9
5	1.58 (m)	52.6
6	1.47 (m)	19.7
7	1.51 (m)	34.1
	1.29 (m)	
8	-	40.1
9	1.57 (m)	51.6
10	-	38.7
11	1.53 (m)	22.9
	1.29 (m)	
12	1.66 (m)	24.7
	1.45 (m)	
13	1.54 (m)	42.7
14	-	50.3
15	1.37 (m)	31.5
	1.05 (m)	
16	1.72 (m)	23.7
17	1.66 (m)	49.8
18	-	75.1
19	1.06 (s)	25.0
20	1.37 (m)	37.1
21	1.47 (m)	19.7
22	4.74 (dd, 10.3, 2.4)	80.5
23	-	72.5
24	1.14 (s)	26.7
25	1.14 (s)	25.2
26	1.02 (s)	29.4
27	0.90 (s)	19.5
28	0.88 (s)	15.3
29	0.84 (s)	16.7
30	4.18 (d, 11.7)	64.5
	4.00 (d, 11.7)	
31	-	171.3
32	1.90 (s)	21.0
33	-	171.2
34	2.05 (s)	21.1

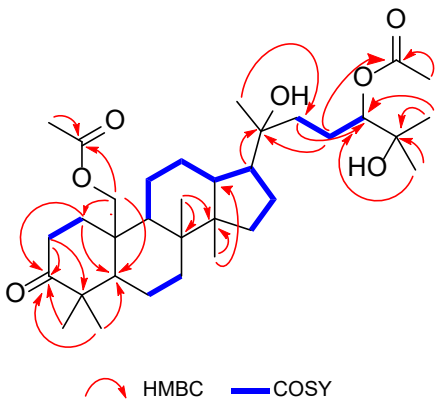

Figure 4.7:*Key HMBC and ^{1}H-^{1}H COSY correlations of compounds* ***1*** *(cleogynone A).*

Two hydroxyl groups as part of the structure were further located. The HMBC correlations from H-24 (δ_H 1.14), H-25 (δ_H 1.14) to C-22 (δ_C 80.5) and to C-23 (δ_C 72.5) illustrated that C-23 carries two methyl groups and a possible hydroxyl group which was later confirmed by single crystal X-ray diffraction (SCXRD) analysis. The HMBC correlations from H-19 (δ_H 1.06) to C-17 (δ_C 49.8), C-18 (δ_C 75.1), C-20 (δ_C 37.1) demonstrated that C-18 neighbours a methylene (C-20) on one end, and attaches a hydroxyl group and a methyl group. While the HMBC correlation from H-17 (δ_H 1.66) to C-18 (δ_C 75.1) demonstrated that on the other end C-18 is connected to the D ring at C-17. C-20 shares an HMBC correlation with H-22 while H-22 shares a ^{1}H-^{1}H COSY correlation with H-21, completing the linkage of the structural moieties.

The location of the further two methyl groups is described by the HMBC correlations from H-28 (δ_H 0.88) to C-7 (δ_C 34.1), C-14 (δ_C 50.3), C-8 (δ_C 40.1) and from H-29 (δ_H 0.84) to C-14 (δ_C 50.3), C-15 (δ_C 31.5) while and the methyl groups are connected at C8 and C14.

The NOESY spectrum of clyogynone A (**1**) showed correlation between H-22, H-24 and H-25 as shown in Figure 4.8 indicating that these are on the same plane demonstrating that the hydroxyl group on C-23 is at the same side as the acetate group that attaches at position C-22. Furthermore, the correlation between H-30 (δ_H 11.7) and H-28 proved that the methyl groupC-28 is in the same face as the oxymethylene at C-30.

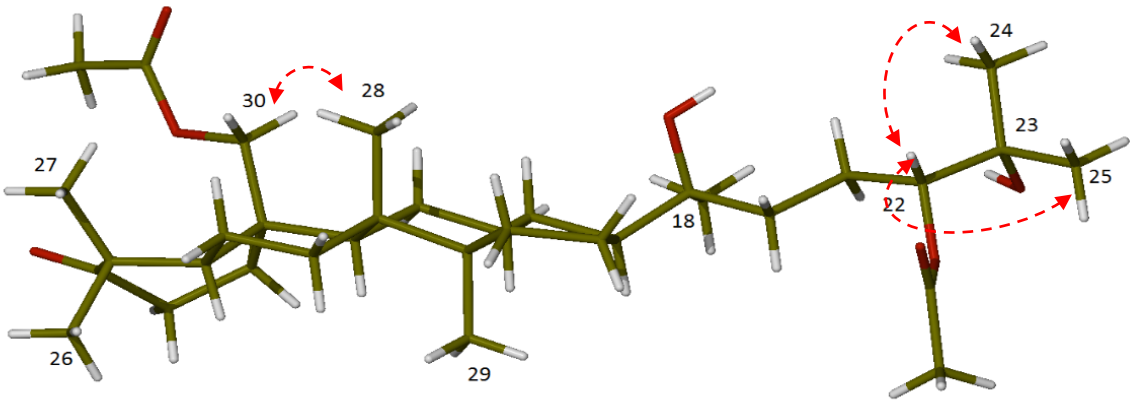

Figure 4.8:*Key NOESY ( ) correlations of compound 1 (cleogynone A).*

Compound **1** crystallised in the chiral space group $P2_1$, revealing nine chiral centres present (seven as part of the triterpenoid skeletal structure, and two as part of the heptyl-acetate based-moiety). The final refinement of the CμKα data in SCXRD analysis, based on the seven oxygen atoms in the molecule, resulted in a Flack parameter [27,28] of 0.04(10), which not only indicated the relative configuration of two methyl groups (Figure 4.9), but also unambiguously determined the absolute stereochemistry of compound **1** to be 5*R*, 8*R*, 9*S*, 10*S*, 13*R*, 14*R*, 17*S*, 18*S*, and 22*R*. All other bond lengths and angles fall within the expected ranges for the respective functional groups.

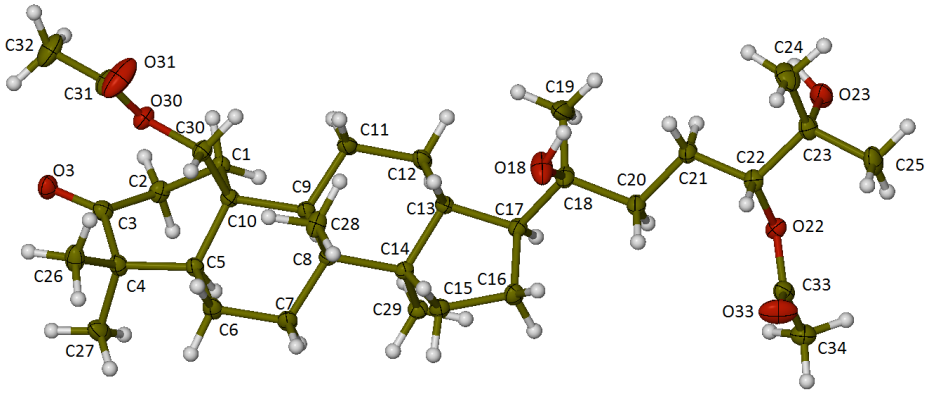

Figure 4.9: *Pictogram of compound **1** structure (CμKα) (ellipsoids shown at the 50 % probability level). Green represents C-atoms, red represents O-atoms while white represents H-atoms.*

The crystal data and refinement parameters are reported in Table 4.7. The monoclinic crystal system and the space group $P2_1$ were confirmed using X-PREP [29]. This chiral space group is consistent with the chiral molecule, cleogynone A (**1**). The structure was solved by direct methods using a SHELXS algorithm [30] and refined using the SHELXL program [31]. All atoms were revealed in the difference Fourier syntheses and were added to the structural model. All non-hydrogen atoms were refined anisotropically. All hydrogen atoms of the molecule were found in difference Fourier maps, attesting to the exceptionally high quality of the crystal. The H atoms were placed in idealised positions and were refined with temperature factors 1.2-1.5 times those of their parent atoms.

Table 4.7:*Data collection and refinement parameters for cleogynone A (**1**).*

Crystal Data	
Formula	$C_{34}H_{56}O_7$
Formula Weight	576.79
Crystal System	Monoclinic
Space group	$P2_1$
a, b, c (Å)	7.8377(5), 16.5237(10), 12.3065(8)
α, β, γ (°)	90, 99.120(2), 90
V (Å^3)	1573.64(17)
Z	2
D_{calc} (g/cm^3)	1.217
μ(CμKa) (mm^{-1})	0.664
F(000)	632
Crystal Size (mm)	0.41 x 0.56 x 0.63
Data Collection	
Temperature (K)	150
Radiation (λ/Å) CμKa	1.54178
θ-range for data-collection (°)	3.6, 70.1
Dataset	-10: 10 ; -22: 22 ; -16: 16
Tot., Uniq. Data, R_{int}	21101, 5925, 0.023
Observed data [I > 2.0 sigma(I)]	5859
Refinement	
N_{ref}, N_{par}	5925, 396
R, wR_2, S	0.0336, 0.1011, 0.96
$(\Delta/\sigma)_{max}$, $(\Delta/\sigma)_{av}$	0.00, 0.00
Flack x	0.04(10)
Δρ excursions (e Å^{-3})	-0.27, 0.23

4.4.4.2. Cleogynone B (2)

White crystalline, mp 142 – 144 °C; [α]20 D +50.8 (c 0.19, MeOH); UV (MeOH) λ_{max} (log ε): 204 (2.00), 220 (2.50), 283 (1.81) nm; IR ν_{max}: 3502, 2941, 2880, 1718, 1699, 1452, 1376, 1350, 1246, 1222, 1173, 1137, 1034, 954, 899cm^{-1};HRESIMS m/z 501.3948. $[M + H - OH]^+$ (calculated for $C_{32}H_{54}O_5$)

Compound **2** (Figure 4.10) wasobtained as a white powder and assigned the molecular formula $C_{32}H_{54}O_5$ from its HRESIMS (*m/z* 501.3948,$[M + H - OH]^+$) ^{1}H NMR, ^{13}C NMR spectraand single crystal X-ray data,with six degrees of unsaturation.

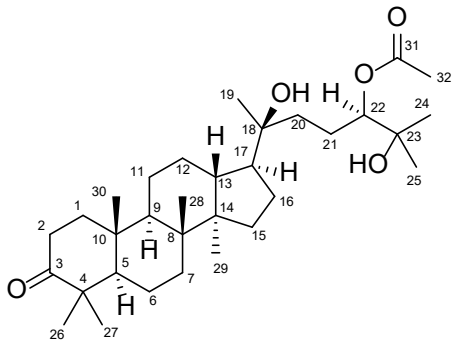

***Figure 4.10**: Structure of compound **2** (cleogynone B) a novel dammerane-type triterpenoid with anticancer activity.*

^{1}H NMR (Table 4.8) revealed signals for nine singlet methyls (δ_H 0.89, 0.95, 1.00, 1.05, 1.09, 1.14, 1.22, 1.22, 2.12), one oxygenated methine at δ_H 4.82 (1H, dd, J = 10.3, 2.4 Hz) and a downfield proton resonance at δ_H 2.48 (2H, m) for a methylene group. Several proton resonances for methylenes and methyls are embedded in the overlapping range between δ_H 1.25 – 1.99.

The ^{13}C NMR and DEPT spectra(Table 4.8) suggested that compound **2** called cleogynone B was also a triterpenoid derivative, with a total of 32 carbons, assigning to nine methyls, ten methylenes, five methines (including one oxygenated δ_C 4.82), and eight quaternary carbons (including two carbonyl δ_C 171.4 and 218.2). With the exception of the two degrees occupied by the two carbonyls, the remaining degrees are attributed to a tetracyclic system.

Table 4.8: *Table 4.9: ^{1}H (400 MHz) and ^{13}C NMR spectroscopic data for compounds **2** in $CDCl_3$.*

Position	δ_H (ppm) (mult., *J* in Hz)	δ_C (ppm)
1	1.93 (m)	39.9
	1.46 (m)	
2	2.48 (m)	34.1
3	-	218.2
4	-	47.4
5	1.38 (m)	55.3
6	1.52 (m)	19.7
7	1.56 (m)	34.5
	1.33 (m)	
8	-	40.3
9	1.44 (m)	50.0
10	-	36.81
11	1.74 (m)	24.8
	1.49 (m)	
12	1.80 (m)	27.6
	1.29 (m)	
13	1.79 (m)	23.7
	1.61 (m)	
14	1.63 (m)	42.5
15	-	50.4
16	1.46 (m)	31.2
	1.10 (m)	
17	1.73 (m)	49.9
18	-	75.2
19	1.14 (s)	25.0
20	1.46 (m)	37.0
21	1.51 (m)	22.0
	1.29 (m)	
22	4.82 (dd, 10.3, 2.4)	80.5
23	-	72.5
24	1.22 (s)	26.6
25	1.22 (s)	25.1
26	1.09 (s)	26.7
27	1.05 (s)	21.1
28	1,00 (s)	15.1
29	0.89 (s)	16.4
30	0.95 (s)	16.0
31	-	171.4
32	2.12 (s)	21.0

Similar to clyogynone A (**1**), the ^{1}H-^{1}H COSY correlation (Figure 4.11) between δ_H 1.46, 1.93 (H-1)/δ_H 2.48 (H-2) and the HMBC correlations (Figure 4.11) from H-1 (δ_H 1.46, 1.93), H-2 (δ_H 2.48), H-26 (δ_H 1.02) and H-27 (δ_H 0.90) to C-3 (δ_C 218.2) confirmed the presence of a ketone at C-3, and that C-4 is substituted by two methyl groups. As in compound **1** an acetyl group was located at C-22, demonstrated by the HMBC correlations between H-22 (δ_H 4.82) and C-31 (δ_C 171.4), H-32 (δ_H 2.12) and C-31 (δ_C 171.4). Furthermore, the correlations from H-30 (δ_H 0.95) to C-1 (δ_C 39.9), C-5 (δ_C 55.3), C-10 (δ_C 36.8) demonstrated the substitution

of C-10 with a methyl, further illustrating the only difference between compounds **1** and **2**, was that while compound **1** has an acetate group linked by a methylene to C-10, compound **2** has a methyl group attached at position C-10. The remaining HMBC correlation between compounds **1** and **2** were identical or similar.

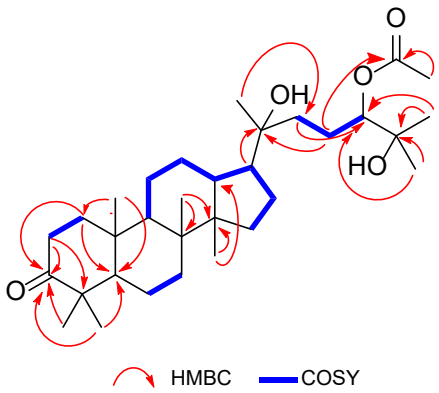

Figure 4.11: *Key HMBC and ^{1}H-^{1}H COSY correlations of compounds* ***2****.*

The NOESY spectrum of cleogynone B (**2**) (as illustrated in Figure 4.12) showed correlation between H-30 and H-28 proving that the methyl group C-28 is in the same face as the methyl at C-30.

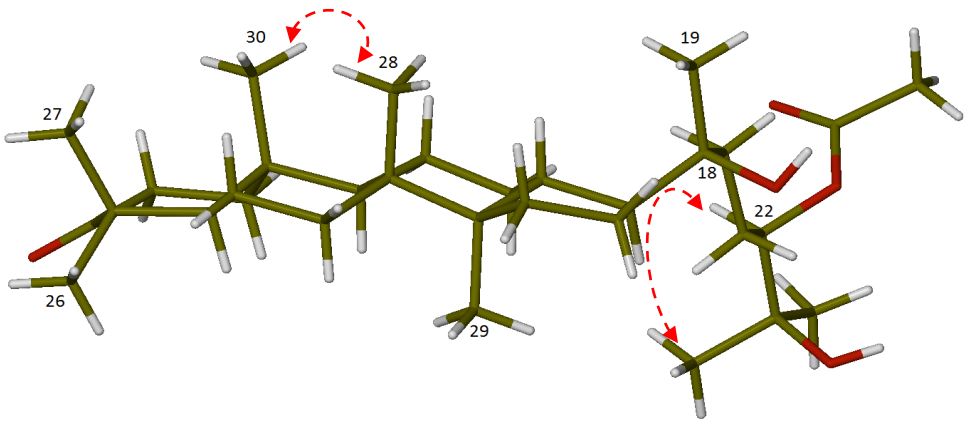

Figure 4.12:Key NOESY ( ) correlations of compound **2**.

Compound **2** crystallised in the chiral space group *P*1, revealing nine chiral centres present as before with compound **1**. The final refinement of the CμKα data in SCXRD analysis, based on the five oxygen atoms in the molecule, resulted in a Flack parameter [27,28] of 0.06(6), which indicated the relative configuration of the three methyl groups on the infused ring backbone (Figure 4.13), while also assisting in unambiguously determining the absolute stereochemistry of compound **2** to be 5*R*, 8*R*, 9*R*, 10*R*, 13*R*, 14*R*, 17*S*, 18*S*, and 22*R*. All bond lengths and angles observed in compound **2** compare well with the corresponding bond lengths and angles observed in compound **1**, and fall within the expected ranges for the respective functional groups.

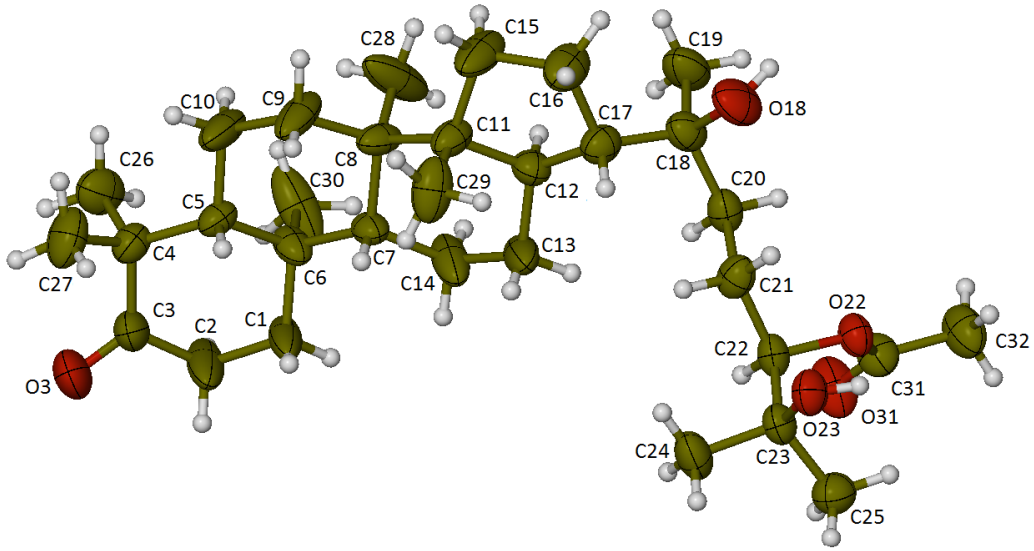

Figure 4.13: *Pictogram of compound **2** structure (CμKα) (ellipsoids shown at the 50 % probability level). Green represents C-atoms, red represents O-atoms while white represents H-atoms.*

The crystal data and refinement parameters are reported in Table 4.9. The triclinic crystal system and the space group *P*1 were confirmed using X-PREP [29].The structure was solved by direct methods using a SHELXS algorithm [30] and refined using the program SHELXL [31]with successive difference Fourier maps revealing the non-hydrogen atoms. The molecule was modelled without difficulties. Owing to the exceptionally high quality of the crystals, all hydrogen atoms were found and were placed ideally and refined with thermal parameters 1.2-1.5 times the U_{iso} values of their parent atoms.

Table 4.10:*Data collection and refinement parameters for cleogynone B (**2**).*

Crystal Data			
Formula			C_{32} H_{54} O_5
Formula Weight			518.75
Crystal System			Monoclinic
Space group			*P1*
a, b, c (Å)	7.4475(5)	7.7239(5)	14.5814(10)
α, β, γ (°)	97.298(3)	93.052(3)	115.003(3)
V ($Å^3$)			748.66(9)
Z			1
D_{calc} (g/cm^3)			1.151
μ(CμKa) (mm^{-1})			0.592
F(000)			286
Crystal Size [mm]			0.18 x 0.24 x 0.37
Data Collection			
Temperature (K)			150
Radiation (λ/Å) CμKa			1.54178
θ-range for data-collection (°)			3.1, 72.1
Dataset			-9: 8 ; -9: 9 ; -17: 17
Tot., Uniq. Data, R_{int}			39127, 5573, 0.049
Observed data [I > 2.0 sigma(I)]			5177
Refinement			
N_{ref}, N_{par}			5573, 345
R, wR_2, S			0.0480, 0.1295, 1.04
$(\Delta/\sigma)_{max}$, $(\Delta/\sigma)_{av}$			0.00, 0.00
Flack x			0.06(6)
Δρ excursions (e $Å^{-3}$)			-0.19, 0.23

4.4.4.3. Cleogynone C (3)

Compound **3,** (Figure 4.14) was obtained as a white powder and assigned the molecular formula C_{32} H_{52} O_5 from its HRESIMS (*m/z* 499.3789, $[M + H - OH]^+$), ^1H NMR, ^{13}C NMR spectra, with seven degrees of unsaturation. Daset al., isolated compound **3** for the first time from *C. gynandra* and acetylation of which resulted in compound **3** without any given name [32] and in this study is named cleogynone C.

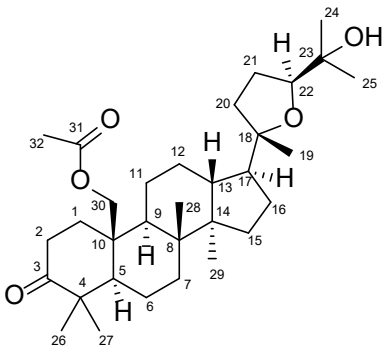

Figure 4.14: *Structure of compound **3** (cleogynone C), a known compound isolated from C. gynandra leaves in this study with anticancer activity.*

^{1}H NMR (Table 4.10) revealed signals for eight singlet methyls (δ_H 0.91, 0.96, 0.97, 1.08, 1.11, 1.15, 1.18, 1.96), the presence of one oxygenated methine at δ_H 3.62 (1H, dd, *J* = 8.1, 5.1 Hz) and one oxygenated methylene with protons at δ_H 4.23 (1H, d, *J* = 11.7 Hz) and 4.06 (1H, d, *J* = 11.7 Hz). In addition, two proton resonances at δ_H 2.56 (1H, m) and 2.33 (1H, m) from one methylene were seen. Several protons for methylenes and methines overlap in the range between δ_H 1.18 and 1.78 (typical of triterpenoids), one of the methylenes had one proton at δ_H 2.13 (1H, m) and the other embedded within the overlapping range. One proton, at δ_H 2.01 (1H, s) further revealed the presence of one hydroxyl groups. Several proton resonances for methylenes and methyls are embedded in the overlapping range between δ_H 1.26 – 1.99.

The ^{13}C NMR and DEPT spectra(Table 4.10) suggested that compound **3** was also a triterpenoid derivative, with a total of 32 carbons, assigning to eight methyls, ten methylenes, five methines (including one oxygenated δ_C 3.62), and eight quaternary carbons (including two carbonyl δ_C 171.4 and 216.9). With the exception of the two degrees occupied by the two carbonyls, the remaining degrees are attributed to a tetracyclic system and a heterocyclic 5-membered ring.

Table 4.11:*Comparison of ^{1}H (400 MHz) and ^{13}C NMR spectroscopic data for compound **3** in $CDCl_3$ and those in literature. Only key ^{1}H NMR data were reported in literature* [32].

Position	δ_C (ppm)	δ_H (ppm) (mult., *J* in Hz)	δ_C, lit.*	δ_H (ppm) (mult., *J* in Hz) lit.*
1	34.6	2.13 (m)	34.2	
2	34.4	2.56 (m)	34.0	
		2.33 (m)		
3	216.9		216.5	
4	45.9		45.6	
5	52.4	1.67 (m)	52.1	
6	19.7	1.52 (m)	19.5	
7	34.2	1.35 (m)	34.2	
8	40.1		39.8	
9	51.8	1.66 (m)	51.5	
10	38.7		38.4	
11	23.1	1.60 (m)	22.9	
		1.30 (m)		
12	26.3	1.77 (m)	25.6	
13	43.1	1.67 (m)	42.9	
14	49.9		49.6	
15	31.7	1.46 (m)	31.5	
16	27.2	1.85 (m)	27.0	
17	49.6	1.90 (m)	49.4	
18	86.6		86.3	
19	27.5	1.18 (s)	27.3	1.11 (s)
20	34.4	1.63 (m)	34.2	
		1.86 (m)		
21	25.9	1.31 (m)	26.1	
22	86.5	3.62 (dd, 8.1, 5.1)	86.3	3.55 (dd, 8.1, 5.1)
23	70.3		70.0	
24	24.1	1.11 (s)	23.9	1.04 (s)
25	27.9	1.15 (s)	27.6	1.07 (s)
26	19.4	0.97 (s)	19.2	0.88 (s)
27	29.5	1.08 (s)	29.3	1.00 (s)
28	16.6	0.91 (s)	16.3	0.84 (s)
29	15.4	0.96 (s)	15.2	0.88 (s)
30	64.5	4.23 (d, 11.7)	64.3	4.15 (d, 11.7)
		4.06 (d, 11.7)		3.97 (d, 11.7)
31	171.4		171.0	
32	21.0	1.96 (s)	20.8	1.87 (s)

* 75.47 MHz, $CDCl_3$, Das et al.

Similar to clyogynones A & B (**1** and **2**), the ^{1}H-^{1}H COSY correlation (Figure 4.15) between δ_H 2.13 (H-1)/δ_H 2.33, 2.56 (H-2) and the HMBC correlations (Figure 4.15) from H-1 (δ_H 2.13, H-2 (δ_H 2.33, 2.56), H-26 (δ_H 0.97) and H-27 (δ_H 1.08) to C-3 (δ_C 216.9) confirmed the presence of a ketone at C-3, and that C-4 is substituted by two methyl groups. Unlike compounds **1** and **2** no acetyl group was located at C-22, demonstrated by the absence of such HMBC correlations. Furthermore, as in compound **1** the correlations from H-30 (δ_H

4.06, 4.23) to C-1 (δ_C 34.6), C-5 (δ_C 52.4), C-9 (δ_C 51.8) and C-31 (δ_C 171.4), and from H-32 (δ_H 1.96) to C-31 (δ_C 171.4) demonstrated the substitution of C-10 with a methylene further linked to an acetyl group. The HMBC correlation from H-22 (δ_H 3.62) to C-18 (δ_C 86.6) reveals the presence of the heterocyclic 5 membered ring, the main distinction of compound **3** in contrast to compounds **1** and **2**. The remaining HMBC correlation between compounds **1**, **2** and **3** were identical or similar.

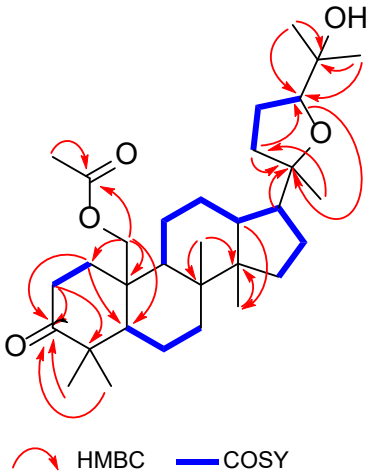

Figure 4.15: *Key HMBC and ^{1}H-^{1}H COSY correlations of compound 3.*

The NOESY spectrum of compound **3** showed correlation between H-19, H-24 and H-25 as shown in Figure 4.16 indicating that these are on the same plane, demonstrating that the moiety consisting of a hydroxyl group and two methyl linked on C-23 attached to the heterocyclic 5-membered ring are the same side as the methyl group linked at position 18 of on the heterocyclic ring. Furthermore, as the case with compound **1** the correlation between H-30 (δH 11.7) and H-28 proved that the methyl group C-28 is in the same face as the oxymethylene at C-30.

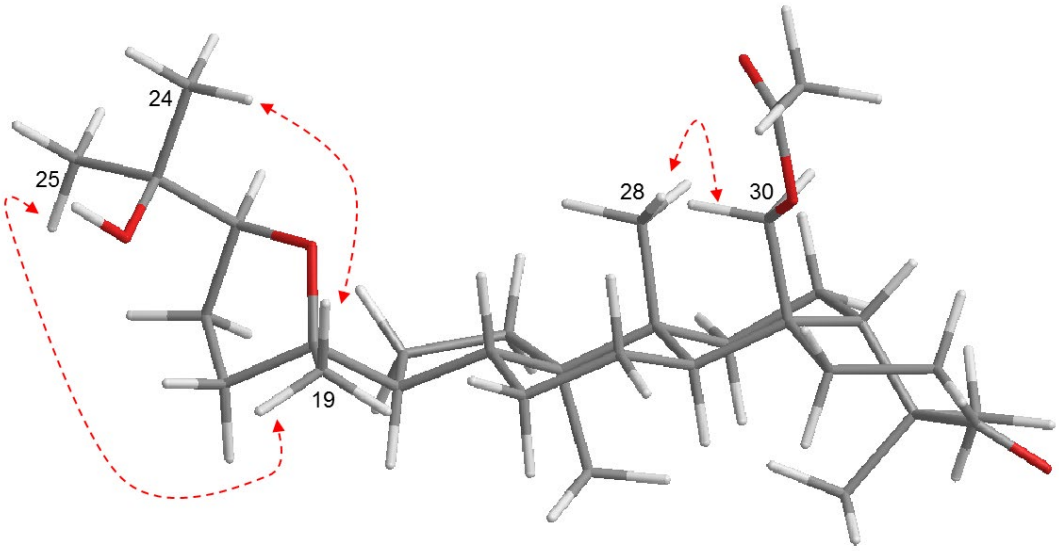

Figure 4.16:*Key NOESY (* ↔ *) correlations of compound* ***3****.*

4.4.5. Anticancer activity of compounds 1-3

The pure compounds were evaluated for their *invitro* anticancer activity. Tables 4.11 - 4.13 demonstrate the anticancer activity of the pure compounds tested at concentrations 25.00, 12.50, 6.25, 3.12, 1.56, 0.78 and 0.39 µg/mL against lung cancer (A549), breast cancer (MDA-MB-468) and colorectal cancer (HCT15 and HCT116) cell lines. Compound **2** displayed a maximum of 51 % inhibition of lung cancer (A549) cell line at 25 µg/mL, over 24 hr treatment, comparable to diallyl disulfide (DADS) inhibition of 48% at 146.2 µg/mL (Table 4.11).

All three compounds displayed concentration dependent inhibition over 48 hr treatment of breast cancer (MDA-MB-468) cell line (Table 4.12).

Table 4.12: *Comparative assessment of cytotoxic potential of compound **2** against A549 lung cancer cell line.*

Compound	Concentration (µg/mL)	%Inhibition 24 hr (Mean ± SE)	%Inhibition 48 hr (Mean ± SE)
DMSO (vehicle control) #		9.89±4.76	4.06±5.58
DADS (positive control)	146.2	46.55±2.12	53.23±2.40
Compound 2	0.39	-4.37±3.08	-0.87±4.03
	0.78	-5.78±2.50	0.42±4.38
	1.56	-6.60±1.91	0.44±4.83
	3.12	-5.46±2.21	0.72±4.43
	6.25	-1.8±3.80	1.33±4.55
	12.50	-5.19±3.13	0.53±4.20
	25.00	51.38±0.39	16.14±1.72

The final concentration of vehicle DMSO control in the treatment media is 1%

Table 4.13: *Comparative assessment of cytotoxic potential of compounds **1**, **2**, **3** against MDA-MB-468 breast cancer cell line.*

Compound	Concentration (µg/mL)	%Inhibition - 24 hr (Mean ± SE)	%Inhibition - 48 hr (Mean ± SE)
DMSO (vehicle control) #	0.00	-0.37±1.22	3.22±2.62
DADS (positive control)	146.2	60.99±2.06	59.13±0.04
Compound 1	0.78	9.33±7.54	11.14±4.23
	1.56	3.87±6.41	20.88±6.26
	3.12	0.32±5.29	21.6±1.97
	6.25	1.42±5.68	23.73±11.92
	12.50	3.74±6.67	28.12±8.34
	25.00	44.48±1.42	52.55±5.42
Compound 2	0.78	-0.99±4.58	-8.10±6.11
	1.56	1.72±2.89	10.7±3.71
	3.12	0.22±3.14	18.65±4.45
	6.25	2.41±1.60	20.3±3.06
	12.50	6.12±3.51	34.95±6.61
	25.00	43.82±2.38	51.28±1.99
Compound 3	0.78	5.71±1.45	-4.67±5.00
	1.56	7.03±1.80	8.33±2.15
	3.12	8.02±2.29	12.13±1.71
	6.25	6.84±2.63	14.89±0.67
	12.50	10.99±2.69	22.18±2.13
	25.00	48.32±2.19	66.58±1.30

The final concentration of vehicle DMSO control in the treatment media was 1%

The compounds exhibited moderate active, above 50 % inhibition at 25 µg/mL over the 48 hr treatment, comparable to DADS at 146.2 µg/mL. The cytotoxicity results for the compounds are shown in Table 4.12.

Compounds **2** and **3** showed 89.34±5.46 and 87.76±1.22 % inhibition activity, respectively, against HCT116 over 24 hr treatment at the highest test concentration of 25 µg/mL,comparable to DADS 89.17±0.90 at 146.2µg/mL (Table 4.13).

Table 4.14: *Comparative assessment of cytotoxic potential of compounds **1**, **2** and **3** against HCT116 colorectal cancer cell line.*

Compound	Concentration (µg/mL)	%Inhibition - 24 hr (Mean ± SE)	%Inhibition - 48 hr (Mean ± SE)
DMSO (vehicle control) #	0.00	18.91±3.18	21.87±1.75
Positive controls	30.11 (Cisplatin)	35.8±2.98	26.76±2.05
	146.2 (DADS)	89.17±0.90	79.84±3.63
Compound 2	0.39	23.6±0.89	-1.52±5.44
	0.78	20.33±0.96	11.18±1.67
	1.56	23.74±2.36	16.25±2.84
	3.12	25.08±3.26	18.07±3.06
	6.25	30.27±3.15	22.93±2.46
	12.50	30.58±1.51	22.94±3.68
	25.00	89.34±5.46	55.79±1.23
Compound 3	0.39	18.25±1.71	0.85±7.16
	0.78	15.26±1.81	12.87±4.43
	1.56	17.15±2.17	16.55±2.93
	3.12	22.34±1.80	21.68±3.13
	6.25	27.68±1.39	24.78±1.55
	12.50	28.02±0.48	24.44±1.76
	25.00	87.76±1.22	60.96±4.95

The final concentration of vehicle DMSO control in the treatment media was 1%

Against the HCT15 colorectal cancer, compounds **1**, **2** and **3** showed 82.97±0.56, 81.74±0.34 and 83.67±3.16 % inhibition at 25 µg/mL concentration over 48 hr treatment, higher than DADS 79.98±1.12 (146.2 µg/mL) and cisplatin 75.92±1.60 (30.11 µg/mL)and all three compounds exhibited less than 75 % inhibition activity over a 24 hr treatment (Table 4.14) 79.98±1.12.

Table 4.15: *Comparative assessment of cytotoxic potential of compounds **1, 2, 3** against HCT15 colorectal cancer cell line.*

Compound	Concentration (µg /mL)	%Inhibition - 24 hr (Mean±SE)	%Inhibition - 48 hr (Mean±SE)
Vehicle DMSO control #		18.62±3.57	21.66±1.16
Positive controls	30.11 (Cisplatin)	45.25±1.95	75.92±1.60
	146.2 (DADS)	63.71±2.88	79.98±1.12
Compound 1	0.39	-7.06±1.71	4.01±1.15
	0.78	-3.51±1.54	-3.58±0.88
	1.56	-4.72±3.15	-3.28±0.23
	3.12	-1.88±8.68	-3.84±0.56
	6.25	8.92±4.87	-2.88±1.00
	12.50	16.16±5.63	7.01±2.43
	25.00	51±6.59	82.97±0.56
Compound 2	0.39	16.85±3.06	1.6±1.52
	0.78	9.98±4.18	-4.38±0.87
	1.56	7.11±5.90	-5.04±0.60
	3.12	8.27±5.85	-4.06±0.38
	6.25	15.1±4.42	-2.74±0.48
	12.50	36.65±4.05	8.82±2.00
	25.00	72.27±3.91	81.74±0.34
Compound 3	0.39	20.46±3.28	-0.35±0.60
	0.78	2.83±6.86	-5.01±1.30
	1.56	1.43±6.82	-5.32±0.31
	3.12	-0.17±8.74	-4.27±0.66
	6.25	7.64±7.70	-4.17±1.07
	12.50	30.44±6.39	7.82±2.75
	25.00	64.85±9.03	83.67±3.16

The final concentration of vehicle DMSO control in the treatment media was 1%

These results reveal that the novel tritepernoids cleogynone A (**1**) and cleogynone B (**2**) as well as the known compound **3** named here cleogynone C are amongst the compounds responsible for the anticancer activity of *C. gynandra* leaf *n*-hexane extract. Their greatest cytotoxicity was against colorectal cancer cell lines as two of the tritepernoids (cleogynone B and C) exhibited activity greater than 87 % inhibition over a 24 hr exposure against HCT116 and all the tritepernoids (cleogynone A, B and C) exhibiting greater than 81 % over the 48 hr exposure against HCT15, better than the positive controls in both cases.

Triterpenoids are highly multifunctional and the antitumor activity of these compounds is measured by their ability to block nuclear factor-kappaB activation, induce apoptosis, inhibit

signal transducer, and activate transcription and angiogenesis [33,34]. Oleanolic acid and its isomer ursolic acid are triterpenoid compounds that exist widely in natural plants and are weakly anti-inflammatory and anti-tumorigenic *in vivo*[33,35]. Synthetic oleanane triterpenoids are the most potent anti-inflammatory and anticarcinogenic triterpenoids known [33]. He et al. (2007) reported triterpenoids isolated from apple peels, 2R-hydroxyursolic acid, maslinic acid, 2R-hydroxy-3â-{[(2E)-3-phenyl-1-oxo-2- propenyl]oxy}olean-12-en-28-oic acid, and 3â-trans-p-coumaroyloxy-2R-hydroxyolean-12-en-28-oic acid, which had potent antiproliferative activity against HepG2 human liver cancer cells, Caco-2 human colon cancer cells, and MCF-7 human breast cancer cells [36]. The triterpenoids were said to be partially responsible for apple's anticancer activity along with other bioactive compounds. Yang et al. (2006) studied the anticancer activity of tirucallane triterpenoids from twigs of *Amoora dasyclada* against human lung cancer cells (AGZY 83-a) and human liver cancer cells (SMMC-7721), two of the tirucallanes exerted weak activity against AGZY 83-a, while one exhibited strong activity against SMMC-7721 [37].

It was deduced that the novel tritepernoids cleogynone A (1) and cleogynone B (2) as well as the known compound cleogynone C in this study are partly responsible for the anticancer activity exhibited by *C. gynandra,*. The activity was distributed across all the primary fractions collected from the *n*-hexane leaf extract and the greatest activity was due by the most polar fraction. This necessitates future work on identifying robust methods to isolating and identifying further compounds responsible for the cancer activity, that is not the scope of this work.

4.5. Conclusion

Bioassay-guided fractionation of anticancer ingredients from the *n*-hexane leaf extract from *C. gynandra* proved successful. The *n*-hexane extract which was most active for lung cancer

(A549) cytotoxicity compared to other sequentially extracted extracts was subjected to bioassay-guided fractionation towards isolating, purifying and identifying the components responsible for the anticancer activity. The primary fractionation revealed that the lung cancer cytotoxicity was distributed at varying strengths across all fractions. The test concentrations were 0.0625, 0.125, 0.25, 0.5 and 1 mg/mL, and over a 24 hr treatment the lung cancer biological activity of the fractions was distributed between 55 % to 86 % inhibition across all the primary fractions at 0.5 µg/mL.Of the most active primary fractions, F7 was the less complex and most abundant and its further fractionation *via* a combination of silica gel 60 (0.063-0.2 mm) and/or silica gel-60 (0.040-0.063 mm) (flash column chromatography) and preparative TLC yielded two novel compounds **1** (cleogynone A) (29 mg) and **2** (cleogynone B) (24 mg), as well as a known compound **3** (cleogynone C) (11 mg). The structures of the two new triterpenoids, cleogynones A and B were elucidated by NMR and mass spectroscopic data analysis and confirmed by single crystal X-ray crystallography. The structure of compound **3** was elucidated by NMR and mass spectroscopic data analysis and confirmed by comparison of the spectroscopic data to those described in literature. The compounds were all dammerane-type triterpenoids.

The pure compounds were screened for their lung cancer (A549), breast cancer (MDA-MB-468) and colorectal cancer (HCT116 and HCT15) cytotoxicity. The compounds displayed concentration dependant anticancer activity at the concentrations 0.39, 0.78, 1.56, 3.12, 6.25, 12.50 and 25.00 µg/mL. Cleogynone B (2) showed moderate activity against lung cancer (A549) while all three compounds displayed moderate cytotoxicity against breast cancer (MDA-MB-468). The best activities were displayed against colorectal cancer cell lines with cleogynone B (**2**) and cleogynone C (**3**) demonstrating greater than 87 % inhibition against HCT116 at the 24 hr exposure at 25 µg/mL, while all compounds displayed greater than 81 % inhibition at the 48 hr exposure against HCT15 at 25 µg/mL concentration.

Compounds **1** - **3** displayed potent anticancer activity against colorectal cancer, and these dammerane-type triterpenoids are partially responsible for the overall anticancer activity of *C. gynandra* along with other bioactive compounds. For the first time a comprehensive study

that involves not only systematic identification of anticancer compounds, but systematic identification of anticancer dammerane-type triterpenoids from *C. gynandra,* was conducted. There is still a chiasm that need to be filled in identifying further compounds, that are potentially novel, responsible for the cancer activity of *C. gynandra,* this study has paved the platform.

4.6. References

1. Tan, W.; Lu, J.; Huang, M.; Li, Y.; Chen, M.; Wu, G.; Gong, J.; Zhong, Z.; Xu, Z.; Dang, Y.; et al. Anti-cancer natural products isolated from chinese medicinal herbs. *Chin. Med.***2011**, *6*, 1–15, doi:10.1186/1749-8546-6-27.
2. Bala, A.; Haldar, P.K.; Kar, B.; Naskar, S.; Saha, P.; Kundusen, S.; Gupta, M.; Mazumder, U.K. Antioxidant activity of the fractions of *Cleome gynandra* promotes antitumor activity in ehrlich ascites carcinoma. *Asian J. Chem.***2011**, *23*, 5055–5060.
3. Molatlhegi, R.P.; Phulukdaree, A.; Anand, K.; Gengan, R.M.; Tiloke, C.; Chuturgoon, A.A. Cytotoxic effect of a novel synthesized carbazole compound on A549 lung cancer cell line. *PLoS One***2015**, *10*, 1–14, doi:10.1371/journal.pone.0129874.
4. Gibbs, J.B. Mechanism-based target identification and drug discovery in cancer research. *Science (80-.).***2000**, *287*, 1969–1973, doi:10.1126/science.287.5460.1969.
5. Mzondo, B.; Dlamini, N.; Malan, F.; Labuschagne, P.; Maharaj, V. Dammarane-type triterpenoids with anti-cancer activity from the leaves of *Cleome gynandra*. *Phytochem. Lett.***2021**, *43*, 16–22.
6. Minna, J.D.; Roth, J.A.; Gazdar, A.F. Focus on lung cancer. *Cancer Cell***2002**, *1*, 49–52, doi:10.1016/S1535-6108(02)00027-2.
7. Alberg, A.J. Epidemiology of lung cancer. *Chest***2003**, *123*, 21–49, doi:10.5114/wo.2021.103829.
8. Collins, L.G.; Haines, C.; Perkel, R.; Enck, R.E. Lung Cancer: Diagnosis and Management. **2007**, *75*, 56–63.
9. Molina, J.R.; Adjei, A.A.; Jett, J.R. Advances in chemotherapy of non-small cell lung cancer. *Chest***2006**, *130*, 1211–1219, doi:10.1378/chest.130.4.1211.
10. Rossi, A.; Di Maio, M. Platinum-based chemotherapy in advanced non-small-cell lung cancer: optimal number of treatment cycles. *Expert Rev. Anticancer Ther.***2016**, *16*, 653–660, doi:10.1586/14737140.2016.1170596.
11. National Cancer Institute Drugs Approved for Lung Cancer - National Cancer Institute Available online: https://www.cancer.gov/about-cancer/treatment/drugs/lung (accessed on Oct 16, 2021).
12. Harris, J.R.; Lippman, M.E.; Veronesi, U.; Willet, W. Breast cancer. *Med. Prog.***1992**, *326*, 319–328.
13. Key, T.J.; Verkasalo, P.K.; Banks, E. Epidemiology of breast cancer. *The lancet oncoogy***2001**, *2*, 133–140, doi:10.1016/j.molcel.2019.06.002.
14. Waks, A.G.; Winer, E.P. Breast Cancer Treatment: A Review. *J. Am. Med. Assoc.***2019**, *321*, 288–300, doi:10.1001/jama.2018.19323.
15. Akram, M.; Iqbal, M.; Daniyal, M.; Khan, A.U. Awareness and current knowledge of breast cancer. *Biol. Res.***2017**, *50*, 1–23, doi:10.1186/s40659-017-0140-9.
16. National Cancer Institute Drugs Approved for Breast Cancer - National Cancer Institute Available online: https://www.cancer.gov/about-cancer/treatment/drugs/breast (accessed on Oct 16, 2021).
17. Center, M.M.; Jemal, A.; Smith, R.A.; Ward, E. Worldwide variations in colorectal cancer. *Dis. Colon Rectum***2010**, *53*, 1099, doi:10.1007/DCR.0b013e3181d60a51.

18. Markowitz, S.D.; Bertagnolli, M.M. Molecular Basis of Colorectal Cancer. *N. Engl. J. Med.***2009**, *361*, 2449–2460, doi:10.1056/nejmra0804588.

19. Meyerhardt, J.A.; Mayer, R.J. Systemic therapy for colorectal cancer. *N. Engl. J. Med.***2005**, *352*, 476–487, doi:10.2298/AOO0304255S.

20. Potter, J.D. Colorectal cancer: Molecules and populations. *J. Natl. Cancer Inst.***1999**, *91*, 916–932, doi:10.1093/jnci/91.11.916.

21. Kudo, S.E.; Kashida, H.; Tamura, T.; Kogure, E.; Imai, Y.; Yamano, H.O.; Hart, A.R. Colonoscopic diagnosis and management of nonpolypoid early colorectal cancer. *World J. Surg.***2000**, *24*, 1081–1090, doi:10.1007/s002680010154.

22. Wolpin, B.M.; Mayer, R.J. Systemic Treatment of Colorectal Cancer. *Gastroenterology***2008**, *134*, 1296–1310, doi:10.1053/j.gastro.2008.02.098.

23. National Cancer Institute Drugs Approved for Colon and Rectal Cancer - National Cancer Institute Available online: https://www.cancer.gov/about-cancer/treatment/drugs/colorectal (accessed on Oct 16, 2021).

24. Garcia-Oliveira, P.; Otero, P.; Pereira, A.G.; Chamorro, F.; Carpena, M.; Echave, J.; Fraga-Corral, M.; Simal-Gandara, J.; Prieto, M.A. Status and challenges of plant-anticancer compounds in cancer treatment. *Pharmaceuticals***2021**, *14*, 1–28, doi:10.3390/ph14020157.

25. Akhtar, M.S.; Swamy, M.K. *Anticancer plants: Clinical trials and nanotechnology*; Akhtar, M.S., Swamy, M.K., Eds.; Springer nature: Singapore, 2018; Vol. 3; ISBN 9789811082160.

26. Efferth, T.; Kuete, V. Biodiversity, Natural Products And Cancer Treatment. *Curr. Diabetes Rev.***2018**, *14*, 36–106.

27. Flack, H.D. On enantiomorph-polarity estimation. *Acta Crystallogr. Sect. A***1983**, *A39*, 876–881.

28. Flack, H.D.; Bernardinelli, G. Reporting and evaluating absolute-structure and absolute-configuration determinations. *J. Appl. Crystallogr.***2000**, *33*, 1143–1148, doi:10.1107/S0021889800007184.

29. Sheldrick, G.M. X-PREP. *Bruker Anal. X-ray Syst.* 2008.

30. Sheldrick, G.M. SHELXT - Integrated space-group and crystal-structure determination. *Acta Crystallogr. Sect. A Found. Adv.***2015**, *A71*, 3–8.

31. Sheldrick, G.M. Crystal structure refinement with SHELXL. *Acta Crystallogr. Sect. C Struct. Chem.***2015**, *C71*, 3–8.

32. Das, P.C.; Patra, A.; Mandal, S.; Mallick, B.; Das, A.; Chatterjee, A. Cleogynol, a novel dammarane triterpenoid from *Cleome gynandra.J. Nat. Prod.***1999**, *62*, 616–618, doi:10.1021/np9803528.

33. Petronellia, A.; Pannitterib, G.; Testaa, U. Triterpenoids as new promising anticancer drugs. *Anticancer. Drugs***2009**, *20*, 880–892, doi:10.1097/CAD.0b013e328330fd90.

34. Liby, K.T.; Yore, M.M.; Sporn, M.B. Triterpenoids and rexinoids as multifunctional agents for the prevention and treatment of cancer. *Nat. Rev. Cancer***2007**, *7*, 357–369, doi:10.1038/nrc2129.

35. Jie, L. Pharmacology of oleanolic acid and ursolic acid. *J. Ethnopharmacol.***1995**, *49*, 57–68, doi:10.1016/0378-8741(95)01310-5.

36. He, X.; Rui, H.L. Triterpenoids isolated from apple peels have potent antiproliferative activity and may be partially responsible for apple's anticancer activity. *J. Agric. Food Chem.***2007**, *55*, 4366–4370, doi:10.1021/jf063563o.

37. Yang, S.M.; Song, Q.S.; Qing, C.; Wu, D.G.; Liu, X.K. Anticancer activity of tirucallane triterpenoids from Amoora dasyclada. *Zeitschrift fur Naturforsch. - Sect. C J. Biosci.***2006**, *61*, 193–195, doi:10.1515/znc-2006-3-407.

Chapter 5:

Formulation of *Cleome gynandran*-hexane extract with β-cyclodextrin, solubility assessments and the anticancer activity of the formulations

5.1. Introduction

5.1.1. Background

Plant constituents may possess poor physicochemical properties which may limit the feasibility of their pharmaceutical formulations. Such physicochemical property hurdles may involve light- and heat-sensitivity, instability at low pH, lack of wettability in water, hygroscopicity, low aqueous solubility, and therefore, poor bioavailability. These adverse properties may eventually impede their use as pharmaceutical or nutraceutical agents [1]. One of the objectives of this study was to overcome some of the problems encountered with the use of such plant bioactive isolates. Cyclodextrins (CDs) are able to incorporate a variety of molecules in their hydrophobic cavity and this has many positive implications, mainly due to the resulting physicochemical properties of the included molecule [2]. The *n*-hexane extract, which was most active for anticancer activity, and whose further fractionation resulted in the isolation and identification of compounds with anticancer activity in chapter 4, was selected for its potential to benefit from CD complexation. This extract possesses low aqueous solubility, and thus poor bioavailability if it were to be developed as an herbal medicine. This chapter involves using strategies of CD inclusion to complex the *n*-hexane extract components in order to identify the best formulation. The focus is based on producing formulations with low toxicity, better stability, good bioavailability, longer shelf life and higher market value. While many techniques such as kneading, spray-drying, freeze drying and co-precipitation, are used for CD complexation formulations, these preparative methods can be time consuming, less efficient, some requiring additional drying step and high residual organic solvent [3]. The requirements for purity are exceptionally high in pharmaceuticals, nutraceuticals and food supplements and conventional methods are not sufficient, therefore, the supercritical fluid (SCF) technique and in particular the supercritical carbon dioxide (SC-

CO_2) technology is another alternative worth considering [4–6]. During the past few decades, SCF has emerged as an effective alternative for many traditional pharmaceutical manufacturing processes and is said to be one of the most renowned high-pressure techniques to obtain products with better performances [7]. SCF technology takes advantage of benign solvents such as CO_2 and water (or food grade solvent) to replace the organic solvents thereby serving as an alternative in synthesising delivery systems [7]. SC-CO_2 technique was selected for this study as it is non-toxic, non-flammable, non-reactive, economical and non-polluting. This green technology has a potentially high impact in the pharmaceutical field to overcome the curbs of the various conventional methods mentioned earlier. It was hypothesised that the extract complexation with CD might lead to new solid species with improved physicochemical properties increasing their chances of eventually being developed as pharmaceuticals, nutraceuticals or herbal medicines. CDs have been in existence for decades and are employed in many different fields, including food and pharmaceuticals. They are used as such as they have very limited bioavailability and distribute among extracellular compartments on absorption [2]. Systemically absorbed CDs are rapidly expelled from the body and appear in the urine unmetabolized [2]. Martin Del Valle (2004) wrote that administered CDs are quite resistant to starch-degrading enzymes, although they can be degraded at very low rates by α-amylases. β-CD is the slowest degradable compound while γ-CD is the fastest, due to their differences in size and flexibility [2]. Furthermore, degradation is not performed by salivary or pancreatic amylases, but by α-amylases from microorganisms from the colon flora.

5.1.2. Cyclodextrins

5.1.2.1. Their discovery, nature and properties

CDs were called “cellulosines” when they were first discovered by A. Villiers in 1891 and later referred to as “Schardinger sugars” after the identification of the naturally occurring α- and β-cyclodextrins by F. Schardinger in 1911. The third naturally occurring CD, γ-

cyclodextrin, was only isolated in 1935. Research spanning a period of over 25 years demonstrated the ability of the CDs to form stable complexes with many chemicals in aqueous solution [2,8]. CDs are formed during bacterial digestion of cellulose and structurally they are truncated cone-shaped oligosaccharides composed of (α-1,4)-linked α-D-glucopyranose units. Naturally occurring CDs are named α-CD (cyclohexaamylose), β-CD (cycloheptaamylose) and γ-CD (cyclooctaamylose) and consist of 6, 7 and 8 glucopyranose units, respectively (Figure 5.1)

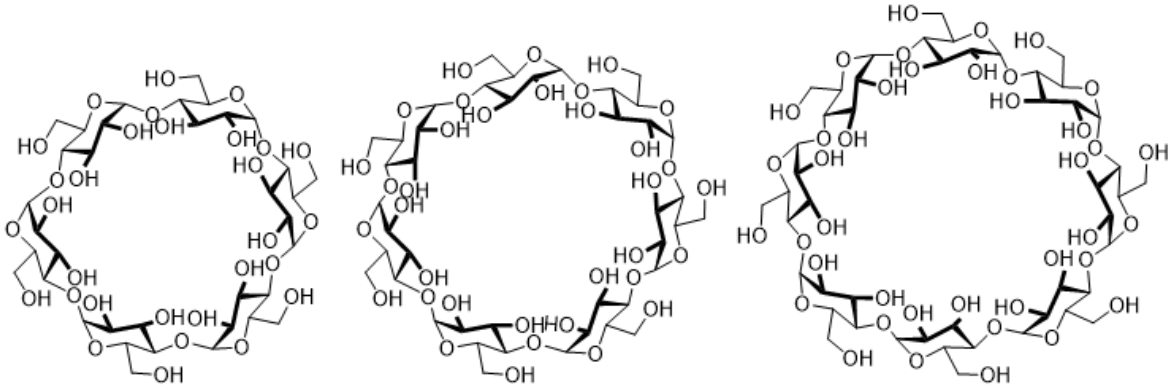

α-cyclodextrin **β-cyclodextrin** **γ-cyclodextrin**

Figure 5.1:*Structure of α-, β-, and γ-cyclodextrin, the naturally occurring cyclodextrins.*

The interior of the CD cavity is hydrophobic, in contrast with the hydrophilic exterior environment, and can thus host less hydrophilic guest molecules [8–10]. The inclusion complex with the guest (e.g., a drug molecule) may involve the incorporation of the lipophilic moiety of a guest molecule in the cavity. The CD has a narrower and a wider rim; the narrower rim possesses one primary hydroxyl group (O6-H) per glucose unit and the wider secondary rim has two hydroxyl groups (O2-H and O3-H) per glucose unit (Figure 5.2).

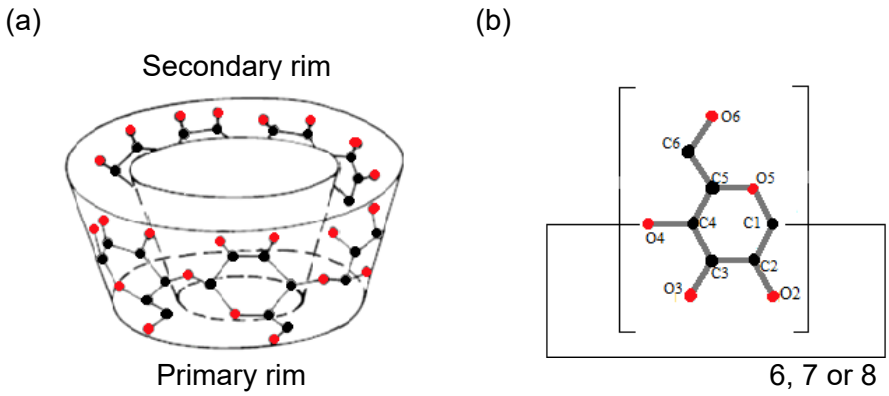

***Figure 5.2**: (a) The truncated-cone shape of a CD molecule illustrating the narrow primary rim and the wider secondary rim and (b) α-D-glucopyranose units. The red and black dots represent oxygen atoms and carbon atoms, respectively, in both (a) and (b). H atoms have been omitted for clarity. Edited from the illustration "The chemical structure and the toroidal shape of a cyclodextrin molecule" by R. Challa et al. (2005)[11].*

There are a series of intramolecular hydrogen bonds (O2···H-O3') between the secondary hydroxyl groups of adjacent glucose rings and these stabilise the CD molecule and negatively affect the aqueous solubility of CDs to some extent [2,12]. The strengths of the hydrogen bonds increase in the order α-CD < β-CD < γ-CD, while the aqueous solubilities are 14.5, 1.85 and 23.2 g per 100 ml, respectively [11]. Table 5.1 is a summary of some properties of the three native CDs.The hydrophilic exterior of CDs is responsible for the relatively high aqueous solubility that these compounds possess.

***Table 5.1**: Properties of native cyclodextrins.*

Cyclodextrin	M_r (g/mol)	Molecular formula	Melting point (°C)	Aqueous solubility (g/L)	Cavity diameter (Å)		Cavity volume (Å^3)
					Inner	Outer	
α-CD	972.84	$C_{36}H_{60}O_{30}$	278	145	4.7 - 5.3	14.6	174
β-CD	1134.98	$C_{42}H_{70}O_{35}$	260	18.5	6.0 - 6.5	15.4	262
γ-CD	1297.12	$C_{48}H_{80}O_{40}$	267	232	7.5 - 8.3	17.5	427

5.1.2.2. Cyclodextrins and their pharmaceutical application

In order to be readily delivered to the cellular membrane, a drug must have a certain minimum level of aqueous solubility, and in this respect most pharmaceutical agents are not sufficiently soluble in water [2]. The traditional formulation systems involve organic solvents,

extreme pH conditions and surfactants; these measures often cause irritation and adverse reactions. CDs are non-irritants and are characteristic stabilisers of active compounds. These compounds also reduce volatility of drugs, and offer masking of malodours and bitter tastes [12]. The ability of CDs to increase solubility of insoluble drugs, results in improvement of the bioavailability of the active ingredient, enhancing pharmacological effect and therefore allowing for a reduced dose of administered drug. CDs are able to enhance drug delivery through the biological membrane: they provide enhancement of penetration by making the bioactive ingredient more available at the biological membrane surface. The membrane is relatively lipophilic and therefore CDs will not penetrate these, but remain in the bulk aqueous medium. Studies revealed that only 2–4% of CDs were adsorbed in the small intestines, and that the remainder is enzymatically degraded and taken up as glucose [2,11].

Loftsson and Duchêne (2007) reported that very few different pharmaceutical products containing CDs were on the market worldwide [13]. They stated the views that even though new CD-based technologies are being developed, CDs are novel excipients of unexplored technology still after 100 years of their discovery. In 2013 the company Cyclolab (Budapest, Hungary) reported the approved and marketed pharmaceutical products containing CDs, showing that most of them contain β-CD or its derivative [14]. Around 50 bioactive formulations with various CDs were listed.

Results obtained by researchers are continually contributing towards the development of oral pharma-/nutraceutical agents containing CD. Research confirmed the inclusion complexation between hydroxypropyl-β-CD and 7-dehydrocholesterol resulting in enhanced solubility compared to uncomplexed 7-dehydrocholesterol [15]. Curcumin, a promising anticancer and antiviral nutraceutical agent with limited solubility in water at both neutral and acidic pH and exhibiting high decomposition at alkaline pH was also complexed with CD [16]. The stability and solubility of curcumin under basic conditions were improved upon complexation. Silymarin, a liver protective nutraceutical, particularly poorly water soluble and thus

exhibiting poor bioavailability, was complexed by co-precipitation method with β-CD [17]. The complexation resulted in increased dissolution rates compared to the uncomplexed drug and more sustained-release profiles were also apparent. Wang et al. (2011) in their study encapsulated garlic oil in β-CD [18]. Garlic oil possesses antioxidant and antimicrobial properties, its inherent volatility and poor physicochemical stability, however, limit its pharmaceutical activity. Using UV-Vis, differential scanning calorimetry, FTIR and X-ray diffraction techniques Wang et al. (2011) established that the garlic oil when incorporated in β-CD was protected from oxidation with improvement in the stability of the complex. Complexation further resulted in enhanced aqueous solubility on garlic oil and *in vitro* dissolution studies suggested that a controlled release rate was also achieved. In a study by Gonnetet al. (2010) the solubility of vitamin A was increased by almost 35000 times through encapsulation in hydroxypropyl-β-CD [19]. Mekjaruskul et al. (2013) performed complexation studies using 2-hydroxypropyl-β-CD to improve the oral bioavailability and permeation parameters of the kaempferia parviflora plant extract [20]. The extract contained methoxyflavones with bioactivity such as anti-inflammatory, anti-allergy and antimicrobial properties. The resulting formulation increased the biological membrane permeability by 3.5 times while the bioavailability was 21-34 times greater compared to the standard extracted formulation. An inclusion complex between the herbal compound, astaxanthin, and hydroxypropyl-β-CD was achieved, resulting in improved solubility of the compound and this also serving as a strategy to control the release of the bioactive molecule at the active site [21,22]. UV, FTIR, ^{1}H NMR and molecular modelling studies were used for the characterisation.

CDs play a very vital role in the pharmaceutical research field; To the best of our knowledge there are no reports on CD complexations studies towards improving the physicochemical properties of *C. gynandra* ingredients. Such studies are useful in paving the way towards developing *C. gynandra* medicinal products. To achieve this, this study employs SC-CO_2

technology whose adoption is not only due to its environmentally benign nature in various processes but also because of its economically promising character [7].

5.1.3. Supercritical fluid technology

5.1.3.1. Background

The technology of supercritical fluids is exploited due to the combination of solvent strength and unique physical properties of the compound at temperature and pressure about its critical point [23]. Each compound has its characteristic phase diagram and the location of the critical point will differ from compound to compound. At the critical point the gas and liquid phases merge to form a single homogeneous fluid phase. Beyond the critical point is the supercritical fluid region. The supercritical fluid is highly dense, and possesses low viscosity and diffusive intermediate between gas and liquid. Combined with their polarity, these characteristics make supercritical fluids powerful solvents. The physicochemical affinity of the solute for the solvent and the apparent density of the solvent determine the solubility of a compound in a supercritical solvent [23]. SC-CO_2 technique has been receiving increased attention over recent years due to the adjustability of the supercritical fluid properties mentioned [3]. SC-CO_2 is the technique of choice due to its safety and the mild temperature and pressure required to achieve the supercritical state. Further, since CO_2 is gaseous at ambient conditions and thus eliminating the residual solvent problem it is an ideal substitute for organic solvents. The favourable properties of SC-CO_2, such as excellent mass transfer properties and high solvating power render this technique suitable for the complexation of thermally labile compounds with CDs [6]. A CO_2 pressure-temperature phase diagram is shown in Figure 5.3.

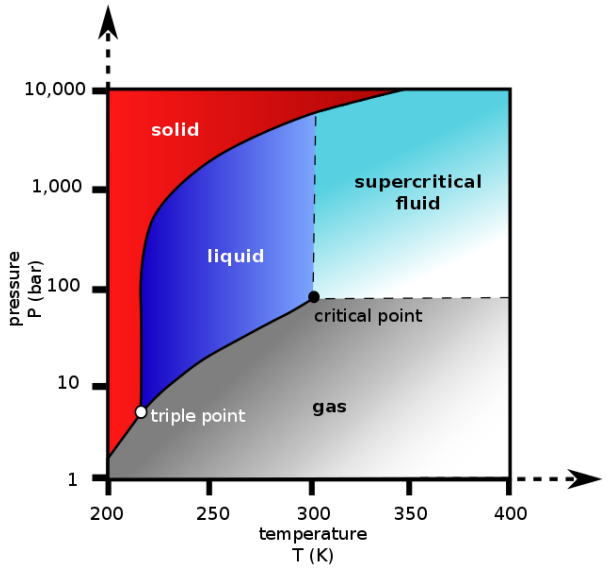

Figure 5.3: *Carbon dioxide pressure-temperature phase diagram, Finney and Jacobs (2010)* [24].

5.1.3.2. Literature on supercritical CO_2 cyclodextrin complex formulation

Palmer et al. (1995) stated that research into the solvent properties of dense gases, near-critical and supercritical fluids over the last 130 years has led to the characterisation of a wide range of solvent systems [23]. The use of CO_2 as a supercritical solvent enables achievement of the supercritical conditions at moderate pressure and temperature, avoiding the degradation of thermolabile substances while providing an inert medium suitable for easy processing of oxidisable compounds [25]. Some processes have been developed to provide means of obtaining inclusion complexes under mild conditions in order to increase the bioavailability of poorly soluble drugs using SC-CO_2 as themedium for the complexation process. The process has the advantage of being carried out under mild, solvent-free conditions reducing energy costs [26]. A novel method for producing a solid budesonide-γ-CD complex in a single-step process involving solution enhanced dispersion by SC-CO_2 method was reported [27]. Enhanced dissolution rate in water was achieved in a study where ibuprofen–methyl-β-CD complexes were prepared by passing ibuprofen-laden CO_2 through a methyl-β-CD packed bed [28]. The enhanced dissolution rate was attributed to the amorphous character and improved wettability of the product. A study that involved

dissolving the drug of interest in SC-CO_2, followed by permeation of the supercritical solution into the pores of the carrier and precipitation of the drug inside the pores presented an almost complete inclusion of *RS*(±)-Ibuprofen in β-CD at the solid state and a significant increase in dissolution rate compared to the untreated *RS*(±)-Ibuprofen [29]. Bounaceur et al. (2007) prepared an inclusion complex of ketoprofen and β-CD using SC-CO_2 [30]. An increase in the parameters related to the process: pressure, temperature, maturation period, agitation and density of SC-CO_2, resulted in increased association rate of ketoprofen with β-CD. The stoichiometry of the complex was 1:2 ketoprofen to β-CD. The importance of adjusting such parameters as temperature, pressure and exposure period is revealed as critical to achieving the desired outcome, and that is the solvating power of the SFC technique. With control of both the operating conditions (pressure, temperature, maturation period, agitation and density of SC-CO_2 and the preparation of the mixture, high percentage of complexation was observed without the use of organic solvent [31]. The influence of temperature, residence time, water content and a ternary agent, l-lysine, was studied in preparation of piroxicam/β-CD complexes by means of SC-CO_2 [32]. A complete inclusion was achieved for a piroxicam/β-CD/l-lysine mixture by keeping a physical mixture of the three compounds (1:2:1.5 molar ratio) for 2 hr in contact with CO_2 at 150 °C and 15 MPa. Jun (2007) successfully prepared a complex of simvastatin with hydroxypropyl-β-CD using supercritical antisolvent [33]. Al-Marzouqi et al. (2006) showed that inclusion complex of itraconazole and β-CD obtained using SC-CO_2 significantly improved the solubility of itraconazole in aqueous solutions. Higher inclusion yields were obtained in the SC-CO_2 method compared to physical mixing and co-precipitation methods [34]. Furthermore, both temperature and pressure had significant effects on itraconazole solubility in SC-CO_2 and the yield of the inclusion complex prepared by SC-CO_2 method. Hazem et al. (2007) further reported studies on enhancement of dissolution amount and *in vivo* bioavailability of itraconazole-β-CD complex obtained using SC-CO_2 [35].

In this study the SC-CO_2 technique is used to formulate the *n*-hexane extract of *C. gynandra* leaves with β-CD aimed at improving the physicochemical properties of the extract.

5.1.4. The spray-drying technique

5.1.4.1. Background

This technique is commonly used in pharmaceuticals to produce a dry powder from a liquid phase. The spray-drying process comprises three major stages [36]. The initial stage involves the atomisation of the liquid stream by an appropriate device. The next stage involves subjecting the fine droplets of the feed to the interaction with a drying gas at adequate temperature, usually higher than that of the feed. At this phase the solvent contained within the dispersion droplets is vaporised, and this results in the formation of solid particles as product. During the last phase the dried particles are separated from the drying gas by an appropriate device and collected by a receptacle tank. For example, in the case of bioactive-CD encapsulation, the CD and bioactive compound are first homogenised as a suspension or slurry in a solvent [37]. The slurry is then fed into a spray-drier, usually a tower heated to temperatures well over the boiling point of the solvent. As the slurry enters the tower, it is atomised. The interaction between the CD and bioactive ingredient results in a slurry of CD-complexed bioactive component. The small size of the atomised droplets results in a relatively large surface-to-volume ratio, allowing rapid drying. The resulting product of this process is a powdery material.

5.1.4.2. Cyclodextrin complex formulations using the spray-drying technique

The spray-drying process is considered to be a fast procedure applied in the formulation and processing of biopharmaceuticals [38]. Spray-drying of cyclodextrin solutions was proven to be an efficient technique for the preparation of highly soluble inclusion compounds of aripiprazole and the β-CD derivative, (2-Hydroxy) propyl-β-cyclodextrin [39]. The spray-dried products were free of crystalline aripiprazole, with higher solubility and dissolution rate, and proved to be stable enough over a prolonged period of storage. Skalko-Basnet et al. (2000) applied a one-step spray-drying method in their preparation of liposomes containing drug and cyclodextrin (CD) [38]. Spray-dried lecithin liposomes, entrapping metronidazole or

verapamil alone or together with hydroxypropyl-β-cyclodextrin, were characterised. The most stable liposomes (still retaining about 10% of the originally entrapped drug even after 24 hr incubation with serum) were liposomes prepared by the direct spray-drying of the mixture of lipid, drug, and hydroxypropyl-β-cyclodextrin. Shan-Yang et al. (1989) prepared inclusion complexes of drugs (acetaminophen, indomethacin, piroxicam and warfarin) with β-CD by using a spray-drying technique [40]. It was found that the spray-drying technique could be used to prepare the amorphous state of drug inclusion complexes. While the flowability and compressibility of the spray-dried products were poor due to the small particle size formed by the spray-drying process, the dissolution rates of drugs from tablets made by the spray-dried products were faster than those of the pure drug and the physical mixture of drug and β-CD. Several research studies have described the complexation of phenolic compounds with CDs [41] and Escobar-Avello et al. (2021) encapsulated phenolic compounds from a grape cane pilot-plant extract in hydroxypropyl β-cyclodextrin and maltodextrin by spray-drying [42]. Alginate and β-CD were used to produce easily dosable and spray-dried microsystems of a dried blood orange extract with antidysmetabolic properties obtained from a by-product fluid extract [43]. The 2% sodium alginate was capable of improving the extract shelf life, while the β-CD (1:1 molar ratio with dried extract) prolonged the extract antioxidant efficiency by 6 hours.

There is sufficient evidence of the capability of the spray-drying technique in CD formulation of bioactive compounds and extracts. Indications are vast on the improvement of physicochemical properties such as solubility, stability and more, due to such formulations. In this study we compare the established, spray-drying technique, with the novel supercritical fluid technique which boasts as the green technology of great interest nowadays.

5.2. Materials and methods

U/HPLC grade solvents (methanol and water) used for UPLC-QTOF-MS samples preparation were purchased from Sigma Aldrich (South Africa), so were the analytical grade solvent(s), reagent(s) and chemical(s) (ethanol, polyvinyl alcohol (PVA) and D-lactose) used in formulation experiments. CAVAMAX® W7 (β-cyclodextrin) was purchased from Wacker Chemie AG (Pinetown, New Germany). Milli-Q® water was used in preparative experimentations involving the use of water. All chemicals were used without further purification.

5.2.1. Formulation using the supercritical fluid technique

Formulations *via* the supercritical CO_2 method were carried out using a Separex pilot-scale reactor (Separex Equipements, Champigneulles, France) described by Labuschagne et al. (2010) [44]. The reactor is shown in Figure 5.4 while a schematic diagram of the reactor with labels is illustrated in Figure 5.5. CO_2 gas is drawn from a standard commercial gas cylinder fitted with a dip-tube and pumped through a pre-heated chamber, set to the reactor temperature, into the mixing chamber. The mixing chamber (0.5L capacity) was pre-heated to the process temperature with electrical heaters.

Figure 5.4: *An image of the Supercritical CO_2 reactor, personal photo.*

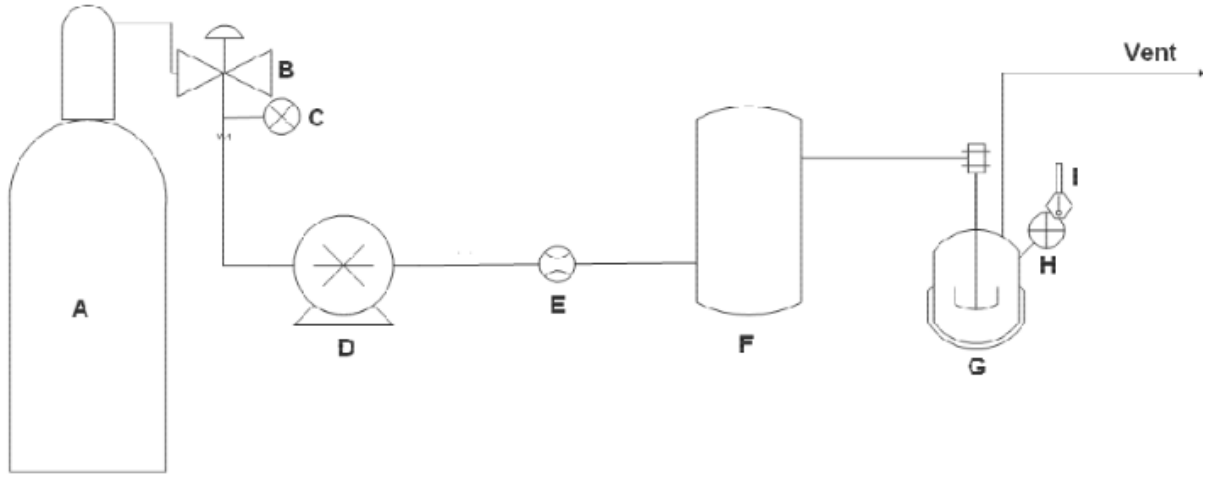

Figure 5.5: *Schematic diagram of the supercritical CO_2 reactor: A) CO_2 cylinder, B) back-pressure regulator, C) pressure gauge, D) diaphragm pump, E) flow meter, F) CO_2 pre-heater, G) mixing chamber, H) pressure gauge, I) temperature probe. Taken from Labuschagne et al. (2010)* [44].

β-CD (60.0 – 70.2 mg) was physically mixed with the *n*-hexane extract (17.3 – 26.1 mg) by co-grinding using a pestle and a mortar with each co-grinding experiment taking no less than 5 min, to prepare several samples for SC-CO_2 reaction at varying operating parameters (temperature, pressure and exposure time). The SC-CO_2 formulations were prepared by placing the β-CD/*n*-hexane physical mixture in the supercritical CO_2 reactor reaction/mixing chamber preheated to 40, 70 or 100 °C. The reactor was sealed and the formulations exposed to the following CO_2 pressure conditions: 0 bar, 100 bar and 300 bar. Experimental exposure time was set at 4 and 8 hours. After completion of reaction, the CO_2 pump was turned off and the CO_2 was released from the reactor to 0 bar over a period of approx. 3 minutes. All formulations were stored in a refrigerator at ±4 °C in airtight containers, prior to analysis. Table 5.2 lists the SC-CO_2 reactor conditions (temperature, pressure and time) used to prepare eighteen samples of β-CD and *n*-hexane extract loading formulations.

***Table 5.2**: β-CD/n-hexane-extract formulations prepared at varying conditions in SC-CO_2 (temperature, pressure and time).*

#	Sample name	Temperature (°C)	CO_2 Pressure (bar)	Exposure time (hr)
1	40·0·4	40	0	4
2	40·100·4	40	100	4
3	40·300·4	40	300	4
4	40·0·8	40	0	8
5	40·100·8	40	100	8
6	40·300·8	40	300	8
7	70·0·4	70	0	4
8	70·100·4	70	100	4
9	70·300·4	70	300	4
10	70·0·8	70	0	8
11	70·100·8	70	100	8
12	70·300·8	70	300	8
13	100·0·4	100	0	4
14	100·100·4	100	100	4
15	100·300·4	100	300	4
16	100·0·8	100	0	8
17	100·100·8	100	100	8
18	100·300·8	100	300	8

5.2.2. Formulation using the spray-drying technique

Formulation using the spray-drying technique was achieved using a Büchi Mini Spray Dryer B-290 (Büchi Labortechnik AG), shown in Figure 5.6.

***Figure 5.6:** An image of a Büchi mini spray dryer used for spray-dried formulations* [45].

The schematic diagram of the general layout of the spray-dryer is shown in Figure 5.7 as illustrated by Kalombo et al. (2019) [46]. As shown in Figure 5.7 the spray-dryer is generally equipped with: {M-1} electric motor for stirrer, {T-1} emulsification tank, {V-1} valve, {PP-1} Pump for emulsion feeding into the atomisation tower T-1 of the spray dryer, {P-1} Compressed fluid (air or nitrogen) line used for spray atomisation, {E-1} Heating system for the drying fluid fed into the atomisation tank, {P-2} Line for dried product to be recovered through the cyclone C-1, {PR-1} Product collector as underflow from the cyclone, {P-3} Line for the overflow separated from the fluid (air/N2) through a filter F-1, {P-4} Line of the solid product recycled from the filter F-1; {P-5} Fluid (Air/N2) separated from solid particles feeding into a vacuum pump VP-1 to be recycled by line P-6 back to the drying tower T-2 after being heated-up through E-1 [46].

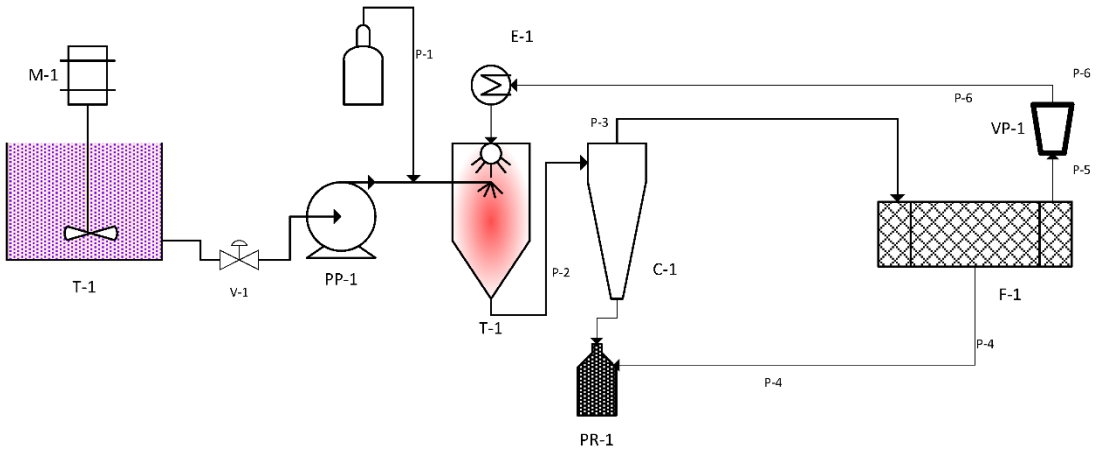

Figure 5.7: *Spray drying technology general layout, Kalombo et al.*[46].

The β-CD formulation of the *n*-hexane extract prepared *via* the spray-drying technique was named 122633 and was prepared as follows:

The *n*-hexane extract (105.9 mg) was dissolved in EtOH (40 ml), β-CD (305.4 mg) was added to the mix and water (40 ml) was added and the mixture was high-speed homogenised using a Silverson L4R high-speed homogeniser at 5000 rpm, yielding a 25.7 % extract loading. The emulsion was directly fed into the bench top Buchi mini-spray dryer

(Model B-290). The spray-drying conditions were as follows: Inlet temperature – 100 °C, pump speed – @2, aspiration – 100 %, outlet temperature – 110 °C with atomising pressure varying between 6 and 7 bar.

5.2.3. Aqueous solubility assessment

UPLC-QTOF-MS was used to generate chromatograms for solubility assessments of the SC-CO_2 as well as spray-dried *n*-hexane extract/β-CD formulations. UPLC was performed using a Waters Acquity UPLC system (Waters Corp., MA USA), equipped with a binary solvent delivery system and an autosampler.

The formulations of approximately 25 % loading of extract were suspended in water (1 mg sample per 1 ml) and sonicated for 5 minutes then centrifuged at 10000 rpm for 2 min, the supernatant was then subjected to UPLC-QTOF-MS analysis. Hundred percent solubility was standardised as 0.25 mg extract in methanol (equivalent to the 25 % loading as formulations) which exhibits complete dissolution of the *n*-hexane extract. In the case of the uncomplexed extract 0.25 mg was suspended in 1 ml water and the similar procedure was carried out as in the case of the formulations.

Separation was performed on a Waters BEH C18, (2.1 mm × 100 mm, 1.7 µm column). The mobile phase consisted of solvent A: 0.1% formic acid in purified water and solvent B: acetonitrile with 0.1% formic acid. The gradient elution was optimized as follows: 3% B (0-0.1 min), 3-30% B (0.1-6.0 min), 30% B (6.0-9.0 min), 30-100% B (9.0-20.0 min), 100% B (20.0-23.5 min), 100-3% B (23.5-24.0), 3% B (24.0-25.0). The flow rate was kept at 0.400 mL/min and the injection volume was 5 µL. The column temperature was 40 °C.

For MS conditions a Waters Synapt G2 high definition QTOF mass spectrometer equipped with an ESI source was used to acquire negative and positive ion data. The system was driven by MassLynx V 4.1 software (Waters Inc., Milford, Massachusetts, USA) for data acquisition. MS calibration was performed by direct infusion of 5 mM sodium formate

solution at a flow rate of 10 µL/min and using Intellistart functionality over the mass range of 50 - 1200 Da. The MS source parameters were set as follows for both the positive and negative mode: Source temperature 110 °C, sampling cone 25 V, extraction cone 4.0 V, desolvation temperature 300 °C, cone gas flow 10 l/h, desolvation gas flow (500 l/h). The capillary was 2.8 kV in the positive and 2.6 kV in the negative modes.

Acquisition

A 2 ng/µL solution of leucine encephalin was used as the lockspray solution that was constantly infused at a rate of 2 µL/min through a separate orthogonal ESI probe to compensate for experimental drift in mass accuracy. Trap collision energies were 30 V (high) and (10 V) for the low energy.

Relative Aqueous Solubility

Six major peaks of the *n*-hexane extract chromatogram were selected for relative solubility increment assessments of the formulation in comparison with the uncomplexed *n*-hexane extract. The integrated areas under each of the six major peaks for the uncomplexed *n*-hexane extract chromatogram served as the baseline for relative aqueous solubility increment or decrement determination of formulations. Such increments or decrements were calculated as follows:

$$Solubility\ increment = \frac{A_{complexed}}{A_{uncomplexed}} \quad (2)$$

Where $A_{complexed}$ is the value of the integrated area under the selected chromatogram peak for the formulation (β-CD complexed extract) and $A_{uncomplexed}$ is the integrated area of the peak for the original extract (*n*-hexane extract uncomplexed).

In cases where the solubility increment is a fraction this indicated a decrement and therefore for plotting the relative solubility graphs a reciprocal of the equation was taken and therefore the equation changes to:

$$solubility\ decrement = \left(\frac{A_{complexed}}{A_{uncomplexed}}\right)^{-1} \quad (3)$$

5.2.4. Anticancer studies for formulations

Anticancer studies were performed at the Cellular and Molecular Biology centre, Department of Biochemistry, JSS Medical College, JSS University, Mysuru, Karnataka, in India, as part of training of myself at the cancer research laboratory (B. G. Vidya, K. G. Mahadeva Swamy and Venugopal R. Bovilla) led by professor SubbaRao V. Madhunapantula. Prepared formulations were evaluated for their lung cancer (A549), breast cancer (MDA-MB-468) and colorectal cancer (HCT 15 and HCT116) cytotoxicity. The formulations were only dissolved in water and filter using a 0.45-micron filter.

Cell culture

All cell lines were cultured at 37°C, 5% CO_2, in Dulbecco's Modified Eagle Medium (DMEM) containing high glucose (containing 4.5 g/L glucose, sodium bicarbonate and phenol red), supplemented with 10 % fetal bovine serum (FBS), Glutamax (2 mM) and PenStrep (0.5 mg/ml).

Method for anticancer bioactivity assay of formulations

Cells were trypsinized at 10,000 cells per well in a 100 µL volume plated in 96 well plate. The cells were incubated in CO_2 to reach 60 - 70% confluence, at which point, they were treated with concentrations 0.25, 0.5 and 1 mg/mL in terms of extract loading and therefore 0.75, 1.5 and 3 in terms of β-CD for each test sample (whereby only H_2O was used for dissolution of test samples) along with positive control (Cisplatin-100 µM and/or diallyl disulphide (DADS) 1mM), incubated over 24 hours and 48 hours and cell viability determined using sulforhodamine B (SRB) assay. After 24- and 48-hour incubation cells were fixed using 50 µL of 50% trichloroacetic acid (TCA) was added to each well, and the plates were kept at 40 °C for 60 min. After fixation of cells, the wells were carefully washed with slow running tap water, and subsequently the plates were allowed to dry. One hundred microliters of SRB was added to each well and the plates incubated for 30 min. Excess unbound SRB was removed and the plates washed with 1% acetic acid. The washed wells were allowed to dry at room temperature. The protein bound SRB was dissolved in 100 µL of 10 mM tris base

solution and the absorbance read at 510 nm on a multimode plate reader (ParkinElmer, Massachusetts, USA).

5.3. Results and discussion

5.3.1. Formulations

The naming of the formulations obtained using the SC-CO_2 technique followed the nomenclature: $T \cdot P \cdot t$, for easy identification, where *T* was the operating temperature (°C), *P* the operating pressure (bar) and *t* the exposure time, in accordance with the SC-CO_2 method for the preparation of the formulation e.g. the formulation prepared at temperature 40 °C, pressure 100 bar and 4-hour exposure time is named 40·100·4. As shown in Table 5.2 eighteen formulations were prepared *via* the SC-CO_2 technology. One sample was prepared *via* the spray-drier method and was named 122633. The formulations were assessed for their aqueous solubility in order to compare with the original crude extract to determine as to whether the solubility was improved upon formulating.

5.3.2. Solubility assessment using UPLC-QTOF-MS

The chromatographic profile of the *n*-hexane extract generated using UPLC-QTOF-MS operating in the ESI positive mode is shown in Figure 5.8. Six major peaks from the chromatographic profile were selected for the solubility assessment studies and are labelled 1,2,3,4,5 and 6 in Figure 5.8, where 0.25 mg of extract was dissolved in methanol. The compounds represented by the peaks 1, 2 and 3 were the three compounds, cleogynone A, B and C, respectively, isolated and structure elucidated as described in chapter 4, and shown to possessing anticancer activity.

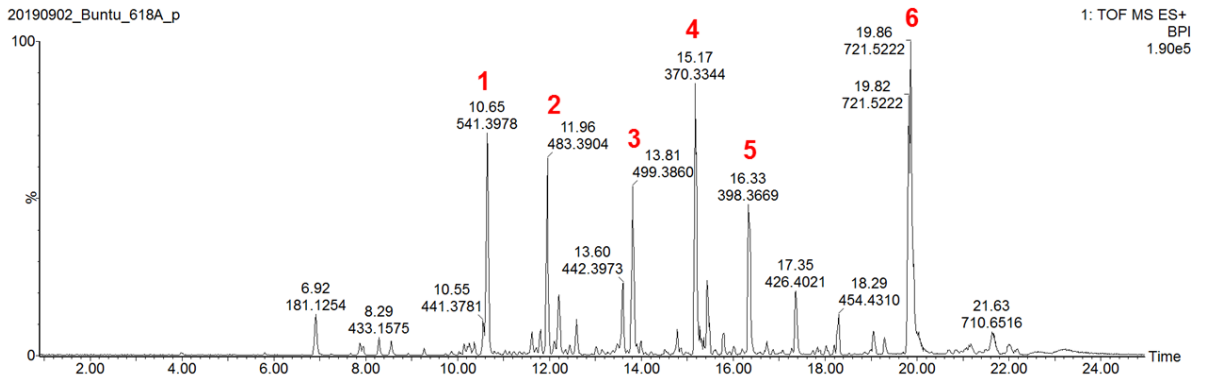

Figure 5.8: *UPLC-QTOF-MS ESI positive mode chromatographic profile of n-hexane extract. Peaks 1, 2, 3, 4, 5 and 6 selected for solubility assessment studies. Peaks 1, 2 and 3 represent cleogynone A, B and C with anticancer activity isolated and structure elucidated in chapter 4.*

The formulations and the crude *n*-hexane extract were separately dissolved in water and each solution was filtered using a 0.45-micron filter. The solutions were analysed using UPLC-QTOF-MS in positive mode. Using the *integrate* functionality in the MassLynx™ spectrometry software the profiles for the samples were area integrated and an example of the integrated chromatographic profile is shown in Figure 5.9. The peak areas were used to calculate the solubilities of the formulations relative to the unformulated extract using the six selected peaks. One additional sample was used for control, prepared by fist dissolving β-CD (3 mg) in water (4 ml) and adding *n*-hexane extract (1 mg) dissolved in β-CD solution, resulting in, extract : β-CD 1:3 mass ratio and given the sample name, extract-BCD-water. Figure 5.10 displays the solubility increment or decrement as a result of formulation compared to the crude *n*-hexane extract. The components (peaks) that indicated an increase in the solubility compared to the uncomplexed *n*-hexane extract protrude above the *x*-axis while those indicating a decrease in aqueous solubility protrude below the *x*-axis while the strength of such relative increment or decrement in solubility is indicated by the bar height in the graph.

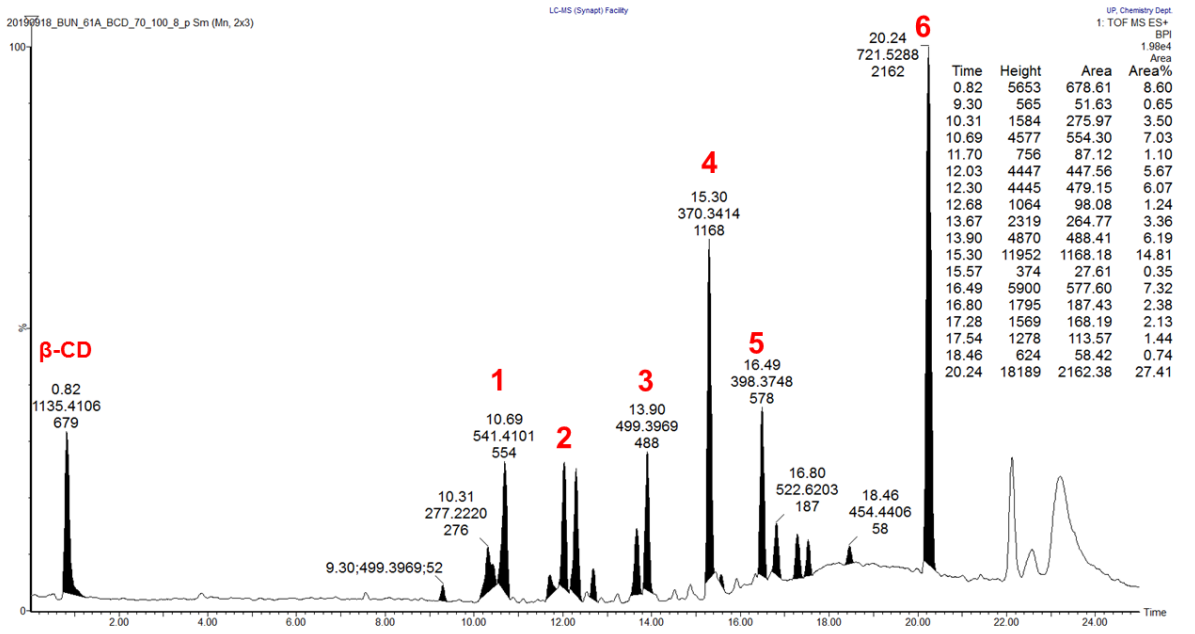

Figure 5.9: *An example peak area integrated chromatographic profile of the formulations, this particular formulation is 70·100·8.*

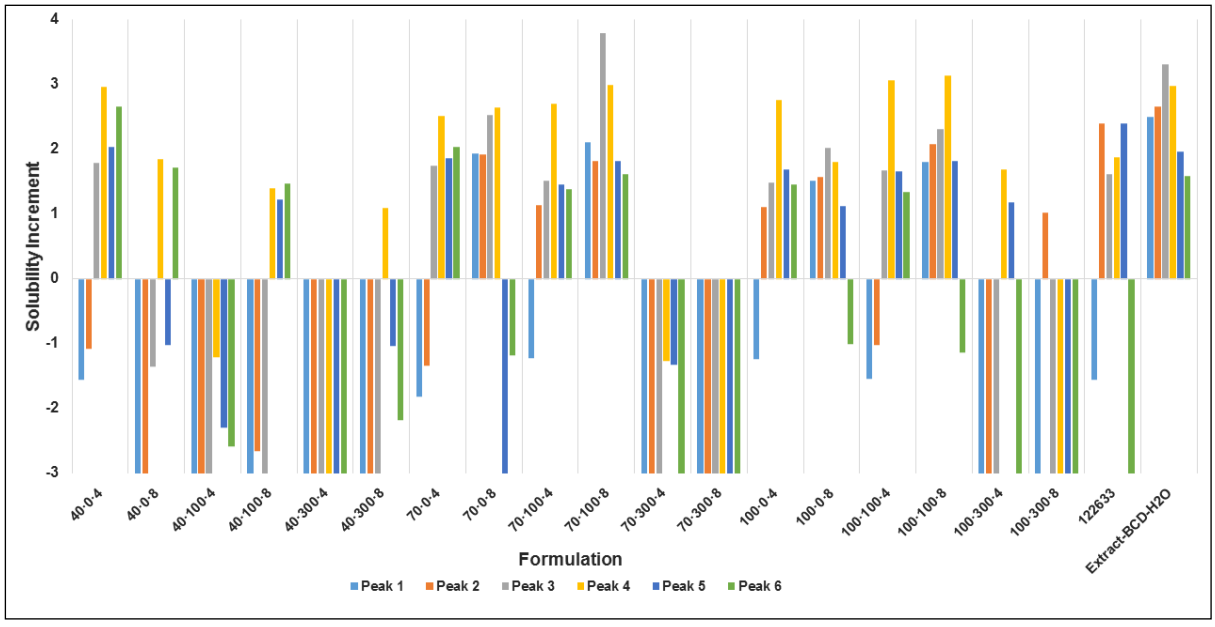

Figure 5.10: *Solubility increment or decrement of formulations with n-hexane extract compared to the crude extract.*

The component represented by peak 4 exhibited the highest solubility improvement overall with its greatest improvement of 3.13-times relative increase in solubility seen for the formulation 100·100·8. Peak 3, which represents cleogynone C, displays the second highest

overall solubility improvement with its bar height revealing a 3.79-times solubility increase (the highest overall improvement), seen for the formulation 70·100·8. Only the formulation 70·100·8 displays positive relative solubility increment on all the six selected peaks. Peak 1: 2.11-, peak 2: 1.82-, peak 3: 3.79-, peak 4: 2.99-, peak 5: 1.82-, and peak 5: 1.61-times solubility increment. Cleogynone C, therefore, displayed the highest solubility, almost four times that of the uncomplexed *n*-hexane extract. Extract-β-CD-water sample reveals that in the presence of β-CD in water, the solubility of the *n*-hexane extract is the greatest improved comparable to all the formulations, with only the compounds represented by peak 3 and 4 the only less soluble, compared to 70·100·8. Furthermore, peak 4 of extract-β-CD-water is also slightly less soluble than that of 40·0·4, 100·100·4 and 100·100·8.

Formulations that display five of the selected six peaks exhibiting solubility increments were: 70·100·4, 100·0·4, 100·0·8 and 100·100·8; while formulations displaying four of the six selected peaks exhibiting the relative solubility improvement were 40·0·4, 70·0·4, 70·0·8, 100·100·4 and the spray-dried formulation 122633.

Furthermore, it is evident that for the formulations that were obtained using the SC-CO_2 method at 300 bar pressure the solubility was highly decreased compared to the original extract (40·300·4, 40·300·8, 70·300·4, 70·300·8, 100·300·4, and 100·300·8). All or most of the selected peaks displayed highly negative relative solubility mostly more than 3-times less, this could be attributed to the loss of compound(s) due to unfavourable partitioning of the extract between the CO_2 and the β-CD. Literature has shown that increased pressure leads to increased compound solubility in CO_2, favouring partitioning of the compound in the CO_2 phase [47]. Upon depressurisation of the system, the compound is extracted with the CO_2. Thus, decreased solubility of extract at higher pressures could in fact be due to much lower extract concentration in the final product. Contrary to the formulations obtained at the pressure of 300 bar all other formulations displayed mainly an increased solubility for the selected six components compared to the uncomplexed extract.

With the positive impact of formulation in the aqueous solubility of the resulting complex their anticancer activities were determined to assess as to whether formulation improves the cancer cytotoxicity, conducted only in aqueous media.

5.3.3. Anticancer activity

The greatest aim for extract formulation with CDs in this study was to improve the solubility of the *n*-hexane extract and in doing so increase the chances of improved bioavailability of the active pharmaceutical ingredient(s) at the active site in the body. The reason for preparing the studied samples in water based media, therefore, is justified as an appropriate measure to assess as to whether the solubility improved components are those highly responsible for the biological activity.

The *n*-hexane extract was tested against breast- (MDA-MB-468), colorectal- (HCT-116) and lung cancer (A549), dissolved in water only and dissolved in β-CD water. Figures 5.11 - 5.13 compare the biological activity of *n*-hexane extract in water *vsn*-hexane extract in β-CD water against these cell lines. The extract was tested in the concentration range 0.2 – 1.0 mg/Ml, while the mass ratio extract : β-CD was 1:3 in all cases. In the presence of β-CD the anticancer activity of the *n*-hexane extract was improved compared to only water used as solvent. In all cases the *n*-hexane extract in water only exhibits activity less than 30% inhibition, while in all cases the activity is improved in the presence of β-CD. The highest activity was exhibited against breast cancer (MDA-MB-468), 79.3 %inhibition. At the highest test concentration (0.5 mg/mL) the extract showed dose-dependent anticancer activity in the range 0.2 – 5.0 mg/mL. Against both the lung- (A549) and colorectal cancer (HCT-116) an improvement in biological activity was evident but less than 65 %inhibition.

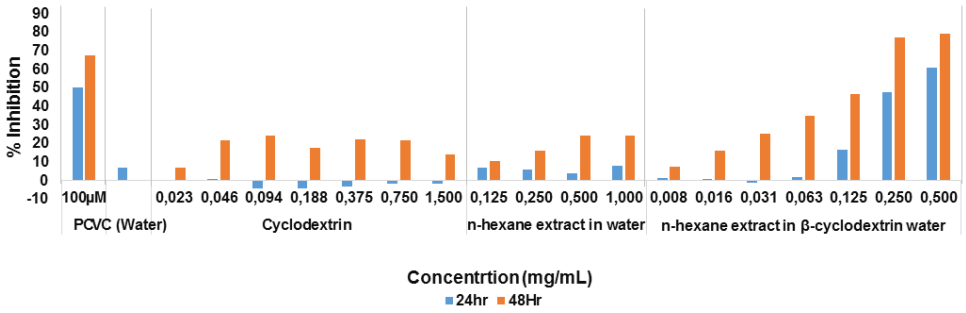

Figure 5.11: *Breast cancer cytotoxicity against MDA-MB-468 cell line in water based media with or without β-cyclodextrin indicating that in the presence of β-cyclodextrin the solubility of the active components is improved. Positive control (PC), Cisplatin.*

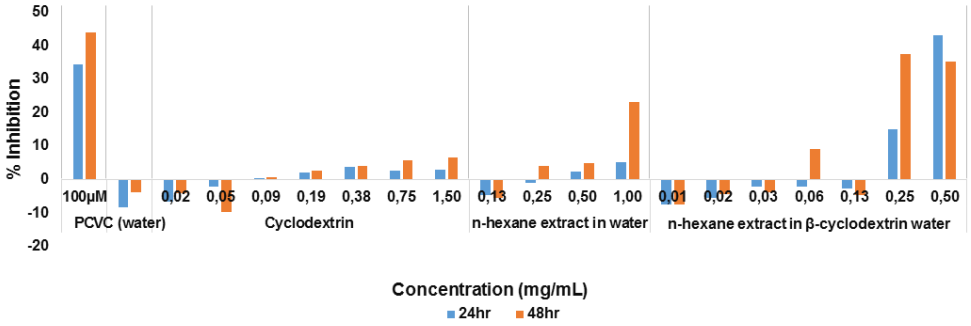

Figure 5.12: *Colorectal cancer cytotoxicity against HCT-116 cell line in water based media with or without β-cyclodextrin indicating that in the presence of β-cyclodextrin the solubility of the active components is improved. Positive control (PC), Cisplatin.*

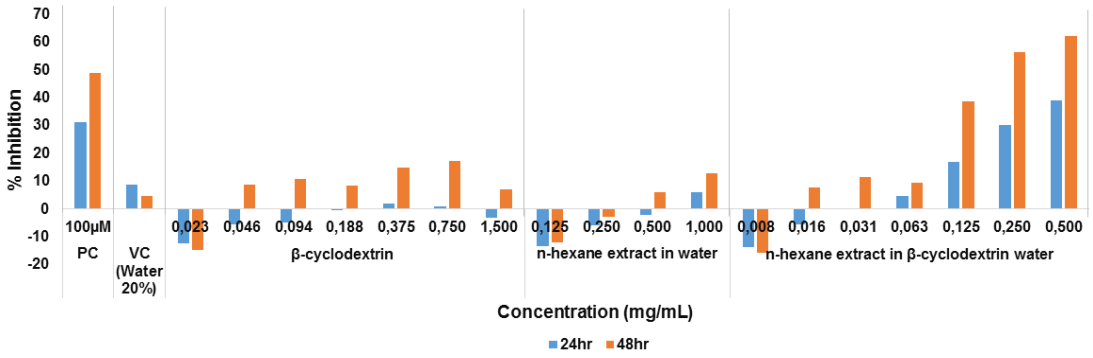

Figure 5.13: *Lung cancer cytotoxicity against the A549 cell line in water based media with or without β-cyclodextrin indicating that in the presence of β-cyclodextrin the solubility of the active components is improved. Positive control (PC), Cisplatin.*

Figures 5.14 and 5.15 display the activity of the formulations against lung cancer (A549) and breast cancer (MDA-MB-468). Better than of the uncomplexed extract and Cisplatin the positive control, the highest overall activity was displayed by the sample obtained *via* the spray-drying technique, 122633, displaying at its highest 83.66 %inhibition against the A549 cell line and 89.46 %inhibition against the MDA-MB-468 cell line at 0.5 mg/mL, tested at the concentrations 0.25, 0.5 and 1.0 mg/mL.

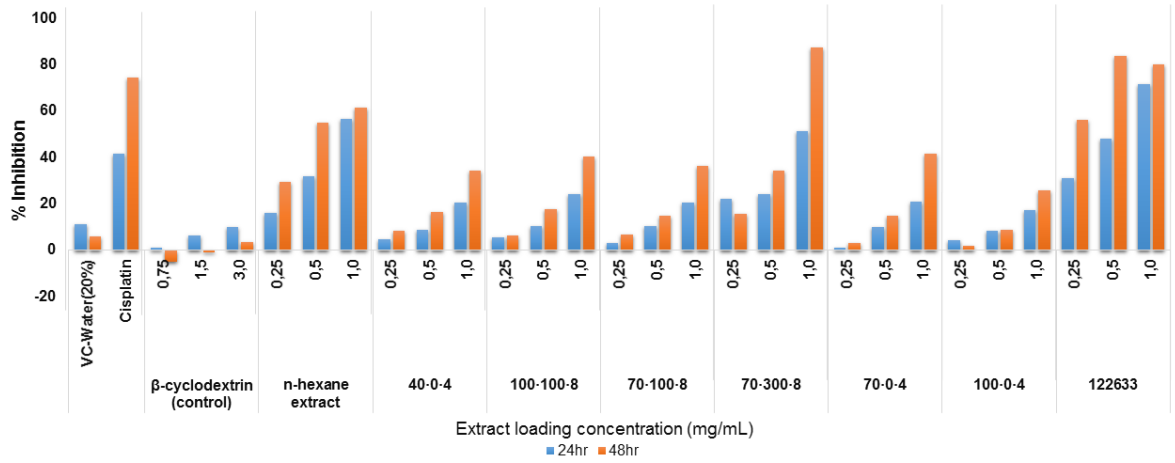

Figure 5.14: *Lung cancer (A549) cytotoxicity of formulations in comparison with the uncomplexed n-hexane extract.*

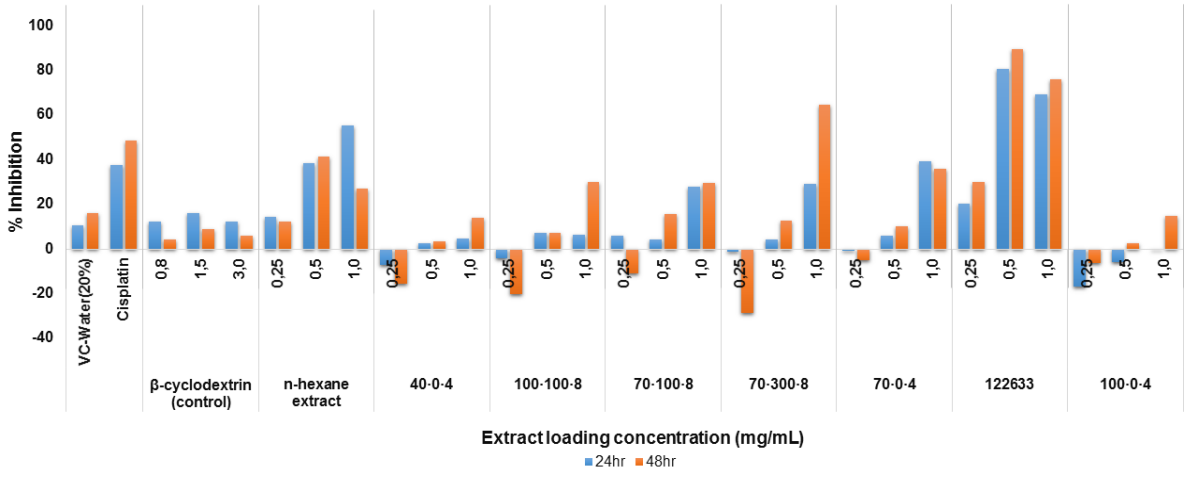

Figure 5.15: *Breast cancer (MDA-MB-468) cytotoxicity of formulations in comparison with unformulated n-hexane extract.*

The SC-CO_2 formulation, 70·100·8, which displayed a relatively higher aqueous solubility overall displayed activity lower than 40 %inhibition against both cell lines, indicating that the most active anticancer ingredients were not those that solubilised. The formulation 70·300·8 which was one of the lowest soluble formulations surprisingly displayed at its highest 87.43 %inhibition at 1 mg/mL and a dose-dependent activity in the range 0.25 – 1.0 mg/mL against the lung cancer (A549) cell line. This activity was the highest peak of all tested formulations. On effects of temperature, pressure and exposure time on the properties of complexes prepared by SC-CO_2 technology literature revealed that high temperature and pressure conditions may lead to greater drug inclusion, however, can influence the dissolution performance of the final product [48]. This may explain the poor solubility but higher bioactivity of 70·300·8.

When assessed against the colorectal cancer (HCT-116), 122633 exhibited the greatest activity overall at its highest displaying 87.03 %inhibition at 1 mg/mL (Figure 5.16). It is evident that even though the spray drying formulation technique was not the best overall in solubility studies, it displayed the greatest improvement in the anticancer biological activity against the lung (549), breast (MDA-MB-468) and colorectal cancer (HCT-116). While the SC-CO_2 formulation resulted in overall better improvement in solubility, the enhancement in anticancer biological activity was not evident for the solubility enhanced formulations.

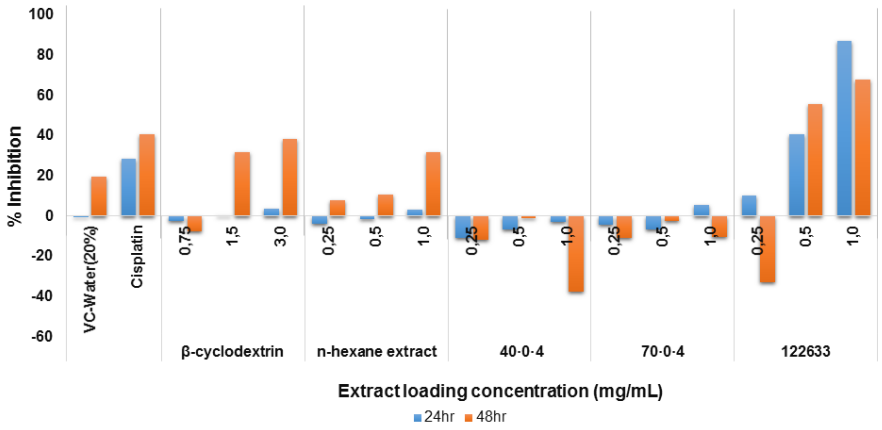

Figure 5.16: *Colorectal cancer (HCT-116) cytotoxicity of selected fractions in contrast with the uncomplexed extract.*

The two novel compounds whose chemical structures were elucidated as discussed in chapter 4 and proved to possess anticancer activity are poorly soluble in water. The compounds were also assessed to study whether they have a potential to benefit from cyclodextrins. Figures 5.17 – 5.19 show that dissolving the compounds in β-CD water has no consequence in terms of bioactivity improvement compared to dissolving the compounds in water only, indicating that β-CD does not enhance their aqueous solubilities. No activity was exhibited against all three cell lines A549, MDA-MB-468 and HCT-116 for both cleogynones A and B.

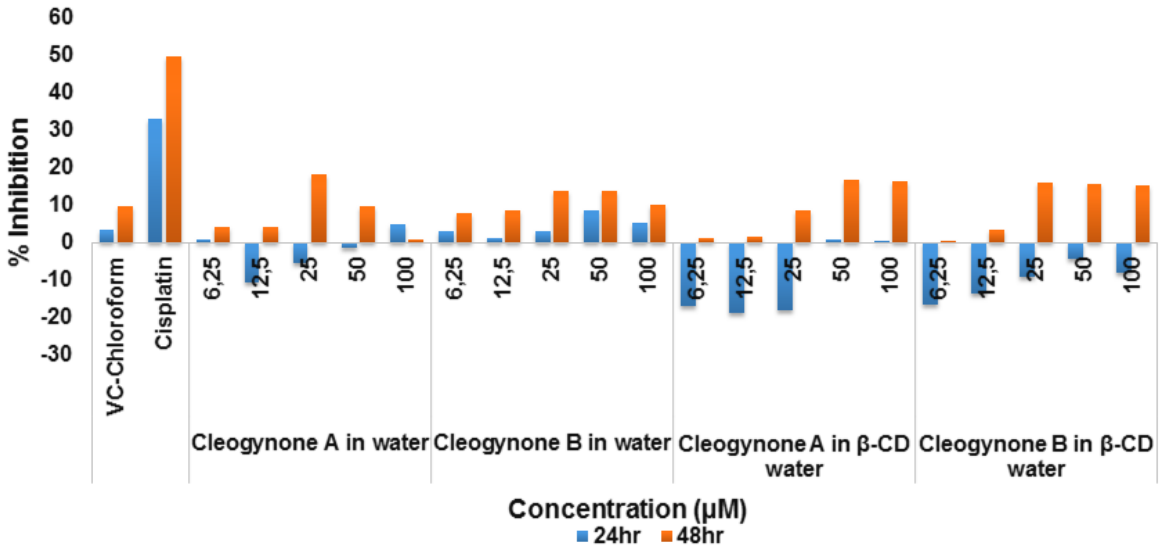

Figure 5.17: *Lung cancer cytotoxicity against the A549 cell line in water based media with or without β-cyclodextrin indicating that the presence of β-cyclodextrin in water for water based assays has no consequence in the bioactivity of cleogynones A and B.*

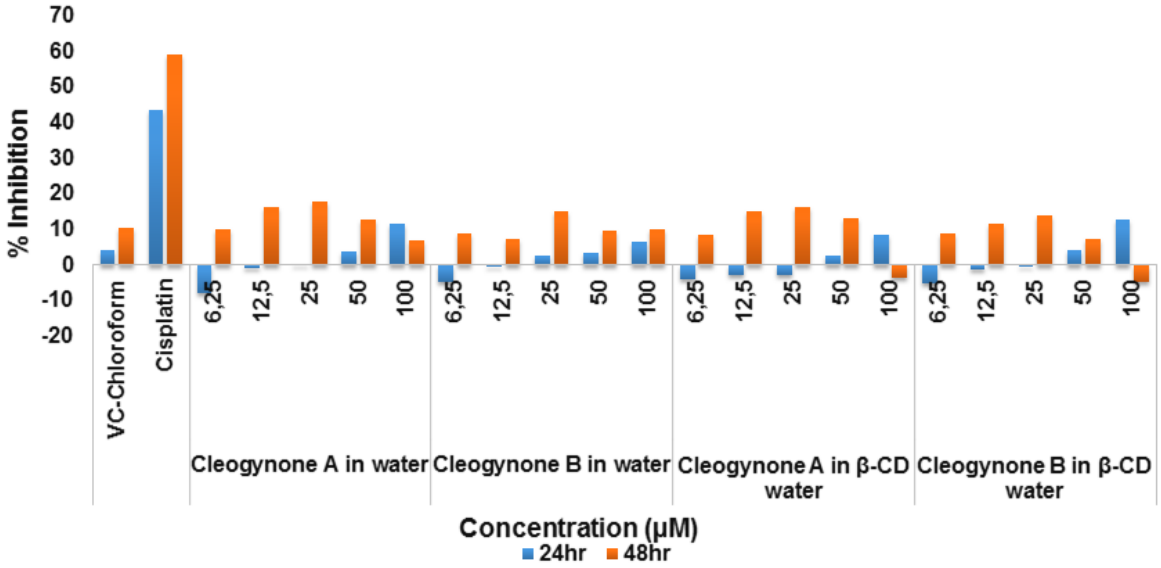

Figure 5.18: *Breast cancer cytotoxicity against the MDA-MB-468 cell line in water based media with or without β-cyclodextrin indicating that the presence of β-cyclodextrin in water based assays has no consequence in the bioactivity of cleogynones A and B, the novel compounds.*

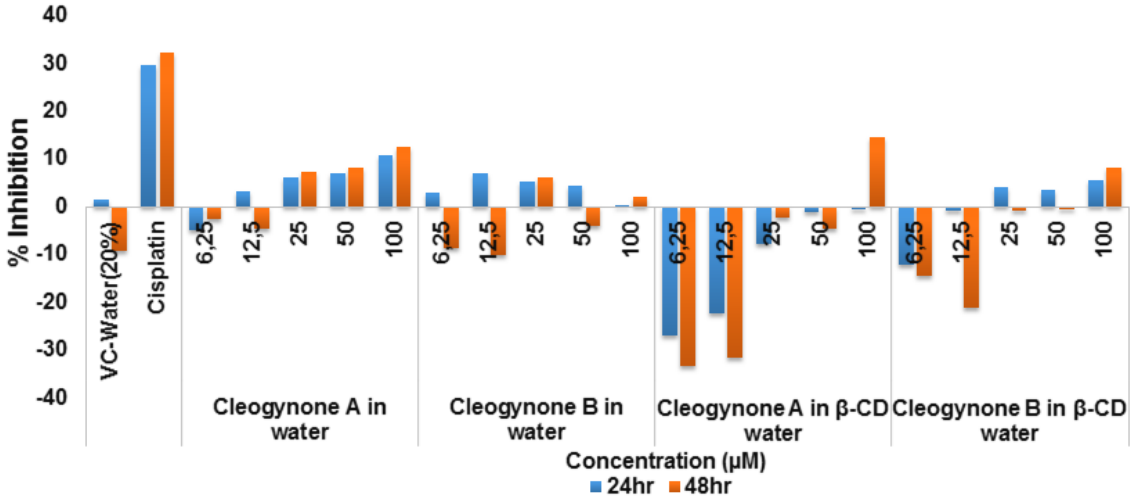

Figure 5.19: *Colorectal cancer (HCT-116) cytotoxicity in water based media with or without β-cyclodextrin indicating that the presence of β-cyclodextrin in water for water based assays has no consequence in the bioactivity of cleogynones A and B.*

5.4. Conclusions

Studies involving inclusion complexation of an anticancer bioactive extract from *C. gynandra* leaves are reported for the first time. Formulation was successful in improving the aqueous solubility for most of the SC-CO_2 formulations as well as the spray-dried formulation. Further it was shown that high pressure formulation condition may have enhanced the formulation but negatively impacts on the solubility. While formulations *via* the SC-CO_2 did not show improvement of anticancer activity the spray drying technique resulted in the greatest anticancer activity improvement. Overall, cyclodextrin formulation imparted an improvement in solubility and bioactivity. The best aqueous solubility increase was seen for the formulation 70·100·8 about 4-times better than the uncomplexed *n*-hexane extract, while the anticancer activity against all of lung-, breast- and colorectal cancer was lower than 40% inhibition on all tested concentrations with the highest concentration being 1 mg/mL. While the spray-dried formulation, 122633, displayed at its best approximately 2.5-times improvement in solubility, only showing improvement for four of the selected peaks, it was the most potent overall compared to other formulations (most of which showed better solubility) against all cell line (*viz.* A549, MDA-MB-468 and HCT-116). The formulation 122633, moreover, displayed the highest bioactivity of 89.46 %inhibition at 0.5 mg/mL against the A549 cell line.

The aqueous solubility of the novel compounds cleogynone A and cleogynone B was not improved in the presence of β-CD in water as these exhibited no improvement of anticancer activity against the lung-, breast and colorectal cancer cell lines. These compounds lack solubility in water and therefore display no activity if dissolved in water as they are filtered off during the assay. Attempts at using different cyclodextrins will need to form the bases of future work towards identifying the appropriate CDs to improve their aqueous solubilities.

In this study the unique versatility of the SC-CO_2 process has been demonstrated where it was shown how adjusting 3 operating parameters (pressure, temperature & time) can have significant impact on the characteristics of the final product.

5.5. References

1. Awasthi, R.; Kulkarni, G.T.; Pawar, V.K. Phytosomes: An approach to increase the bioavailability of plant extracts. *Int. J. Pharm. Pharm. Sci.***2011**, *3*, 1–3.
2. Del Valle, E.M.M. Cyclodextrins and their uses: A review. *Process Biochem.***2004**, *39*, 1033–1046, doi:10.1016/S0032-9592(03)00258-9.
3. Banchero, M.; Manna, L. Investigation of the piroxicam/hydroxypropyl-β-cyclodextrin inclusion complexation by means of a supercritical solvent in the presence of auxiliary agents. *J. Supercrit. Fluids***2011**, *57*, 259–266, doi:10.1016/j.supflu.2011.04.006.
4. Nguez, Ä. Supercritical CO_2 Extraction and Purification of Compounds with Antioxidant Activity. *J. Agric. Food Chem***2006**, *54*, 2441–2469.
5. Pasquali, I.; Bettini, R.; Giordano, F. Supercritical fluid technologies: An innovative approach for manipulating the solid-state of pharmaceuticals. *Adv. Drug Deliv. Rev.***2008**, *60*, 399–410, doi:10.1016/j.addr.2007.08.030.
6. Charoenchaitrakool, M.; Dehghani, F.; Foster, N.R. Utilization of supercritical carbon dioxide for complex formation of ibuprofen and methyl-beta-cyclodextrin. *Int. J. Pharm.***2002**, *239*, 103–112, doi:10.1016/S0378-5173(02)00078-9.
7. Kankala, R.K.; Zhang, Y.S.; Wang, S. Bin; Lee, C.H.; Chen, A.Z. Supercritical Fluid Technology: An Emphasis on Drug Delivery and Related Biomedical Applications. *Adv. Healthc. Mater.***2017**, *6*, doi:10.1002/adhm.201700433.
8. Eastburn, S.D.; Tao, B.Y. Applications of modified cyclodextrins. *Biotechnol. Adv.* 1994, *12*, 325–339.
9. Loftsson, T.; Brewster, M.E. Pharmaceutical applications of cyclodextrins: Drug solubilisation and stabilization. *J. Pharm. Sci.***1996**, *85*, 1017–1025.
10. Loftsson, T.; Matthíasson, K.; Másson, M. The effects of organic salts on the cyclodextrin solubilization of drugs. *Int. J. Pharm.***2003**, *262*, 101–107, doi:10.1016/S0378-5173(03)00334-X.
11. Challa, R.; Ahuja, A.; Ali, J.; Khar, R.K. Cyclodextrins in drug delivery: an updated review. *AAPS PharmSciTech***2005**, *6*, E329–E357, doi:10.1208/pt060243.
12. Frömming, K.-H.; Szejtli, J. Cyclodextrins in Pharmacy 1993, *30*, 224.
13. Loftsson, T.; Duchêne, D. Cyclodextrins and their pharmaceutical applications. *Int. J. Pharm.***2007**, *329*, 1–11, doi:10.1016/j.ijpharm.2006.10.044.
14. Cyclolab Approved pharmaceutical products containing cyclodextrins. *Cyclodext. news***2013**, *27*, 1–16.
15. S. C. Gupta, J. H. Kim, S. Prasad, B.B.A. Regulation of survival, proliferation, invasion, angiogenesis, and Cancer metastasis of tumor cells through modulation of inflammatory pathways by nutraceuticals. *Cancer Metastasis Rev***2010**, *29*, 405–434, doi:10.1007/s10555-010-9235-2.Regulation.

16. Tønnesen, H.H.; Másson, M.; Loftsson, T. Studies of curcumin and curcuminoids. XXVII. Cyclodextrin complexation: Solubility, chemical and photochemical stability. *Int. J. Pharm.***2002**, *244*, 127–135, doi:10.1016/S0378-5173(02)00323-X.

17. Ghosh, a; Biswas, S.; Ghosh, T. Preparation and Evaluation of Silymarin β-cyclodextrin Molecular Inclusion Complexes. *J. Young Pharm.***2011**, *3*, 205–10, doi:10.4103/0975-1483.83759.

18. Wang, J.; Cao, Y.; Sun, B.; Wang, C. Physicochemical and release characterisation of garlic oil-beta-cyclodextrin inclusion complexes. *Food Chem.***2011**, *127*, 1680–1685, doi:10.1016/j.foodchem.2011.02.036.

19. Gonnet, M.; Lethuaut, L.; Boury, F. New trends in encapsulation of liposoluble vitamins. *J. Control. Release***2010**, *146*, 276–290, doi:10.1016/j.jconrel.2010.01.037.

20. Mekjaruskul, C.; Yang, Y.T.; Leed, M.G.D.; Sadgrove, M.P.; Jay, M.; Sripanidkulchai, B. Novel formulation strategies for enhancing oral delivery of methoxyflavones in Kaempferia parviflora by SMEDDS or complexation with 2-hydroxypropyl-β- cyclodextrin. *Int. J. Pharm.***2013**, *445*, 1–11, doi:10.1016/j.ijpharm.2013.01.052.

21. Yuan, C.; Jin, Z.; Xu, X.; Zhuang, H.; Shen, W. Preparation and stability of the inclusion complex of astaxanthin with hydroxypropyl-β-cyclodextrin. *Food Chem.***2008**, *109*, 264–268, doi:10.1016/j.foodchem.2007.07.051.

22. Yuan, C.; Jin, Z.; Xu, X. Inclusion complex of astaxanthin with hydroxypropyl-??-cyclodextrin: UV, FTIR, 1H NMR and molecular modeling studies. *Carbohydr. Polym.***2012**, *89*, 492–496, doi:10.1016/j.carbpol.2012.03.033.

23. Palmer, M.V.; Ting, S.S.T. Applications for supercritical fluid technology in food processing. *Food Chem.***1995**, *52*, 345–352, doi:10.1016/0308-8146(95)93280-5.

24. Finney, B.; Jacobs, M. “Carbon dioxide pressure-temperature phase diagram” 2010.

25. Sekhon, B.S. Supercritical fluid technology: An overview of pharmaceutical applications. *Int. J. PharmTech Res.***2010**, *2*, 810–826.

26. Perrut, M. Supercritical Fluid Applications : Industrial Development and Economic Issues. *Ind. Eng. Chem. Res.***2000**, *39*, 4531–4535.

27. Toropainen, T.; Velaga, S.; Heikkila, T.; Matilainen, L.; Jarho, P.; Carlfors, J.; Lehto, V.-P.; Jarvinen, T.; Jarvinen, K. Preparation of Budesonide/gemma-Cyclodextrin Complexes in Supercritical Fluids with a Novel SEDS Method. *J. Pharm. Sci.***2006**, *95*, 2245, doi:10.1002/jps.

28. Hirunsit, P.; Huang, Z.; Srinophakun, T.; Charoenchaitrakool, M.; Kawi, S. Particle formation of ibuprofen-supercritical CO_2 system from rapid expansion of supercritical solutions (RESS): A mathematical model. *Powder Technol.***2005**, *154*, 83–94, doi:10.1016/j.powtec.2005.03.020.

29. Türk, M.; Upper, G.; Steurenthaler, M.; Hussein, K.; Wahl, M.A. Complex formation of Ibuprofen and β-Cyclodextrin by controlled particle deposition

(CPD) using SC-CO_2. *J. Supercrit. Fluids***2007**, *39*, 435–443, doi:10.1016/j.supflu.2006.02.009.

30. Bounaceur, A.; Rodier, E.; Fages, J. Maturation of a ketoprofen/beta-cyclodextrin mixture with supercritical carbon dioxide. *J. Supercrit. Fluids***2007**, *41*, 429–439, doi:10.1016/j.supflu.2006.11.004.

31. Bounaceur, A.; Rodier, E.; Fages, J. Maturation of a ketoprofen/??-cyclodextrin mixture with supercritical carbon dioxide. *J. Supercrit. Fluids***2007**, *41*, 429–439, doi:10.1016/j.supflu.2006.11.004.

32. Sauceau, M.; Rodier, E.; Fages, J. Preparation of inclusion complex of piroxicam with cyclodextrin by using supercritical carbon dioxide Preparation of Inclusion Complex of Piroxicam with Cyclodextrin by Using Supercritical Carbon Dioxide. *J. Supercrit. Fluids***2008**, *47*, 326–332.

33. Jun, S.W.; Kim, M.-S.; Kim, J.-S.; Park, H.J.; Lee, S.; Woo, J.-S.; Hwang, S.-J. Preparation and characterization of simvastatin/hydroxypropyl-β-cyclodextrin inclusion complex using supercritical antisolvent (SAS) process. *Eur. J. Pharm. Biopharm.***2007**, *66*, 413–21, doi:10.1016/j.ejpb.2006.11.013.

34. Al-Marzouqi, A.H.; Shehatta, I.; Jobe, B.; Dowaidar, A. Phase solubility and inclusion complex of itraconazole with β-cyclodextrin using supercritical carbon dioxide. *J. Pharm. Sci.***2006**, *95*, 292–304, doi:10.1002/jps.20535.

35. Hassan, H.A.; Al-Marzouqi, A.H.; Jobe, B.; Hamza, A.A.; Ramadan, G.A. Enhancement of dissolution amount and in vivo bioavailability of itraconazole by complexation with β-cyclodextrin using supercritical carbon dioxide. *J. Pharm. Biomed. Anal.***2007**, *45*, 243–250, doi:10.1016/j.jpba.2007.06.011.

36. Cal, K.; Sollohub, K. Spray Drying Technique. I: Hardware and Process Parameters. *J. Pharm. Sci.***2010**, *99*, 575–586, doi:10.1002/jps.

37. Kumar, A.; Awasthi, A. *Bioseparation Engineering*; I.K. International Publishing House Pvt. Ltd: New Delhi, 2009;

38. Skalko-Basnet, N.; Pavelic, Z.; Becirevic-Lacan, M. Liposomes containing drug and cyclodextrin prepared by the one-step spray-drying method. *Drug Dev. Ind. Pharm.***2000**, *26*, 1279–1284, doi:10.1081/DDC-100102309.

39. Mihajlovic, T.; Kachrimanis, K.; Graovac, A.; Djuric, Z.; Ibric, S. Improvement of aripiprazole solubility by complexation with (2-hydroxy)propyl-β-cyclodextrin using spray drying technique. *AAPS PharmSciTech***2012**, *13*, 623–631, doi:10.1208/s12249-012-9786-3.

40. Shan-Yang, L.; Yuh-Horng, K. Solid particulates of drug-β-cyclodextrin inclusion complexes directly prepared by a spray-drying technique. *Int. J. Pharm.***1989**, *56*, 249–259.

41. Pinho, E.; Grootveld, M.; Soares, G.; Henriques, M. Cyclodextrins as encapsulation agents for plant bioactive compounds. *Carbohydr. Polym.***2014**, *101*, 121–135, doi:10.1016/j.carbpol.2013.08.078.

42. Escobar-Avello, D.; Avendaño-Godoy, J.; Santos, J.; Lozano-Castellón, J.; Mardones, C.; von Baer, D.; Luengo, J.; Lamuela-Raventós, R.M.; Vallverdú-Queralt, A.; Gómez-Gaete, C. Encapsulation of phenolic compounds from a

grape cane pilot-plant extract in hydroxypropyl beta-cyclodextrin and maltodextrin by spray drying. *Antioxidants***2021**, *10*, 1–18, doi:10.3390/antiox10071130.

43. Lauro, M.R.; Crascì, L.; Giannone, V.; Ballistreri, G.; Fabroni, S.; Sansone, F.; Rapisarda, P.; Panico, A.M.; Puglisi, G. An alginate/cyclodextrin spray drying matrix to improve shelf life and antioxidant efficiency of a blood orange by-product extract rich in polyphenols: MMPs inhibition and antiglycation activity in dysmetabolic diseases. *Oxid. Med. Cell. Longev.***2017**, *2017*, doi:10.1155/2017/2867630.

44. Labuschagne, P.W.; John, M.J.; Sadiku, R.E. Investigation of the degree of homogeneity and hydrogen bonding in PEG/PVP blends prepared in supercritical CO_2: Comparison with ethanol-cast blends and physical mixtures. *J. Supercrit. Fluids***2010**, *54*, 81–88, doi:10.1016/j.supflu.2010.03.012.

45. BÜCHI *SpeedExtractor E-916/E-914 Operation Manual*; Version D.; BÜCHI Labortechnik AG: Flawil, Switzerland, 2009;

46. Kalombo, L.; Lemmer, Y.; Semete-Makokotlela, B.; Ramalapa, B.; Nkuna, P.; Booysen, L.L.L.I.J.; Naidoo, S.; Hayeshi, R.; Verschoor, J.A.; Swai, H.S. Spray-dried, nanoencapsulated, multi-drug anti-tuberculosis therapy aimed at once weekly administration for the duration of treatment. *Nanomaterials***2019**, *9*, doi:10.3390/nano9081167.

47. Ngo, T.T.; Liotta, C.L.; Eckert, C.A.; Kazarian, S.G. Supercritical fluid impregnation of different azo-dyes into polymer: in situ UV/Vis spectroscopic study. *J. Supercrit. Fluids***2003**, *27*, 215–221, doi:https://doi.org/10.1016/S0896-8446(02)00239-5.

48. Al-Marzouqi, A.H.; Jobe, B.; Dowaidar, A.; Maestrelli, F.; Mura, P. Evaluation of supercritical fluid technology as preparative technique of benzocaine–cyclodextrin complexes—Comparison with conventional methods. *J. Pharm. Biomed. Anal.***2007**, *43*, 566–574, doi:https://doi.org/10.1016/j.jpba.2006.08.019.

Chapter 6:

General Conclusion

Ingredients with varying bioactivity from varying leaf extracts of *C. gynandra*have been effectively prepared. Enzyme-based biological activities of several crude extracts revealed the potential of the ingredients of leaf extracts of *C. gynandra* to be developed as herbal medicines for the management of hyperglycaemia, management of cholesterol, control of blood pressure and cardio-protection as well as protection against hyperuricemia and management of gout.The extracts showed inhibition activities at varying levels against α-glucosidase, xanthine oxidase, renin and HMG-CoA reductase. Noteworthy, in enzyme-based work is the ethyl acetate extract, which was subjected to bioassay-guided fractionation for several potential yet unknown possibly novel biomarkers of high molecular mass using UPLC-QTOF-MS, while the poor UV visible nature of these compounds were a setback that hindered their isolation and potential structure elucidation.

The antimicrobial potential of *C. gynandra* ingredients was demonstrated, the ethanol extract indicating such potential, with its bioassay-guided fractionation subsequently revealing a semi-pure fraction exhibiting the greatest activity. The semi-pure fraction in turn revealed eight sub-fractions with MIC values in the range 0.012 – 0.094 mg/mL comparable to gentamicin. UPLC-QTOF-MS analysis using MassLynx and UNIFI®information system revealed the major compounds that make the tentative composition of this most active fraction as rutin, kaempferol-3-glucoside-3''-rhamnoside, isorhamnetin 3-*O*-robinoside, and nictoflorin while some of the minor compounds were kaempferol, quercetin and nepitrin. The conclusion could not be drawn as to which of the compounds exhibited the evident*E. coli* inhibitory activity seen in this study, with the contradictory literature. Standards were purchased for the major compounds rutin and nictoflorin,however,the standards displayed no bio-activity against *E. coli*or*S. aureus*.

Three anticancer compounds were isolated from an *n*-hexane extractof *C. gynandra* leaves, two of the compounds were novel compounds while one was a known compound. The compounds were named cleogynone A (**1**), cleogyone B (**2**)and cleogynone C (**3**), all displaying at the highest activity, greater than 81 % inhibitionagainst the colorectal cancer (HCT15), at 25 µg/mL concentration over 48 hr treatment. Cleogynones B and C both displayed the greatest activity at 89.34±5.46 and 87.76±1.22 % inhibition, respectively, against colorectal cancer (HCT116) over 24 hr treatment at the highest test concentration (25 µg/mL). The compounds displayed moderate activity against breast cancer (MDA-MB-468) while all three compounds displayed poor activity against lung cancer (A549).

The structure elucidation of the isolated compounds was successfully done by a set of modern spectroscopic techniques including IR, MS, NMR spectroscopy and single crystal X-ray diffraction. These techniques were combined to chemical methods for the determination of the absolute configuration of the chiral cleogynones A (**1**), B (**2**) and C (**3**). The chemical profiling of the extracts, fractions and sub-fractions was effectively done using UPLC-QTOF-MS.

While plant ingredients are known to possess poor physicochemical properties which may hinder their pathway to commercialisation, formulation of the *C. gynandra*ingredients in β-CD *via*the green technology SC-CO_2as well as the spray-drying techniquehave resulted in complexes with either/or/both increased aqueous solubility and improved biological activity which may render them more bioavailable at the active site in the final formulation. Several SC-CO_2 β-CD complexes of the *n*-hexane extract in this study displayed between 2 and 4 times increase in aqueous solubility while spray dried formulation not only showed increase in solubility but also showed improvement in anticancer activity. Complexes obtained using high pressure conditions did not show solubility increase but rather decreased solubility. The effects of temperature, pressure and exposure time on the properties of complexes prepared by the SC-CO_2 technology reveal that high temperature and pressure conditions may lead to greater drug inclusion, however, can influence the dissolution performance of the final

product. This is evident of the formulation 70·300·8 which was one of the lowest soluble formulations obtained at 300 bar pressure displaying at its highest 87.43 %inhibition at 1 mg/mL and a dose-dependent activity in the range 0.25 – 1.0 mg/mL against the lung cancer (A549) cell line, better than some of the more soluble complexes.In the presence of β-CD in water, however, the novel compounds cleogynones A (**1**) and B (**2**) did not display any improvement in biological activity.

For the first time, a comprehensive investigation of the biologically active ingredients from *C. gynandra* and attempts at improving inherent physicochemical properties of some of the ingredients through formulation with β-cyclodextrin *via* the environmentally benign SC-CO_2 technology. This study yielded two novel compounds with lung cancer, breast cancer and colorectal cancer activity, while several known compounds were also identified as potential contributors to the biological activity of *C. gynandra*including those as potentialcontributors to anti-carcinogenic, cardioprotective, antihypertension, anti-uricaemic, cholesterol lowering and antimicrobial properties for management of conditions such as diarrhoea.

This study has paved the way for future exploration with respect to *C. gynandra* ingredients for eventually landing marketable medicinal products with good bioavailability, particularly, products with antidiabetic, anticancer medicinal properties as well as antimicrobial properties.*Cleome gynandra* merits commercialisation.